

Canadian Technical Report of
Hydrography and Ocean Sciences 245

2006

**Wind Forcing of Ice Drift in the Southern Gulf
of St. Lawrence: Satellite-tracked Ice Beacon
Program 2004**

by

A. van der Baaren^{*} and S. J. Prinsenber

Ocean Sciences Division
Maritimes Region
Fisheries and Oceans Canada
Bedford Institute of Oceanography
P. O. Box 1006
Dartmouth, Nova Scotia
Canada, B2Y 4A2

^{*} contractor, 8 Toye Lane, Wolfville, Nova Scotia, B4P2C8

© Her Majesty the Queen in Right of Canada, 2006

Cat. No. FS 97-18/245E ISSN 0711-6764

Correct Citation for this publication:

van der Baaren, A. and S. J. Prinsenbergh. 2006. Wind Forcing of Ice Drift in the Southern Gulf of St. Lawrence: Satellite-tracked Ice Beacon Program 2004. *Can. Tech. Rep. Hydrogr. Ocean Sci.* 245: xvii + 188 p.

CONTENTS

CONTENTS	iii
LIST OF FIGURES	v
LIST OF TABLES	xv
ABSTRACT	xvi
RÉSUMÉ	xvii
1 INTRODUCTION	1
2 INSTRUMENTATION AND DATA	1
3 DATA PROCESSING AND ANALYSIS	3
3.1 GPS location beacons and Argos basic ice beacon	3
3.2 Meteorological data	11
3.3 Least squares regression	16
3.4 Results	22
3.4.1 Analysis with low-pass filtered drift data	50
REFERENCES	69
ACKNOWLEDGEMENTS	69
4 APPENDIX I: A comparison of forecast model wind and observed wind	70
4.1 Data	70
4.1.1 Observations @ hourly intervals	73
4.2 Analysis	82
4.2.1 Compare Charlottetown; winter	87
4.2.1.1 Compare Charlottetown with analysis 6-hourly; winter	87
4.2.1.2 Compare Charlottetown with low resolution forecast 6-hourly; winter	89
4.2.1.3 Compare Charlottetown with high resolution forecast 3-hourly	91
4.2.2 Compare Summerside; winter	93
4.2.2.1 Compare Summerside with analysis 6-hourly; winter	93
4.2.2.2 Compare Summerside with low resolution forecast 6-hourly; winter	95
4.2.2.3 Compare Summerside with high resolution forecast 3-hourly; winter	97
4.2.3 Compare Iles de la Madeleine; winter	99
4.2.3.1 Compare Iles de la Madeleine with analysis 6-hourly; winter	99

4.2.3.2	Compare Iles de la Madeleine with low resolution forecast 6-hourly; winter	101
4.2.3.3	Compare Iles de la Madeleine with high resolution forecast 3-hourly; winter	103
4.2.4	Compare wave buoy 44150; summer	105
4.2.4.1	Compare wave buoy 44150 with analysis 6-hourly; summer	105
4.2.4.2	Compare wave buoy 44150 with low resolution forecast 6-hourly; summer	107
4.2.4.3	Compare wave buoy 44150 with high resolution forecast 3-hourly; summer	109
4.2.5	Compare wave buoy 44161; summer	111
4.2.5.1	Compare wave buoy 44161 with analysis 6-hourly; summer	111
4.2.5.2	Compare wave buoy 44161 with low resolution forecast 6-hourly; summer	113
4.2.5.3	Compare wave buoy 44161 with high resolution forecast 3-hourly; summer	115
4.2.6	Compare Charlottetown; summer	117
4.2.6.1	Compare Charlottetown with analysis 6-hourly; summer	117
4.2.6.2	Compare Charlottetown with low resolution forecast 6-hourly; summer	119
4.2.7	Compare Summerside; summer	123
4.2.7.1	Compare Summerside with analysis 6-hourly; summer	123
4.2.7.2	Compare Summerside with low resolution forecast 6-hourly; summer	125
4.2.8	Compare Iles de la Madeleine; summer	129
4.2.8.1	Compare Iles de la Madeleine with analysis 6-hourly; summer	129
4.2.8.2	Compare Iles de la Madeleine with low resolution forecast 6-hourly; summer	131
4.3	Beacon drift analysis with 6-hourly analysis winds	135
4.4	Beacon drift analysis with 3-hourly high resolution forecast model wind output	144
4.5	References Appendix I	169
5	APPENDIX II: Field report and field notes	170
5.1	Sea Ice 2004 Gulf field report	170
5.2	2004 DFO Ice Pic and Probe field program field notes 14-20 February	182
6	APPENDIX III: Computational code	187

LIST OF FIGURES

Figure 1	Track of beacon 00973 from Argos message header position information.....	4
Figure 2	Track of beacon 02754 from Argos message header position information. The long straight line indicates the gap in the time series for the positions (see Figure 7).	4
Figure 3	Track of beacon 26370 from Argos message header position information.....	5
Figure 4	Track of beacon 26375 from Argos message header position information.....	5
Figure 5	Track of beacon 26386 from Argos message header position information.....	6
Figure 6	Latitude and longitude for beacon 00973	7
Figure 7	Latitude and longitude for beacon 02754	8
Figure 8	Latitude and longitude for beacon 26370	9
Figure 9	Latitude and longitude for beacon 26375	10
Figure 10	Latitude and longitude for beacon 26386.....	11
Figure 11	6-hourly forecast wind for beacon 00973 and the wind at the 4 gridpoints surrounding the beacon that were used for bilinear interpolation; 17 Feb to 22 Feb.	12
Figure 12	6-hourly forecast wind for beacon 02754 and the wind at the 4 gridpoints surrounding the beacon that were used for bilinear interpolation; 17 Feb to 22 Feb.	13
Figure 13	6-hourly forecast wind for beacon 26370 and the wind at the 4 gridpoints surrounding the beacon that were used for bilinear interpolation; 18 Feb to 25 Mar	14
Figure 14	6-hourly forecast wind for beacon 26375 and the wind at the 4 gridpoints surrounding the beacon that were used for bilinear interpolation; 16 Feb to 22 Feb.	15
Figure 15	6-hourly forecast wind for beacon 26386 and the wind at the 4 gridpoints surrounding the beacon that were used for bilinear interpolation; 18 Feb to 25 Mar	16
Figure 16	Hourly ice drift and 6-hourly wind data for beacon 00973	17
Figure 17	6-hourly ice drift and 6-hourly wind data for beacon 02754.....	18
Figure 18	Hourly ice drift and 6-hourly wind data for beacon 26370	19
Figure 19	Hourly ice drift and 6-hourly wind data for beacon 26375	20
Figure 20	Hourly ice drift and 6-hourly wind data for beacon 26386	21
Figure 21	Results of complex least squares regression of wind and drift data for beacon 00973. The figure shows hourly wind and beacon drift, the predicted drift values (ie. fitted series), the angle difference between wind vectors and drift vectors (with mean angle difference), and the ratio of drift speed to wind speed (with mean ratio).	24
Figure 22	Scatter of hourly drift speed vs. wind speed for beacon 00973. Lines for various reponse are also shown. Squares indicate the predicted relationship from regression.	25
Figure 23	Results of complex least squares regression of wind and drift data for beacon 02754. The figure shows 6-hourly wind and beacon drift, the predicted drift values (ie. fitted series), the angle difference between wind vectors and drift vectors (with mean angle difference), and the ratio of drift speed to wind speed (with mean ratio).	26
Figure 24	Scatter of 6-hourly drift speed vs. wind speed for beacon 02754. Lines for various reponse are also shown. Squares indicate the predicted relationship from regression.	27
Figure 25	Results of complex least squares regression of wind and drift data for beacon 26370. The figure shows hourly wind and beacon drift, the predicted drift values (ie.	

fitted series), the angle difference between wind vectors and drift vectors (with mean angle difference), and the ratio of drift speed to wind speed (with mean ratio).	28
Figure 26 Scatter of hourly drift speed vs. wind speed for beacon 26370. Lines for various reponse are also shown. Squares indicate the predicted relationship from regression.	29
Figure 27 Results of complex least squares regression of wind and drift data for beacon 26375. The figure shows hourly wind and beacon drift, the predicted drift values (ie. fitted series), the angle difference between wind vectors and drift vectors (with mean angle difference), and the ratio of drift speed to wind speed (with mean ratio).	30
Figure 28 Scatter of hourly drift speed vs. wind speed for beacon 26375. Lines for various reponse are also shown. Squares indicate the predicted relationship from regression.	31
Figure 29 Results of complex least squares regression of wind and drift data for beacon 26386. The figure shows hourly wind and beacon drift, the predicted drift values (ie. fitted series), the angle difference between wind vectors and drift vectors (with mean angle difference), and the ratio of drift speed to wind speed (with mean ratio).	32
Figure 30 Scatter of hourly drift speed vs. wind speed for beacon 26386. Lines for various reponse are also shown. Squares indicate the predicted relationship from regression.	33
Figure 31 Results of complex least squares regression of wind and drift data for beacon 26370 before Feb 20. The figure shows hourly wind and beacon drift, the predicted drift values (ie. fitted series), the angle difference between wind vectors and drift vectors (with mean angle difference), and the ratio of drift speed to wind speed (with mean ratio).....	34
Figure 32 Scatter of hourly drift speed vs. wind speed for beacon 26370 before Feb 20. Lines for various reponse are also shown. Squares indicate the predicted relationship from regression.....	35
Figure 33 Results of complex least squares regression of wind and drift data for beacon 26386 before Feb 20. The figure shows hourly wind and beacon drift, the predicted drift values (ie. fitted series), the angle difference between wind vectors and drift vectors (with mean angle difference), and the ratio of drift speed to wind speed (with mean ratio).....	36
Figure 34 Scatter of hourly drift speed vs. wind speed for beacon 26386 before Feb 20. Lines for various reponse are also shown. Squares indicate the predicted relationship from regression.....	37
Figure 35 Results of complex least squares regression of wind and drift data for beacon 26370 after Feb 20. The figure shows hourly wind and beacon drift, the predicted drift values (ie. fitted series), the angle difference between wind vectors and drift vectors (with mean angle difference), and the ratio of drift speed to wind speed (with mean ratio).....	38
Figure 36 Scatter of hourly drift speed vs. wind speed for beacon 26370 after Feb 20. Lines for various reponse are also shown. Squares indicate the predicted relationship from regression.....	39
Figure 37 Results of complex least squares regression of wind and drift data for beacon 26386 after Feb 20. The figure shows hourly wind and beacon drift, the predicted drift values (ie. fitted series), the angle difference between wind vectors and drift	

vectors (with mean angle difference), and the ratio of drift speed to wind speed (with mean ratio).....	40
Figure 38 Scatter of hourly drift speed vs. wind speed for beacon 26386 after Feb 20. Lines for various reponse are also shown. Squares indicate the predicted relationship from regression.....	41
Figure 39 Results of complex least squares regression of wind and drift data for beacon 26370 after Mar 4. The figure shows hourly wind and beacon drift, the predicted drift values (ie. fitted series), the angle difference between wind vectors and drift vectors (with mean angle difference), and the ratio of drift speed to wind speed (with mean ratio).....	42
Figure 40 Scatter of hourly drift speed vs. wind speed for beacon 26370 after Mar 4. Lines for various reponse are also shown. Squares indicate the predicted relationship from regression.....	43
Figure 41 Results of complex least squares regression of wind and drift data for beacon 26386 after Mar 4. The figure shows hourly wind and beacon drift, the predicted drift values (ie. fitted series), the angle difference between wind vectors and drift vectors (with mean angle difference), and the ratio of drift speed to wind speed (with mean ratio).....	44
Figure 42 Scatter of hourly drift speed vs. wind speed for beacon 26386 after Mar 4. Lines for various reponse are also shown. Squares indicate the predicted relationship from regression.....	45
Figure 43 Results of complex least squares regression of wind and drift data for beacon 26370 before Feb. 20 with drift lagged behind wind by 3 hours. The figure shows hourly wind and beacon drift, the predicted drift values (ie. fitted series), the angle difference between wind vectors and drift vectors (with mean angle difference), and the ratio of drift speed to wind speed (with mean ratio).....	46
Figure 44 Results of complex least squares regression of wind and drift data for beacon 26370 before Feb. 20 with drift lagged behind wind by 6 hours. The figure shows hourly wind and beacon drift, the predicted drift values (ie. fitted series), the angle difference between wind vectors and drift vectors (with mean angle difference), and the ratio of drift speed to wind speed (with mean ratio).....	47
Figure 45 Results of complex least squares regression of wind and drift data for beacon 26386 before Feb. 20 with drift lagged behind wind by 3 hours. The figure shows hourly wind and beacon drift, the predicted drift values (ie. fitted series), the angle difference between wind vectors and drift vectors (with mean angle difference), and the ratio of drift speed to wind speed (with mean ratio).....	48
Figure 46 Results of complex least squares regression of wind and drift data for beacon 26386 before Feb. 20 with drift lagged behind wind by 6 hours. The figure shows hourly wind and beacon drift, the predicted drift values (ie. fitted series), the angle difference between wind vectors and drift vectors (with mean angle difference), and the ratio of drift speed to wind speed (with mean ratio).....	49
Figure 47 Time series of beacon 00973 hourly drift with mean drift (low-passed) superimposed.....	51
Figure 48 Time series of beacon 26370 hourly drift with mean drift (low-passed) superimposed.....	52

Figure 49 Time series of beacon 26375 hourly drift with mean drift (low-passed) superimposed.....	53
Figure 50 Time series of beacon 26386 hourly drift with mean drift (low-passed) superimposed.....	54
Figure 51 Results of complex least squares regression of wind and low-pass drift data for beacon 00973. The figure shows hourly wind and beacon drift, the predicted drift values (ie. fitted series), the angle difference between wind vectors and drift vectors (with mean angle difference), and the ratio of drift speed to wind speed (with mean ratio).	55
Figure 52 Scatter of 6-hourly low-pass filtered drift speed vs. wind speed for beacon 00973. Lines for various reponse are also shown. Squares indicate the predicted relationship from regression.	56
Figure 53 Results of complex least squares regression of wind and low-pass drift data for beacon 26375. The figure shows hourly wind and beacon drift, the predicted drift values (ie. fitted series), the angle difference between wind vectors and drift vectors (with mean angle difference), and the ratio of drift speed to wind speed (with mean ratio).	57
Figure 54 Scatter of 6-hourly low-pass filtered drift speed vs. wind speed for beacon 26375. Lines for various reponse are also shown. Squares indicate the predicted relationship from regression.	58
Figure 55 Results of complex least squares regression of wind and low-pass drift data for beacon 26370. The figure shows hourly wind and beacon drift, the predicted drift values (ie. fitted series), the angle difference between wind vectors and drift vectors (with mean angle difference), and the ratio of drift speed to wind speed (with mean ratio).	59
Figure 56 Scatter of 6-hourly low-pass filtered drift speed vs. wind speed for beacon 26370. Lines for various reponse are also shown. Squares indicate the predicted relationship from regression.	60
Figure 57 Results of complex least squares regression of wind and low-pass drift data for beacon 26370 before Feb 20. The figure shows hourly wind and beacon drift, the predicted drift values (ie. fitted series), the angle difference between wind vectors and drift vectors (with mean angle difference), and the ratio of drift speed to wind speed (with mean ratio).	61
Figure 58 Scatter of 6-hourly low-pass filtered drift speed vs. wind speed for beacon 26370 before Feb. 20. Lines for various reponse are also shown. Squares indicate the predicted relationship from regression.	62
Figure 59 Results of complex least squares regression of wind and low-pass drift data for beacon 26370 after Mar 4. The figure shows hourly wind and beacon drift, the predicted drift values (ie. fitted series), the angle difference between wind vectors and drift vectors (with mean angle difference), and the ratio of drift speed to wind speed (with mean ratio).	63
Figure 60 Scatter of 6-hourly low-pass filtered drift speed vs. wind speed for beacon 26370 after Mar. 4. Lines for various reponse are also shown. Squares indicate the predicted relationship from regression.	64
Figure 61 Results of complex least squares regression of wind and low-pass drift data for beacon 26386. The figure shows hourly wind and beacon drift, the predicted drift	

values (ie. fitted series), the angle difference between wind vectors and drift vectors (with mean angle difference), and the ratio of drift speed to wind speed (with mean ratio).....	65
Figure 62 Scatter of 6-hourly low-pass filtered drift speed vs. wind speed for beacon 26386. Lines for various reponse are also shown. Squares indicate the predicted relationship from regression.....	66
Figure 63 Results of complex least squares regression of wind and low-pass drift data for beacon 26386 after Mar. 4. The figure shows hourly wind and beacon drift, the predicted drift values (ie. fitted series), the angle difference between wind vectors and drift vectors (with mean angle difference), and the ratio of drift speed to wind speed (with mean ratio).....	67
Figure 64 Scatter of 6-hourly low-pass filtered drift speed vs. wind speed for beacon 26386 after Mar. 4. Lines for various reponse are also shown. Squares indicate the predicted relationship from regression.....	68
Figure 65 Map showing locations of Environment Canada weather stations and locations of wave buoys equipped to monitor atmosphere.....	73
Figure 66 Wind velocity components, mean sea level pressure, and air temperature for Iles de la Madeleine, Summerside, and Charlottetown in February 2004; wind speed has been adjusted to 10 m reference level.....	74
Figure 67 Wind velocity components, mean sea level pressure, and air temperature for Iles de la Madeleine, Summerside, and Charlottetown in June 2004; wind speed has been adjusted to 10 m reference level.....	75
Figure 68 Wind velocity components, mean sea level pressure, and air temperature for Iles de la Madeleine, Summerside, and Charlottetown in July 2004; wind speed has been adjusted to 10 m reference level.....	76
Figure 69 Wind velocity components, mean sea level pressure, and air temperature for 2 wave buoys in the Northumberland Strait and in the Gulf of St. Lawrence in June 2004; wind speed has been adjusted to 10 m reference level.....	77
Figure 70 Annual wind speed statistics for the Gulf of St. Lawrence, Magdalen taken from http://www.meds-sdmm.dfo-mpo.gc.ca/alphapro/wave/TDCAtlas/TDCAtlasGS.htm	78
Figure 71 Annual wind statistics for the Gulf of St. Lawrence, Magdalen taken from http://www.meds-sdmm.dfo-mpo.gc.ca/alphapro/wave/TDCAtlas/TDCAtlasGS.htm	79
Figure 72 Monthly wind statistics: frequency of wind speed by direction for the Gulf of St. Lawrence, Magdalen taken from http://www.meds-sdmm.dfo-mpo.gc.ca/alphapro/wave/TDCAtlas/TDCAtlasGS.htm	80
Figure 73 Monthly wind statistics: percent occurrence of wind speed for the Gulf of St. Lawrence, Magdalen taken from http://www.meds-sdmm.dfo-mpo.gc.ca/alphapro/wave/TDCAtlas/TDCAtlasGS.htm	81
Figure 74 Monthly wind statistics: percent exceeding of wind speed for the Gulf of St. Lawrence, Magdalen taken from http://www.meds-sdmm.dfo-mpo.gc.ca/alphapro/wave/TDCAtlas/TDCAtlasGS.htm	82
Figure 75 Time series of Charlottetown winter meteorological observations and 6-hourly analysis output; scatter plots of the same with correlation coefficients.....	87

Figure 76 Time series of Charlottetown winter wind vector observations and 6-hourly analysis output with results of least squares fit.....	88
Figure 77 Time series of Charlottetown winter meteorological observations and 6-hourly low resolution forecast output; scatter plots of the same with correlation coefficients	89
Figure 78 Time series of Charlottetown winter wind vector observations and 6-hourly low resolution forecast output with results of least squares fit	90
Figure 79 Time series of Charlottetown winter meteorological observations and 3-hourly high resolution forecast output; scatter plots of the same with correlation coefficients	91
Figure 80 Time series of Charlottetown winter wind vector observations and 3-hourly high resolution forecast output with results of least squares fit	92
Figure 81 Time series of Summerside winter meteorological observations and 6-hourly analysis output; scatter plots of the same with correlation coefficients.....	93
Figure 82 Time series of Summerside winter wind vector observations and 6-hourly analysis output with results of least squares fit.....	94
Figure 83 Time series of Summerside winter meteorological observations and 6-hourly low resolution forecast output; scatter plots of the same with correlation coefficients	95
Figure 84 Time series of Summerside winter wind vector observations and 6-hourly low resolution forecast output with results of least squares fit	96
Figure 85 Time series of Summerside winter meteorological observations and 3-hourly high resolution forecast output; scatter plots of the same with correlation coefficients	97
Figure 86 Time series of Summerside winter wind vector observations and 3-hourly high resolution forecast output with results of least squares fit	98
Figure 87 Time series of Iles de la Madeleine winter meteorological observations and 6-hourly analysis output; scatter plots of the same with correlation coefficients	99
Figure 88 Time series of Iles de la Madeleine winter wind vector observations and 6-hourly analysis output with results of least squares fit.....	100
Figure 89 Time series of Iles de la Madeleine winter meteorological observations and 6-hourly low resolution forecast output; scatter plots of the same with correlation coefficients	101
Figure 90 Time series of Iles de la Madeleine winter wind vector observations and 6-hourly low resolution forecast output with results of least squares fit.....	102
Figure 91 Time series of Iles de la Madeleine winter meteorological observations and 3-hourly high resolution forecast output; scatter plots of the same with correlation coefficients	103
Figure 92 Time series of Iles de la Madeleine winter wind vector observations and 3-hourly high resolution forecast output with results of least squares fit.....	104
Figure 93 Time series of wave buoy 44150 summer meteorological observations and 6-hourly analysis output; scatter plots of the same with correlation coefficients	105
Figure 94 Time series of wave buoy 44150 summer wind vector observations and 6-hourly analysis output with results of least squares fit.....	106

Figure 95 Time series of wave buoy 44150 summer meteorological observations and 6-hourly low resolution forecast output; scatter plots of the same with correlation coefficients.	107
Figure 96 Time series of wave buoy 44150 summer wind vector observations and 6-hourly low resolution forecast output with results of least squares fit.....	108
Figure 97 Time series of wave buoy 44150 summer meteorological observations and 3-hourly high resolution forecast output; scatter plots of the same with correlation coefficients.	109
Figure 98 Time series of wave buoy 44150 summer wind vector observations and 3-hourly high resolution forecast output with results of least squares fit.....	110
Figure 99 Time series of wave buoy 44161 summer meteorological observations and 6-hourly analysis output; scatter plots of the same with correlation coefficients.	111
Figure 100 Time series of wave buoy 44161 summer wind vector observations and 6-hourly analysis output with results of least squares fit.....	112
Figure 101 Time series of wave buoy 44161 summer meteorological observations and 6-hourly low resolution forecast output; scatter plots of the same with correlation coefficients	113
Figure 102 Time series of wave buoy 44161 summer wind vector observations and 6-hourly low resolution forecast output with results of least squares fit.....	114
Figure 103 Time series of wave buoy 44161 summer meteorological observations and 3-hourly high resolution forecast output; scatter plots of the same with correlation coefficients	115
Figure 104 Time series of wave buoy 44161 summer wind vector observations and 3-hourly high resolution forecast output with results of least squares fit.....	116
Figure 105 Time series of Charlottetown summer meteorological observations and 6-hourly analysis output; scatter plots of the same with correlation coefficients	117
Figure 106 Time series of Charlottetown summer wind vector observations and 6-hourly analysis output with results of least squares fit.....	118
Figure 107 Time series of Charlottetown summer meteorological observations and 6-hourly low resolution forecast output; scatter plots of the same with correlation coefficients	119
Figure 108 Time series of Charlottetown summer wind vector observations and 6-hourly low resolution forecast output with results of least squares fit	120
Figure 109 Time series of Charlottetown summer meteorological observations and 3-hourly high resolution forecast output; scatter plots of the same with correlation coefficients	121
Figure 110 Time series of Charlottetown summer wind vector observations and 3-hourly high resolution forecast output with results of least squares fit	122
Figure 111 Time series of Summerside summer meteorological observations and 6-hourly analysis output; scatter plots of the same with correlation coefficients	123
Figure 112 Time series of Summerside summer wind vector observations and 6-hourly analysis output with results of least squares fit.....	124
Figure 113 Time series of Summerside summer meteorological observations and 6-hourly low resolution forecast output; scatter plots of the same with correlation coefficients	125

Figure 114 Time series of Summerside summer wind vector observations and 6-hourly low resolution forecast output with results of least squares fit	126
Figure 115 Time series of Summerside summer meteorological observations and 3-hourly high resolution forecast output; scatter plots of the same with correlation coefficients	127
Figure 116 Time series of Summerside summer wind vector observations and 3-hourly high resolution forecast output with results of least squares fit	128
Figure 117 Time series of Iles de la Madeleine summer meteorological observations and 6-hourly analysis output; scatter plots of the same with correlation coefficients. ...	129
Figure 118 Time series of Iles de la Madeleine summer wind vector observations and 6-hourly analysis output with results of least squares fit	130
Figure 119 Time series of Iles de la Madeleine summer meteorological observations and 6-hourly low resolution forecast output; scatter plots of the same with correlation coefficients	131
Figure 120 Time series of Iles de la Madeleine summer wind vector observations and 6-hourly low resolution forecast output with results of least squares fit	132
Figure 121 Time series of Iles de la Madeleine summer meteorological observations and 3-hourly high resolution forecast output; scatter plots of the same with correlation coefficients	133
Figure 122 Time series of Iles de la Madeleine summer wind vector observations and 3-hourly high resolution forecast output with results of least squares fit	134
Figure 123 Results of complex least squares regression of 1-hourly analysis wind and drift data for beacon 26370. The figure shows hourly wind and beacon drift, the predicted drift values (ie. fitted series), the angle difference between wind vectors and drift vectors (with mean angle difference), and the ratio of drift speed to wind speed (with mean ratio)	136
Figure 124 Results of complex least squares regression of 1-hourly analysis wind and drift data for beacon 26386. The figure shows hourly wind and beacon drift, the predicted drift values (ie. fitted series), the angle difference between wind vectors and drift vectors (with mean angle difference), and the ratio of drift speed to wind speed (with mean ratio)	137
Figure 125 Results of complex least squares regression of 1-hourly analysis wind and drift data for beacon 26370 until 20 February only. The figure shows hourly wind and beacon drift, the predicted drift values (ie. fitted series), the angle difference between wind vectors and drift vectors (with mean angle difference), and the ratio of drift speed to wind speed (with mean ratio)	138
Figure 126 Results of complex least squares regression of 1-hourly analysis wind and drift data for beacon 26386 until 20 February only. The figure shows hourly wind and beacon drift, the predicted drift values (ie. fitted series), the angle difference between wind vectors and drift vectors (with mean angle difference), and the ratio of drift speed to wind speed (with mean ratio)	139
Figure 127 Results of complex least squares regression of 6-hourly analysis wind and drift data for beacon 26370. The figure shows hourly wind and beacon drift, the predicted drift values (ie. fitted series), the angle difference between wind vectors and drift vectors (with mean angle difference), and the ratio of drift speed to wind speed (with mean ratio)	140

Figure 128 Results of complex least squares regression of 6-hourly analysis wind and drift data for beacon 26386. The figure shows hourly wind and beacon drift, the predicted drift values (ie. fitted series), the angle difference between wind vectors and drift vectors (with mean angle difference), and the ratio of drift speed to wind speed (with mean ratio).....	141
Figure 129 Results of complex least squares regression of 6-hourly analysis wind and drift data for beacon 26370 until 20 February. The figure shows hourly wind and beacon drift, the predicted drift values (ie. fitted series), the angle difference between wind vectors and drift vectors (with mean angle difference), and the ratio of drift speed to wind speed (with mean ratio).....	142
Figure 130 Results of complex least squares regression of 6-hourly analysis wind and drift data for beacon 26386 until 20 February. The figure shows hourly wind and beacon drift, the predicted drift values (ie. fitted series), the angle difference between wind vectors and drift vectors (with mean angle difference), and the ratio of drift speed to wind speed (with mean ratio).....	143
Figure 131 Time series of beacon 26370 wind obtained from CMC high resolution prognostic grid. Also shown are the 4 grid corners used to interpolate the wind at beacon positions.	146
Figure 132 Time series of beacon 26386 wind obtained from CMC high resolution prognostic grid. Also shown are the 4 grid corners used to interpolate the wind at beacon positions.	147
Figure 133 Scatter plot of hourly drift magnitude vs. hourly wind magnitude for both beacons: a) 26370 and b) 26386 with 0-hour lag. Tidal signal is retained in drift data.	148
Figure 134 Scatter plot of 3-hourly drift magnitude vs. 3-hourly wind magnitude for both beacons: a) 26370 and b) 26386 with 0-hour lag. Tidal signal is retained in drift data.	148
Figure 135 Hourly time series of least squares fit for beacon 26370 drift and 3-hourly high resolution forecast wind to 20 Feb. Wind has been interpolated to be hourly. Lag is 0 hours.	149
Figure 136 Hourly time series of least squares fit for beacon 26370 drift and 3-hourly high resolution forecast wind to 20 Feb. Wind has been interpolated to be hourly. Lag is 1 hour.	150
Figure 137 Hourly time series of least squares fit for beacon 26370 drift and 3-hourly high resolution forecast wind to 20 Feb. Wind has been interpolated to be hourly. Lag is 2 hours.	151
Figure 138 Hourly time series of least squares fit for beacon 26370 drift and 3-hourly high resolution forecast wind to 20 Feb. Wind has been interpolated to be hourly. Lag is 3 hours.	152
Figure 139 Hourly time series of least squares fit for beacon 26370 drift and 3-hourly high resolution forecast wind to 20 Feb. Wind has been interpolated to be hourly. Lag is 4 hours.	153
Figure 140 Hourly time series of least squares fit for beacon 26370 drift and 3-hourly high resolution forecast wind to 20 Feb. Wind has been interpolated to be hourly. Lag is 5 hours.	154

Figure 141 Hourly time series of least squares fit for beacon 26370 drift and 3-hourly high resolution forecast wind to 20 Feb. Wind has been interpolated to be hourly. Lag is 6 hours.	155
Figure 142 Hourly time series of least squares fit for beacon 26386 drift and 3-hourly high resolution forecast wind to 20 Feb. Wind has been interpolated to be hourly. Lag is 0 hours.	156
Figure 143 Hourly time series of least squares fit for beacon 26386 drift and 3-hourly high resolution forecast wind to 20 Feb. Wind has been interpolated to be hourly. Lag is 1 hour.	157
Figure 144 Hourly time series of least squares fit for beacon 26386 drift and 3-hourly high resolution forecast wind to 20 Feb. Wind has been interpolated to be hourly. Lag is 2 hours.	158
Figure 145 Hourly time series of least squares fit for beacon 26386 drift and 3-hourly high resolution forecast wind to 20 Feb. Wind has been interpolated to be hourly. Lag is 3 hours.	159
Figure 146 Hourly time series of least squares fit for beacon 26386 drift and 3-hourly high resolution forecast wind to 20 Feb. Wind has been interpolated to be hourly. Lag is 4 hours.	160
Figure 147 Hourly time series of least squares fit for beacon 26386 drift and 3-hourly high resolution forecast wind to 20 Feb. Wind has been interpolated to be hourly. Lag is 5 hours.	161
Figure 148 Hourly time series of least squares fit for beacon 26386 drift and 3-hourly high resolution forecast wind to 20 Feb. Wind has been interpolated to be hourly. Lag is 6 hours.	162
Figure 149 Time series of least squares fit for beacon 26370 drift and 3-hourly high resolution forecast wind to 20 Feb. Wind and drift are both 3-hourly. Lag is 0 hours.	163
Figure 150 Time series of least squares fit for beacon 26370 drift and 3-hourly high resolution forecast wind to 20 Feb. Wind and drift are both 3-hourly. Lag is 3 hours.	164
Figure 151 Time series of least squares fit for beacon 26370 drift and 3-hourly high resolution forecast wind to 20 Feb. Wind and drift are both 3-hourly. Lag is 6 hours.	165
Figure 152 Hourly time series of least squares fit for beacon 26386 drift and 3-hourly high resolution forecast wind to 20 Feb. Wind and drift are both 3-hourly. Lag is 0 hours.	166
Figure 153 Hourly time series of least squares fit for beacon 26386 drift and 3-hourly high resolution forecast wind to 20 Feb. Wind and drift are both 3-hourly. Lag is 3 hours.	167
Figure 154 Hourly time series of least squares fit for beacon 26386 drift and 3-hourly high resolution forecast wind to 20 Feb. Wind and drift are both 3-hourly. Lag is 6 hours.	168

LIST OF TABLES

Table 1 List of ice beacons and data deployment record basics; dates are in calendar days	2
Table 2 List of ice beacons and data record basics; dates are in calendar days.....	2
Table 3 Positional extremes for ice beacons taken from hourly records, or, in the case of 2754, the irregular series; dates are in calendar days.....	3
Table 4 Regression results for least squares fit of wind to drift; data were hourly except for beacon 02754. $R^2 > 50\%$ and $\text{Gain} \geq 1.9\%$ are in bold.	23
Table 5 Regression results for least squares fit of wind to low pass filtered drift.....	50
Table 6 Coefficient of correlation: winter forecast and analysis output with observed winter data.....	83
Table 7 Coefficient of correlation: summer forecast and analysis output with observed summer data	84
Table 8 Regression statistics: winter forecast and analysis wind velocity output to observed winter wind velocity data.....	85
Table 9 Regression statistics: summer forecast and analysis wind velocity output to observed summer wind velocity data.....	86
Table 10 Regression results for least squares fit of drift to 6-hourly analysis wind. $R^2 > 50\%$ and $\text{Gain} \geq 1.9\%$ are in bold.	135
Table 11 Results for least squares fit of drift to wind; data were <i>hourly</i> ; drift lags were by the hour; data were up to but not including Feb. 20, 2004.....	144
Table 12 Results for least squares fit of drift to wind; data were <i>3-hourly</i> ; drift lags were by the 3-hour; data were up to but not including Feb. 20, 2004	145

ABSTRACT

van der Baaren, A. and S. J. Prinsenberg. 2006. Wind Forcing of Ice Drift in the Southern Gulf of St. Lawrence: Satellite-tracked Ice Beacon Program 2004. *Can. Tech. Rep. Hydrogr. Ocean Sci.* 245: xvii + 188 p.

Five satellite-tracked ice beacons were deployed on sea ice near Prince Edward Island in February 2004 providing ice drift record lengths from three days to five weeks. The drift records of two beacons showed that during times of free ice drift the average angles that the ice bore to the wind were 15° and 22° with gain of 3% for both beacons. Least squares regressions gave R^2 values of 0.88 and 0.87.

A low-pass filter removed the tidal signal in the ice drift. Data were then decimated to be 6-hourly. This procedure changed the resulting regression such that, for the beacon that experienced the longest time of “free drift” before February 20, the turning angle was 10° with R^2 of 0.91. It was seen that after March 4 one other beacon experienced a period of free drift such that its R^2 was 0.67 for the regression of tide-free drift to wind with turning angle and gain of 0.7° and 1.48, respectively.

Modelled winds were also compared to land station and wave buoy meteorological data from the Gulf of St. Lawrence/Northumberland Strait. The two wave buoys were located in the strait with one being more exposed than the other. Correlating four scalar quantities (U, V wind components, air temperature, and mean sea level pressure) from the three model outputs with real winter and summer observations measured at three land stations (Summerside, Charlottetown, and Iles de la Madeleine) gave coefficients of correlation ranging from 0.8 to near 1.0. The best correlation was for the mean sea level pressure. It was found that model output underestimated wind speed at land stations during winter and summer with gains from 53% to 87%. In summer gains were 90% to 106% for the more exposed wave buoy and 108% to 118% for the more sheltered one. The best regression results of model output to observation winds were produced by the analysis winds during summer with turning angles of 0.1° to 0.3° and R^2 of 0.64 to 0.86.

RÉSUMÉ

van der Baaren, A. et Prinsenbergh, S. J. « Wind Forcing of Ice Drift in the Southern Gulf of St. Lawrence: Satellite-tracked Ice Beacon Program 2004 ». Dans *Can. Tech. Rep. Hydrogr. Ocean Sci.* n° 245 (2006), xvii + 188 p.

Cinq balises des glaces suivies par satellite ont été déployées sur les glaces de mer, près de l'Île-du-Prince-Édouard, en février 2004, afin d'enregistrer leur dérives pendant une durée de trois jours à cinq semaines. Les données enregistrées par deux balises montrent que durant la dérive libre des glaces, l'angle moyen de dérive des glaces par rapport à la direction du vent s'établissait entre 15° et 22° et la réponse était 3 % pour les deux balises. Une régression par la méthode des moindres carrés a donné des valeurs de R^2 allant de 0,88 et 0,87.

L'utilisation d'un filtre passe-bas a permis d'éliminer l'effet de la marée sur la dérive des glaces en utilisant des données échantillonnées à un intervalle de six heures. La régression résultante a été modifiée, de sorte que pour la balise ayant enregistré la plus longue période de « dérive libre » avait une valeur de R^2 de 0,67, un angle de rotation de $0,7^{\circ}$ et une réponse à 1,48 %.

La mise en corrélation des quatre grandeurs scalaires (soit U, les composantes du vent V, la température de l'air et la pression au niveau moyen de la mer) des trois sorties du modèles avec des observations hivernales et estivales réelles effectuées en trois stations terrestres (Summerside, Charlottetown et Îles de la Madeleine) a respectivement donné des coefficients de corrélation s'étendant de 0,8 à près de 1,0. Les meilleures corrélations étaient celles établies avec les pressions au niveau moyen de la mer. On a constaté que le modèle sous-estimait la vitesse du vent en hiver, respectivement de 53 % à 87 % aux stations de Summerside, Charlottetown, et Îles de la Madeleine. En été, les réponses se situaient entre 108 % et 118 %, dans le cas de la bouée de mesure des vagues la plus abritée, et entre 90 % et 106 %, dans celui de la bouée la plus exposée. Les meilleurs résultats pour la régression établie entre les sorties des modèles et les observations ont été obtenus lors de l'analyse des vents estivaux, les plus petits écarts angulaires s'établissant de $0,1^{\circ}$ à $0,3^{\circ}$ et la valeur de R^2 , de 0,64 à 0,86.

1 INTRODUCTION

The 2004 field program of ice beacons in the Gulf of St. Lawrence involved deploying five Seimac GPS ice beacons north of Prince Edward Island and in Northumberland Strait. The objective was to monitor the evolution of ice thickness tracked by beacons. The work supports ice-ocean numerical modeling verification that is funded through the Program of Energy Research and Development (PERD). The field program also supports satellite image identification work that is funded through the Canadian Space Agency's Government Related Initiatives Program (GRIP).

This report discusses how the location beacon data, as an indicator of ice drift, relates to the wind forcing using simple correlation analysis and a least squares regression. First there is a brief description of instrumentation and data. Preliminary processing procedure is presented and then the correlation between 6-hourly wind data and hourly drift data is presented. Results are reported with and without the drift data being lagged behind the wind. Another analysis is presented with drift data that were low-pass filtered to eliminate the tidal signal. In the first of two appendices there is an examination of the difference that several wind model outputs would make to the analysis. Lastly, an appendix is presented that contains field reports and notes written during the deployment of the instruments.

2 INSTRUMENTATION AND DATA

The GPS ice beacons manufactured by Seimac Ltd. of Dartmouth, N. S. provided positional information of ice movement. Beacon electronic components are contained within a sealed fiberglass shell and the instrument is deployed such that the bottom section sits in a shallow ice hole. The beacons are designed to sink when the ice floe, on which they are deployed, melts. The beacons will quit transmitting after three months. The battery pack in the beacons is capable of powering the internal components for at least 60 days at -35°C and 90 days at temperatures averaging -20°C . Beacons transmit data to Service Argos satellites when they pass overhead. The Argos data message always has a message header with a beacon latitude and longitude which is determined by the satellite at the time of its pass. It can also contain data recorded by specific sensors on the beacons.

These five ice beacons were equipped with GPS sensors that permitted hourly positions to be obtained and stored internally. The most recent 8 hours of data are transmitted to Argos satellites when they pass overhead. A regular hourly time series can be constructed from the transmitted data found in the body of the Argos message. An irregular time series of positions can also be obtained from the Argos message header. These header data can be used to verify the hourly series. GPS beacon specifications and details of performance during stationery tests are given in van der Baaren and Prinsenberg (2000).

Shortly after deployment, three of the five deployed beacons immediately became mired in the pack ice deformation process after deployment due to an unusually fierce winter storm that began on February 19. The remaining two, that were deployed north of the

island, survived through the ridging and rafting process caused by the storm. They were tracked for at least 4 to 5 weeks before being recovered. The floes containing these beacons stayed intact; at least 10 m x 10 m of ice surrounded each beacon. The three other beacons were probably in ridges or rolled off during ridging into cracks in the ice and sank. Table 1 and Table 2 list the beacon IDs, the type of beacon (GPS or basic), deployment location, the length of the position record (if any), and basic statistics of the record.

Table 3 lists the positional extremes for the beacons. You will likely notice that more data are recovered from Argos message headers than from the hourly GPS record. This is not necessarily the case since many of the Argos messages occur within minutes of each other and are essentially repeated messages; the positions are virtually the same. Note also that the precision of the data obtained from the message headers is much less than that of the GPS data. For these reasons, if GPS data are available, it is better to use them for analysis rather than position data from Argos message headers. Unfortunately for beacon 02754, its GPS unit or transmitter malfunctioned so there were no hourly data recovered. For this report, header data from the GPS beacons were used for beacon 02754 and for drawing the beacon tracks in Figure 1 to Figure 5.

Table 1 List of ice beacons and data deployment record basics; dates are in calendar days

Beacon ID	Deployment			
	Start day	End day	where	# days
00973	48	53	Strait	6
02754	45	53	Strait	9
26370	47	83	Gulf	38
26375	47	50	Gulf	4
26386	49	83	Gulf	36

Table 2 List of ice beacons and data record basics; dates are in calendar days

Beacon ID	Data Record from Message Header				Hourly GPS Data Record			
	Start day	End day	# points	# missing	Start day	End day	# points	# missing
00973	41.7142	53.9737	199	68	48 1800	53 2300	126	0
02754	45.4286	53.0570	157	57	NA	NA	NA	NA
26370	47.8641	83.8306	1273	365	47 2000	83 2100	866	6
26375	47.6606	50.9063	130	48	47 1600	50 2100	78	0
26386	49.6984	83.8312	1269	428	49 1600	83 1900	820	9

Table 3 Positional extremes for ice beacons taken from hourly records, or, in the case of 2754, the irregular series; dates are in calendar days

ID	Position (from hourly series if available)					
	First	Last	Northernmost	Southernmost	Easternmost	Westernmost
00973			Day 50 0600	Day 51 0200	Day 50 0700	Day 53 1800
	45.862442	45.853745	45.917282	45.837645	45.85060	45.914866
	-62.483719	-62.668312	-62.411072	-62.6800012	-62.409676	-62.703407
02754			Day 50 0250	Day 47 1774	Day 46 0512	Day 50 1532
	46.274	46.242	46.776	46.229	46.291	46.624
	-63.132	-64.026	-64.364	-63.186	-63.062	-64.487
26370			Day 47 2000	Day 62 0900	Day 50 0100	Day 47 2000
	46.747302	46.460861	46.747302	46.167957	46.658966	46.747302
	-63.460457	-63.057198	-63.460457	-63.244786	-62.923628	-63.460457
26375			Day 50 0600	Day 50 2100	Day 50 0100	Day 50 2100
	47.095273	47.020557	47.134216	47.020557	47.120475	47.020557
	-64.127220	-64.179642	-63.972412	-64.179642	-63.938710	-64.179642
26386			Day 50 0600	Day 82 0000	Day 83 1900	Day 60 2000
	46.801186	46.603973	46.825958	46.338595	46.603973	46.367556
	-62.127499	-61.354378	-62.084261	-61.875310	-61.354378	-62.832982

Meteorological data were obtained from an archive of Canadian Meteorological Centre prognostic data maintained at the Bedford Institute of Oceanography. The 6-hourly data are from the low-resolution model 48-hour forecast. The archived winds are on a $1^{\circ} \times 1^{\circ}$ grid defined from (20°N , 80°W) to (70°N , 30°W). There are also 3-hourly data available from the high resolution regional model (24 km x 24 km grid). Those data were used in a smaller analysis discussed in Appendix I.

3 DATA PROCESSING AND ANALYSIS

3.1 GPS location beacons and Argos basic ice beacon

Positions were plotted for each beacon from Argos message header files to roughly check the beacon tracks (Figure 1 to Figure 5). Hourly GPS positions were then extracted from the Argos data transmission messages from 00973, 26370, 26375, and 26386. Spurious positions were edited for the four GPS records. Hourly positions were compared to positions contained in the Argos header information collected during satellite passes. Header information was available for all beacons (00973, 02754, 26370, 26375, and 26386; see Table 1 to Table 2). Beacons 26370 and 26386 survived the longest and were removed from the pack ice at the end of the survey.

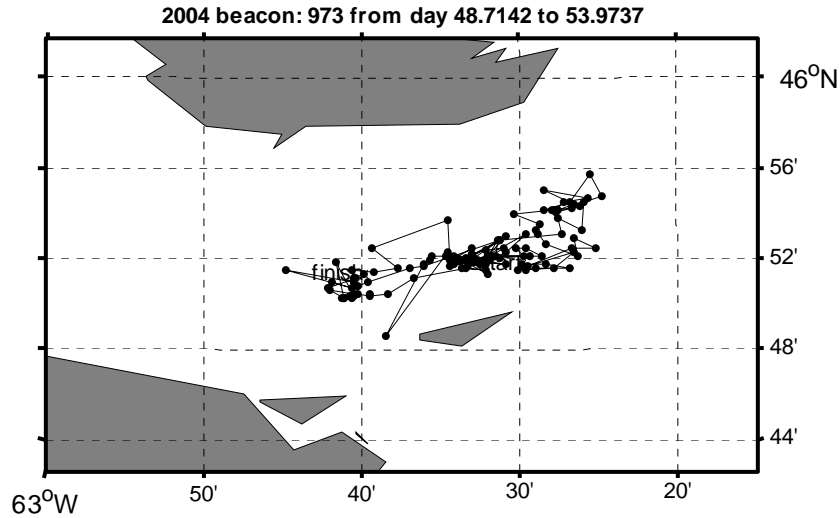


Figure 1 Track of beacon 00973 from Argos message header position information

There are approximately 24 hours of missing data from the Argos record that belongs to beacon 02754. This gap occurs at the time of the February storm. During this event the beacon drifted southeasterly approximately 20 km from a northwest position in Northumberland Strait (Figure 2).

2004 beacon: 2754 from day 48.6455 to 53.057

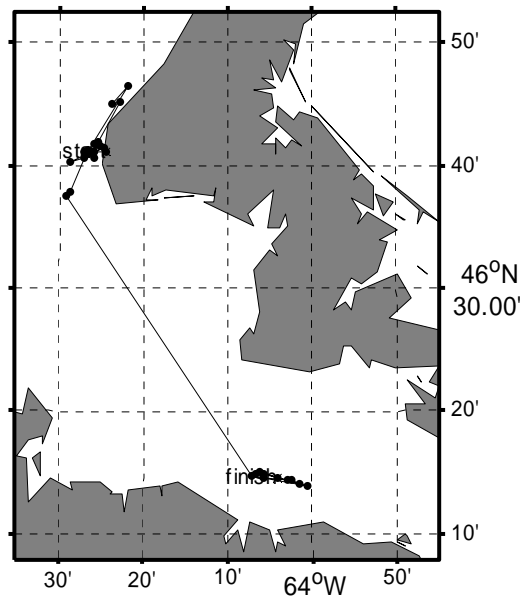


Figure 2 Track of beacon 02754 from Argos message header position information. The long straight line indicates the gap in the time series for the positions (see Figure 7).

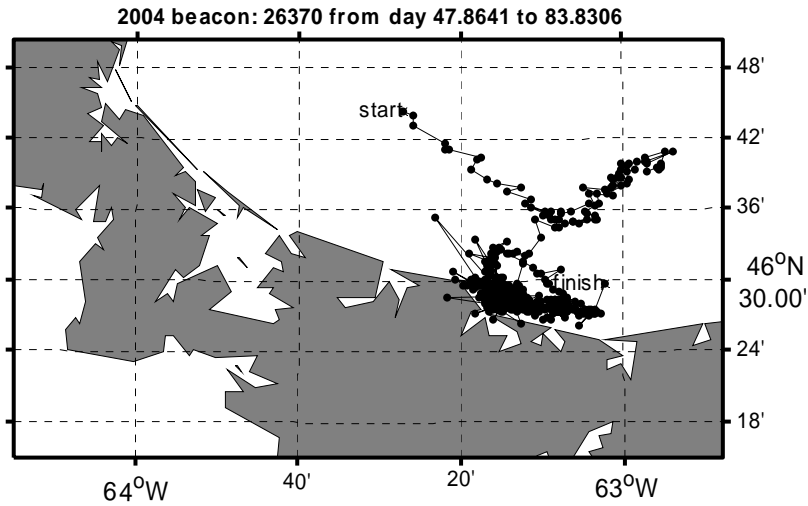


Figure 3 Track of beacon 26370 from Argos message header position information.

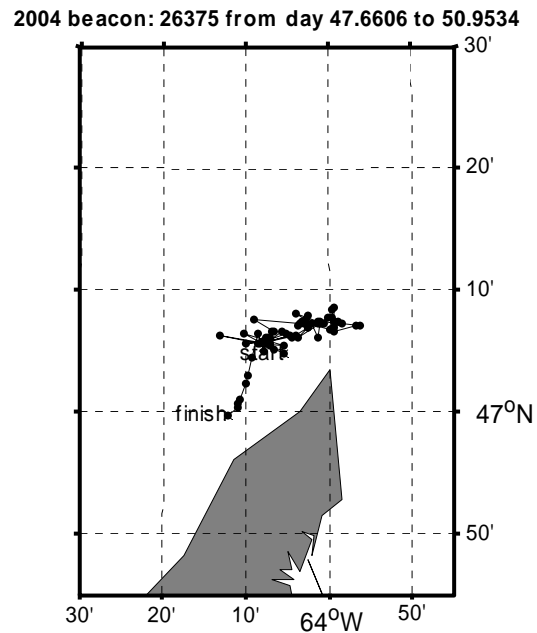


Figure 4 Track of beacon 26375 from Argos message header position information

Despite the short time that data were available for beacon 26375, the relationship of the ice drift to wind was investigated and provided insight on the effect of coastal boundaries on pack ice drift.

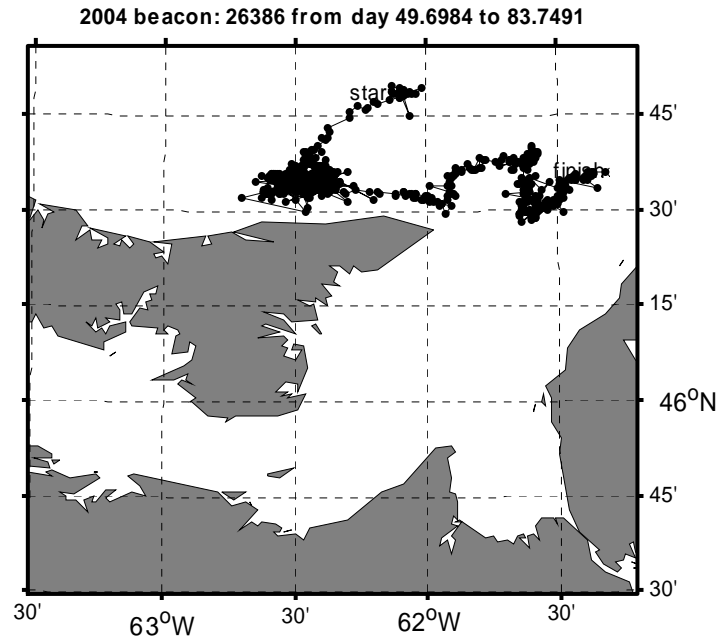


Figure 5 Track of beacon 26386 from Argos message header position information

Hourly ice drift was computed in m/s from the spherical earth distance between two successive points in the hourly beacon latitude and longitude records.

Beacon position data used in analyses are plotted as time series in Figure 6 to Figure 10. Figure 8 and Figure 10 show times when the beacons 26370 and 26386 were not moving due to being jammed against the coast. Each time series shows clearly when the severe northeasterly storm occurred (calendar day 50.5). What can also be seen from the time series figures is the presence of a strong tidal signal in some of the records: Figure 6 especially; Figure 7 a little; Figure 8 after day 65 but weakly; and Figure 10 day 56 weakly and after day 65 weakly.

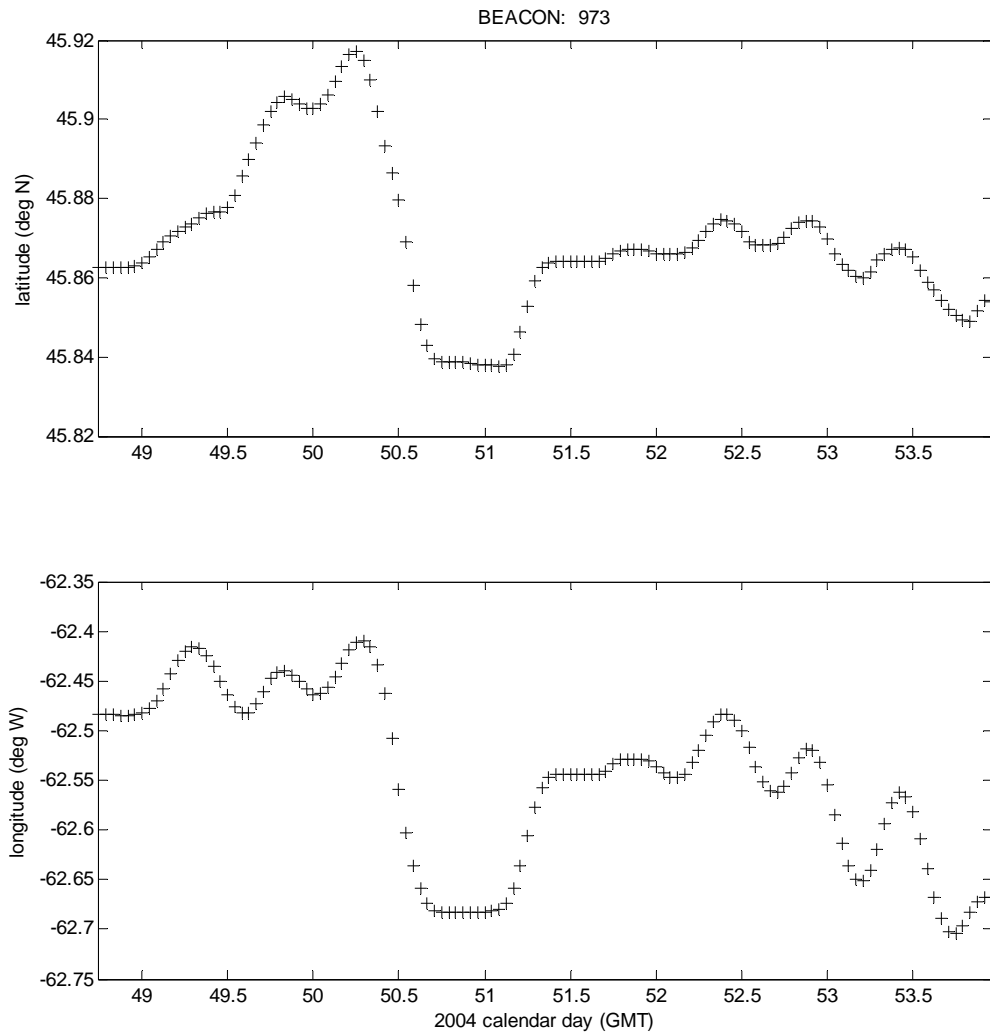


Figure 6 Latitude and longitude for beacon 00973

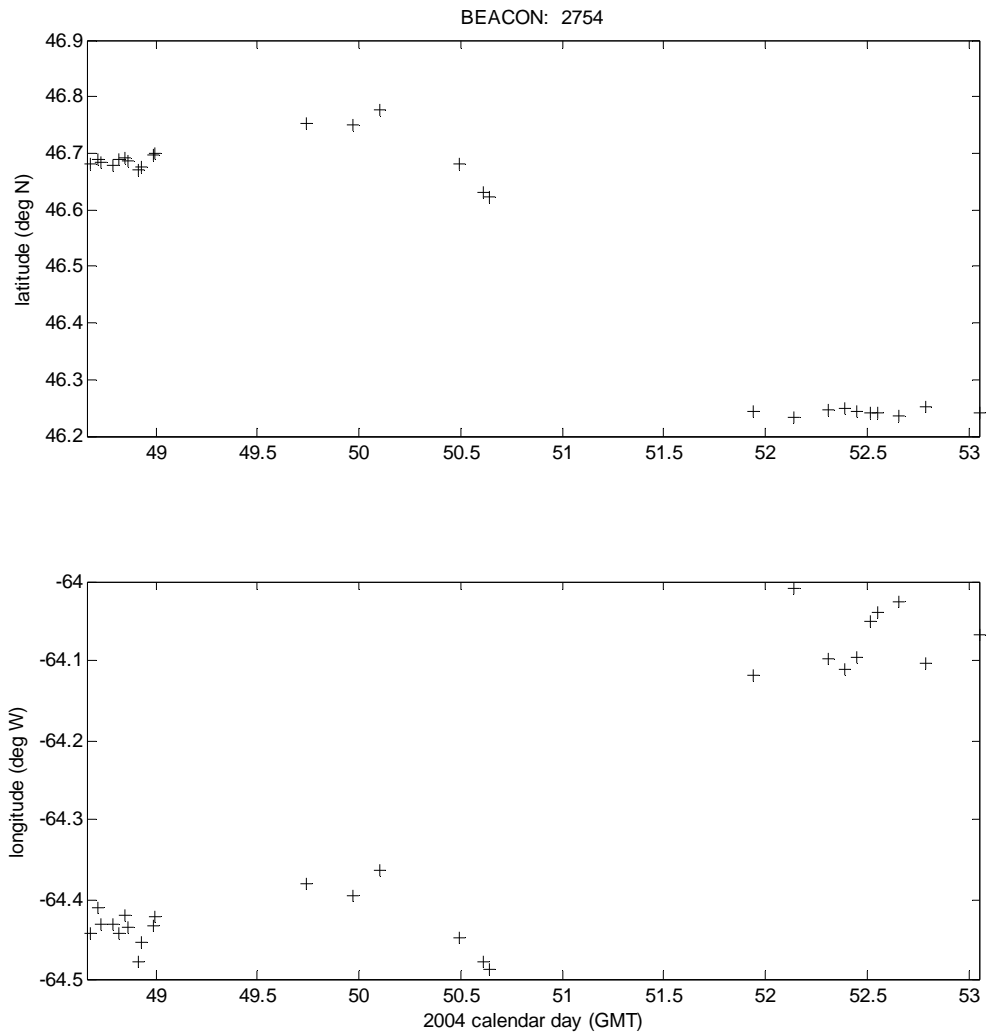


Figure 7 Latitude and longitude for beacon 02754

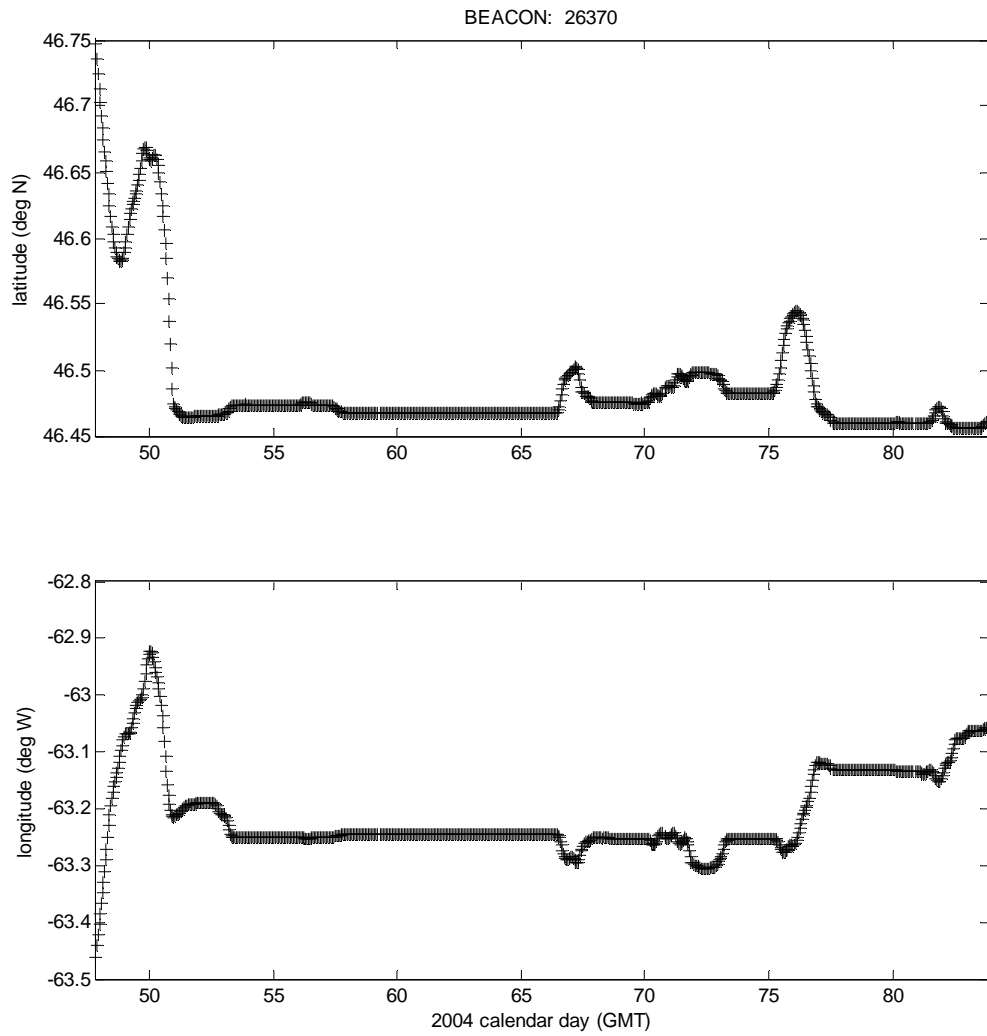


Figure 8 Latitude and longitude for beacon 26370

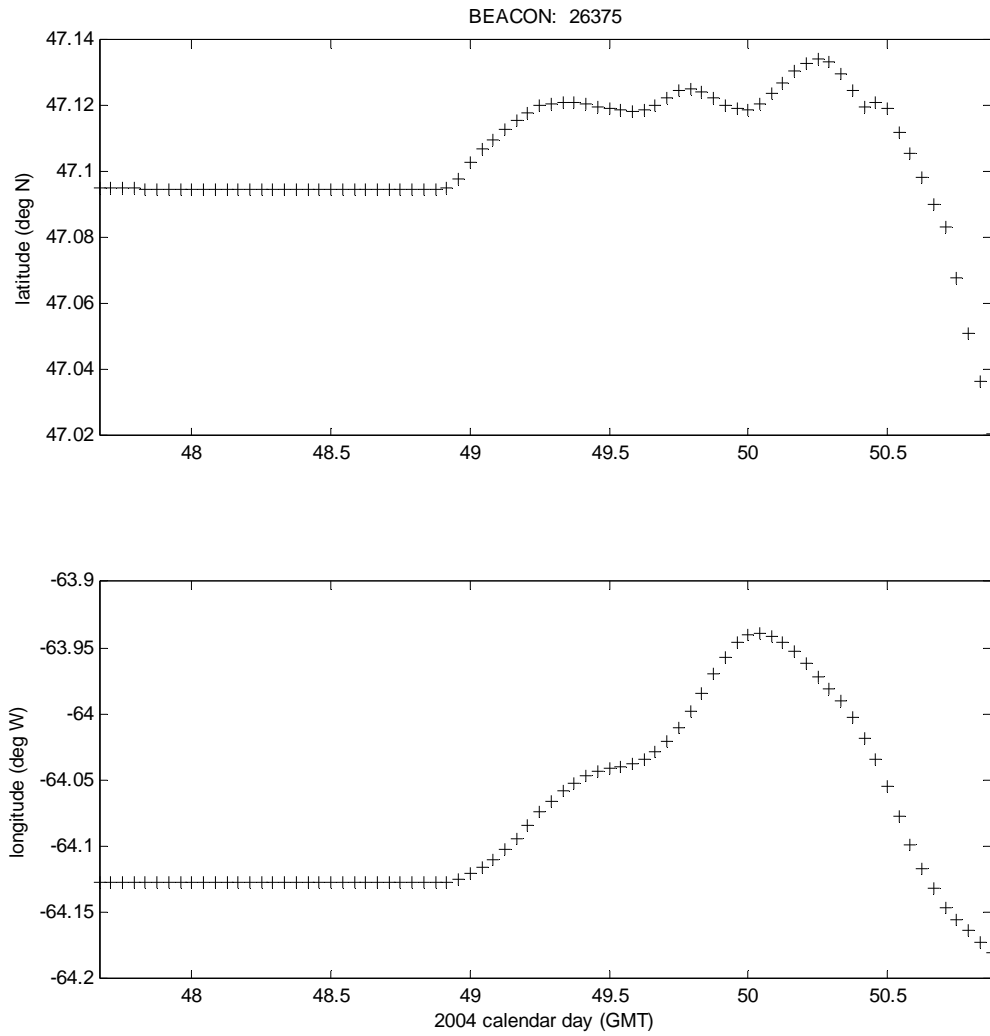


Figure 9 Latitude and longitude for beacon 26375

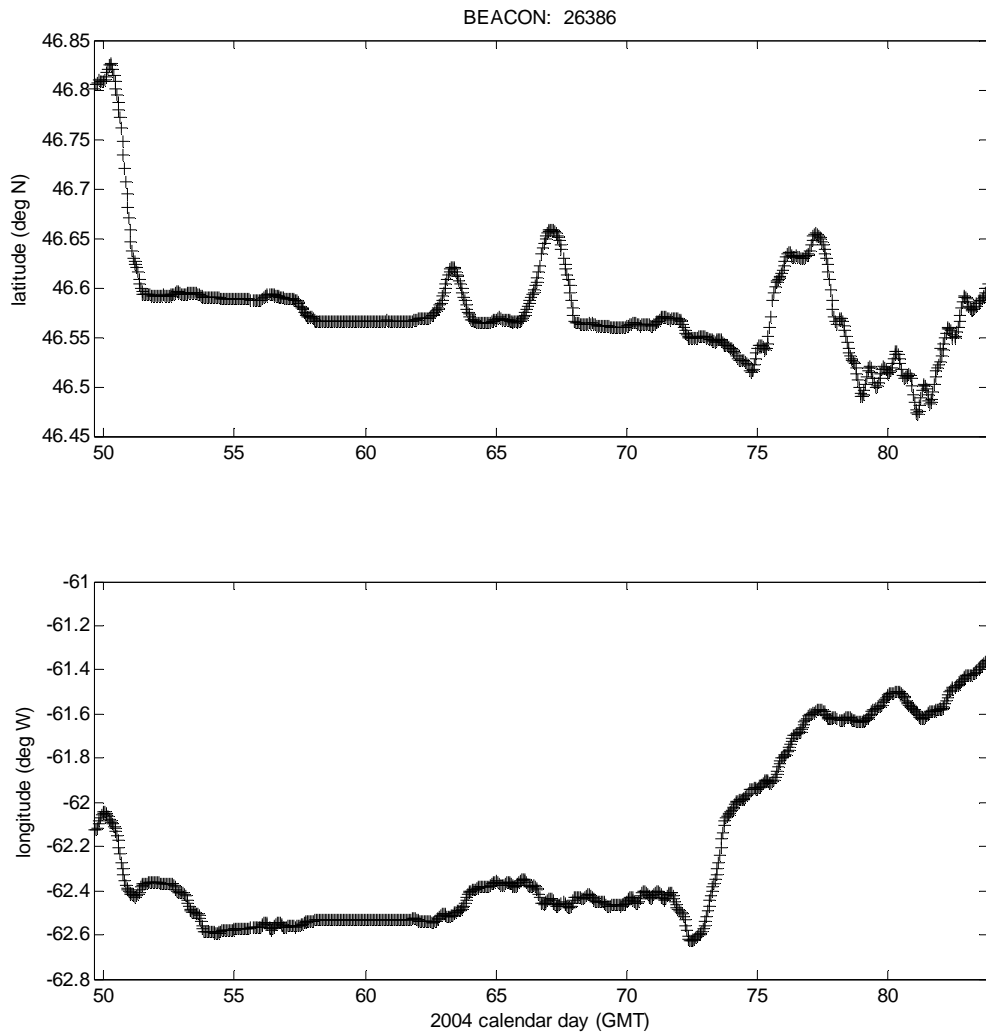


Figure 10 Latitude and longitude for beacon 26386

3.2 Meteorological data

The Bedford Institute of Oceanography archives the 6-hourly CMC atmospheric data from a low-resolution regional prognostic numerical model. It is 48-hour forecast data on a 1 deg x 1 deg grid (defined from (20N, 80W) to (70N, 30W)). Archived data includes wind U, wind V (both in knots, converted to m/s, at assumed 10 m), sea level pressure (at surface), and surface air temperature (assumed at 2 m). Greenan and Prinsenberg (1998) indicated that forecast winds from the Regional Finite Element model overestimated the magnitude of winds measured by anemometers mounted on ice beacons by 10-40%. Since the Greenan and Prinsenberg report was published, however, the regional model was changed. To check the validity of using the new regional model output wind for this analysis the output was compared to measured wind from three land stations and two wave buoys in the southern Gulf (Appendix A). The 6-hourly forecast wind components and scalar quantities were found to correlate with $r \sim 0.9$ in all cases.

The 6-hourly meteorological forecast data were matched temporally to beacon positions at 6-hour intervals. Then bilinear interpolation was used to find the wind data at the each of these beacon positions using the 4 grid points surrounding the beacon at that 6-hour mark. Since beacon 02754 had an irregular time series, its positions were first interpolated to be 6-hourly. Similar bilinear interpolations were performed for analyses in Greenan et al. (1997).

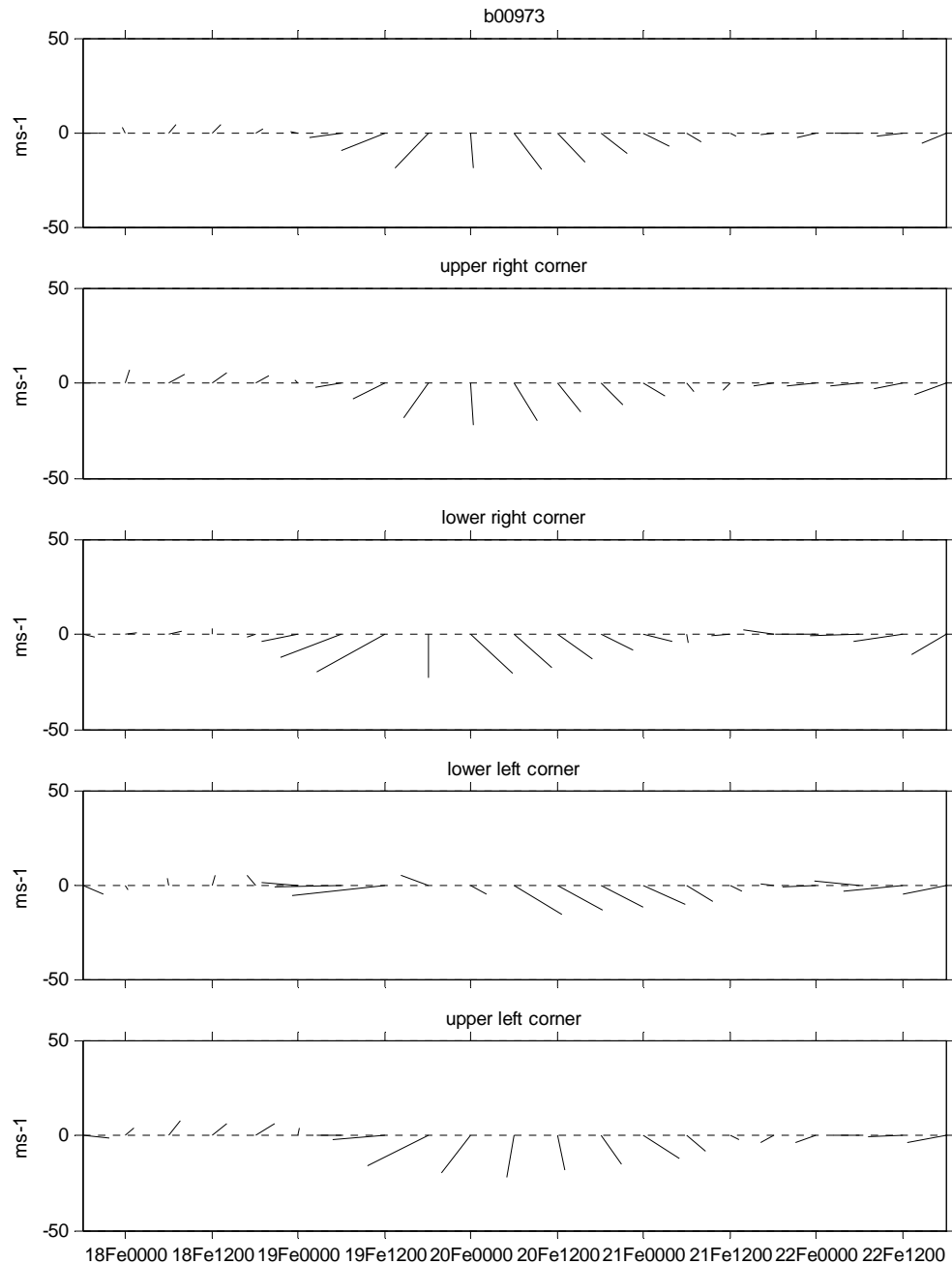


Figure 11 6-hourly forecast wind for beacon 00973 and the wind at the 4 gridpoints surrounding the beacon that were used for bilinear interpolation; 17 Feb to 22 Feb

To check the interpolation, wind data from the 4 nearest model grid points surrounding the beacon position were extracted and plotted as time series with the interpolated beacon wind data. These graphs are presented for beacons 02754, 00973, 26375, 26370, and 26386 (Figure 11 to Figure 15). For the most part the data from the 4 corners of the interpolating square reveal similar features and magnitude. In particular we note that the major winter storm that began on 19 February is forecast clearly in all cases.

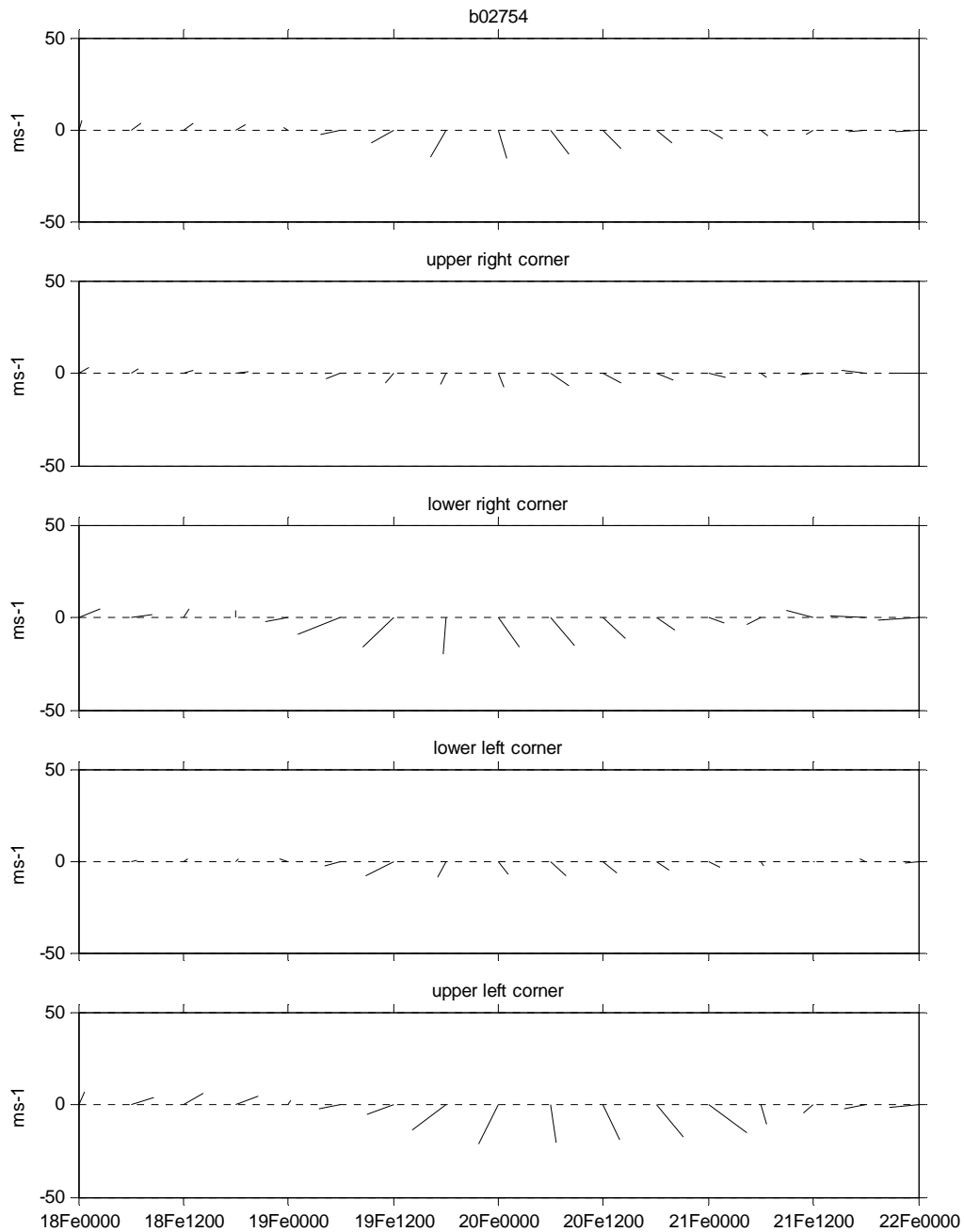


Figure 12 6-hourly forecast wind for beacon 02754 and the wind at the 4 gridpoints surrounding the beacon that were used for bilinear interpolation; 17 Feb to 22 Feb

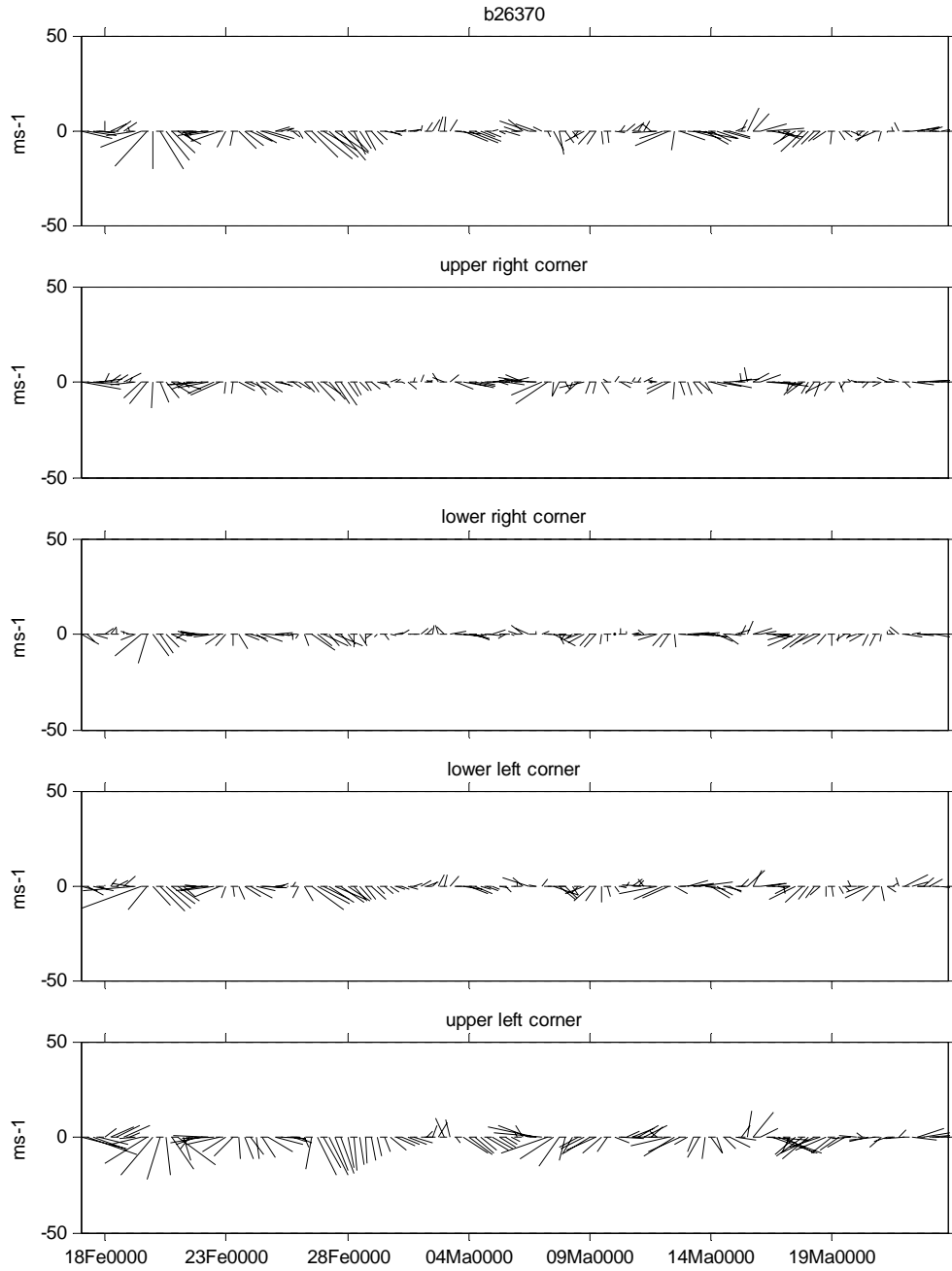


Figure 13 6-hourly forecast wind for beacon 26370 and the wind at the 4 gridpoints surrounding the beacon that were used for bilinear interpolation; 18 Feb to 25 Mar

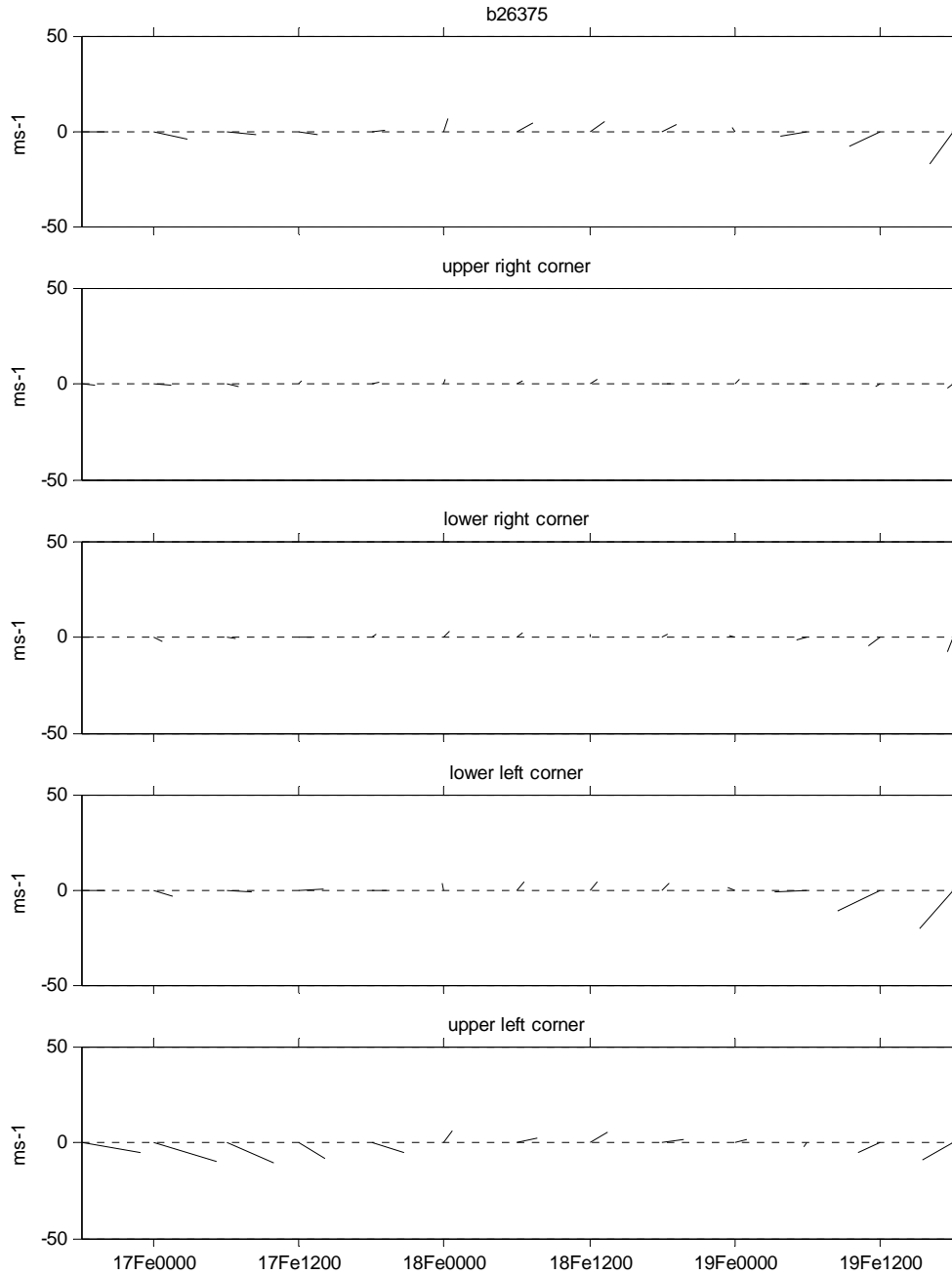


Figure 14 6-hourly forecast wind for beacon 26375 and the wind at the 4 gridpoints surrounding the beacon that were used for bilinear interpolation; 16 Feb to 22 Feb

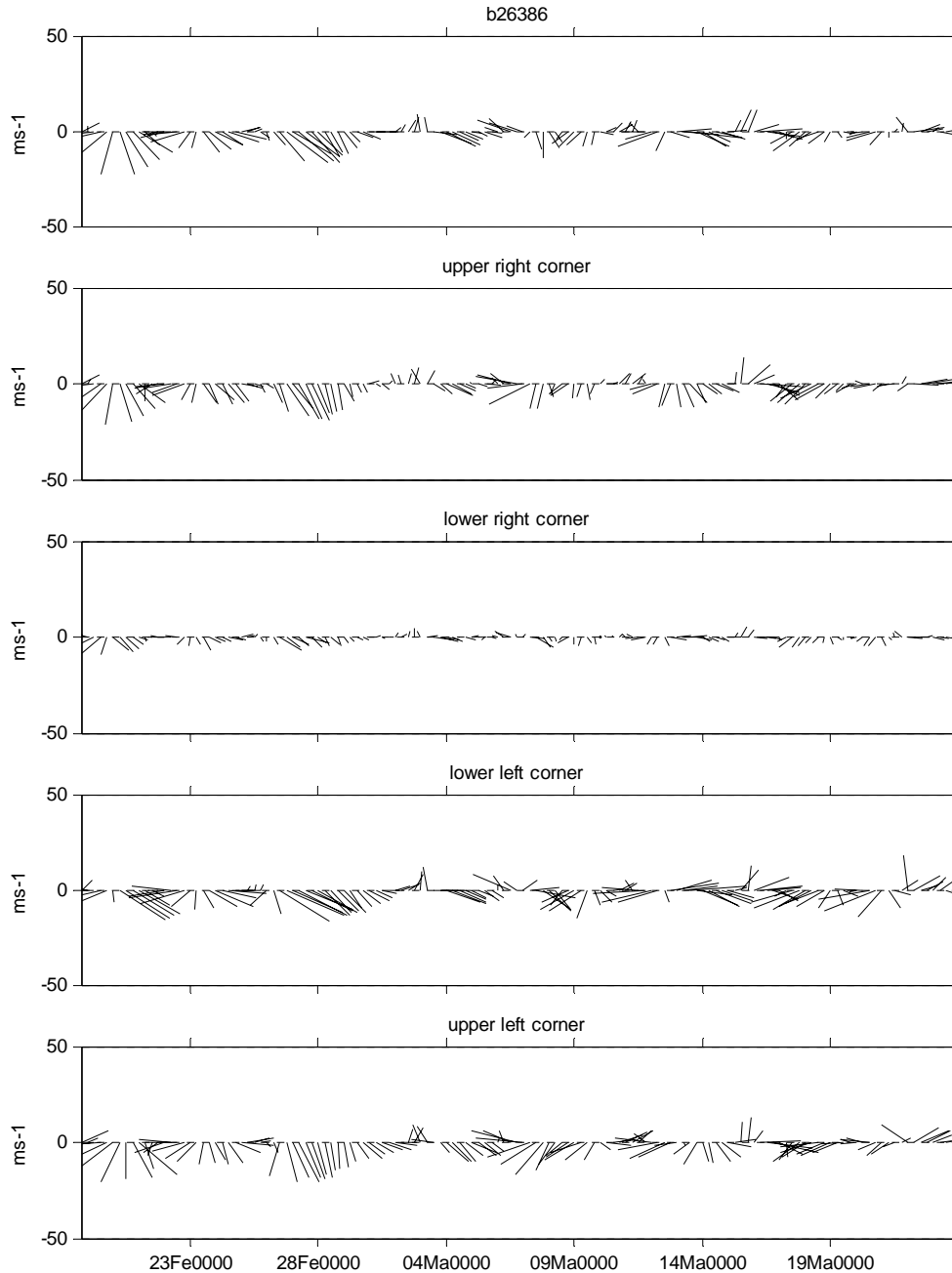


Figure 15 6-hourly forecast wind for beacon 26386 and the wind at the 4 gridpoints surrounding the beacon that were used for bilinear interpolation; 18 Feb to 25 Mar

3.3 Least squares regression

Hourly ice drift was computed for beacons 00973, 26370, 26375, and 26386. Six-hourly ice drift was computed for beacon 02754 since the position data were less frequent. Wind data were interpolated to be hourly for those beacons with hourly position data. Ice drift and wind data are shown in Figure 16 to Figure 20. Note again the strong tidal signal in the drift records in Figure 16, Figure 18, and Figure 20.

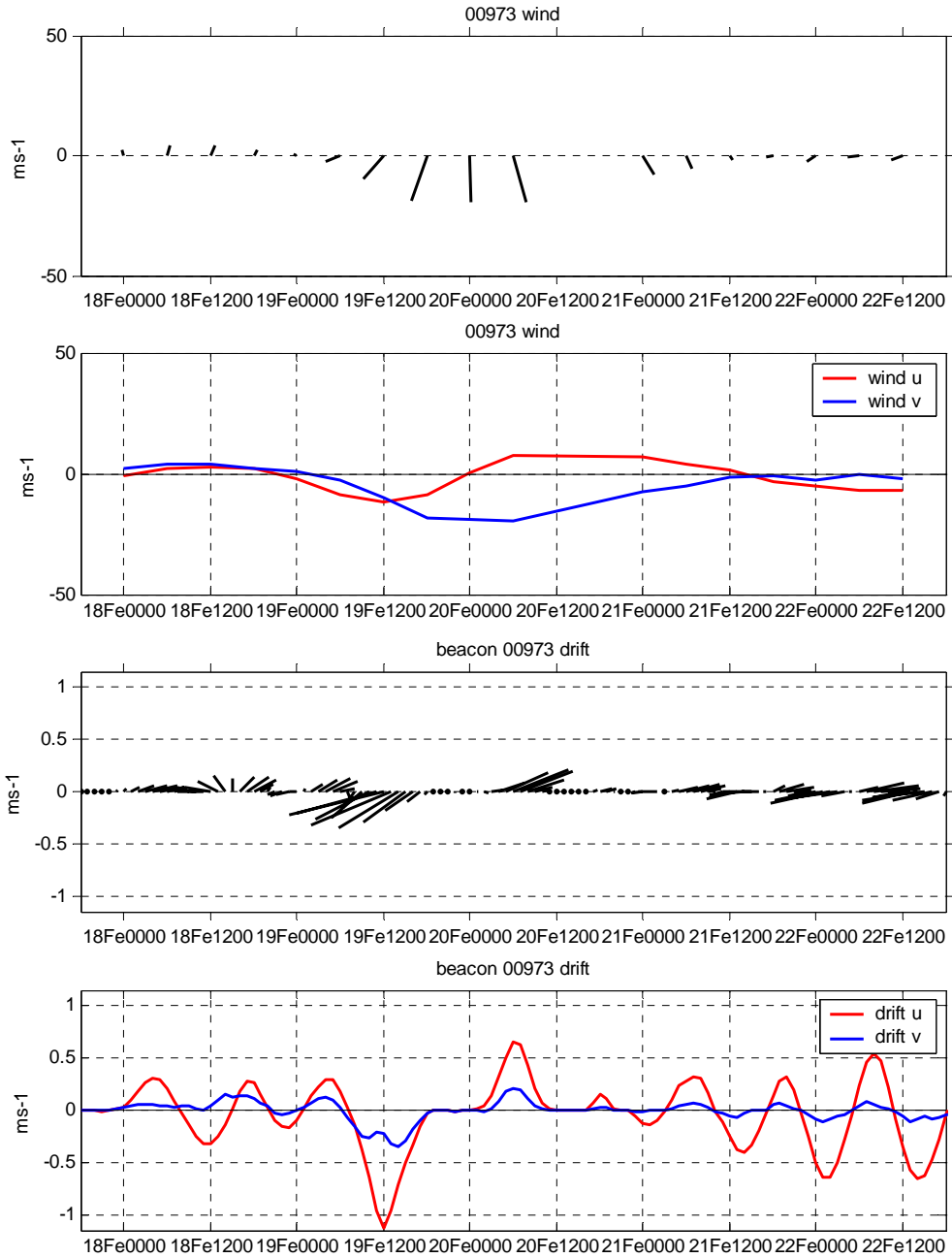


Figure 16 Hourly ice drift and 6-hourly wind data for beacon 00973

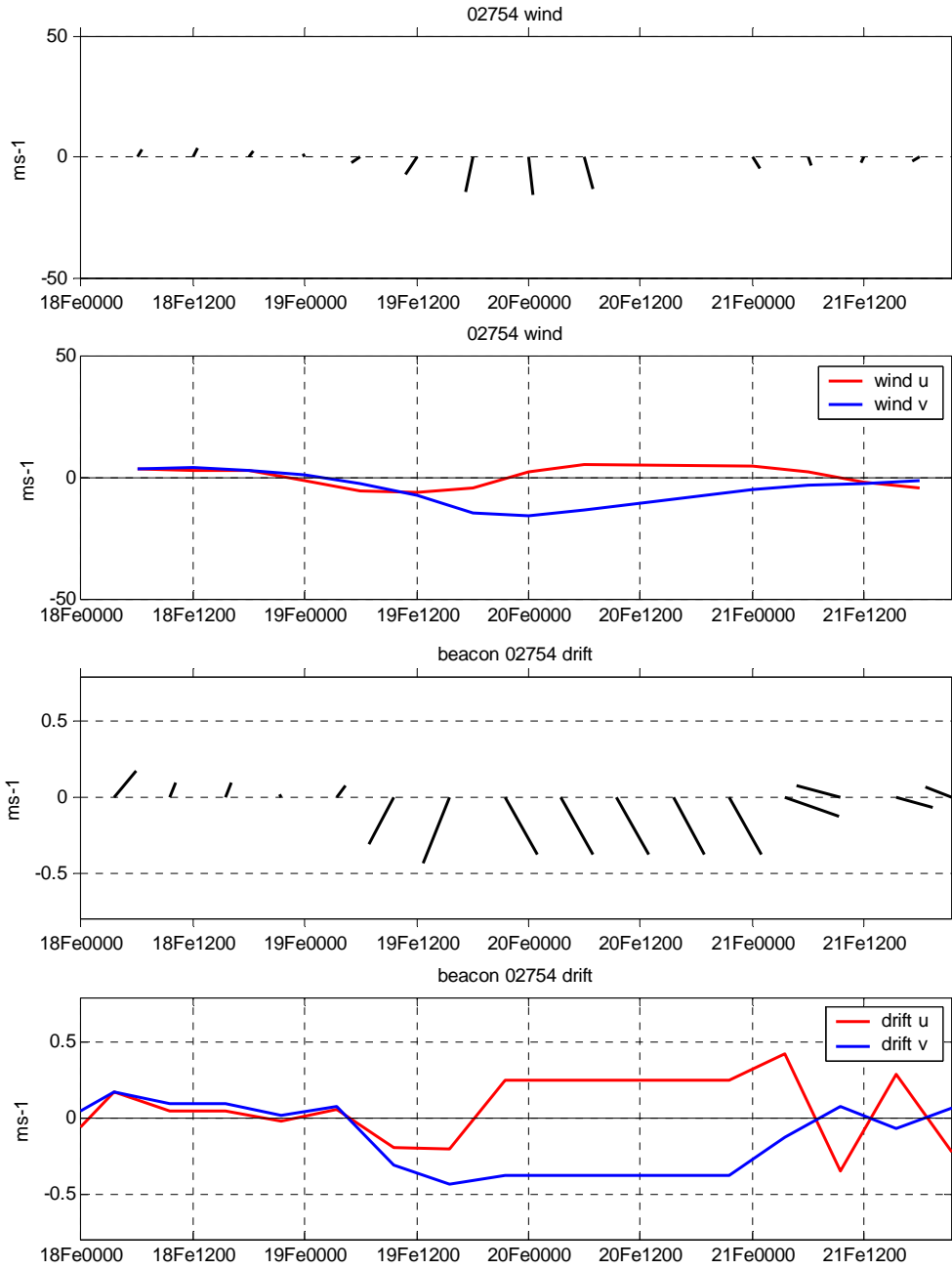


Figure 17 6-hourly ice drift and 6-hourly wind data for beacon 02754

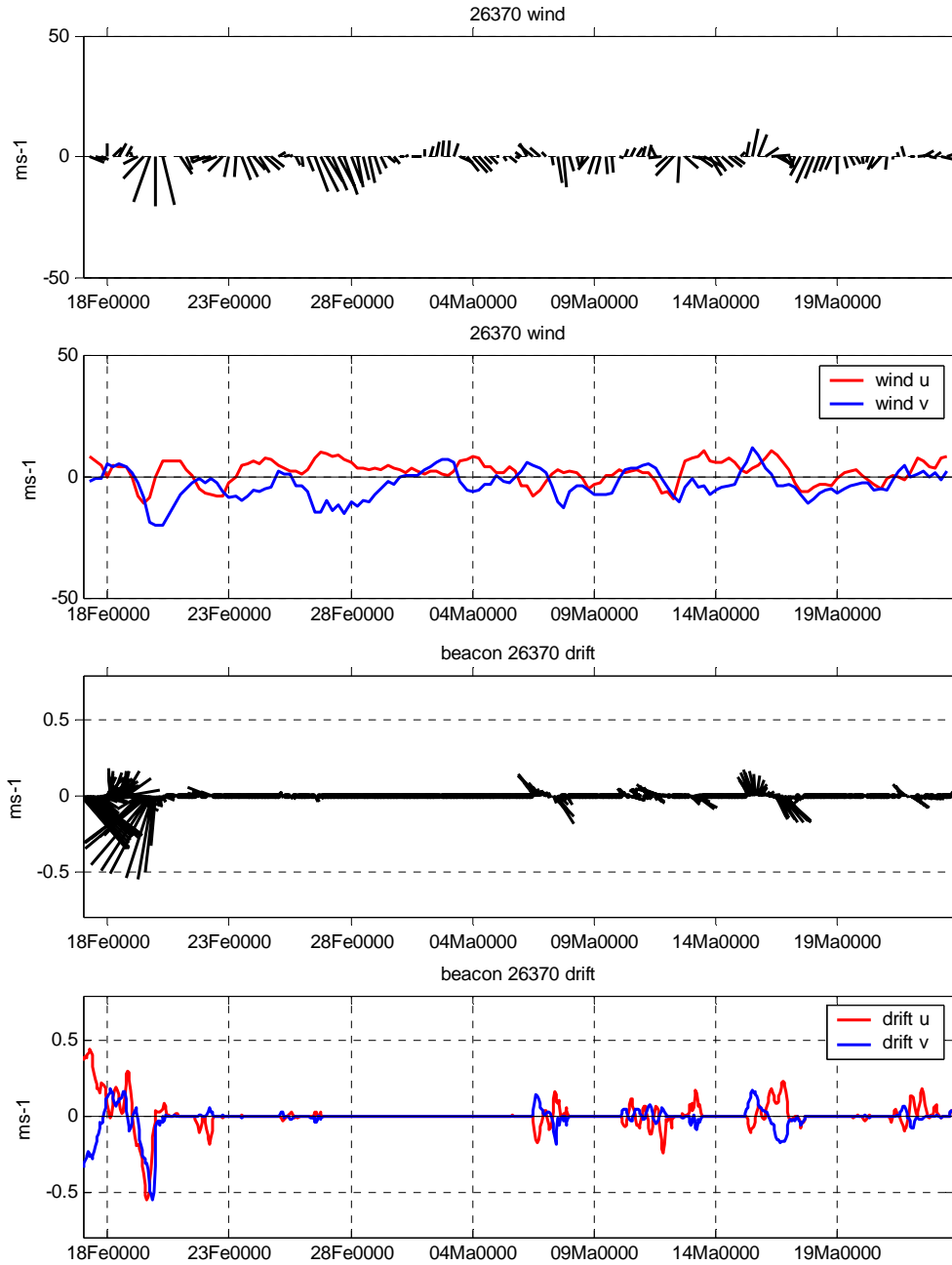


Figure 18 Hourly ice drift and 6-hourly wind data for beacon 26370

Figure 18 shows that when the wind was very strong northeasterly on February 20th beacon 26370 moved directly to shore and into the pack ice after which it barely moved for 3 weeks.

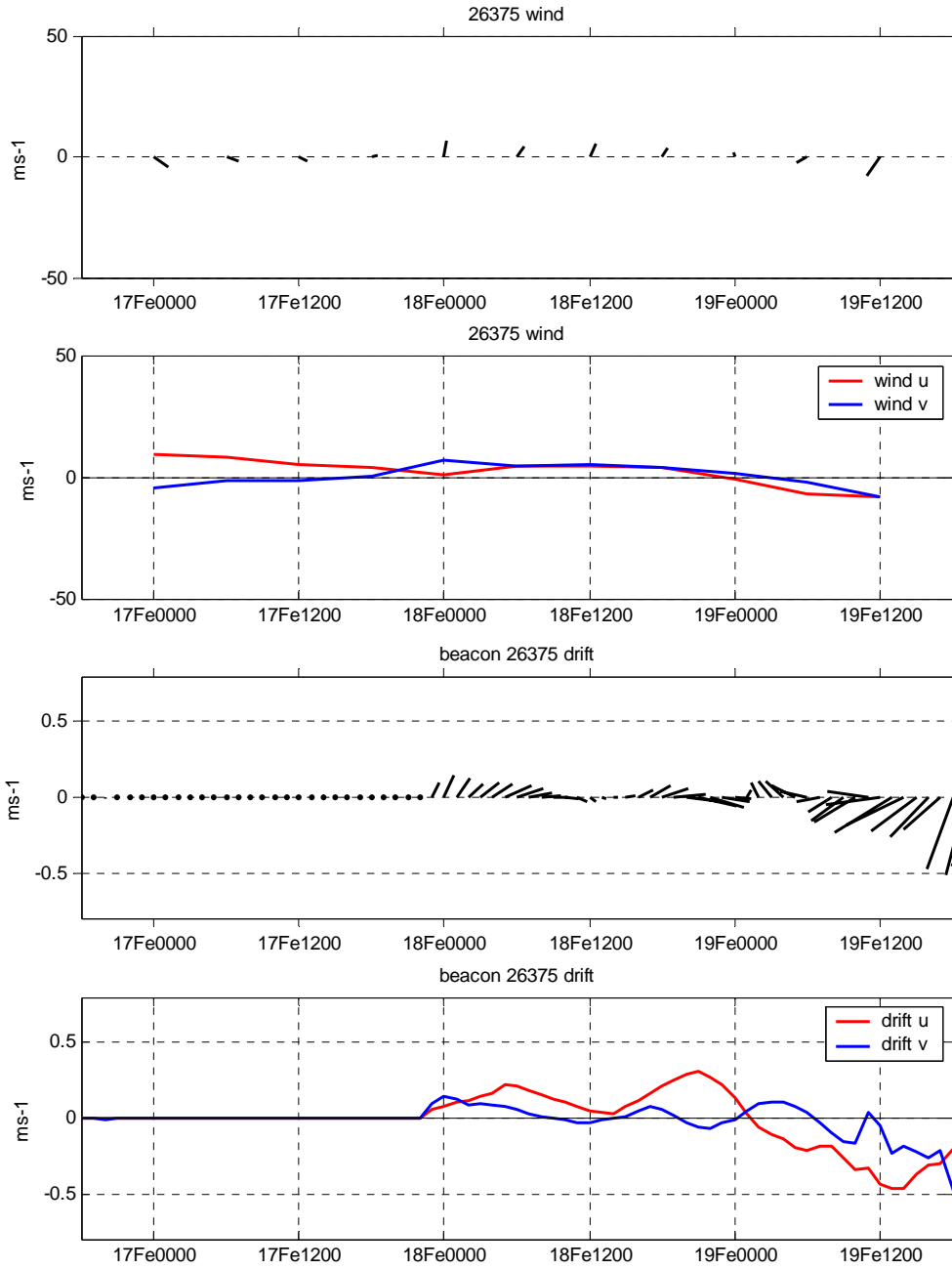


Figure 19 Hourly ice drift and 6-hourly wind data for beacon 26375

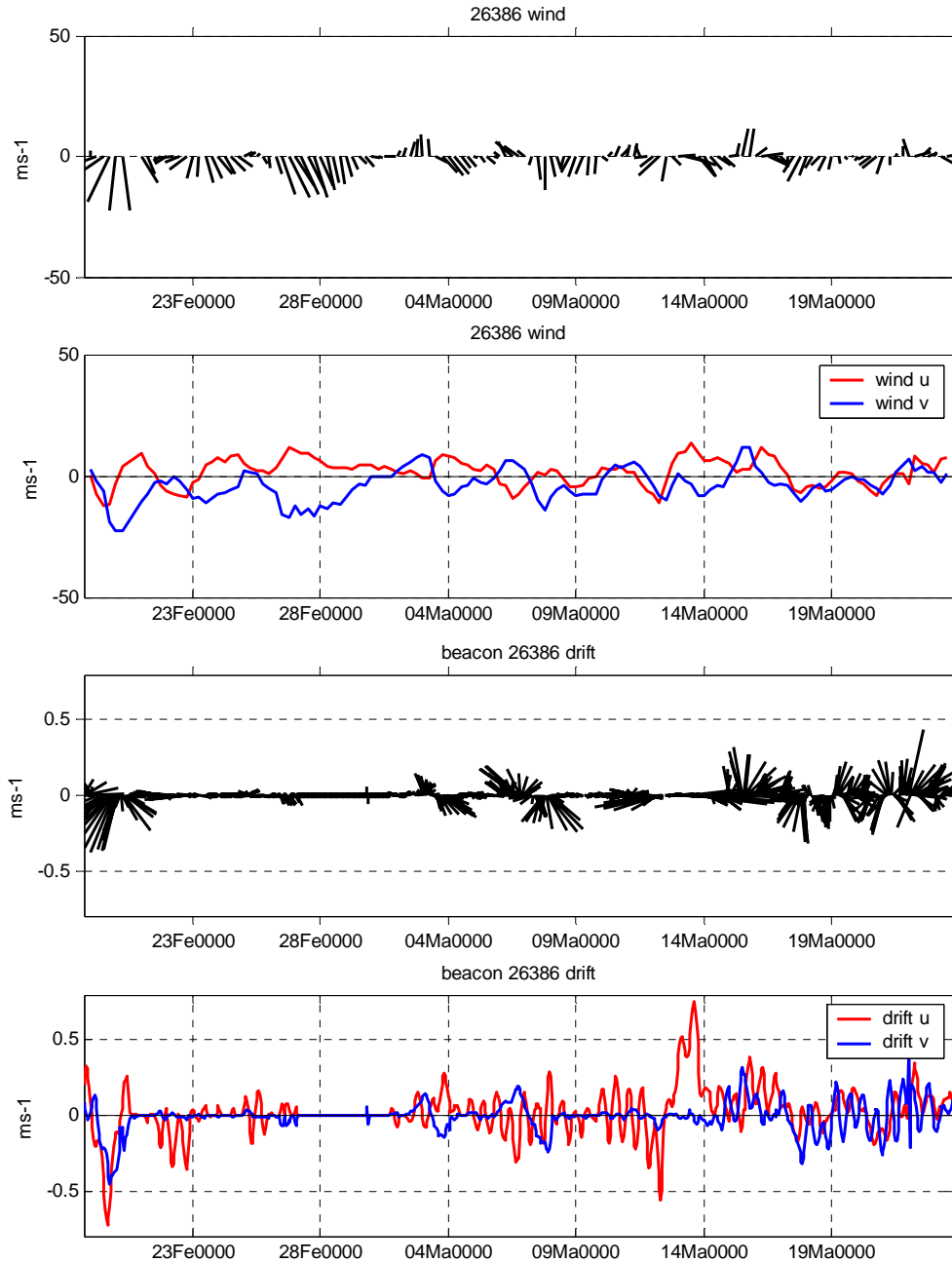


Figure 20 Hourly ice drift and 6-hourly wind data for beacon 26386

Beacon 26386 seemed to have survived the February 20th storm but did not completely break from the landfast ice along the north coast of Prince Edward Island until the beginning of March. There was a bit of east/west movement around February 25 when the wind was calm and after another nor'easter began at that time.

The relationship between ice drift vectors and wind vector data was investigated using a complex least squares regression defined by the following expression:

$$Y = XAe^{i\theta} + \varepsilon$$

Y and X are the ice drift vectors and wind vectors respectively. A is defined physically as the scaling factor, gain, or response of the drift to the wind. Mathematically it is the slope of the best-fit line. θ is the turning angle between the vectors measured clockwise; that is, the mean angle that ice drift would bear to the right of the wind. ε is the residual of the fit. The ice drift vectors and wind vectors were expressed as complex values: $a + ib$. Horizontal components are the real part of the complex value and vertical vector components are the imaginary part. X is a matrix consisting of a column of ones and a column of wind velocities. This configuration provides an offset for the predicted drifts which represents the mean drift of the system (i.e. a y-intercept). The result of the regression produces two complex coefficients: one whose magnitude represents the mean drift (y-intercept) velocity; the other whose magnitude represents the gain and whose angle represents the turning angle.

3.4 Results

Results of the least squares fits are shown in Figure 21 to Figure 38. The figures include time series plots of the modeled wind and observed ice drift vectors as well as predicted ice drift series due to wind forcing. The time series of the angles between the wind and drift vectors and the ratio of wind speed to ice drift are also shown. Scatter plots of wind speed vs. drift speed are also presented. Analysis was performed for the entire series for all beacons. For the two longer time series of beacons 26370 and 26386, the analysis was performed to check the influence of the storm by looking at the time before the storm and after it had passed (i.e. Feb. 20) and after Mar. 4 when it was thought that both beacons were moving freely again. Also, for those 2 beacons, data were lagged by 3 and 6 hours for the time before Feb. 20 to see if this improved results (scatter plots are not shown for lagged analysis). Note that hourly data were used for all beacons except for beacon 02754 where 6-hourly data were used.

Statistics of the least squares fit are given in Table 4. For free ice drifts, van der Baaren and Prinsenberg (2000) found that for beacon data from 1995 to 1998 from the Gulf of St. Lawrence and Labrador Shelf, the gain was about 2%. In that program, anemometers mounted on ice beacons provided observed wind data. In this analysis using forecast winds, the gain was similar (between 1% and 3%) except for beacon 26370 where it was only 0.66%. Beacon 26370 spent most of the time pressed against the north shore coastline so this result is not surprising. In the 2000 report turning angles were found to be 14° and the wind accounted for 38% of the variance.

In this study, the turning angles varied greatly from -6° for 26386 to -31° for 26375 for complete records. Note that beacons 00973 and 26375, deployed in Northumberland Strait (east) and off the NW tip of Prince Edward Island, respectively, the largest turning angles of 23° and -31° for their entire records. Before Feb. 20, the turning angle magnitudes for 26370 and 26386 were -15° and -22° , but, after Mar. 4, the turning angles for 26370 and 26386 were -5° and -2° , respectively. Figure 18 and Figure 20 show that despite the wind, after Mar. 4, beacon 26370 was mostly trying to move southeasterly whereas beacon 26386 seemed to respond to the wind more with drift and wind vectors pointing in similar directions. Lagging the data did not change the turning angles

substantially except for 26386 with 6 hours lag for data before Feb. 20; angle decreased from -22° to 16° .

R^2 values were greatest for 02754, 26375, 26370, and 26386 before the storm of Feb. 20 (0.56 to 0.88). The mean gain of the four was 2.8%. The value of beacon 00973 was excluded; its drift was affected greatly by tidal currents in addition to wind forcing. Results after Feb. 20 are biased due to restrictions imposed by the coast/landfast ice. Comparing R^2 values for 26370 and 26386 for after Feb. 20 (influence of storm), there is improvement when only times of “free float” were used after Mar. 4: R^2 goes from 0.13 to 0.21 for 26370 and from 0.28 to 0.42 for 26386. For the beacons in Northumberland Strait, 00973 looked to be more influenced by tides than wind (Figure 6 and Figure 16) with a small gain of 1.15% and R^2 of 0.12. Mean drift speed for beacons 00973, 26370, and 26386 before the storm was 8, 6, and 6 cm/s. 00973 traveled in a mean SE direction while 26370 and 26386 both traveled northeastward. This is confirmed from drift tracks shown in Figure 1, Figure 3, and Figure 5. After Mar. 4, beacons 26370 and 26386 slowed to 1 and 5 cm/s, respectively.

Lagging data for 26370 and 26386 for the short time before Feb. 20 did not seem to improve regression results.

Table 4 Regression results for least squares fit of wind to drift; data were hourly except for beacon 02754. $R^2 > 50\%$ and Gain $\geq 1.9\%$ are in bold.

Beacon	R^2	Turning angle (deg)	Gain (%)	Mean drift speed (m/s)	# points
<i>Entire data record</i>					
00973	0.12	23.46	1.15	0.08	120
02754	0.86	10.36	2.91	0.05	18 (6-hrly)
26370	0.19	-9.97	0.66	0.02	858
26375	0.56	-30.74	1.97	0.04	72
26386	0.32	-5.82	1.24	0.04	816
<i>Storm influence</i>					
26370 before Feb. 20	0.88	-14.91	3.26	0.06	72
26386 before Feb. 20	0.87	-22.37	3.07	0.06	30
26370 after Feb. 20	0.13	-2.52	0.29	0.01	786
26386 after Feb. 20	0.28	-4.84	1.05	0.04	786
26370 after Mar. 4	0.21	-4.93	0.49	0.01	474
26386 after Mar. 4	0.42	-2.36	1.69	0.05	474
<i>Lagging data</i>					
26370 lag = 3 hrs before Feb. 20	0.87	-4.14	3.43	0.05	69
26370 lag = 6 hrs before Feb. 20	0.78	5.59	3.54	0.07	66
26386 lag = 3 hrs before Feb. 20	0.84	-5.04	2.91	0.07	27
26386 lag = 6 hrs before Feb. 20	0.87	16.27	2.86	0.19	24

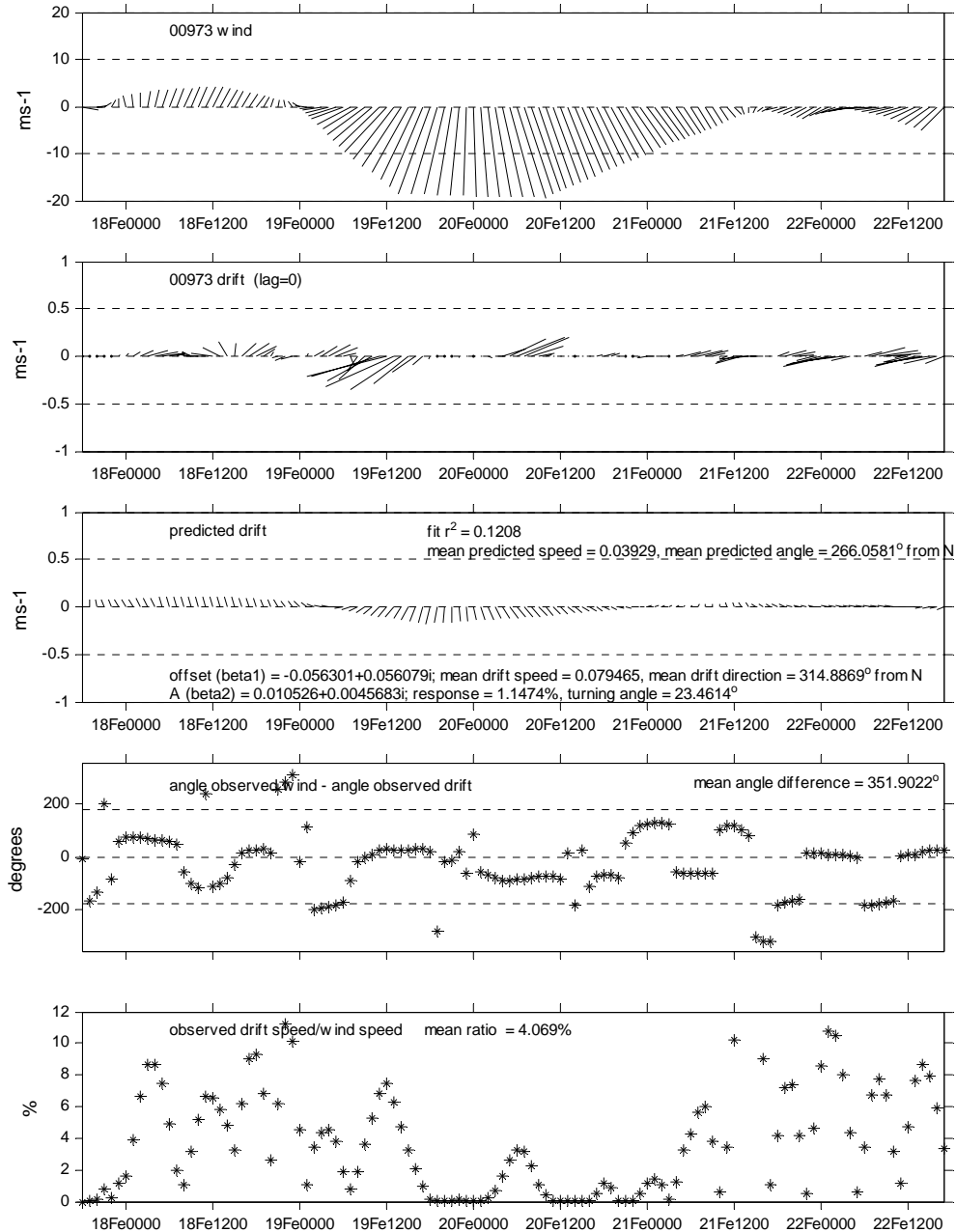


Figure 21 Results of complex least squares regression of wind and drift data for beacon 00973. The figure shows hourly wind and beacon drift, the predicted drift values (ie. fitted series), the angle difference between wind vectors and drift vectors (with mean angle difference), and the ratio of drift speed to wind speed (with mean ratio).

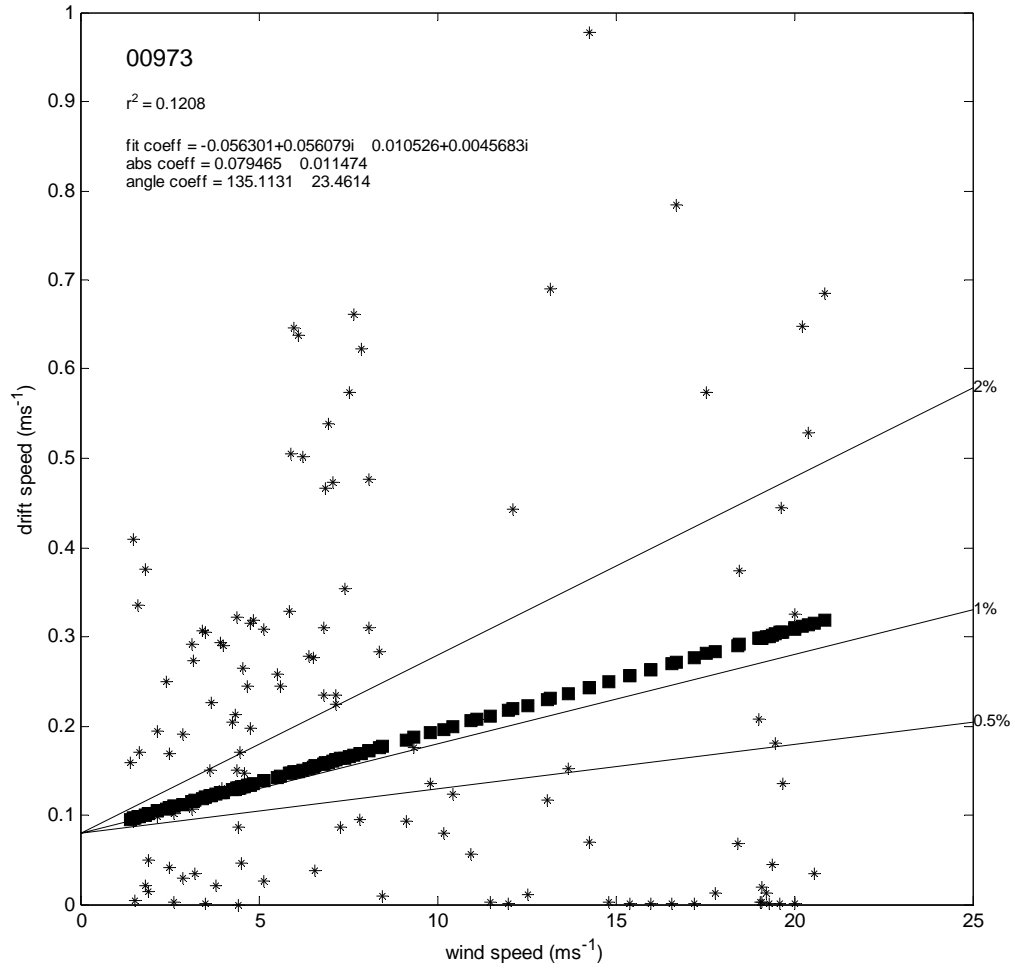


Figure 22 Scatter of hourly drift speed vs. wind speed for beacon 00973. Lines for various reponse are also shown. Squares indicate the predicted relationship from regression.

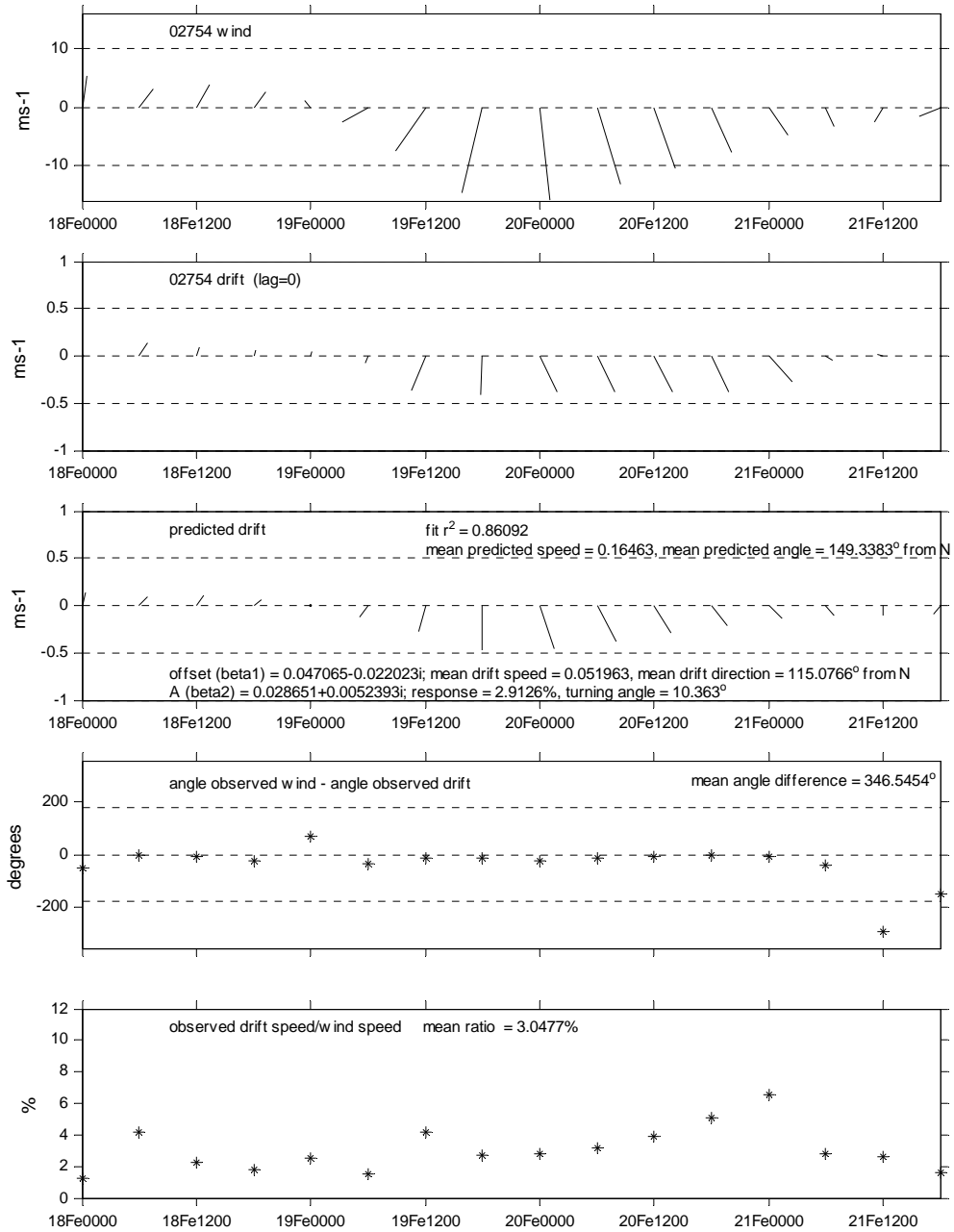


Figure 23 Results of complex least squares regression of wind and drift data for beacon 02754. The figure shows 6-hourly wind and beacon drift, the predicted drift values (ie. fitted series), the angle difference between wind vectors and drift vectors (with mean angle difference), and the ratio of drift speed to wind speed (with mean ratio).

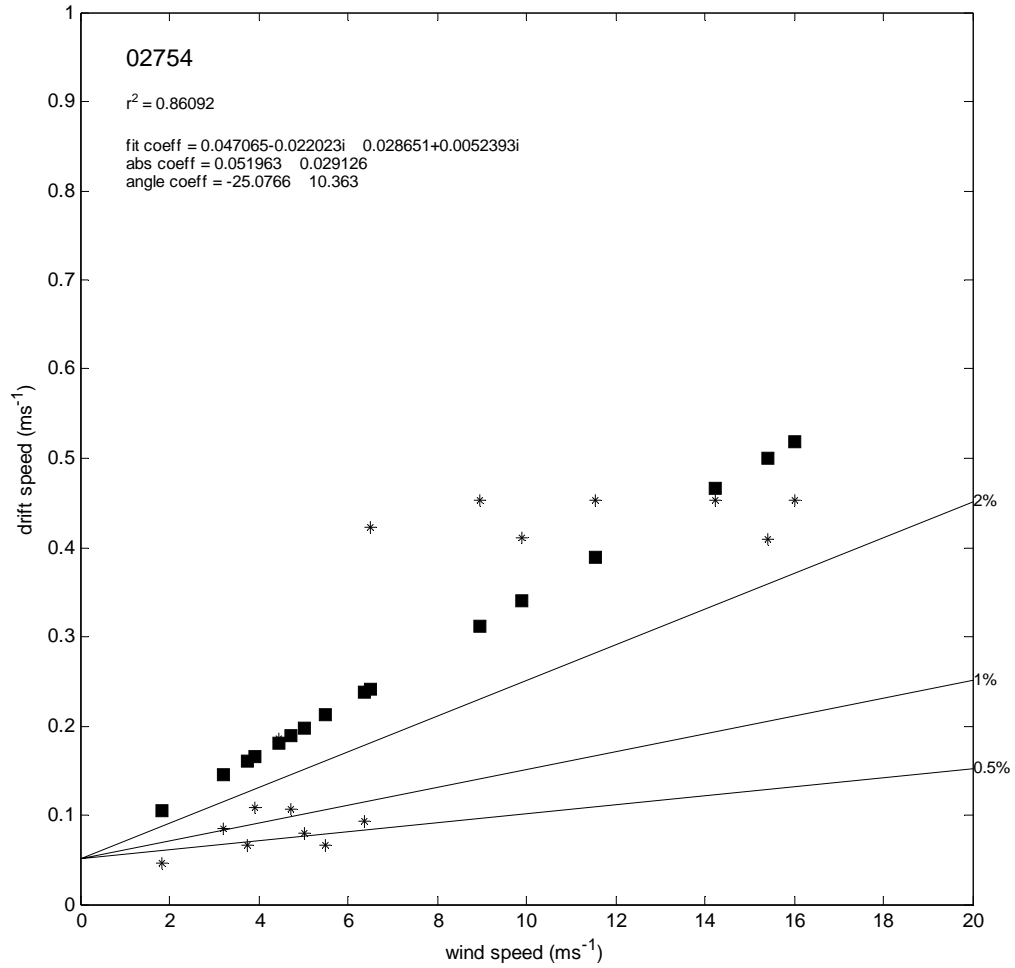


Figure 24 Scatter of 6-hourly drift speed vs. wind speed for beacon 02754. Lines for various response are also shown. Squares indicate the predicted relationship from regression.

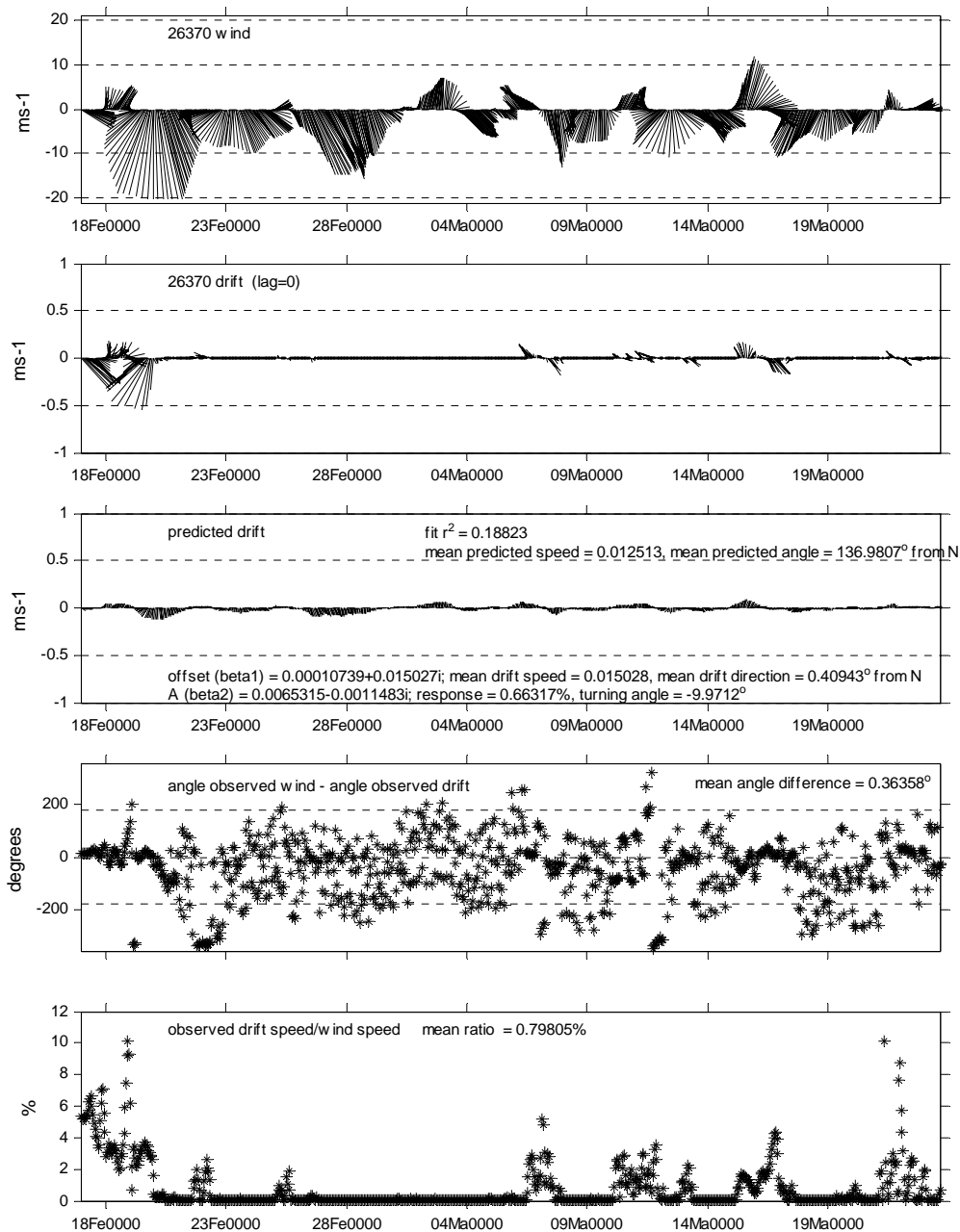


Figure 25 Results of complex least squares regression of wind and drift data for beacon 26370. The figure shows hourly wind and beacon drift, the predicted drift values (ie. fitted series), the angle difference between wind vectors and drift vectors (with mean angle difference), and the ratio of drift speed to wind speed (with mean ratio).

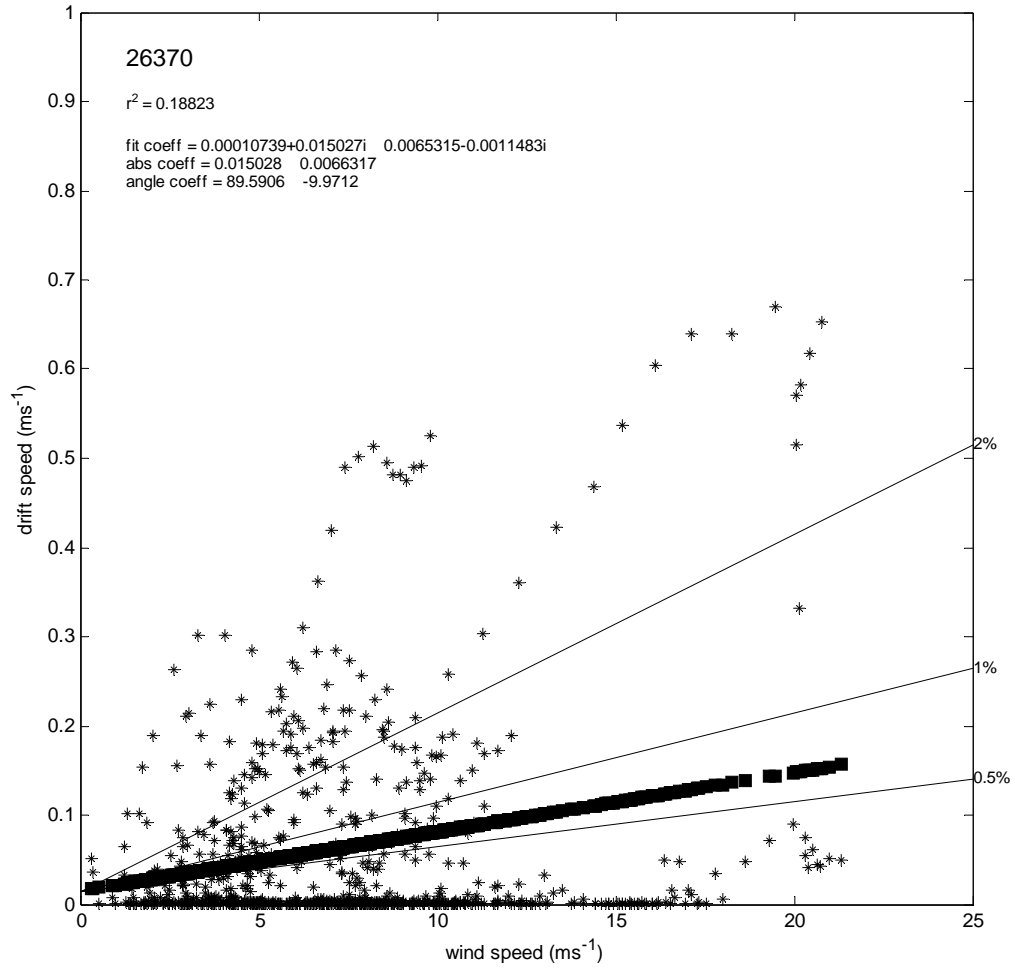


Figure 26 Scatter of hourly drift speed vs. wind speed for beacon 26370. Lines for various response are also shown. Squares indicate the predicted relationship from regression.

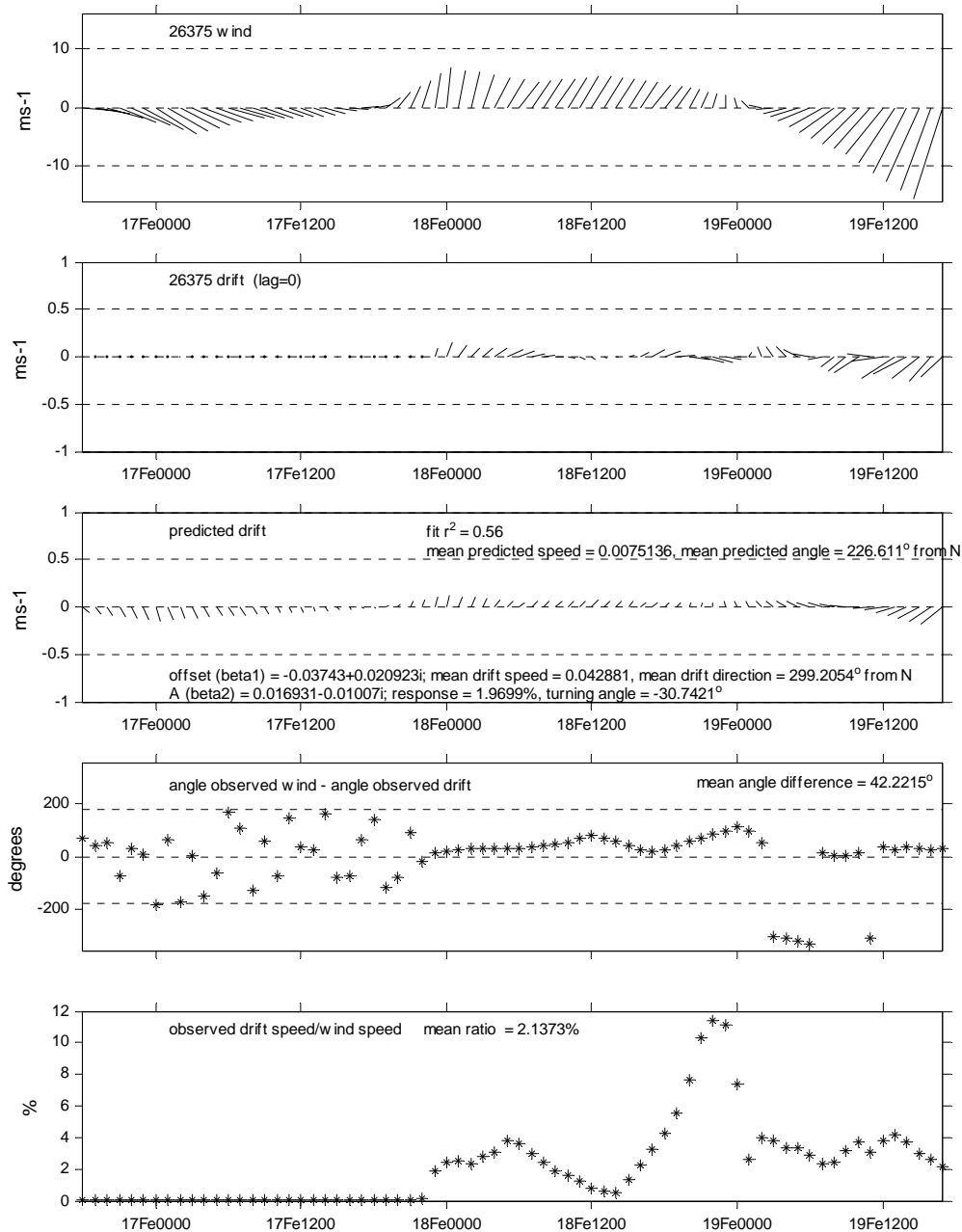


Figure 27 Results of complex least squares regression of wind and drift data for beacon 26375. The figure shows hourly wind and beacon drift, the predicted drift values (ie. fitted series), the angle difference between wind vectors and drift vectors (with mean angle difference), and the ratio of drift speed to wind speed (with mean ratio).

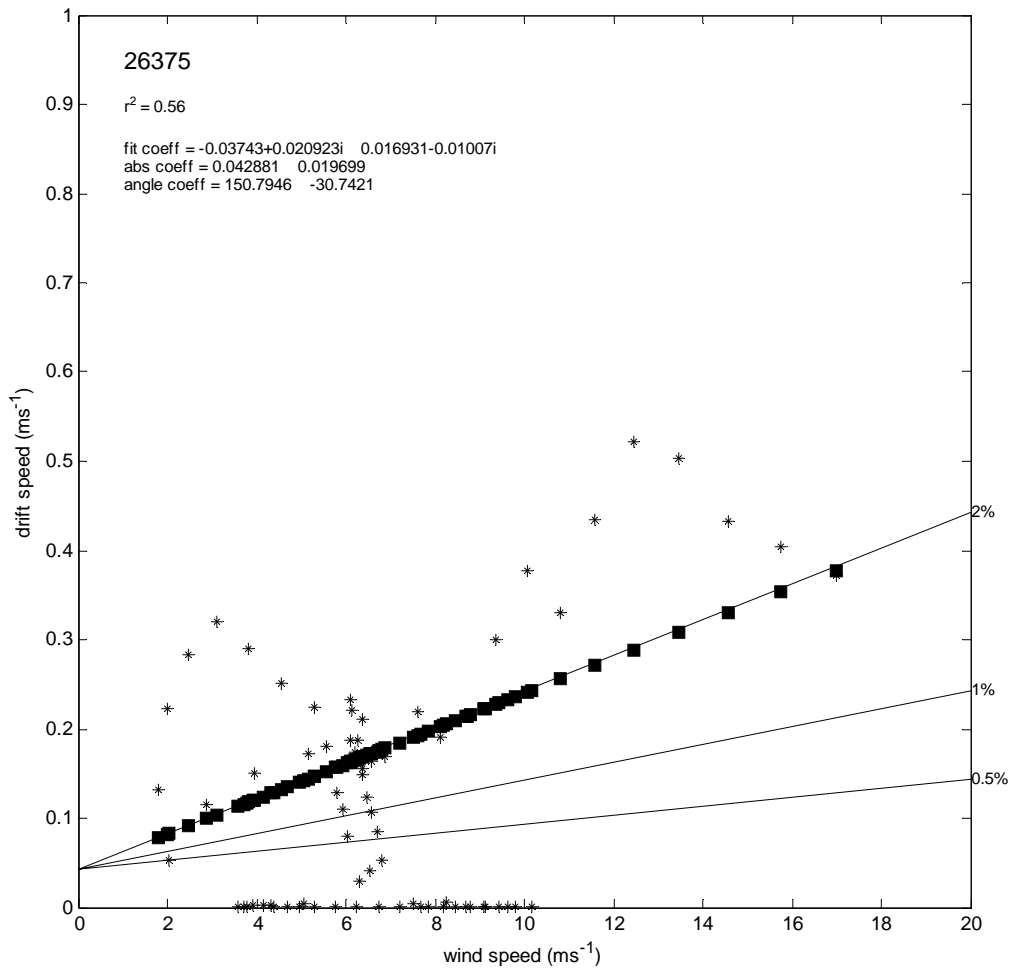


Figure 28 Scatter of hourly drift speed vs. wind speed for beacon 26375. Lines for various response are also shown. Squares indicate the predicted relationship from regression.

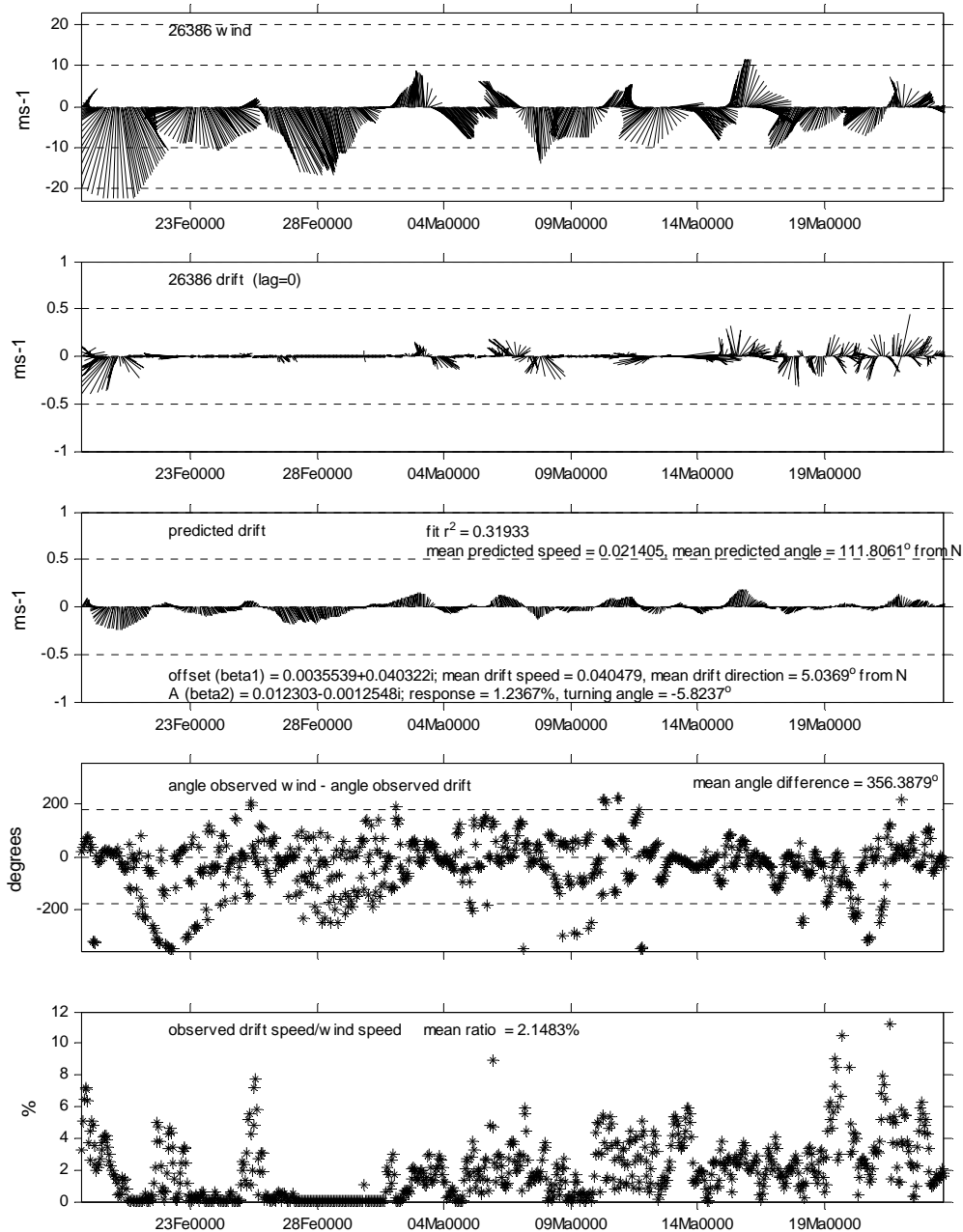


Figure 29 Results of complex least squares regression of wind and drift data for beacon 26386. The figure shows hourly wind and beacon drift, the predicted drift values (ie. fitted series), the angle difference between wind vectors and drift vectors (with mean angle difference), and the ratio of drift speed to wind speed (with mean ratio).

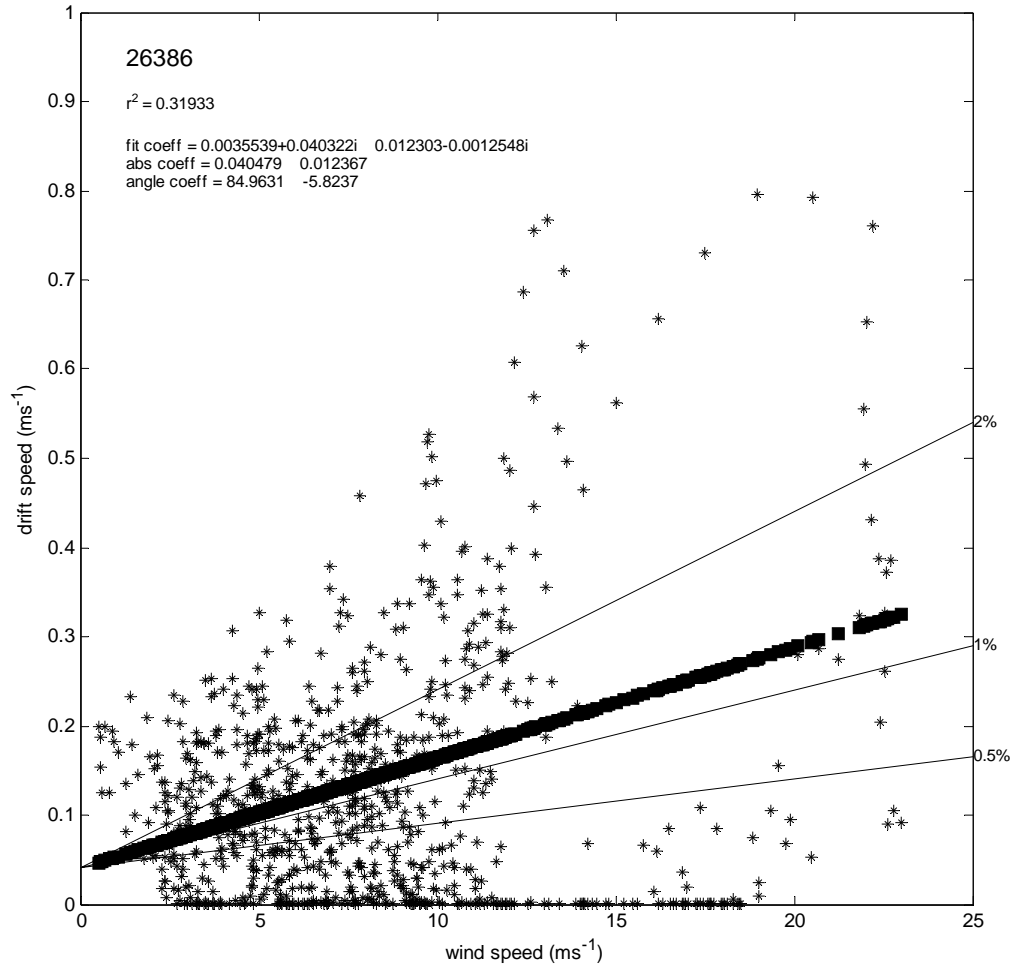


Figure 30 Scatter of hourly drift speed vs. wind speed for beacon 26386. Lines for various response are also shown. Squares indicate the predicted relationship from regression.

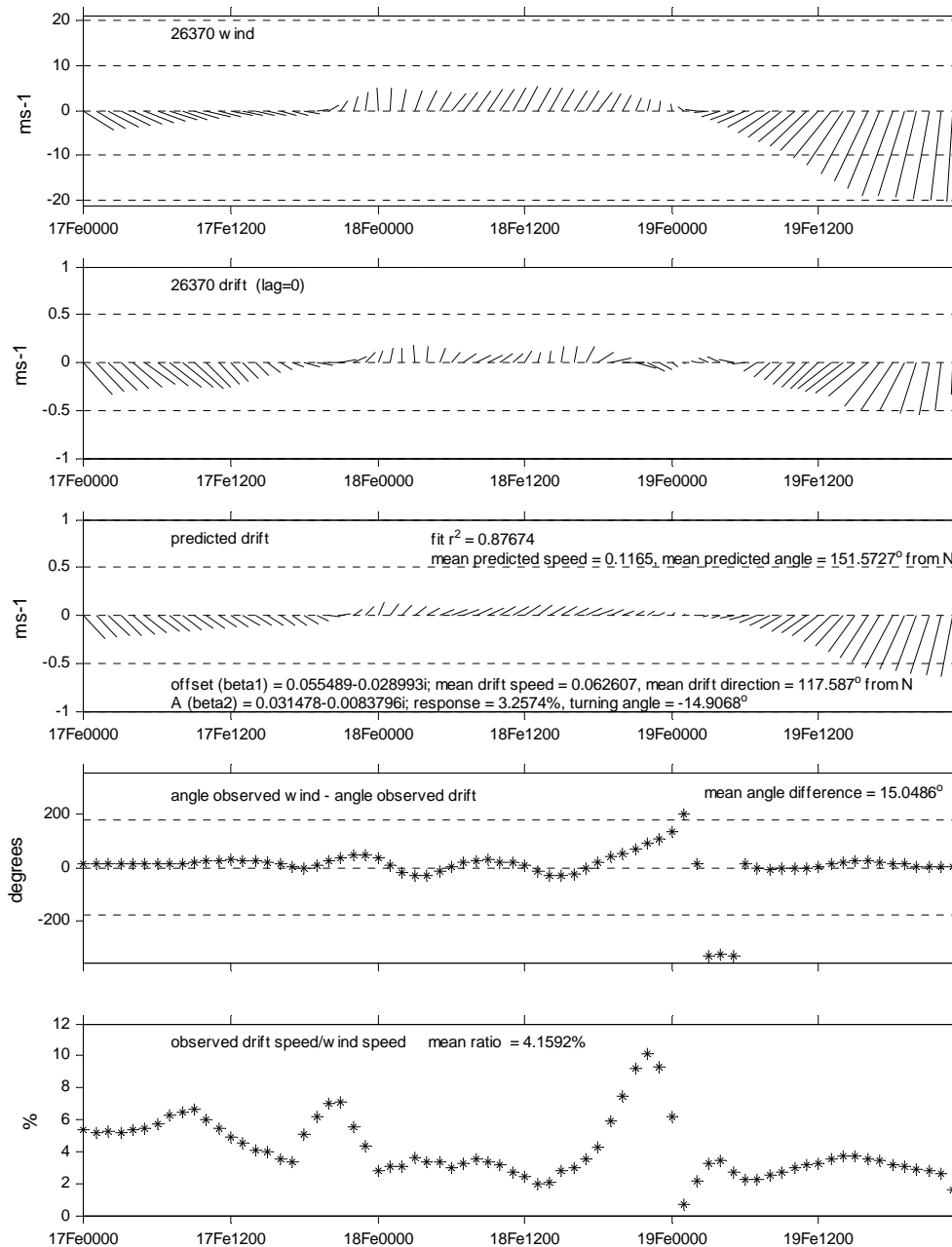


Figure 31 Results of complex least squares regression of wind and drift data for beacon 26370 before Feb 20. The figure shows hourly wind and beacon drift, the predicted drift values (ie. fitted series), the angle difference between wind vectors and drift vectors (with mean angle difference), and the ratio of drift speed to wind speed (with mean ratio).

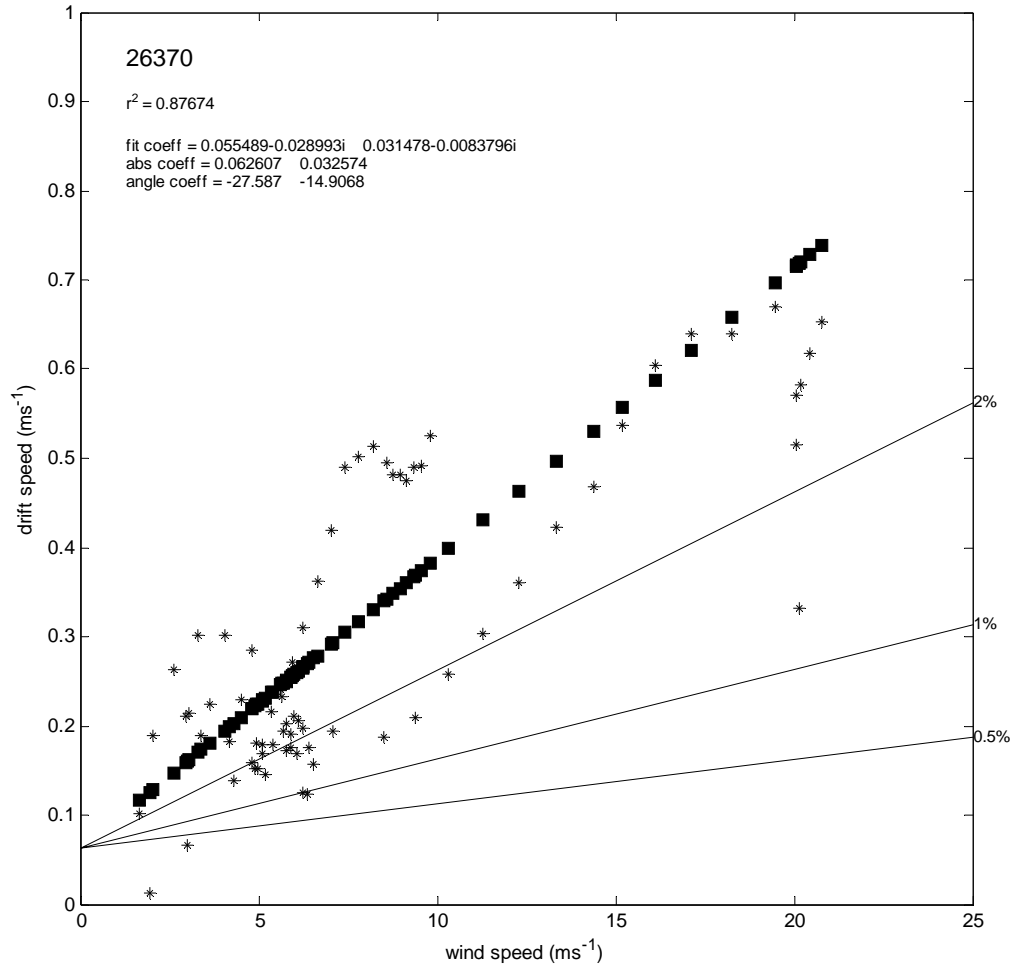


Figure 32 Scatter of hourly drift speed vs. wind speed for beacon 26370 before Feb 20. Lines for various reponse are also shown. Squares indicate the predicted relationship from regression.

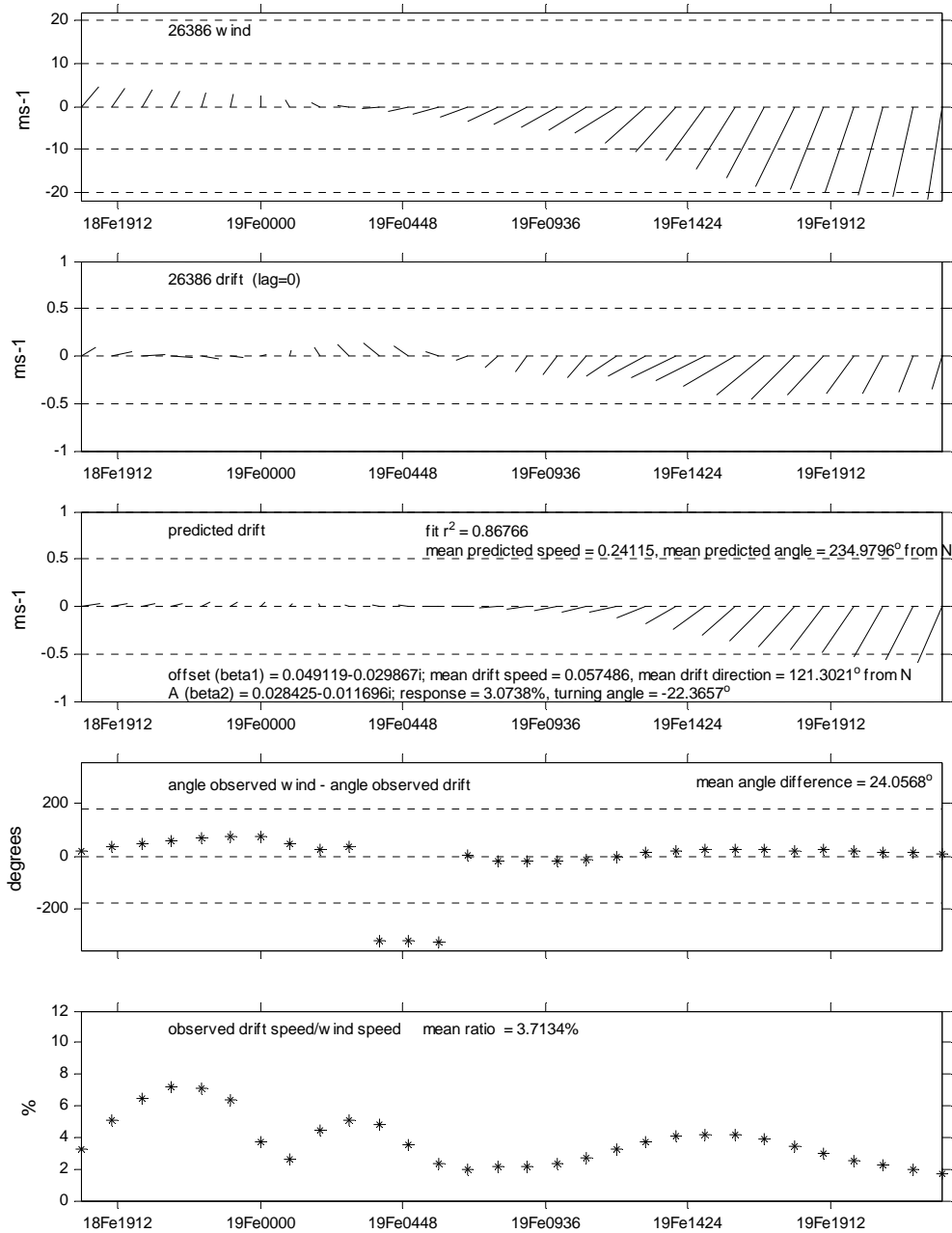


Figure 33 Results of complex least squares regression of wind and drift data for beacon 26386 before Feb 20. The figure shows hourly wind and beacon drift, the predicted drift values (ie. fitted series), the angle difference between wind vectors and drift vectors (with mean angle difference), and the ratio of drift speed to wind speed (with mean ratio).

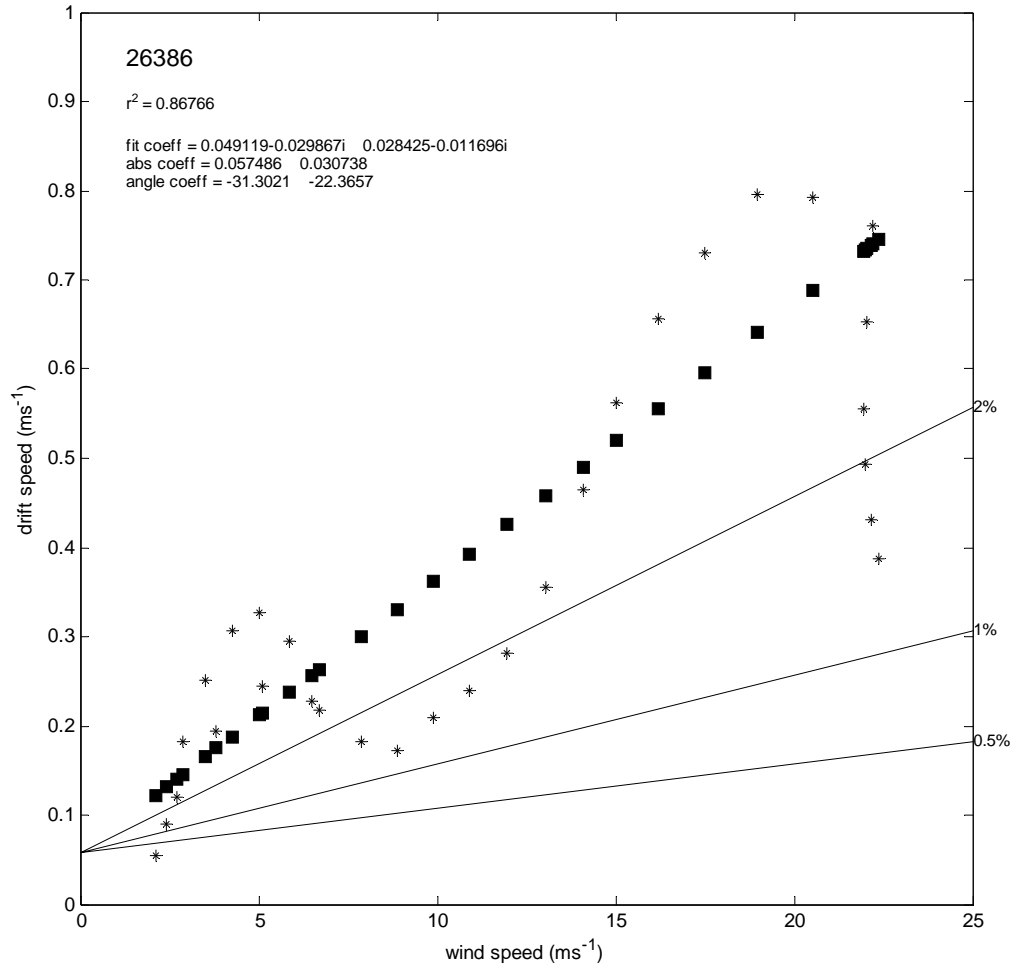


Figure 34 Scatter of hourly drift speed vs. wind speed for beacon 26386 before Feb 20. Lines for various reponse are also shown. Squares indicate the predicted relationship from regression.

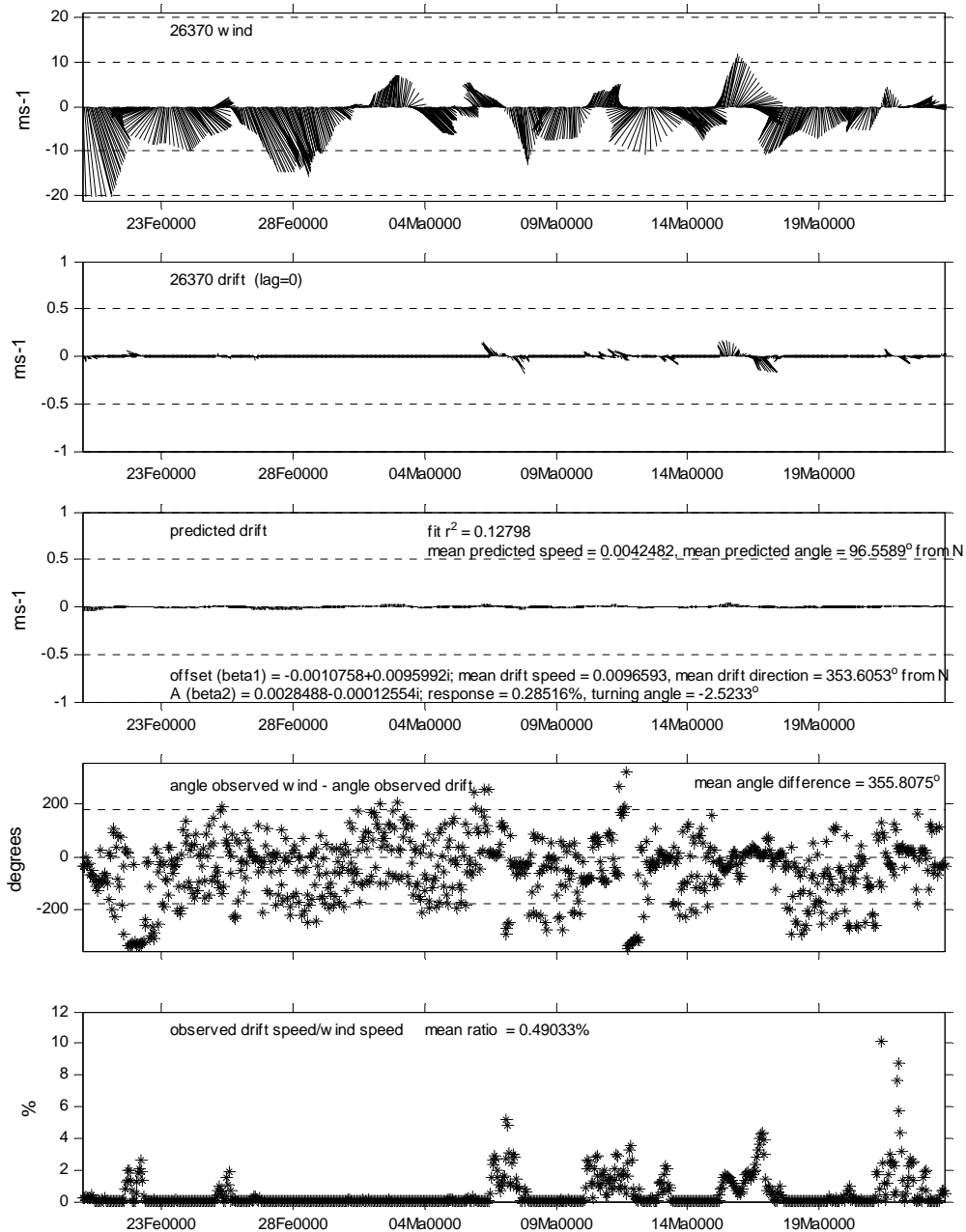


Figure 35 Results of complex least squares regression of wind and drift data for beacon 26370 after Feb 20. The figure shows hourly wind and beacon drift, the predicted drift values (ie. fitted series), the angle difference between wind vectors and drift vectors (with mean angle difference), and the ratio of drift speed to wind speed (with mean ratio).

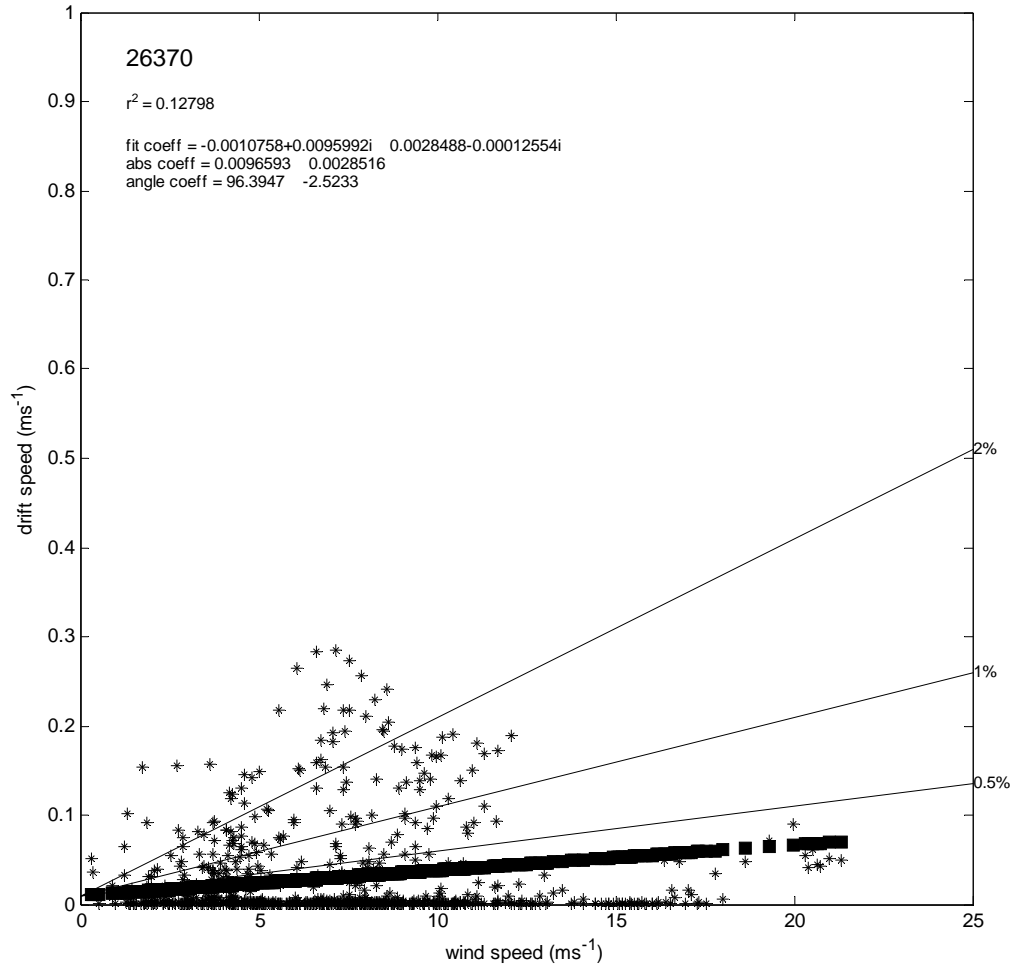


Figure 36 Scatter of hourly drift speed vs. wind speed for beacon 26370 after Feb 20. Lines for various reponse are also shown. Squares indicate the predicted relationship from regression.

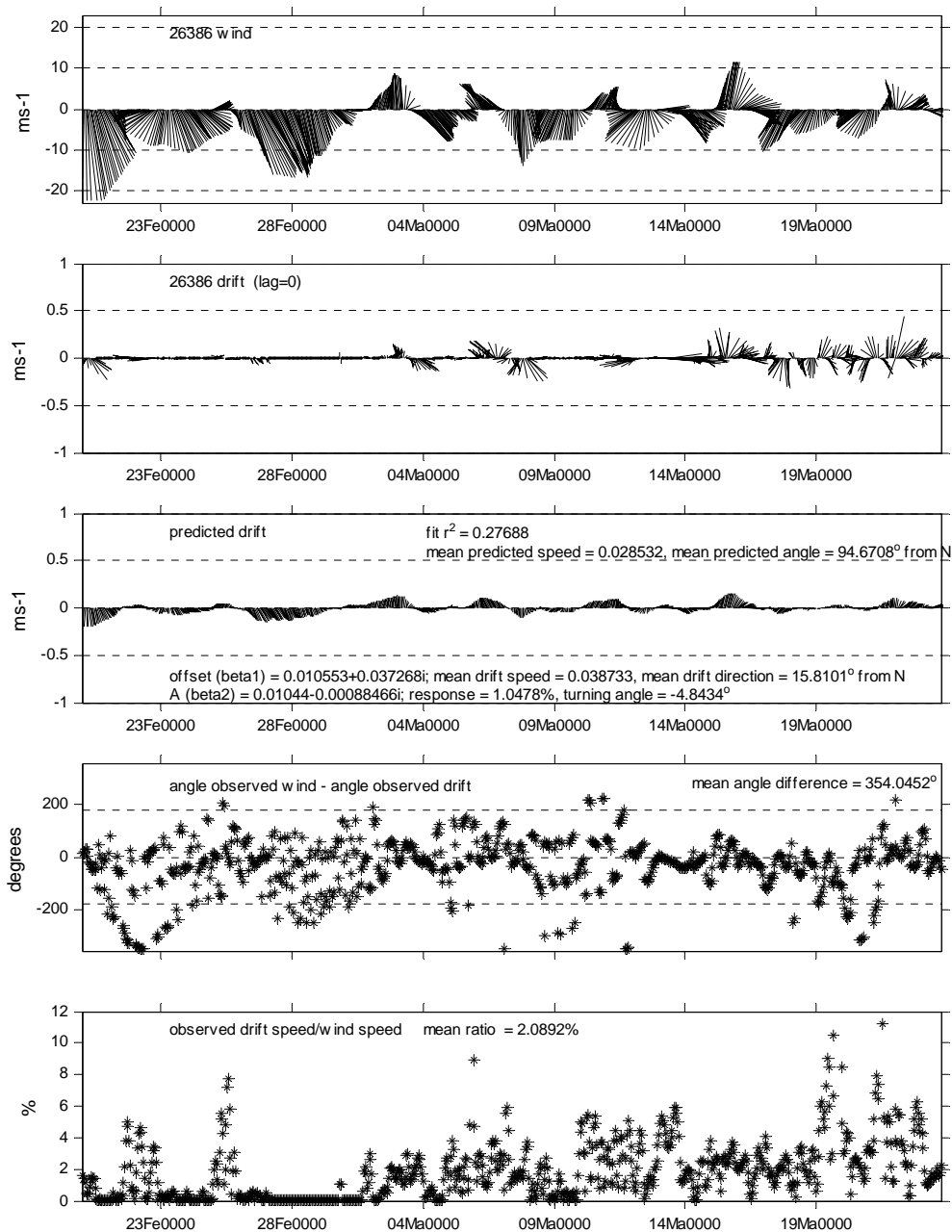


Figure 37 Results of complex least squares regression of wind and drift data for beacon 26386 after Feb 20. The figure shows hourly wind and beacon drift, the predicted drift values (ie. fitted series), the angle difference between wind vectors and drift vectors (with mean angle difference), and the ratio of drift speed to wind speed (with mean ratio).

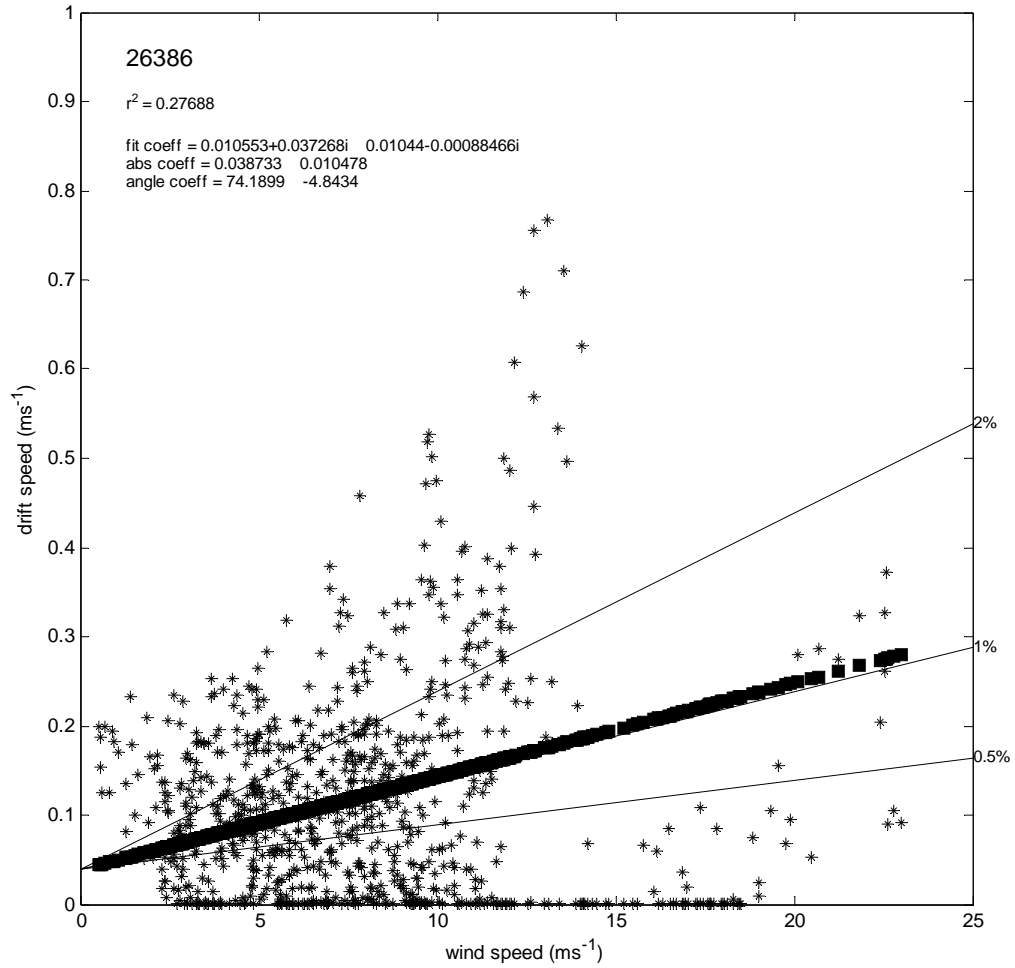


Figure 38 Scatter of hourly drift speed vs. wind speed for beacon 26386 after Feb 20. Lines for various reponse are also shown. Squares indicate the predicted relationship from regression.

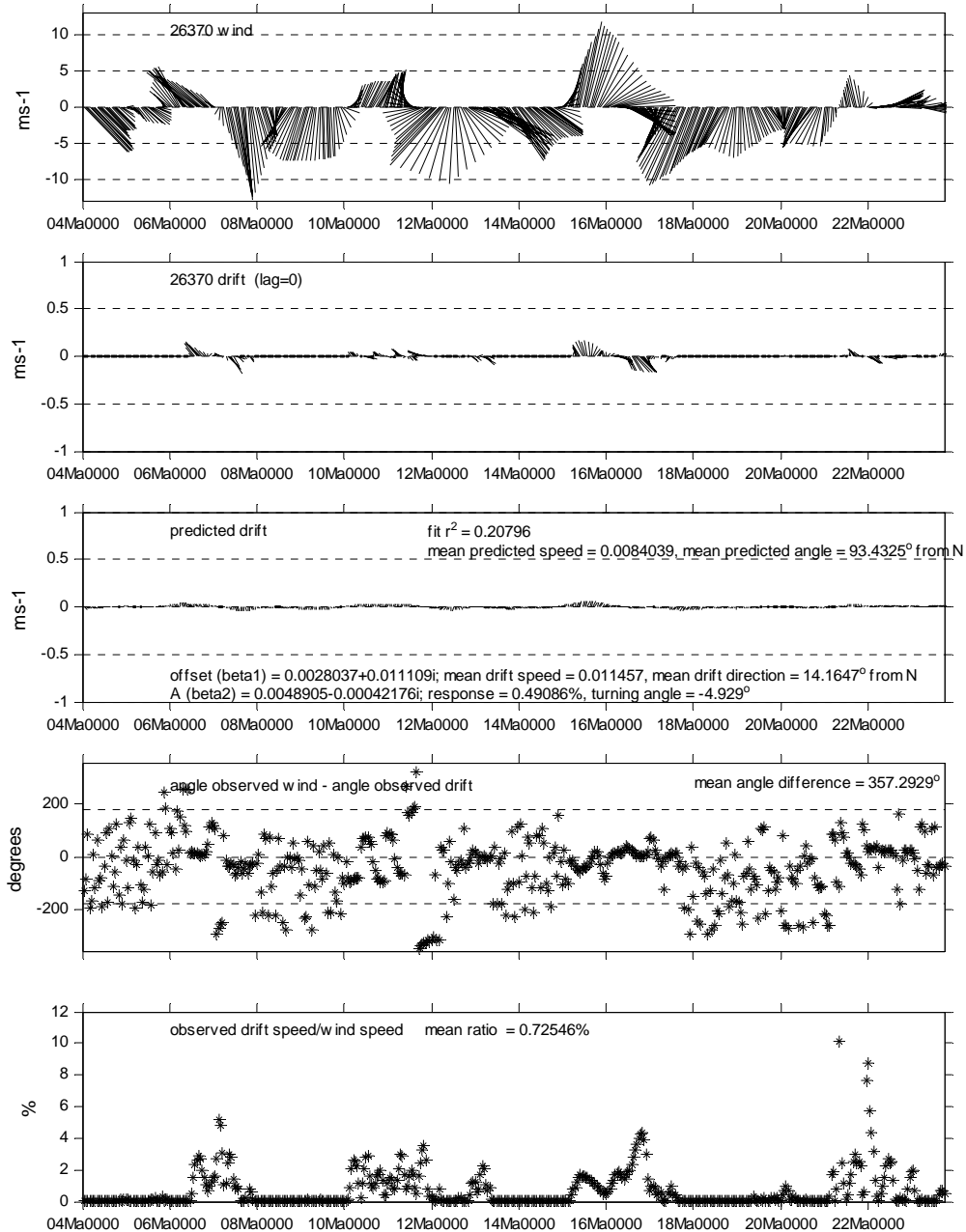


Figure 39 Results of complex least squares regression of wind and drift data for beacon 26370 after Mar 4. The figure shows hourly wind and beacon drift, the predicted drift values (ie. fitted series), the angle difference between wind vectors and drift vectors (with mean angle difference), and the ratio of drift speed to wind speed (with mean ratio).

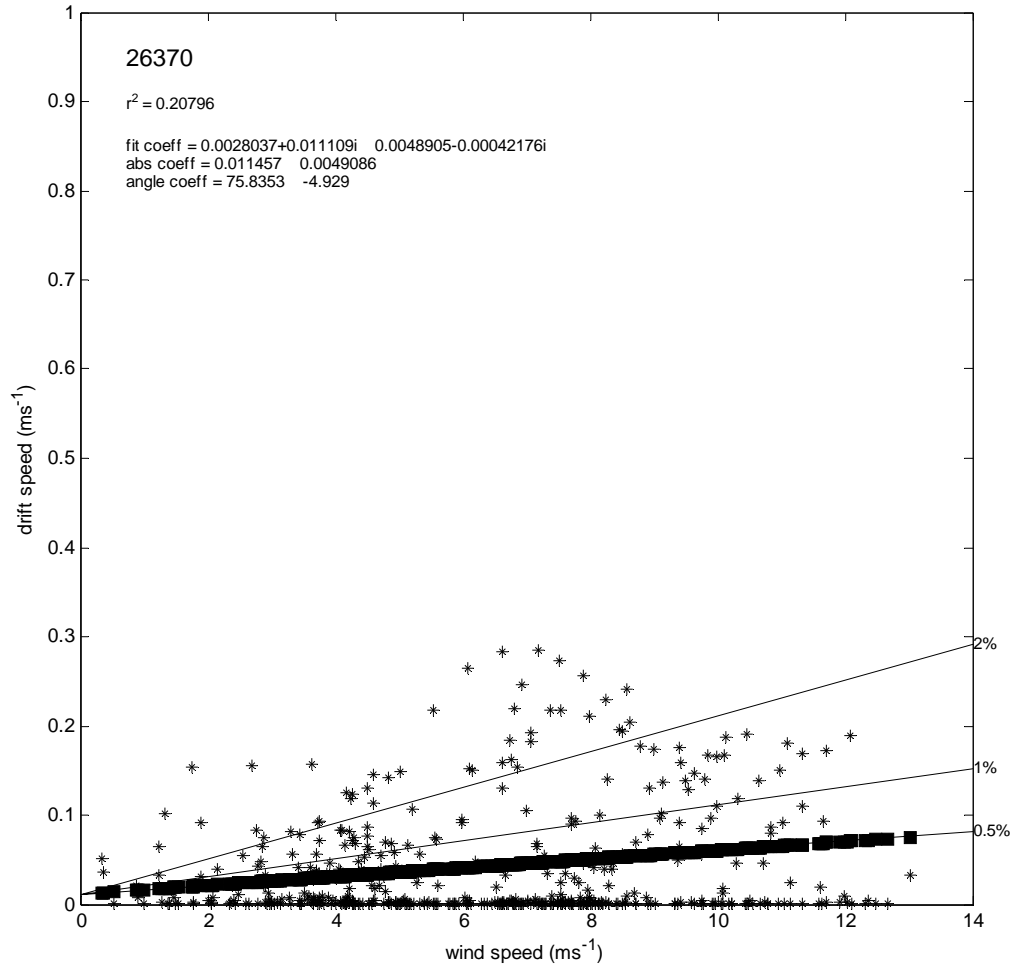


Figure 40 Scatter of hourly drift speed vs. wind speed for beacon 26370 after Mar 4. Lines for various response are also shown. Squares indicate the predicted relationship from regression.

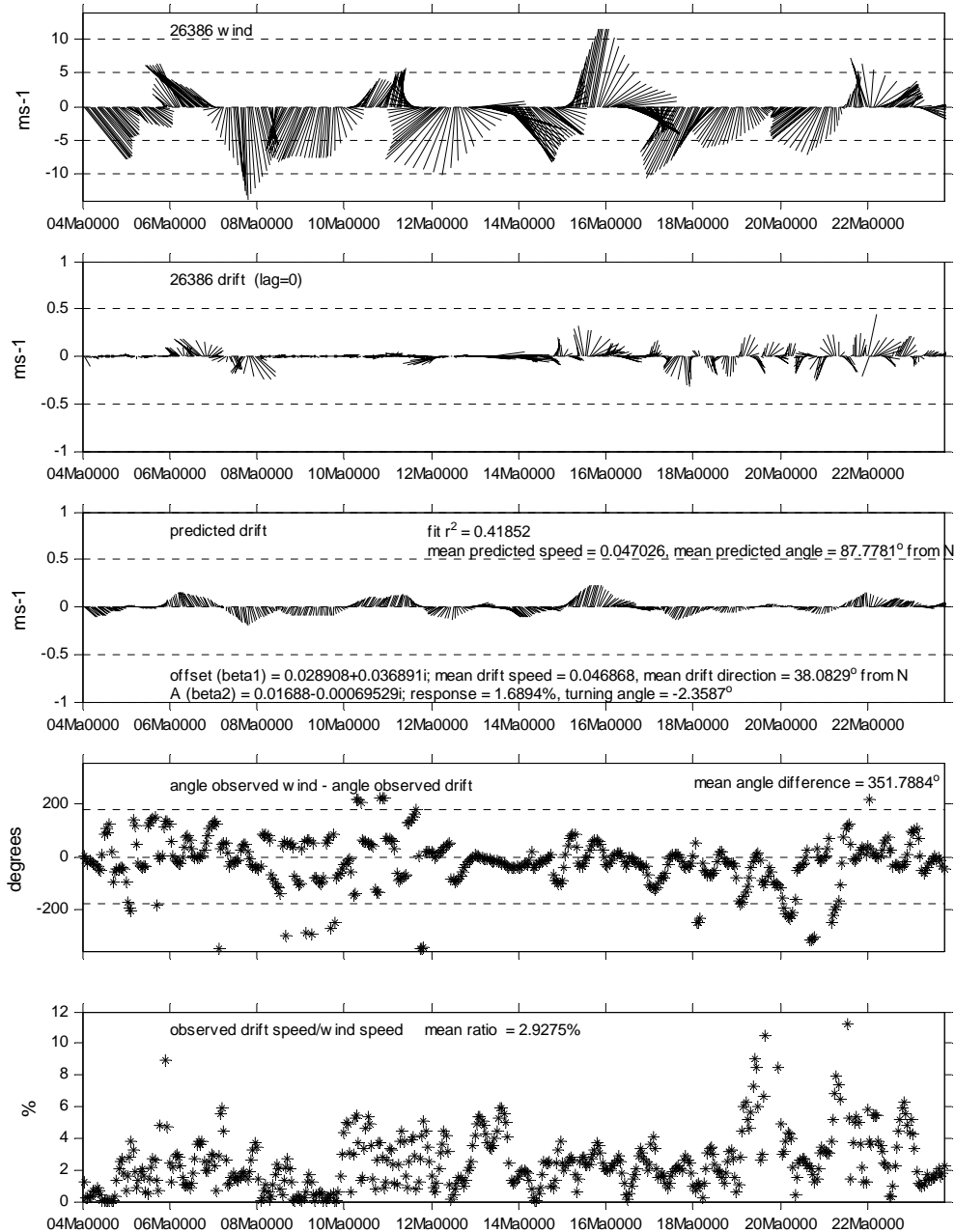


Figure 41 Results of complex least squares regression of wind and drift data for beacon 26386 after Mar 4. The figure shows hourly wind and beacon drift, the predicted drift values (ie. fitted series), the angle difference between wind vectors and drift vectors (with mean angle difference), and the ratio of drift speed to wind speed (with mean ratio).

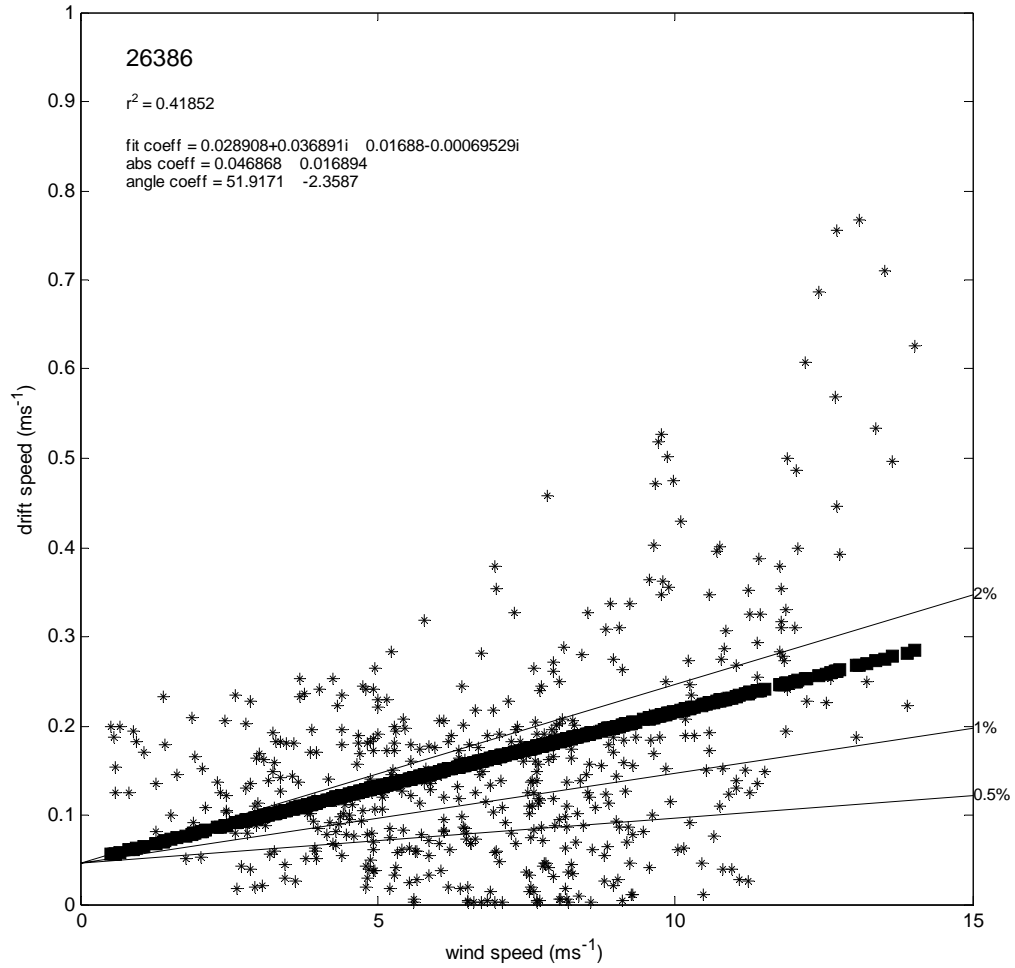


Figure 42 Scatter of hourly drift speed vs. wind speed for beacon 26386 after Mar 4. Lines for various response are also shown. Squares indicate the predicted relationship from regression.

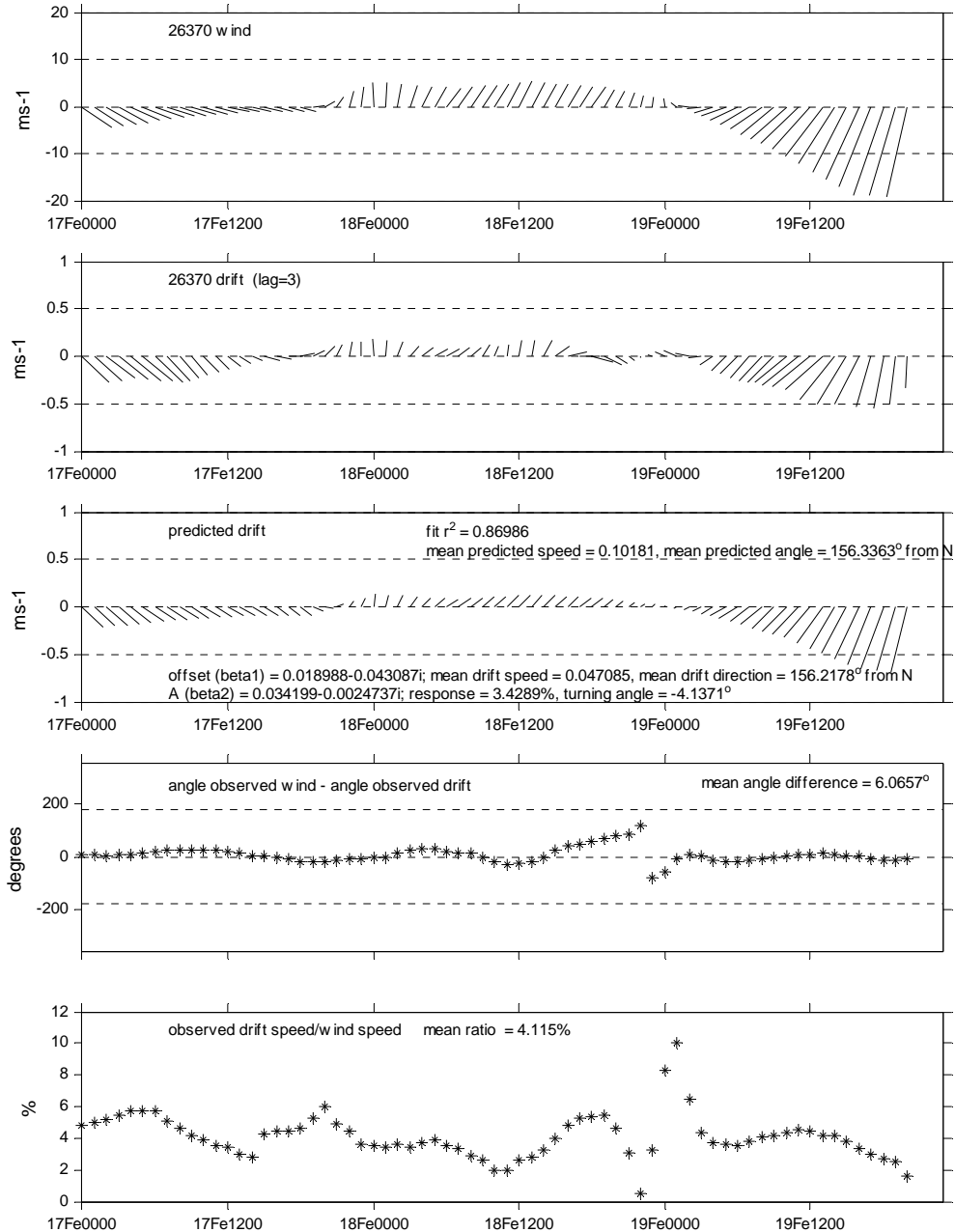


Figure 43 Results of complex least squares regression of wind and drift data for beacon 26370 before Feb. 20 with drift lagged behind wind by 3 hours. The figure shows hourly wind and beacon drift, the predicted drift values (ie. fitted series), the angle difference between wind vectors and drift vectors (with mean angle difference), and the ratio of drift speed to wind speed (with mean ratio).

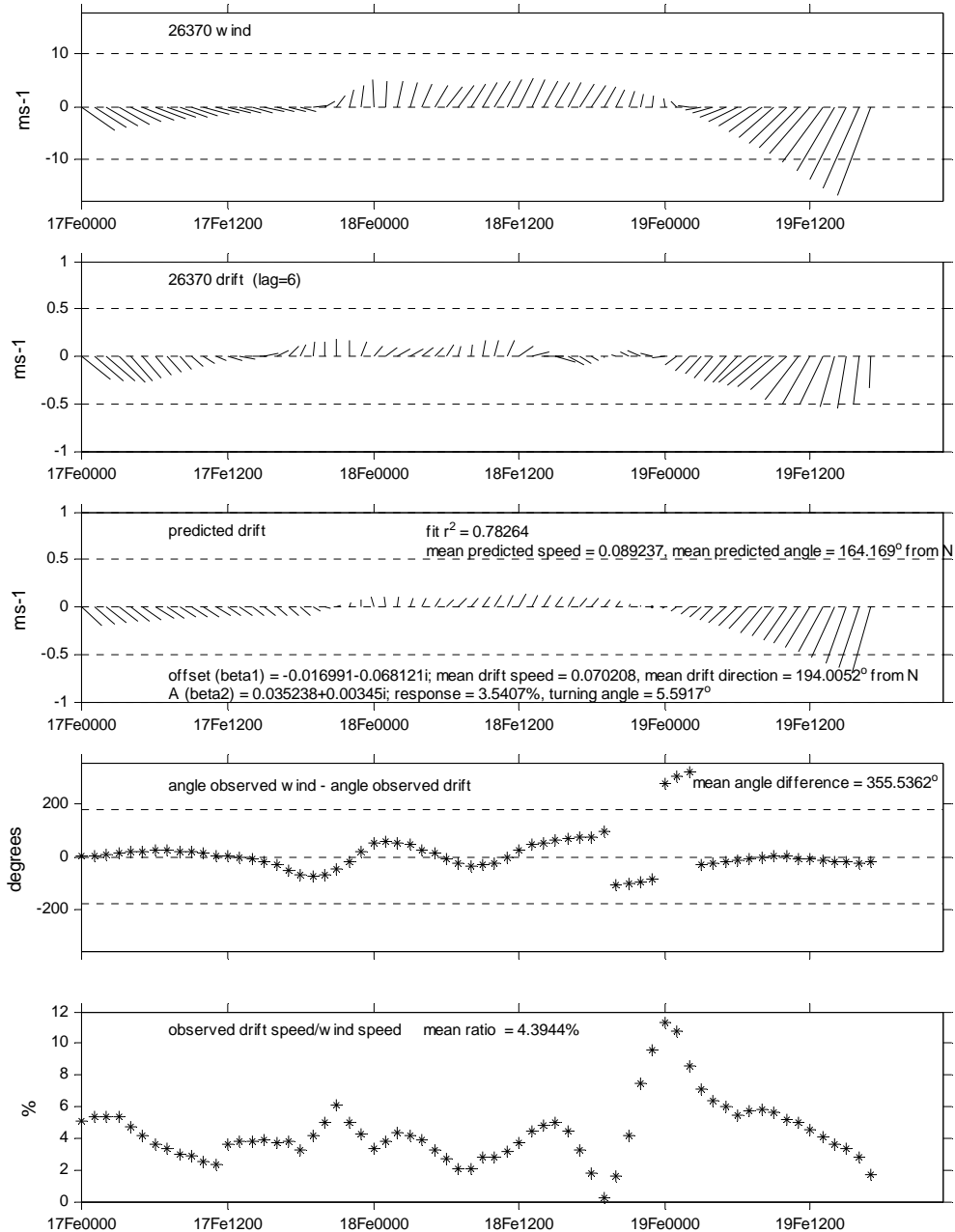


Figure 44 Results of complex least squares regression of wind and drift data for beacon 26370 before Feb. 20 with drift lagged behind wind by 6 hours. The figure shows hourly wind and beacon drift, the predicted drift values (ie. fitted series), the angle difference between wind vectors and drift vectors (with mean angle difference), and the ratio of drift speed to wind speed (with mean ratio).

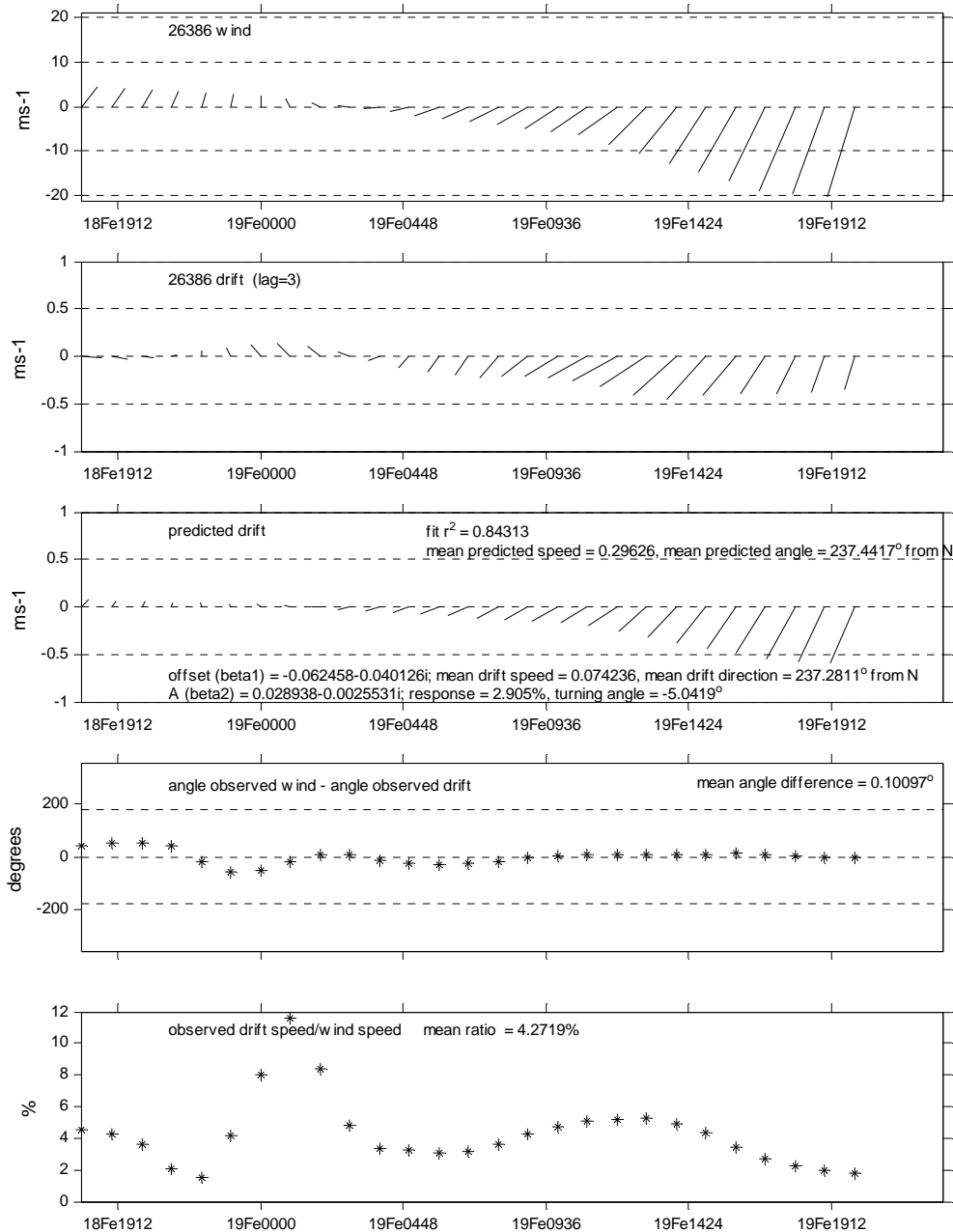


Figure 45 Results of complex least squares regression of wind and drift data for beacon 26386 before Feb. 20 with drift lagged behind wind by 3 hours. The figure shows hourly wind and beacon drift, the predicted drift values (ie. fitted series), the angle difference between wind vectors and drift vectors (with mean angle difference), and the ratio of drift speed to wind speed (with mean ratio).

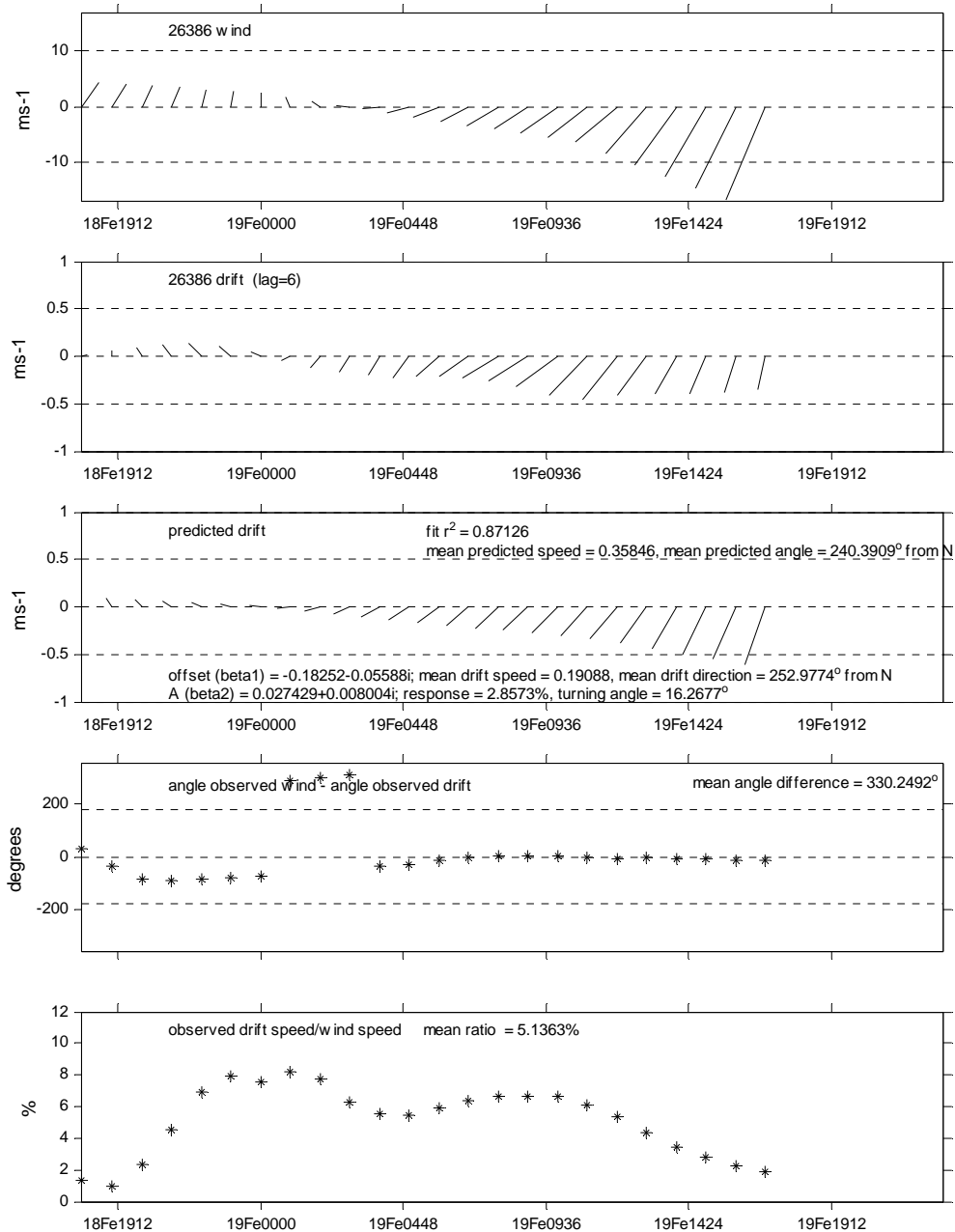


Figure 46 Results of complex least squares regression of wind and drift data for beacon 26386 before Feb. 20 with drift lagged behind wind by 6 hours. The figure shows hourly wind and beacon drift, the predicted drift values (ie. fitted series), the angle difference between wind vectors and drift vectors (with mean angle difference), and the ratio of drift speed to wind speed (with mean ratio).

3.4.1 Analysis with low-pass filtered drift data

We have seen from earlier figures (e.g. Figure 1 and Figure 6 to Figure 10), that the tides had a strong presence in the drift records and influenced the free drift of the beacons. Therefore the tides would also bias the regression analysis. Drift tracks in van der Baaren and Prinsenbergh (2001) also show the same tidal influence around Prince Edward Island, especially in the Northumberland Strait. In order to properly obtain a mean drift, and hence a more correct and presumably stable turning angle, the drift data were low-pass filtered (Cartwright filter) to eliminate the diurnal and semi-diurnal tides (Figure 47 to Figure 50). The data were then decimated to 6-hourly intervals and the regression was performed again. Data from beacon 02754 were not included in this analysis since that time series was too short to low-pass filter. For beacon 26386 there were not enough data before Feb 20 to run the regression for those data up to that date. No drift data were lagged in this case. Results are listed in Table 5. In general R^2 increased for similar data sets.

Table 5 Regression results for least squares fit of wind to low pass filtered drift

Beacon	R^2	Turning angle (deg)	Gain (%)	Mean drift speed (m/s)	# points
<i>Entire data record</i>					
00973	0.32	25.12	1.09	0.08	17
02754	NA	NA	NA	NA	NA
26370	0.28	-9.25	0.48	0.01	137
26375	0.58	-38.61	1.64	0.02	9
26386	0.47	-6.17	1.03	0.03	136
<i>Storm influence</i>					
26370 before Feb. 20	0.91	-10.44	2.15	0.04	9
26386 before Feb. 20	NA	NA	NA	NA	NA
26370 after Mar. 4	0.38	-6.54	0.39	0.01	73
26386 after Mar. 4	0.67	-0.70	1.48	0.05	72

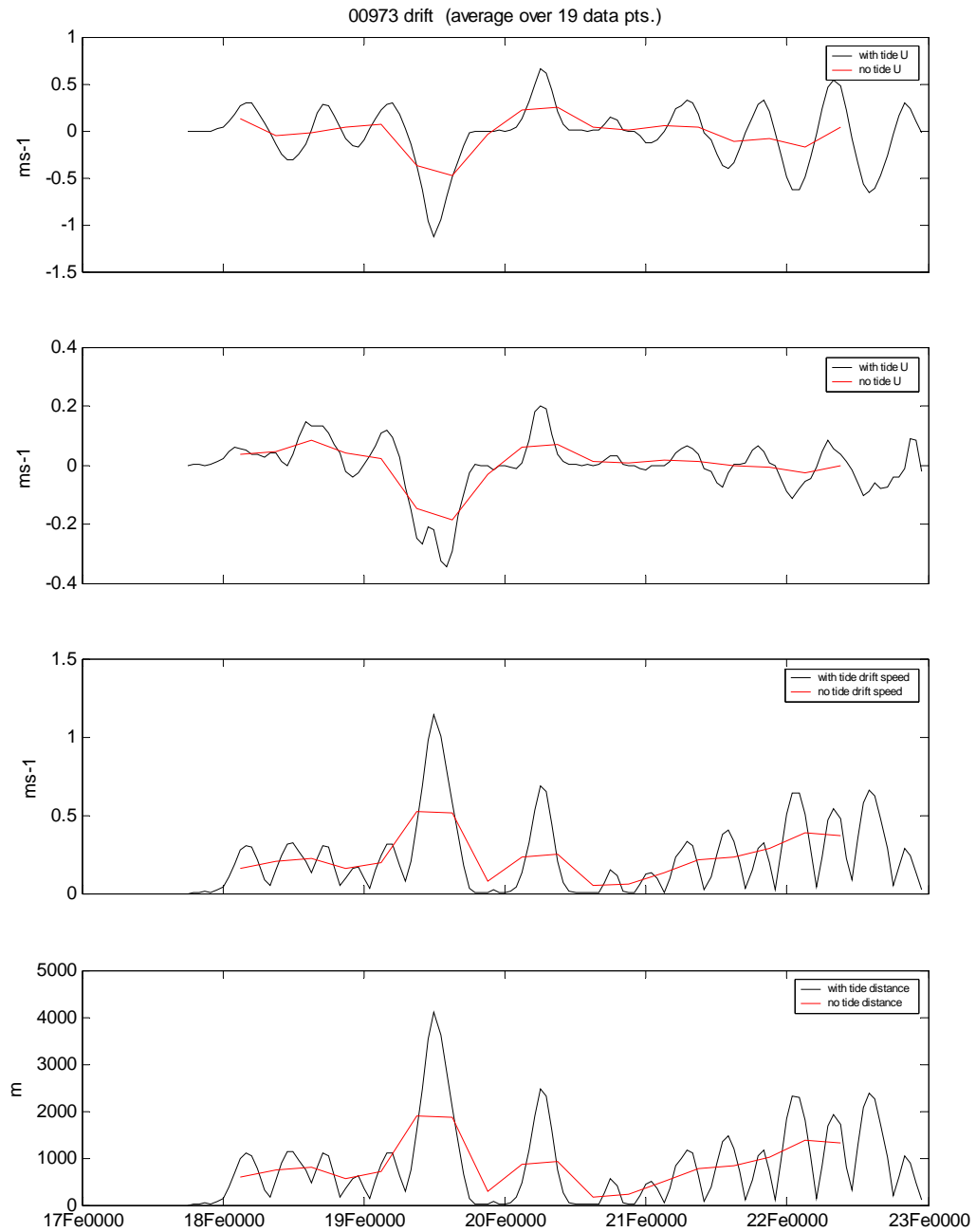


Figure 47 Time series of beacon 00973 hourly drift with mean drift (low-passed) superimposed

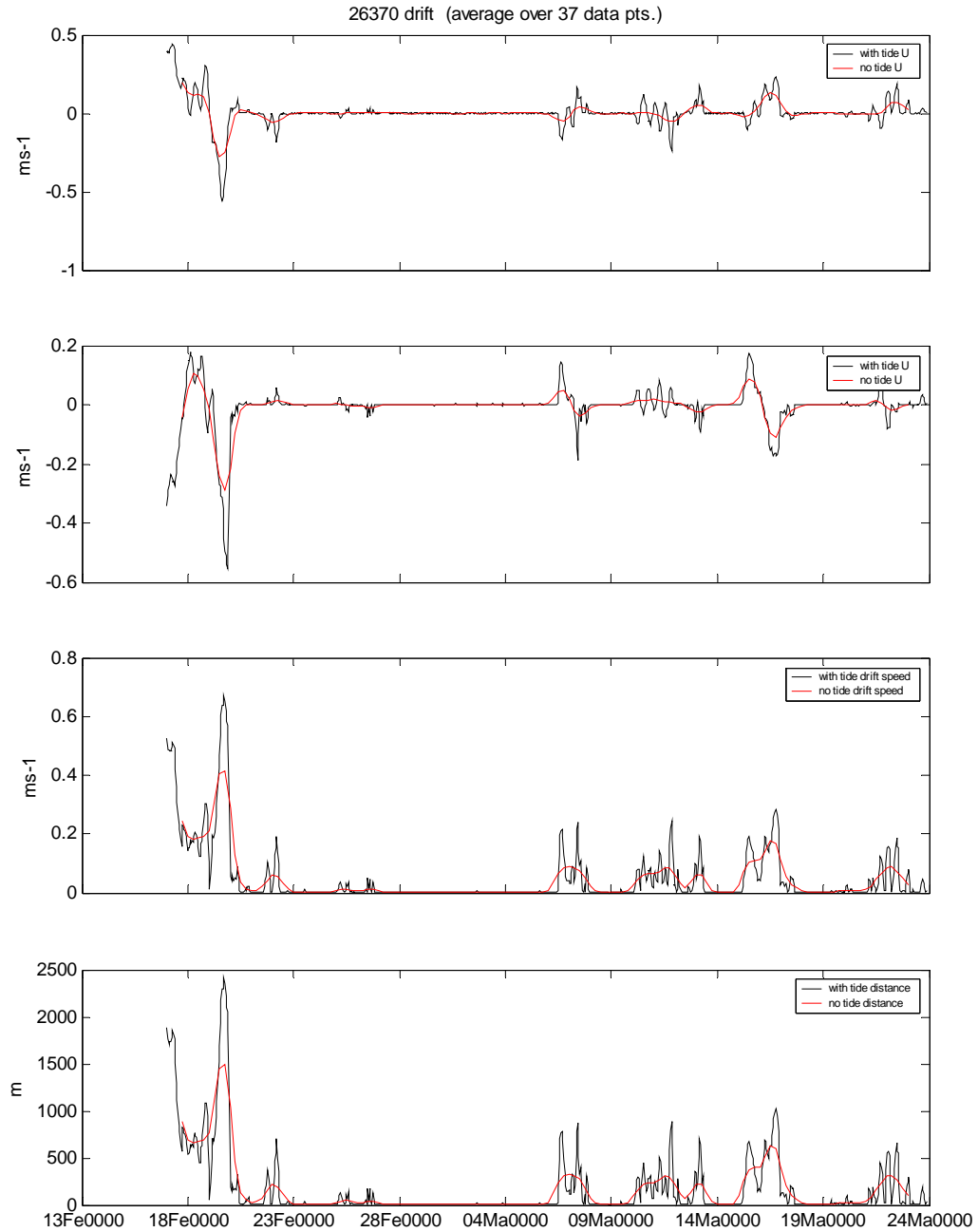


Figure 48 Time series of beacon 26370 hourly drift with mean drift (low-passed) superimposed

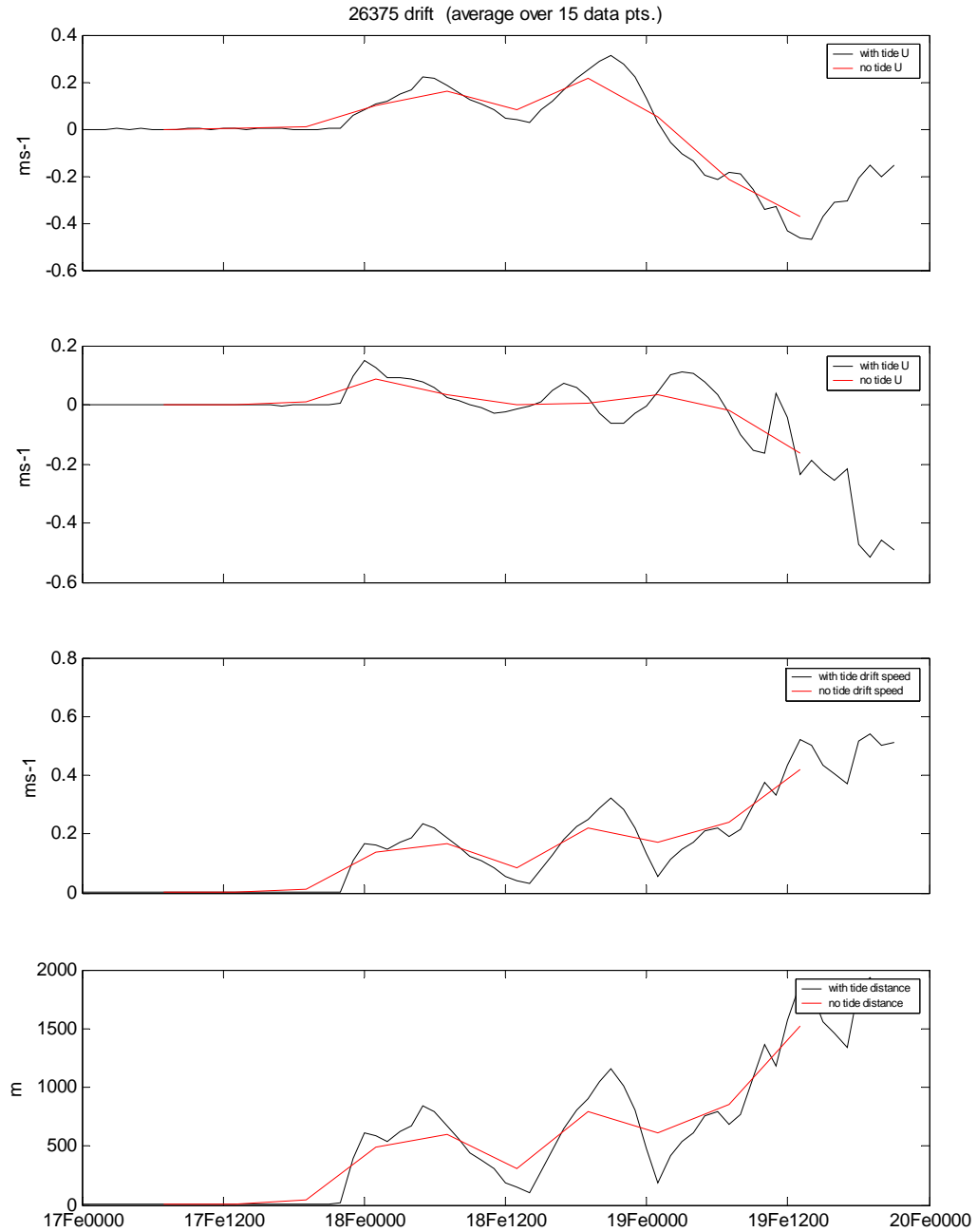


Figure 49 Time series of beacon 26375 hourly drift with mean drift (low-pass) superimposed

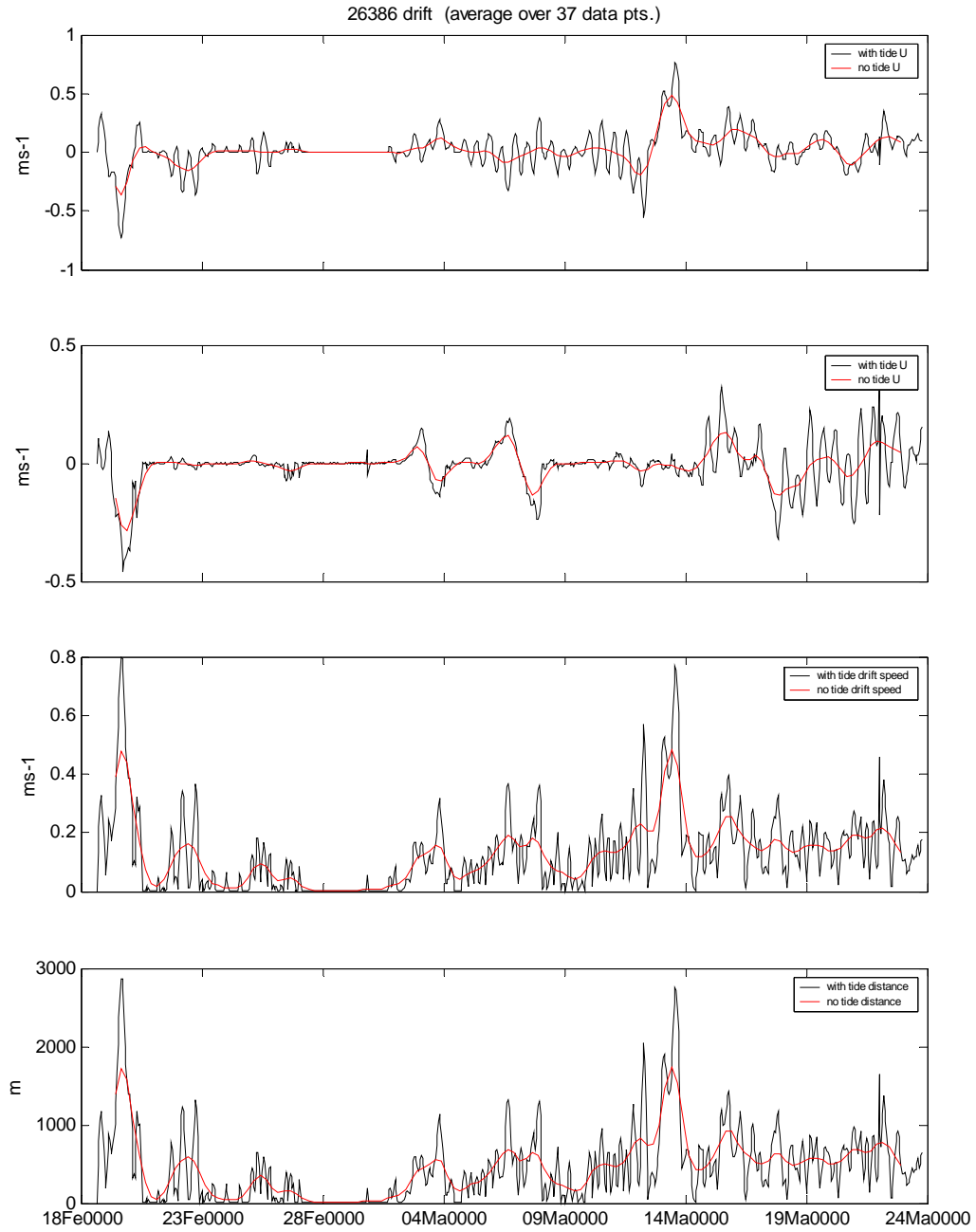


Figure 50 Time series of beacon 26386 hourly drift with mean drift (low-passed) superimposed

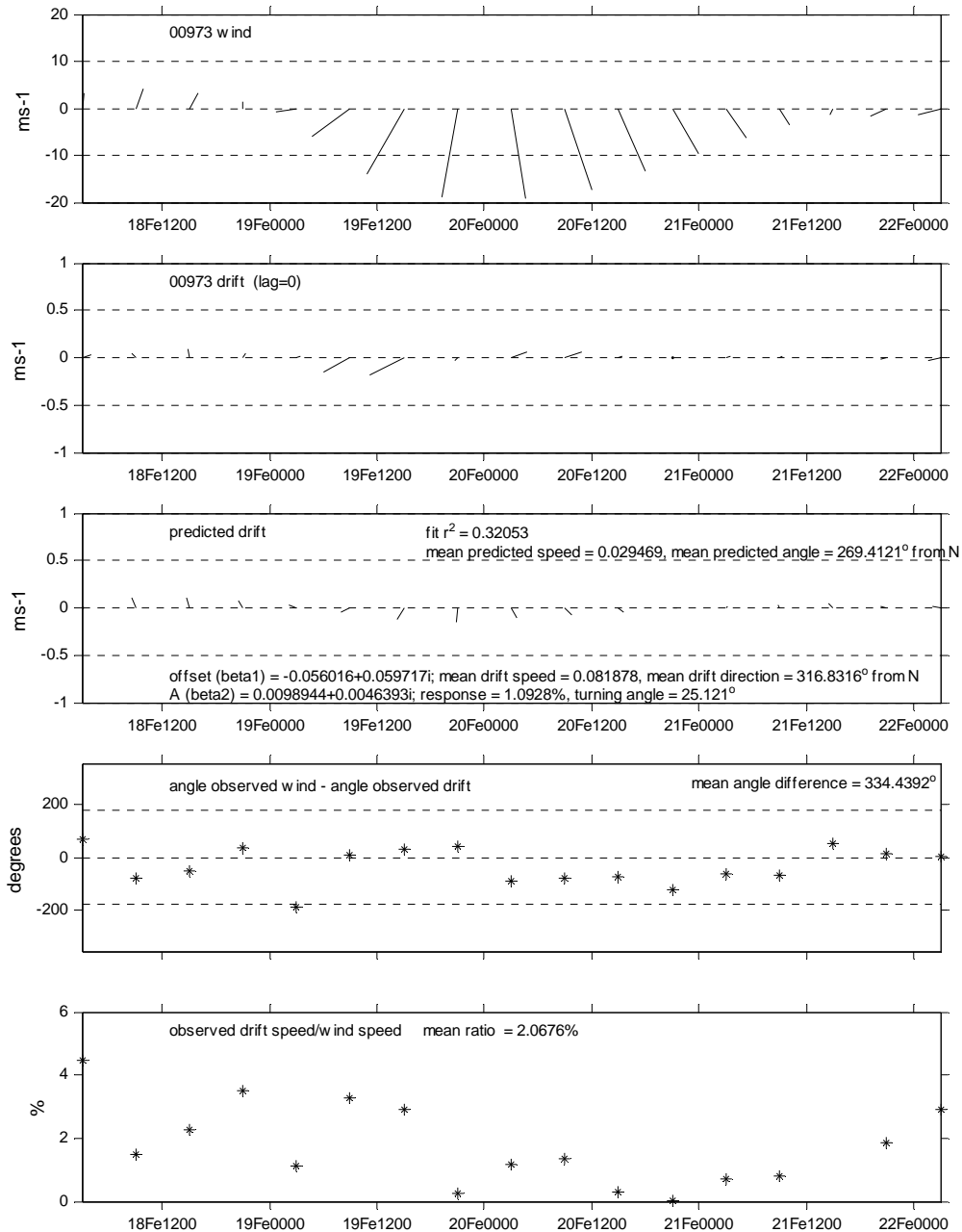


Figure 51 Results of complex least squares regression of wind and low-pass drift data for beacon 00973. The figure shows hourly wind and beacon drift, the predicted drift values (ie. fitted series), the angle difference between wind vectors and drift vectors (with mean angle difference), and the ratio of drift speed to wind speed (with mean ratio).

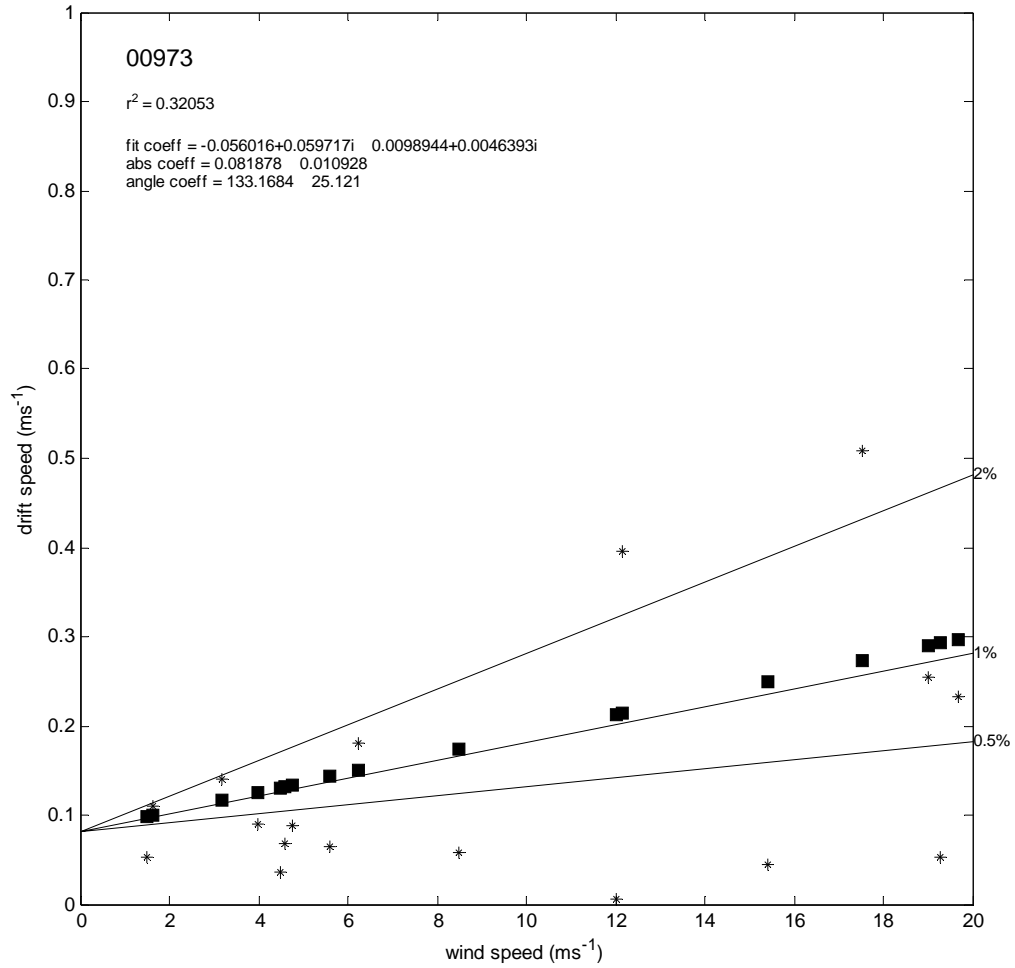


Figure 52 Scatter of 6-hourly low-pass filtered drift speed vs. wind speed for beacon 00973. Lines for various reponse are also shown. Squares indicate the predicted relationship from regression.

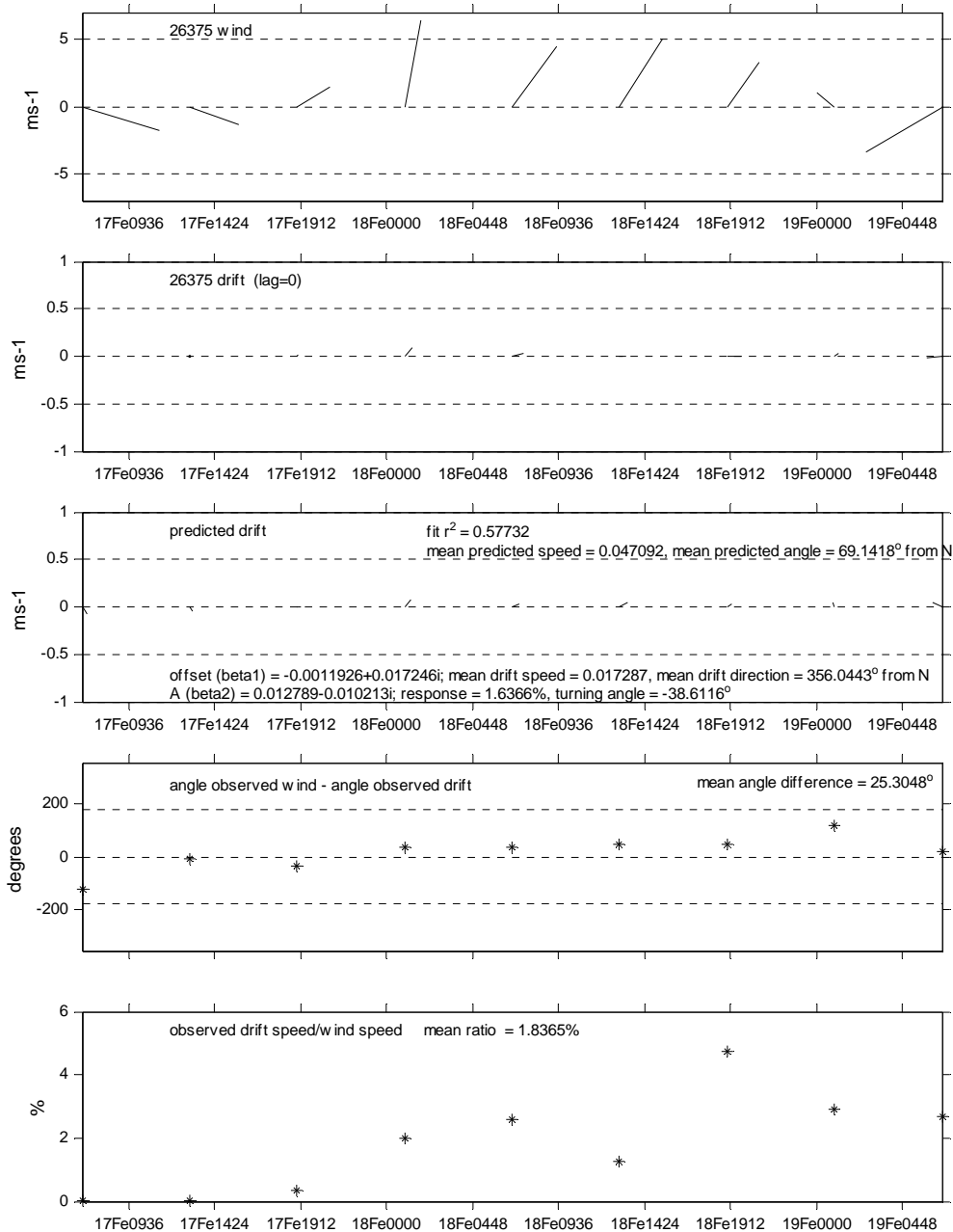


Figure 53 Results of complex least squares regression of wind and low-pass drift data for beacon 26375. The figure shows hourly wind and beacon drift, the predicted drift values (ie. fitted series), the angle difference between wind vectors and drift vectors (with mean angle difference), and the ratio of drift speed to wind speed (with mean ratio).

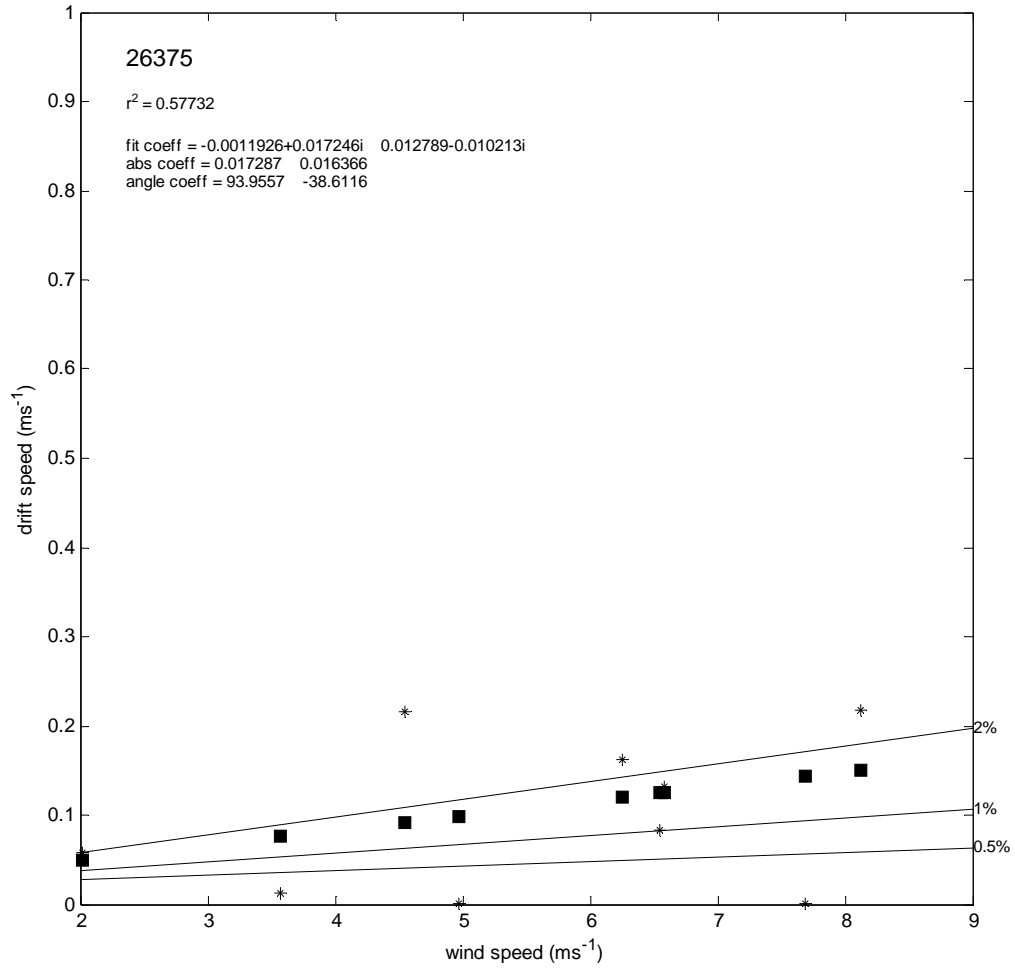


Figure 54 Scatter of 6-hourly low-pass filtered drift speed vs. wind speed for beacon 26375. Lines for various response are also shown. Squares indicate the predicted relationship from regression.

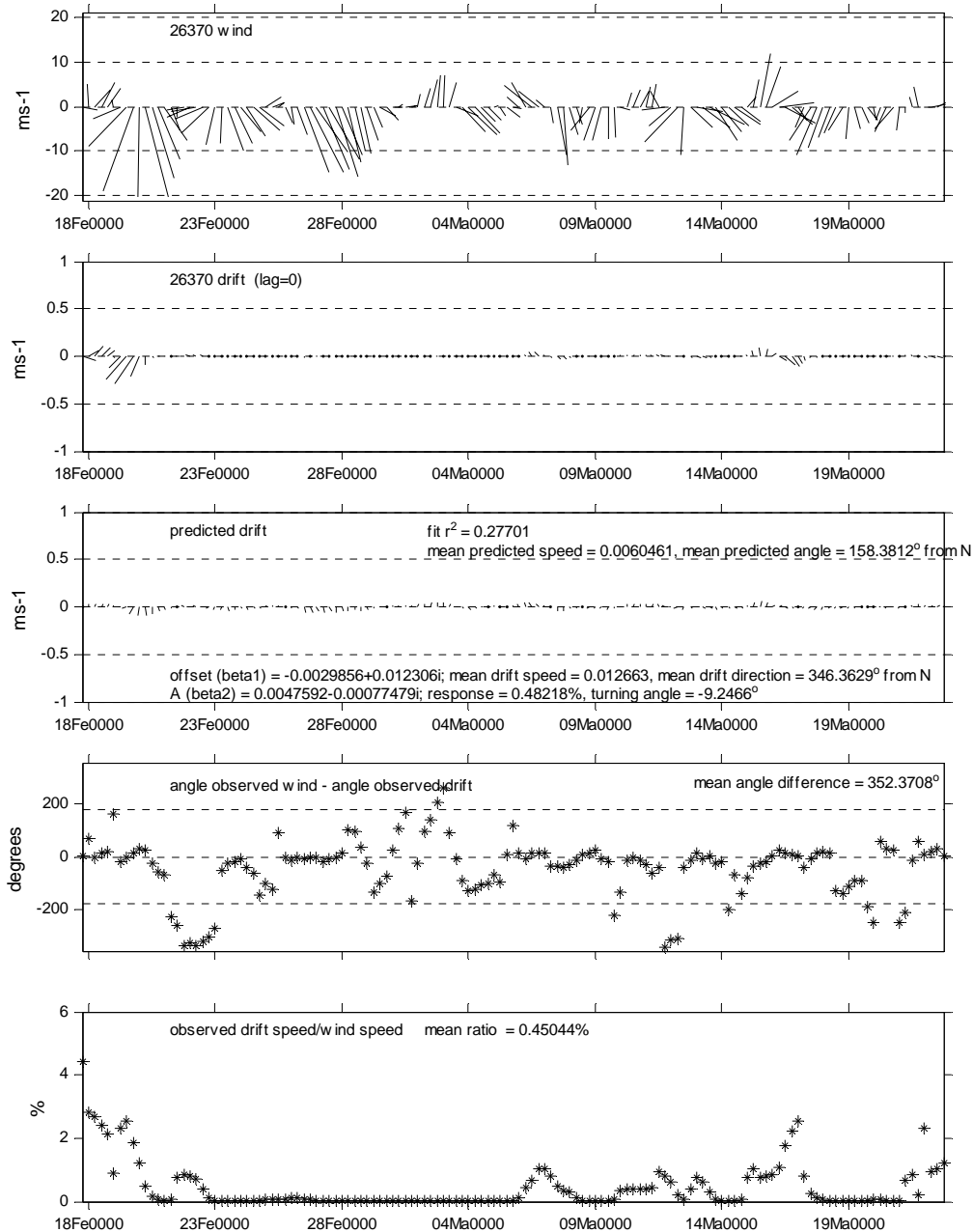


Figure 55 Results of complex least squares regression of wind and low-pass drift data for beacon 26370. The figure shows hourly wind and beacon drift, the predicted drift values (ie. fitted series), the angle difference between wind vectors and drift vectors (with mean angle difference), and the ratio of drift speed to wind speed (with mean ratio).

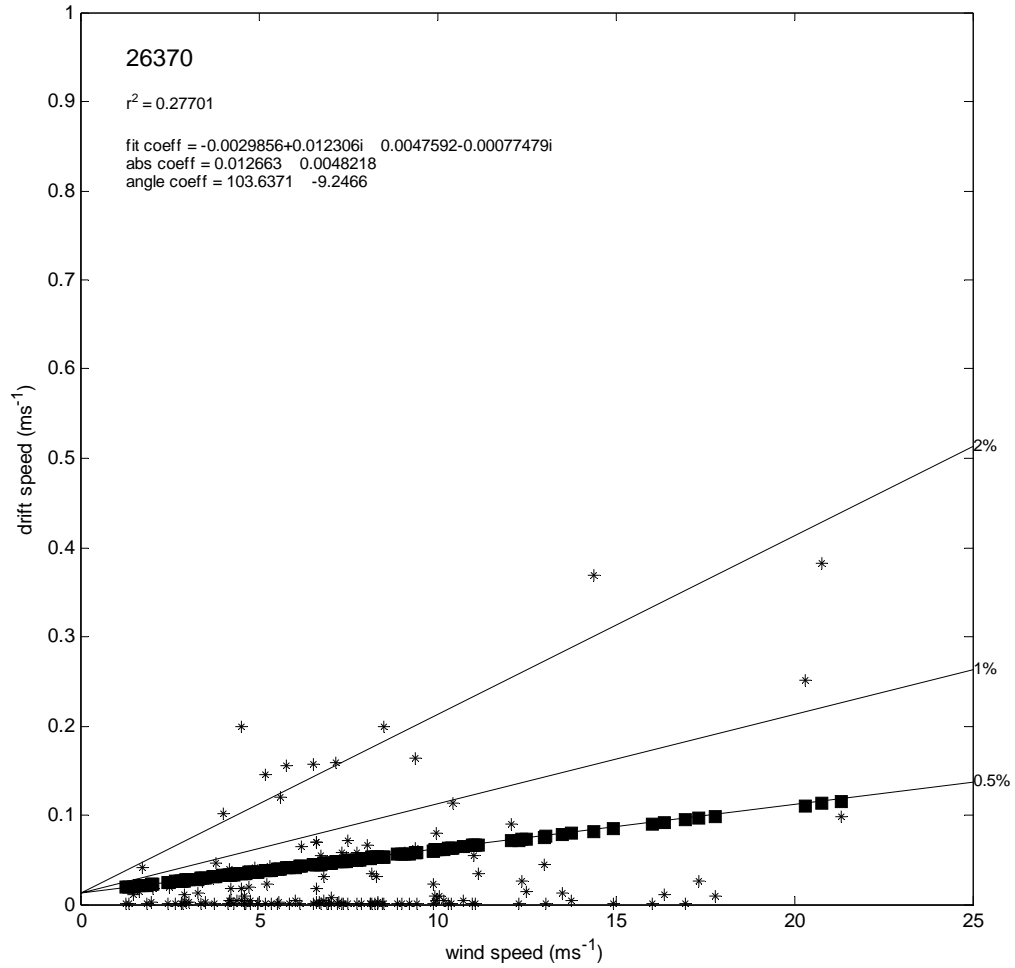


Figure 56 Scatter of 6-hourly low-pass filtered drift speed vs. wind speed for beacon 26370. Lines for various response are also shown. Squares indicate the predicted relationship from regression.

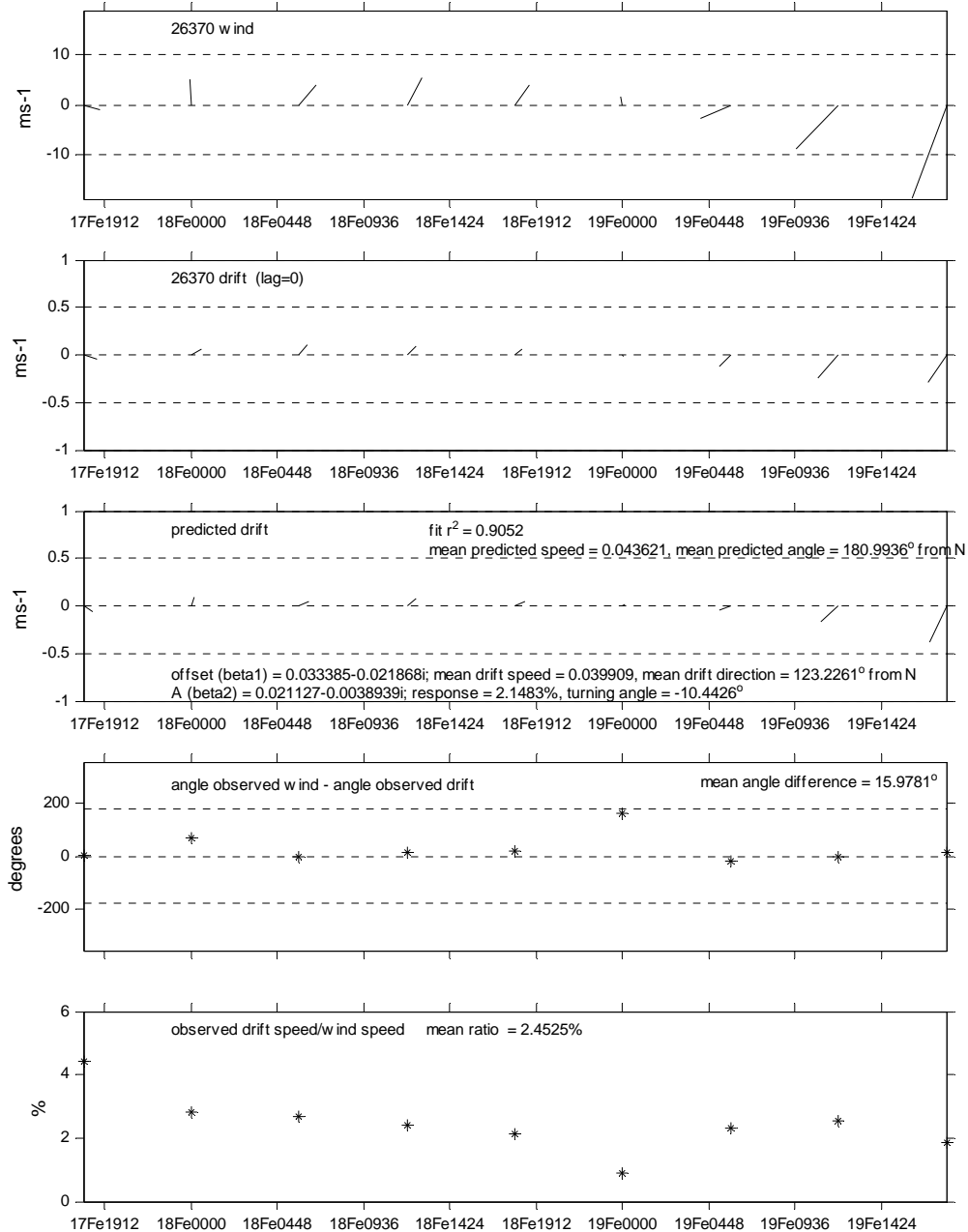


Figure 57 Results of complex least squares regression of wind and low-pass drift data for beacon 26370 before Feb 20. The figure shows hourly wind and beacon drift, the predicted drift values (ie. fitted series), the angle difference between wind vectors and drift vectors (with mean angle difference), and the ratio of drift speed to wind speed (with mean ratio).

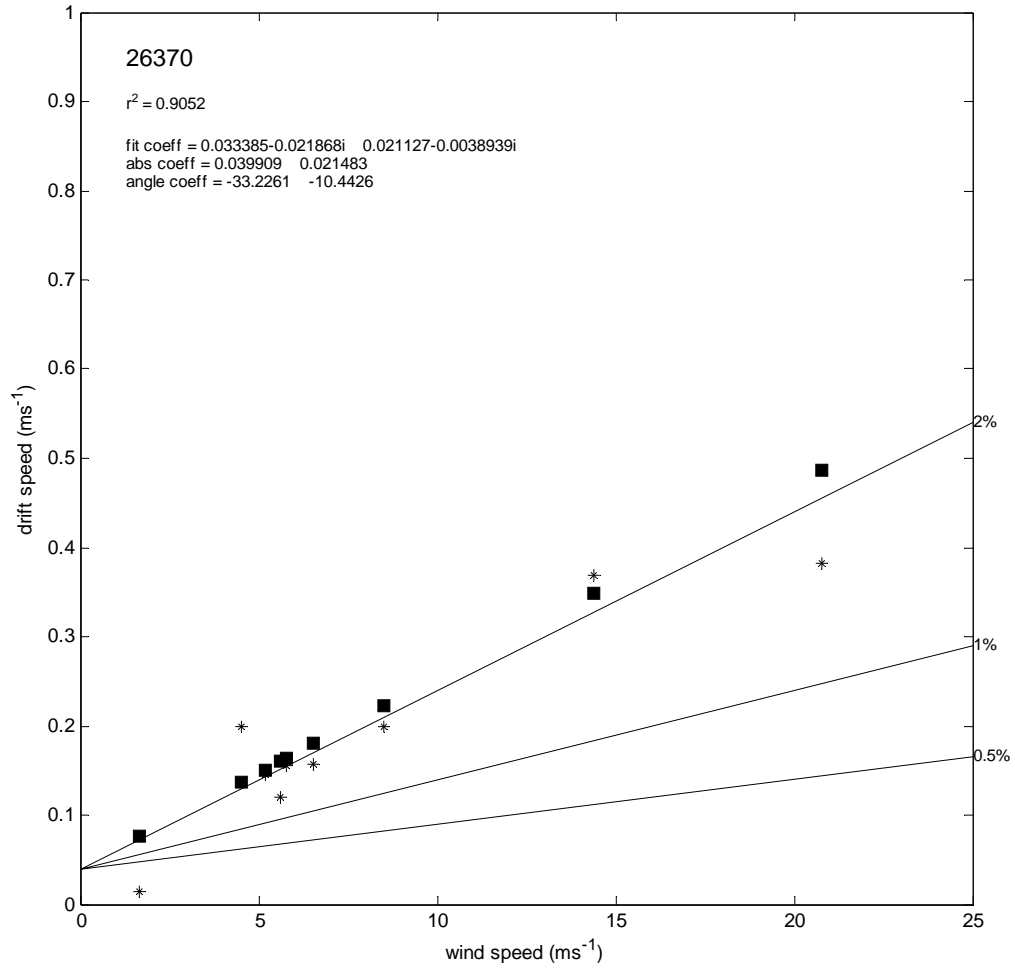


Figure 58 Scatter of 6-hourly low-pass filtered drift speed vs. wind speed for beacon 26370 before Feb. 20. Lines for various reponse are also shown. Squares indicate the predicted relationship from regression.

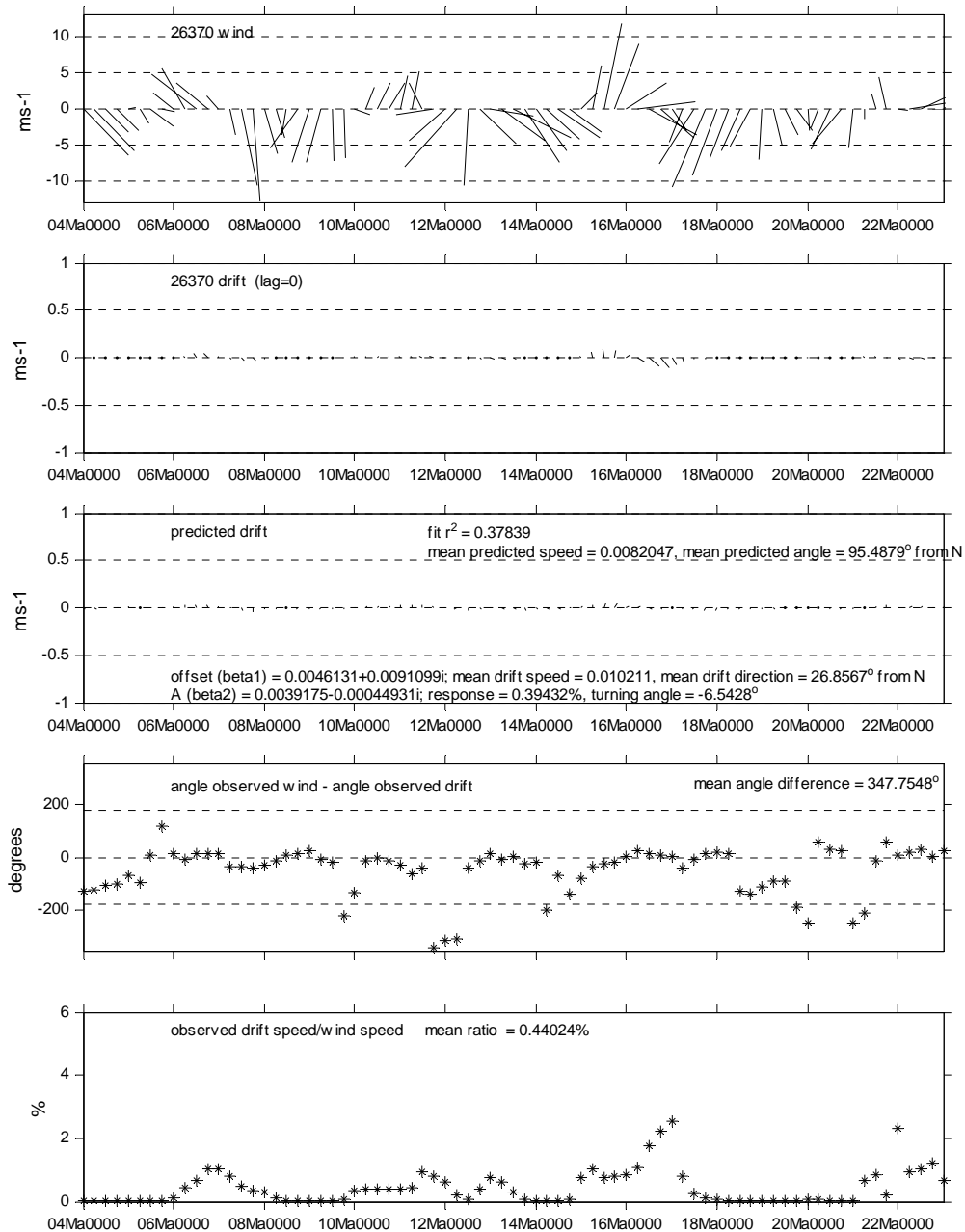


Figure 59 Results of complex least squares regression of wind and low-pass drift data for beacon 26370 after Mar 4. The figure shows hourly wind and beacon drift, the predicted drift values (ie. fitted series), the angle difference between wind vectors and drift vectors (with mean angle difference), and the ratio of drift speed to wind speed (with mean ratio).

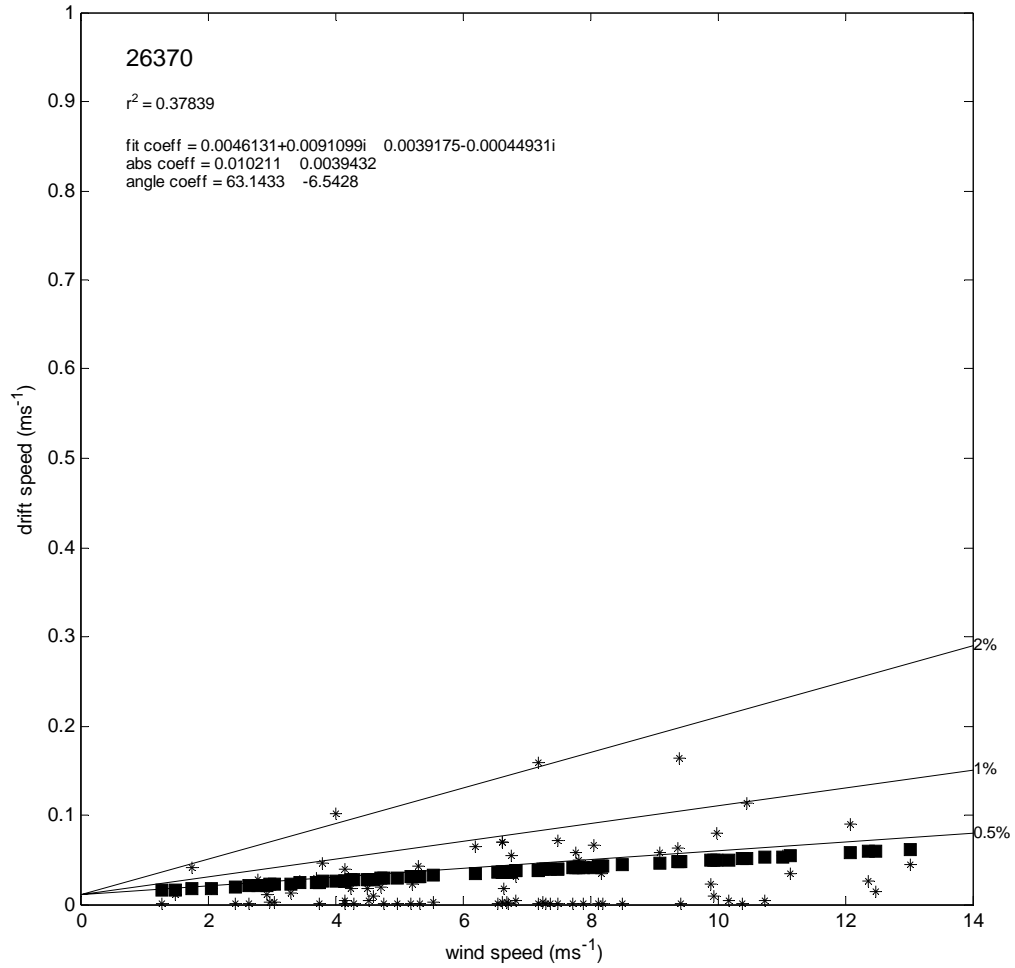


Figure 60 Scatter of 6-hourly low-pass filtered drift speed vs. wind speed for beacon 26370 after Mar. 4. Lines for various response are also shown. Squares indicate the predicted relationship from regression.

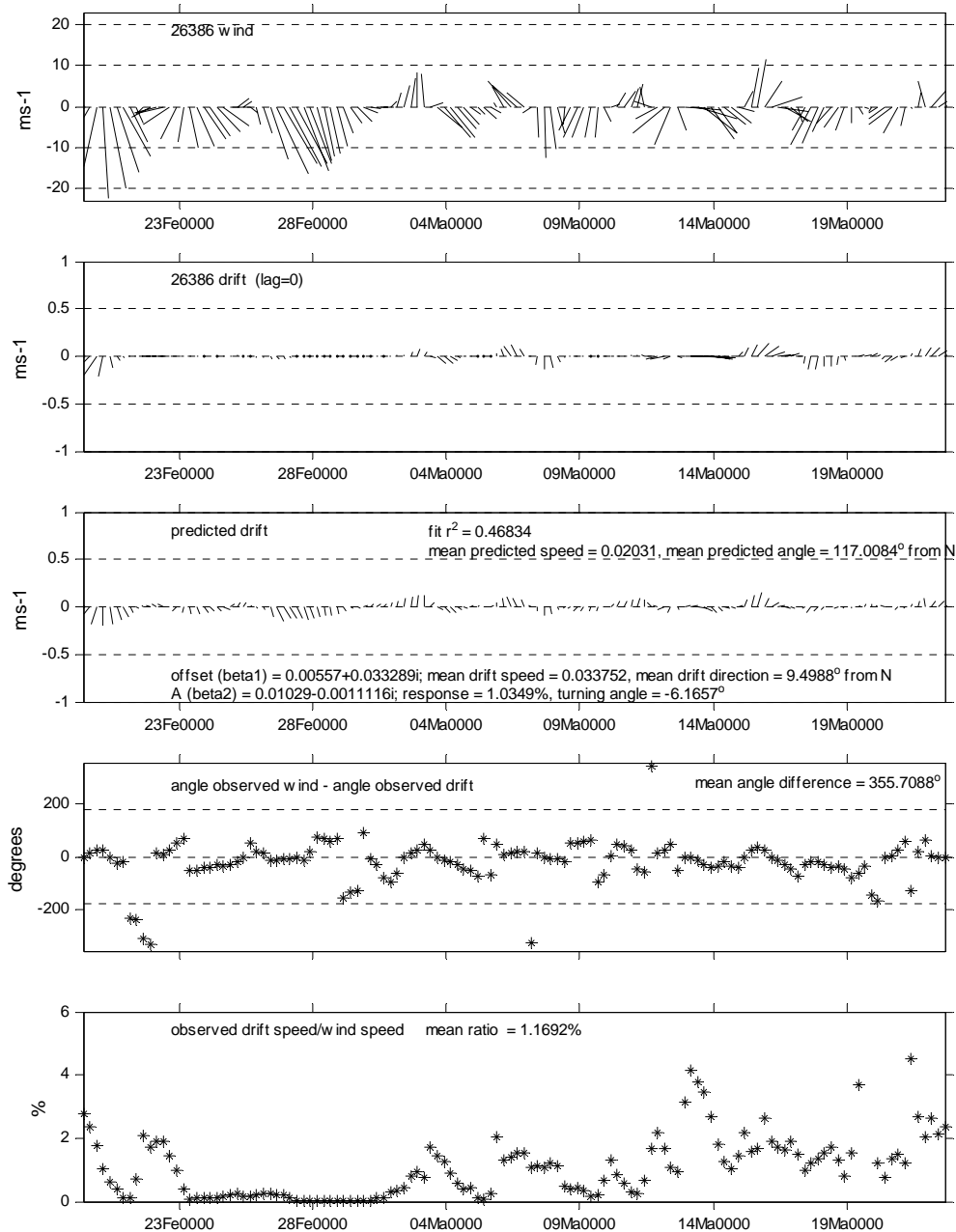


Figure 61 Results of complex least squares regression of wind and low-pass drift data for beacon 26386. The figure shows hourly wind and beacon drift, the predicted drift values (ie. fitted series), the angle difference between wind vectors and drift vectors (with mean angle difference), and the ratio of drift speed to wind speed (with mean ratio).

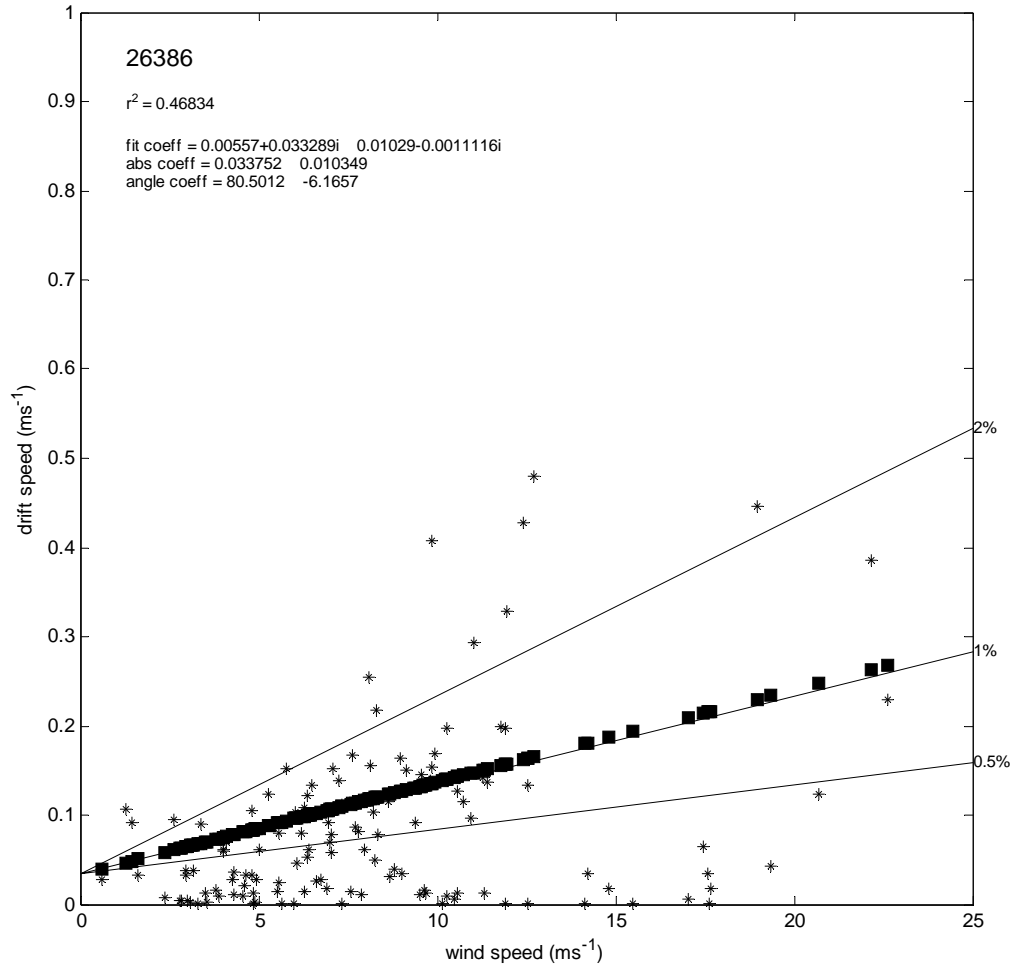


Figure 62 Scatter of 6-hourly low-pass filtered drift speed vs. wind speed for beacon 26386. Lines for various response are also shown. Squares indicate the predicted relationship from regression.

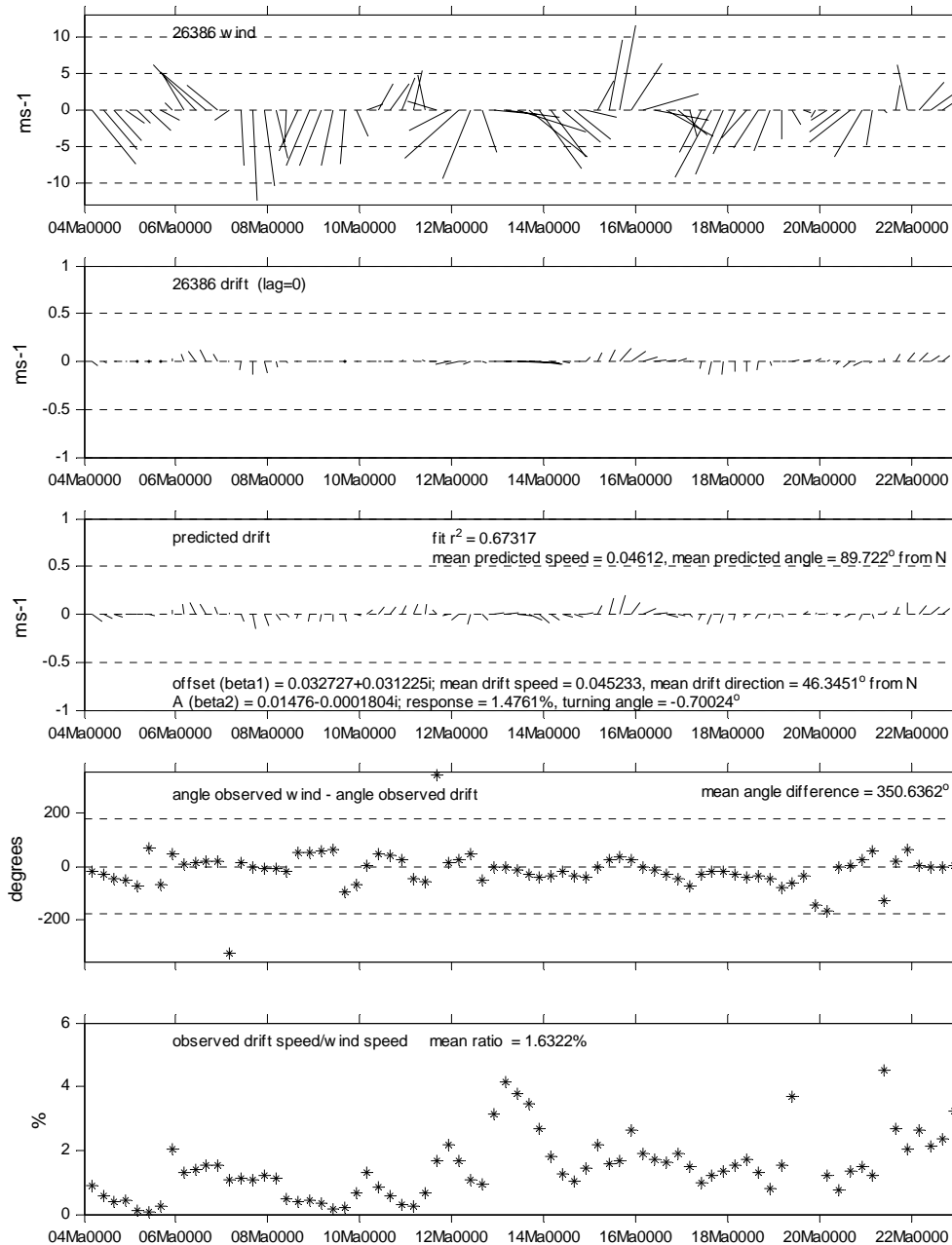


Figure 63 Results of complex least squares regression of wind and low-pass drift data for beacon 26386 after Mar. 4. The figure shows hourly wind and beacon drift, the predicted drift values (ie. fitted series), the angle difference between wind vectors and drift vectors (with mean angle difference), and the ratio of drift speed to wind speed (with mean ratio).

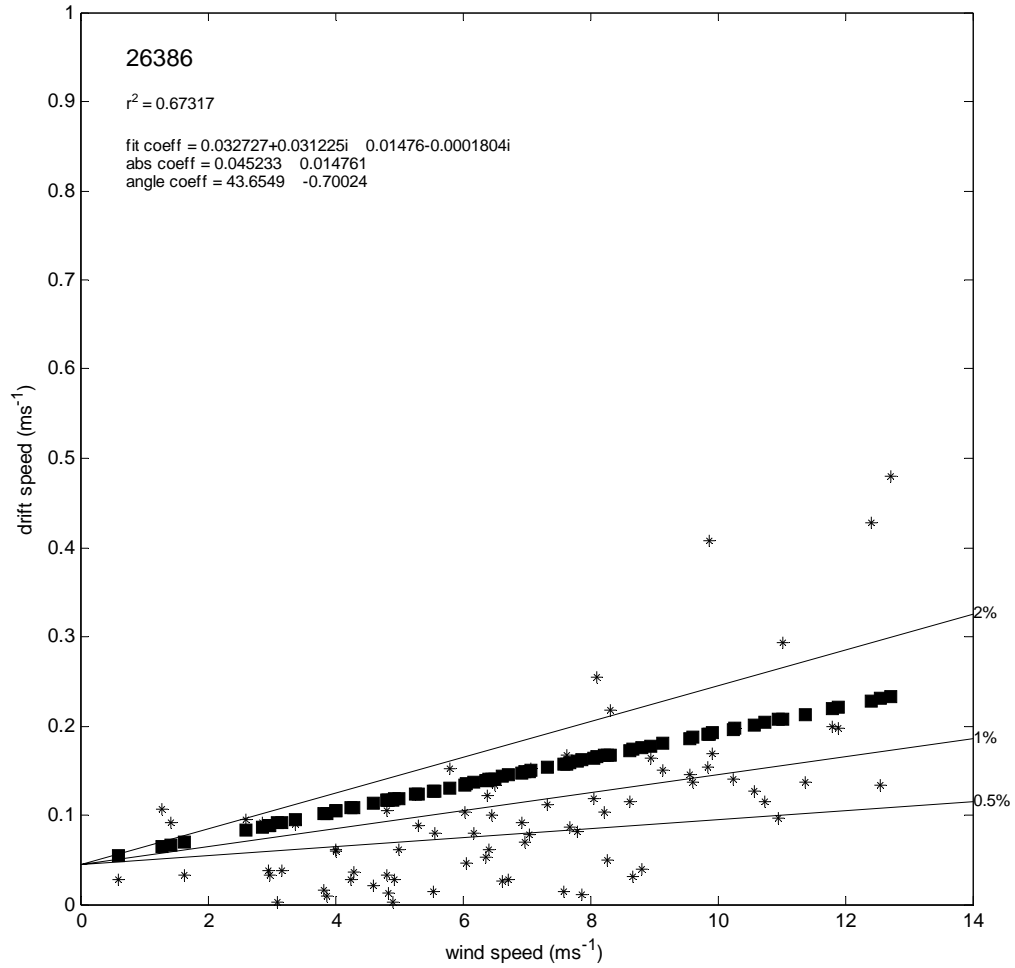


Figure 64 Scatter of 6-hourly low-pass filtered drift speed vs. wind speed for beacon 26386 after Mar. 4. Lines for various response are also shown. Squares indicate the predicted relationship from regression.

REFERENCES

- Greenan, B. J. W., S. J. Prinsenberg, and A. van der Baaren. 1997. Moored Acoustic Doppler Current Profiler Measurements on the Labrador Shelf, 1993-1994. Can. Tech. Rep. Hydrogr. Ocean Sci. 188: vii+149 p.
- Greenan, B. J. W., S. J. Prinsenberg. 1998. "Wind Forcing of Ice Cover in the Labrador Shelf Marginal Ice Zone". *Atmosphere-Ocean* 36(2), 71-93.
- van der Baaren A. and S. Prinsenberg. 2001. Satellite-tracked Ice Beacon Program, 1999-2001. Can. Tech. Rep. Hydrogr. Ocean. Sci. 214: x + 88 p.
- van der Baaren A. and S. Prinsenberg. 2000. Satellite-tracked Ice Beacon Tests for Accuracy and Positioning, 1997-1998. Can. Tech. Rep. Hydrogr. Ocean. Sci. 209: vii + 47 p.
- van der Baaren A. and S. Prinsenberg. 2000. Labrador Shelf and Gulf of St. Lawrence Sea Ice Program, 1995-1998. Can. Tech. Rep. Hydrogr. Ocean. Sci. 207: vii + 213 p.

ACKNOWLEDGEMENTS

We gratefully acknowledge the support given by the Program of Energy Research and Development (PERD) and the Canadian Space Agency. We are also very grateful for the helicopter support from the Canadian Coast Guard while working in Prince Edward Island. B. deTracey of BIO provided us with the archived meteorological forecast data for which we are grateful. S. Prinsenberg wishes to thank S. Holladay of Geosensors, Inc. for his work in the field. The authors also acknowledge the helpful comments of R. Pettipas, R. Anderson, and the assistance of M. Ouellet of MEDS.

4 APPENDIX I: A COMPARISON OF FORECAST MODEL WIND AND OBSERVED WIND

Meteorological data (speed and direction or velocity vector components, air temperature, and mean sea level pressure) are used regularly when analyzing oceanographic data. However, reliable concurrent meteorological measurements (“wind data”) are not always available. Oceanographers often use wind data supplied by Environment Canada from land stations, wave buoys, or from forecast model output to overcome this shortfall. Model output gives the best coverage but, theoretically, direct observations are more reliable.

In order to complete the ice beacon and wind analysis for this report a choice of three meteorological data sources was available: 3-hourly high resolution forecast output, 6-hourly low resolution forecast output, and 6-hourly analysis data. Using simple correlation analysis it was discovered that all three appeared to closely reflect observations with 90% variance accounted for on average. In general, it was found that winter winds are overestimated for land stations (forecast winds too strong). Summer winds, however, are underestimated for offshore regions but overestimated for land stations. If winter winds offshore over pack ice were underestimated as well, then ice drift gains obtained in the analysis of ice drift would be on the high side.

For the beacon analysis reported in the main part of this document, the 6-hourly forecast output was used since it proved to be most economic in terms of computing output, availability (already archived on site), and cost (none). In this appendix the correlation analysis of the gridded meteorological data to observations is presented. Gridded data are from prediction model output and the measured quantities are from meteorological stations (land sites) and ocean wave buoys (open water sites). The time frames used in the comparative study are “winter” (February 2004) for land stations and “summer” (June/July 2004) for wave buoy data.

In the last section of this appendix drift data for beacons 26370 and 26386 are regressed with the other two different wind records from the high resolution regional forecast model (3-hourly) and lower resolution analysis wind data. Results are compared to those of the main report where the low resolution 6-hourly forecast output was used.

4.1 Data

Model output data were supplied by the Canadian Meteorological Centre (CMC) in Dorval, Quebec (Environment Canada). Data were either purchased or obtained from an archive at the Bedford Institute of Oceanography (BIO). Station observations were supplied by the Marine Environmental Data Service (MEDS, Fisheries and Oceans Canada) as part of the Atlantic Zone Monitoring Program (original data from Environment Canada) and the wave buoy wind data were also supplied by the MEDS. The observed data were downloaded from the MEDS web site. Wave buoy data are only available from spring to autumn. The meteorological parameters studied were wind velocity vector components, air temperature, and mean sea level pressure. Model output

parameters give wind velocities at 10 m and air temperature at 2 m. Observations are unadjusted wind velocities at anemometer heights plus station/buoy elevation above sea level and air temperature at sensor height plus station/buoy elevation. Observed winds needed to be adjusted to a standard 10 m reference level. Land station anemometer heights are 10 m above the ground and temperature sensor heights are 2 m above the ground for all stations. Wave buoy anemometer and temperature sensor heights depend on type of buoy. To adjust the observed wind speeds to correctly compare them to 10 m model output wind speed we assumed neutral stability with a 10 m drag coefficient. U_{10} was computed following Smith (1988). The Matlab[®] code used for this computation is reprinted in Appendix III (§6) and can be found @ <http://woodshole.er.usgs.gov/operations/sea-mat/>; Air-Sea Toolbox.

Model output:

- 6-hourly model analysis data from regional model, interpreted to a $1^{\circ} \times 1^{\circ}$ grid (purchased)
- 6-hourly model prognostic data from low resolution regional model grid, interpreted to a $1^{\circ} \times 1^{\circ}$ grid (lower left corner @ 20N, -80W) (archived)
- 3-hourly model prognostic data from high resolution regional model grid, interpreted to a $0.21^{\circ} \times 0.21^{\circ}$ grid (lower left corner @ 20N, -80W) (archived)

The analysis data must be purchased from CMC directly (contact Marc Besner @RPN = CMC, Dorval) at the cost of the extraction, ordinarily \$90/hr where the total extraction costs about \$500 regardless of quantity in most cases. These data can be obtained in any format the user wishes but arbitrarily a $1^{\circ} \times 1^{\circ}$ grid was chosen. It is possible to download forecast data daily in GRIB (WMO format) *gratis* through a user agreement with CMC. Advantages of using prognostic data over analysis data are that there are many more parameters archived, higher temporal frequencies and spatial resolution are available, and it is more readily available. The advantage of using analysis data over prognostic data is that these data are model output data that have been “corrected” by observations.

The following paragraph is an excerpt from November 2004 correspondence with Marc Besner @ RPN, Dorval regarding analysis and prognostic data:

”As for the meteorological variables that you require, most of them are available within our operational analysis system. These are:

UU and VV surface winds

mean sea level pressure (MSLP) : I presume that this is what you are looking for and not actually surface pressure. Please confirm.

surface air temperature

surface dew-point depression: we do not analyze dew point but rather dew-point depression (temperature-dew point).

However, precipitation and cloud cover are not analyzed variables. We do have a low resolution “experimental” precipitation analysis but it is of low quality. These parameters are really only available as outputs from the GEM model forecasts. Also, precipitation estimates are only reasonable for forecast time greater or equal to 6 hours for these types of meteorological fields. This is due to the fact that these variables require a spin-up time at the beginning of the model integration.

Analysis data from our archive are available every 6 hours (00, 06, 12 and 18Z). Model outputs from GEM regional model are available at a higher temporal frequency but we would recommend that you use the 6 and 12 hour forecast of the 00Z and 12Z model runs as precipitation and cloud cover estimates

On another subject, we confirm that you already receive at BIO, the 3-hourly forecast data from the GEM-regional model on a 24km x 24 km grid resolution on a specific geographical area. **Note that the 00 hour forecast of that dataset in pressure coordinates actually corresponds to the analysis at that time.** The data format is a special ASCII format which was developed a very long time ago. Note that this data format is no longer supported at our end. “

It seems that the 0000 hour 3-hourly forecast data should be identical to the 0000 analysis data since the latter initiates the former.

Observations:

- Station data from Charlottetown; (station elevation = 48.8 m), Summerside (station elevation = 19.5 m), and Iles de la Madeleine (station elevation = 10.4 m), February 2004
- Wave buoy data from Northumberland Strait, Gulf of St. Lawrence, June 2004:
 1. Watchkeeper buoy 44150 (moored) anemometer @ 3.3 m above water line and air temperature height = 2.7 m above waterline: 46.85N, 64.64W
 2. 3 m discus buoy 44161 anemometers @ 5.25 m and 4.27 m above waterline and air temperature sensors at 3.73 m above waterline (used only data from 5.25 m anemometer)

The effective heights of the anemometers are:

Charlottetown	58.8 m
Summerside	29.5 m
Iles de la Mad.	20.4 m
44150	3.3 m
44161	5.25 m

The locations of the weather stations and wave buoys are shown in Figure 65. One wave buoy, 44150, is more exposed than the other. The more sheltered buoy (44161) is tucked along the south shore of Northumberland Strait.

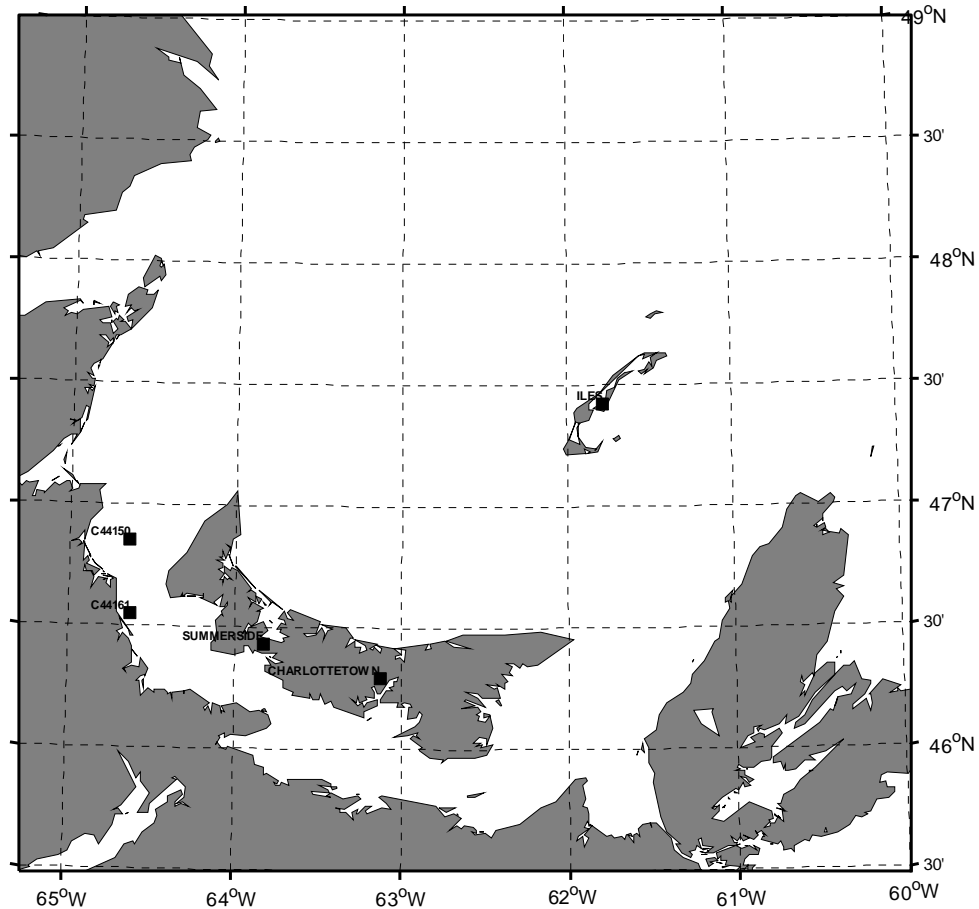


Figure 65 Map showing locations of Environment Canada weather stations and locations of wave buoys equipped to monitor atmosphere.

4.1.1 Observations @ hourly intervals

Figure 66 and Figure 67 show the hourly observations for stations in Iles de la Madeleine, Charlottetown, and Summerside for February 2004 and June 2004, respectively. Summerside and Charlottetown show similar features, as expected, including the February 19-20 storm. Low frequency features, especially east-west wind speed, are similar at all stations. Winter Iles de la Madeleine observations deviate from the other two stations in that low frequency features seem to slightly lag the other two. Summer Iles de la Madeleine mean sea level pressure observations appear to slightly lag and are slightly more intense than those same observations from the other two land stations. Wind speeds for July at Iles de la Madeleine also differ in low frequency intensity and timing from wind speeds at Charlottetown and Summerside (Figure 68). Note that Summerside is missing almost 10 days of data in the first two weeks of the month so that only data after 15 July were used for Summerside in summer.

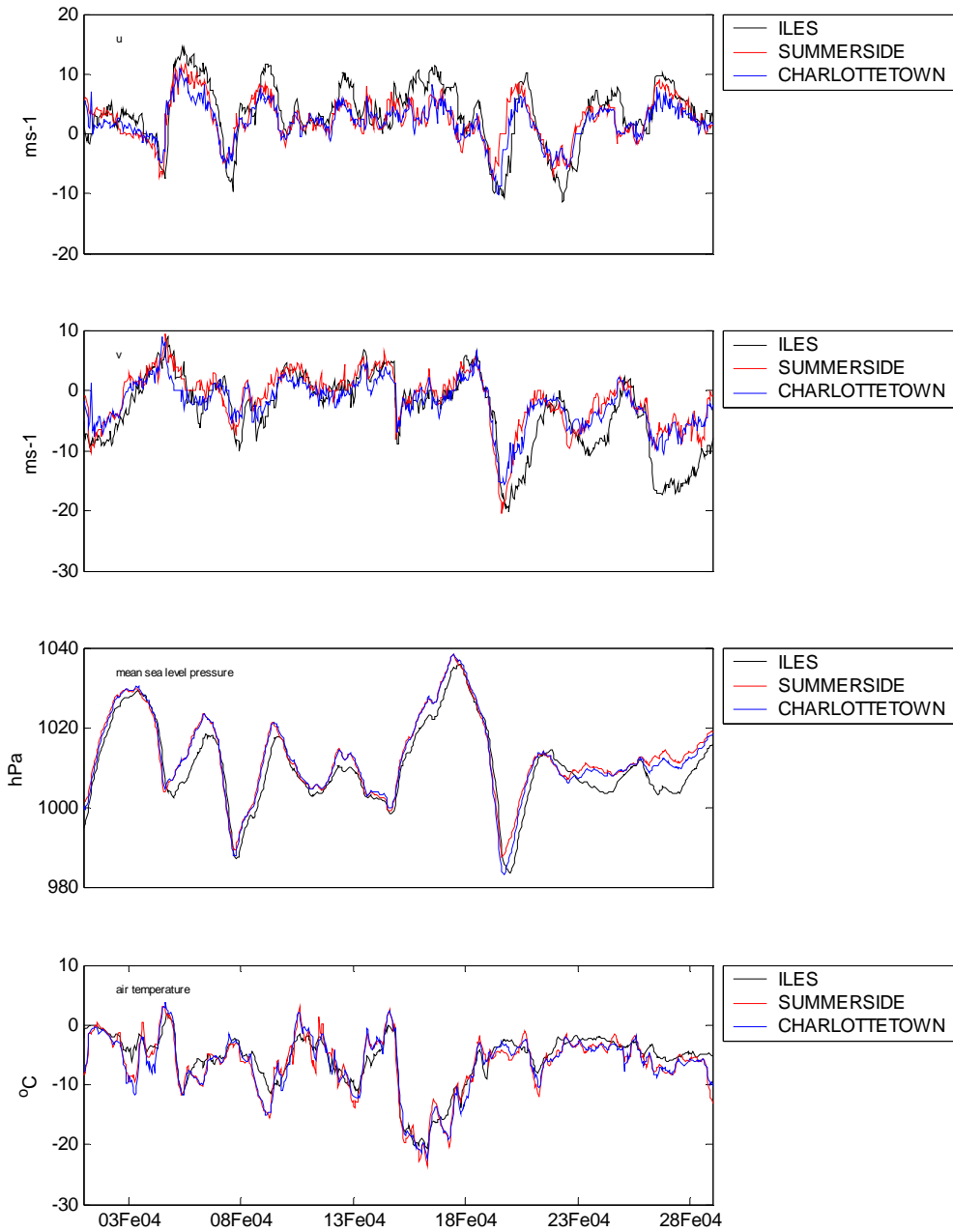


Figure 66 Wind velocity components, mean sea level pressure, and air temperature for Iles de la Madeleine, Summerside, and Charlottetown in February 2004; wind speed has been adjusted to 10 m reference level

Figure 69 shows the hourly observations measured by the wave buoys that were located in the Northumberland Strait during June 2004. Both buoys show similar wind features as expected but the measurements of air temperature, sea level pressure, and sea surface temperature are slightly different for high frequency features. Low frequency features and trends are similar for both buoys.

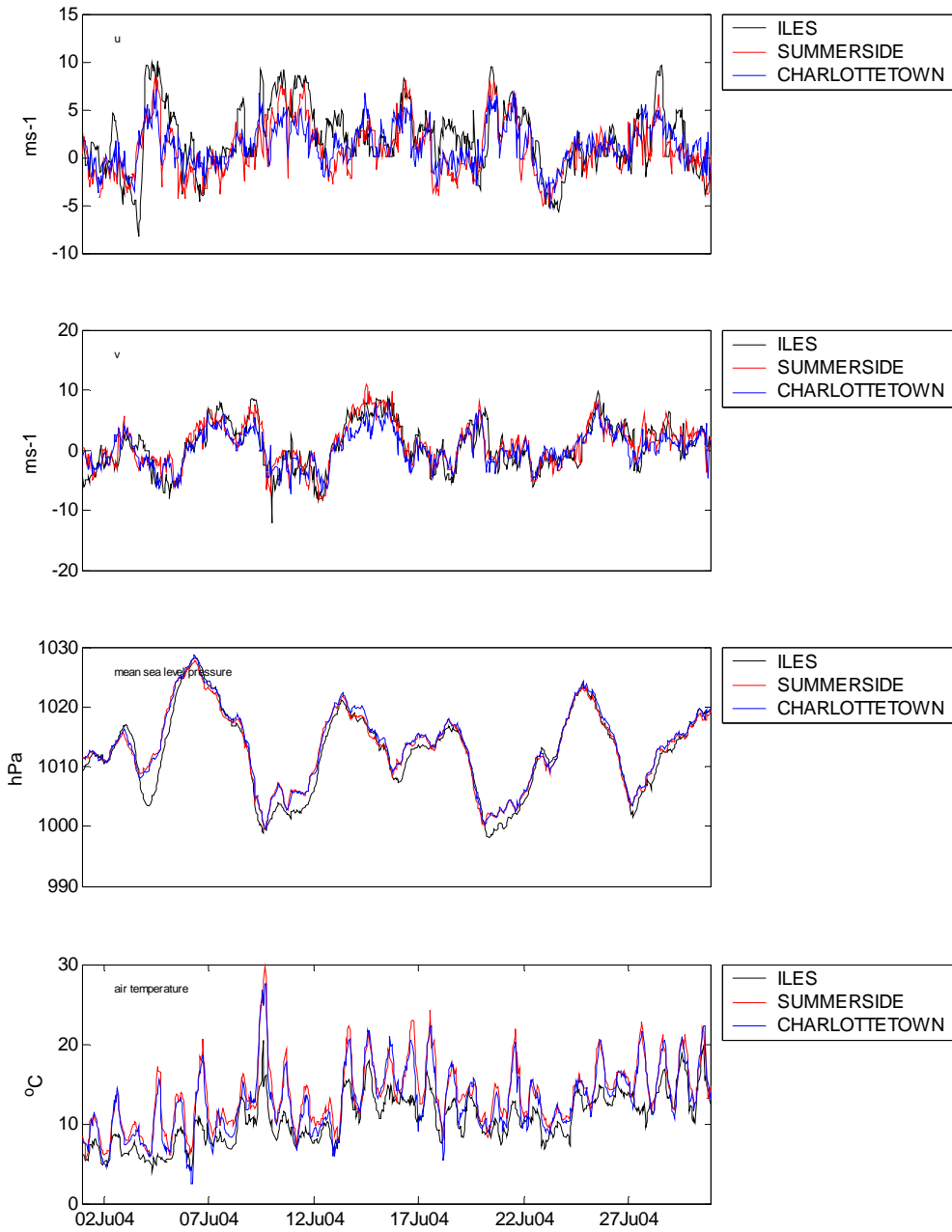


Figure 67 Wind velocity components, mean sea level pressure, and air temperature for Iles de la Madeleine, Summerside, and Charlottetown in June 2004; wind speed has been adjusted to 10 m reference level

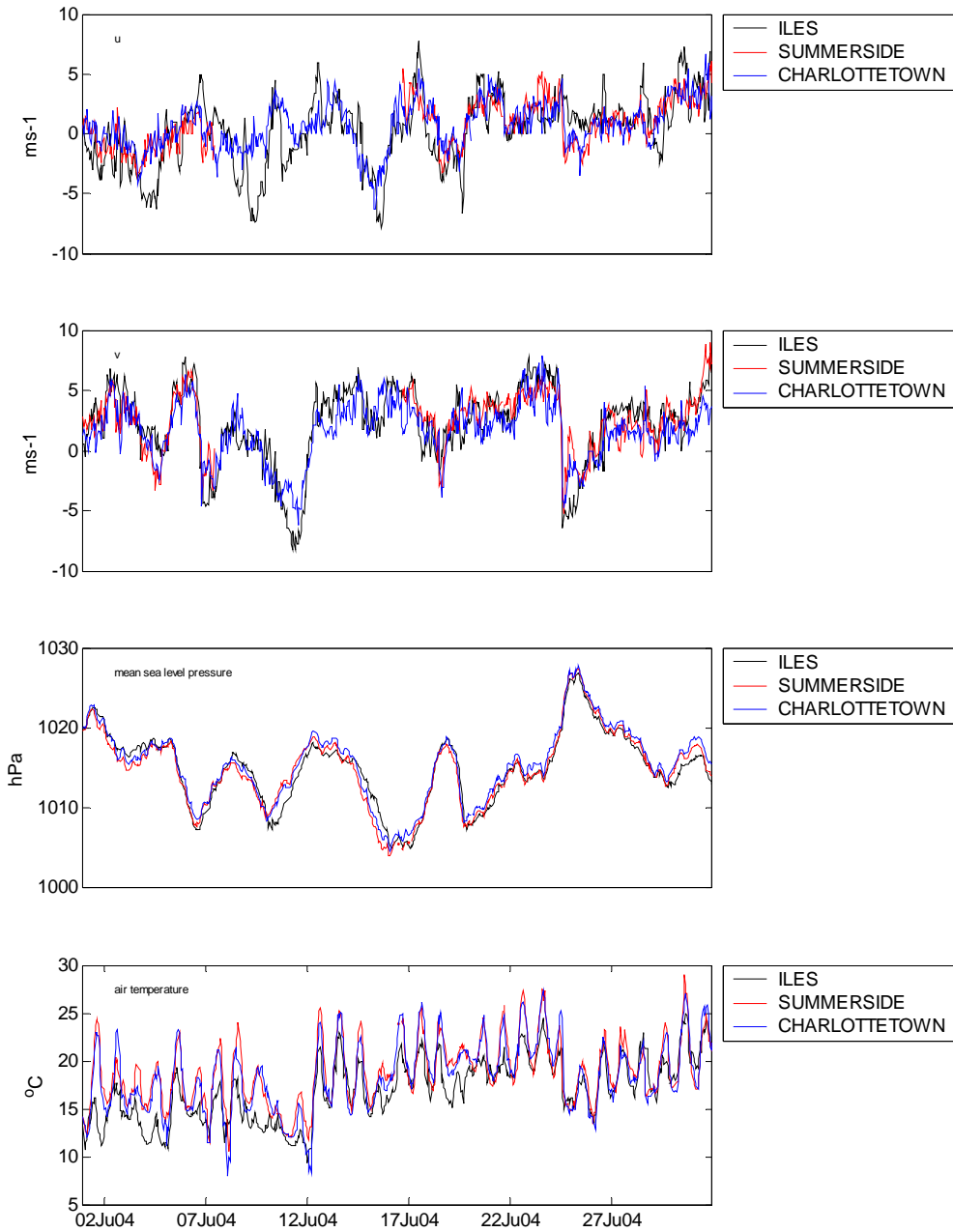


Figure 68 Wind velocity components, mean sea level pressure, and air temperature for Iles de la Madeleine, Summerside, and Charlottetown in July 2004; wind speed has been adjusted to 10 m reference level

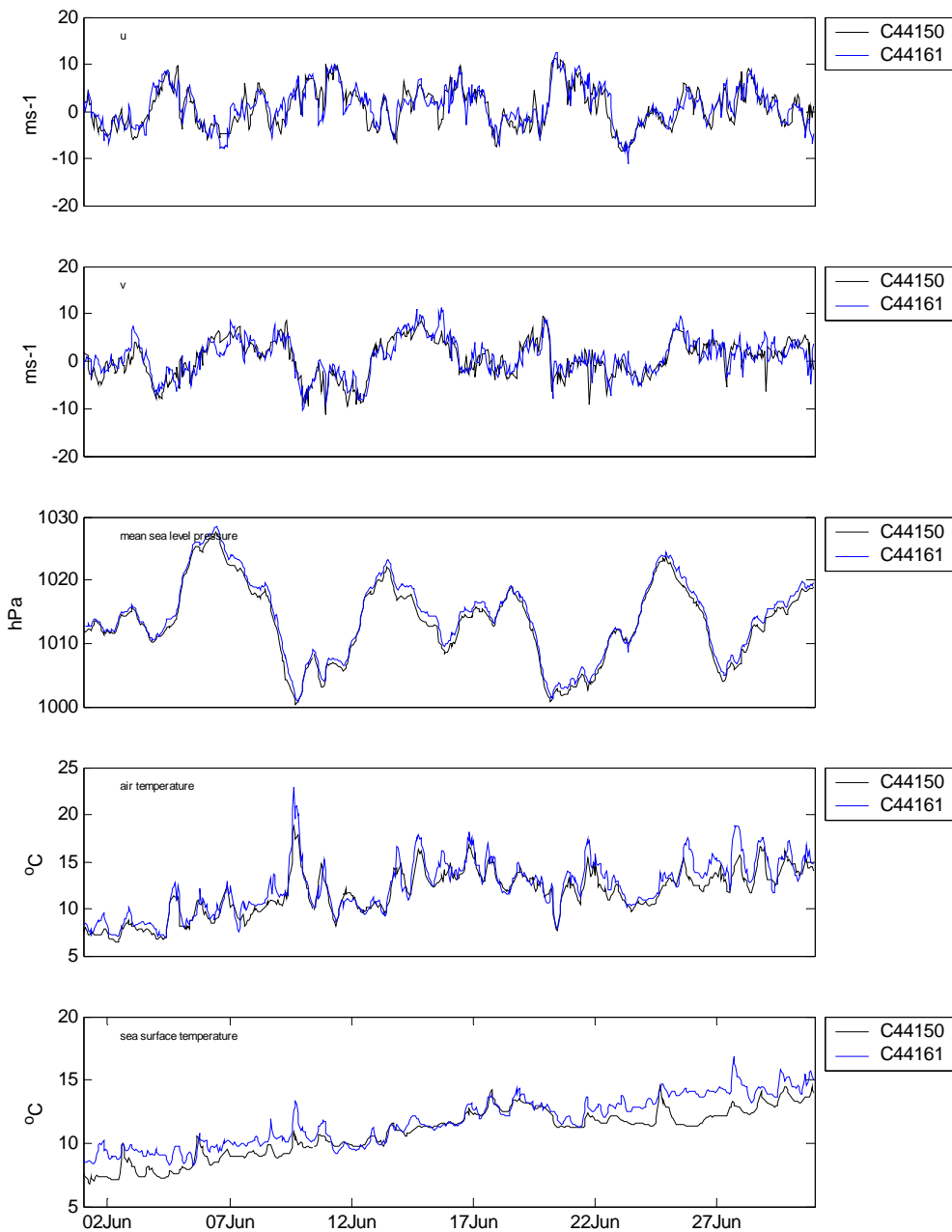


Figure 69 Wind velocity components, mean sea level pressure, and air temperature for 2 wave buoys in the Northumberland Strait and in the Gulf of St. Lawrence in June 2004; wind speed has been adjusted to 10 m reference level

A wind and wave climate atlas was published in 1993 for Transport Canada (Eid et al., 1993) giving monthly wind statistics. The next four figures are reproduced from this atlas as posted on the Marine Environmental Data Service web site (<http://www.meds-sdmm.dfo-mpo.gc.ca/alphapro/wave/TDCAtlas/TDCAtlasGS.htm>) for the Gulf of St. Lawrence, region Magdalen. Figure 70 to Figure 74 show that in February the monthly mean wind speed is around 17.7 kts $\sim 9.1 \text{ ms}^{-1}$ and in June/July it is 15.2 and 15.0 kts \sim

7.8 and 7.7 ms^{-1} , respectively. For the most part the wind comes from the northwest in February and southwest in June and July.

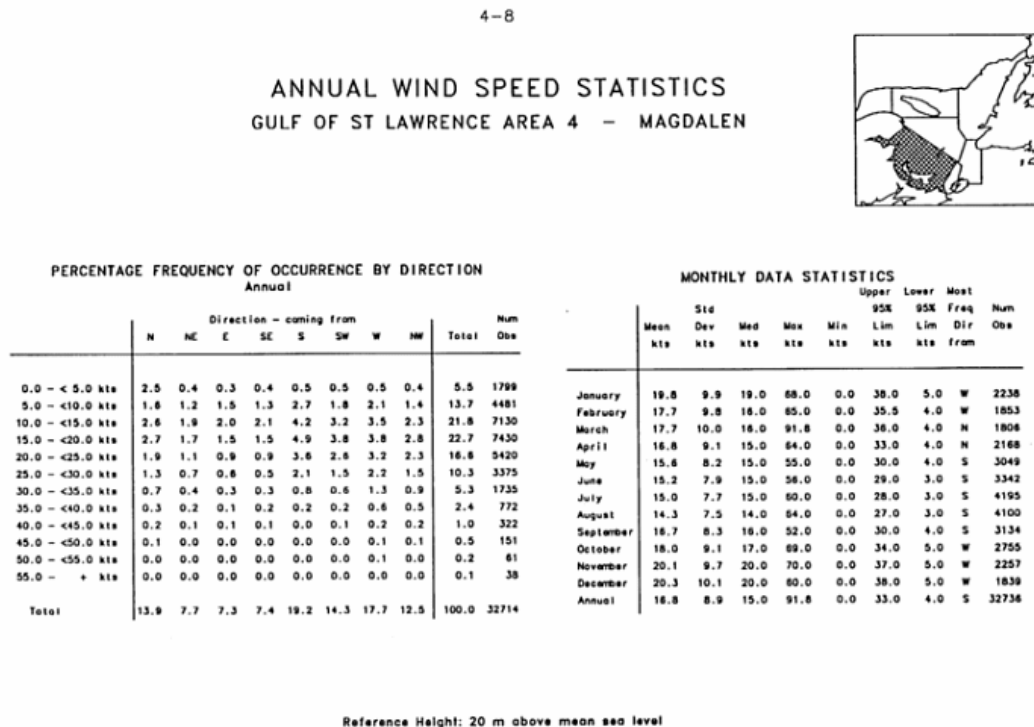


Figure 70 Annual wind speed statistics for the Gulf of St. Lawrence, Magdalen taken from <http://www.meds-sdmm.dfo-mpo.gc.ca/alphapro/wave/TDCAtlas/TDCAtlasGS.htm>

4-1

ANNUAL WIND STATISTICS
GULF OF ST. LAWRENCE AREA 4 - MAGDALEN

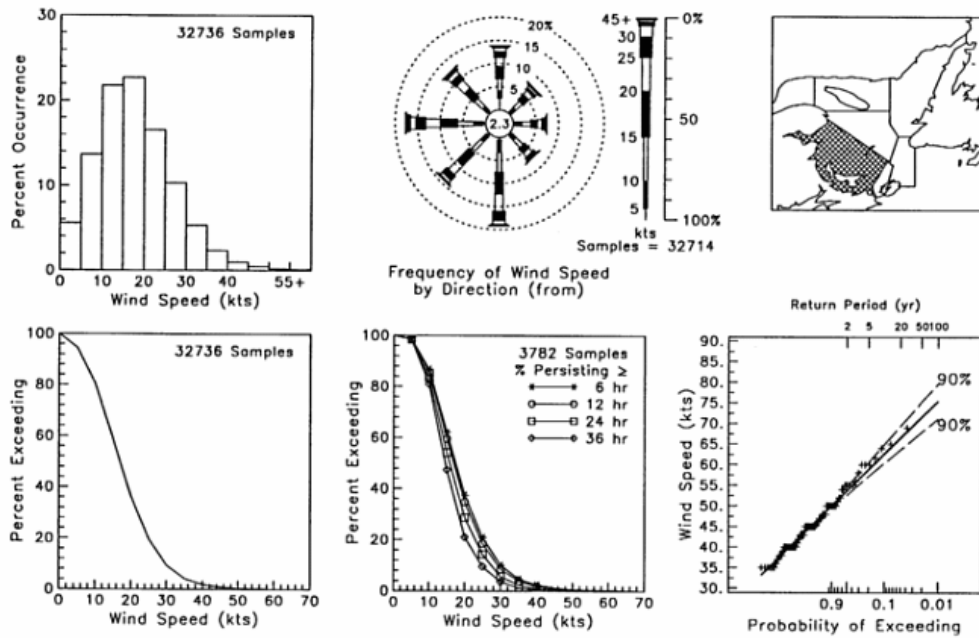


Figure 71 Annual wind statistics for the Gulf of St. Lawrence, Magdalen taken from <http://www.meds-sdmm.dfo-mpo.gc.ca/alphapro/wave/TDCAtlas/TDCAtlasGS.htm>

4-2

MONTHLY WIND STATISTICS
 GULF OF ST. LAWRENCE AREA 4 - MAGDALEN
 FREQUENCY OF WIND SPEED BY DIRECTION (FROM)

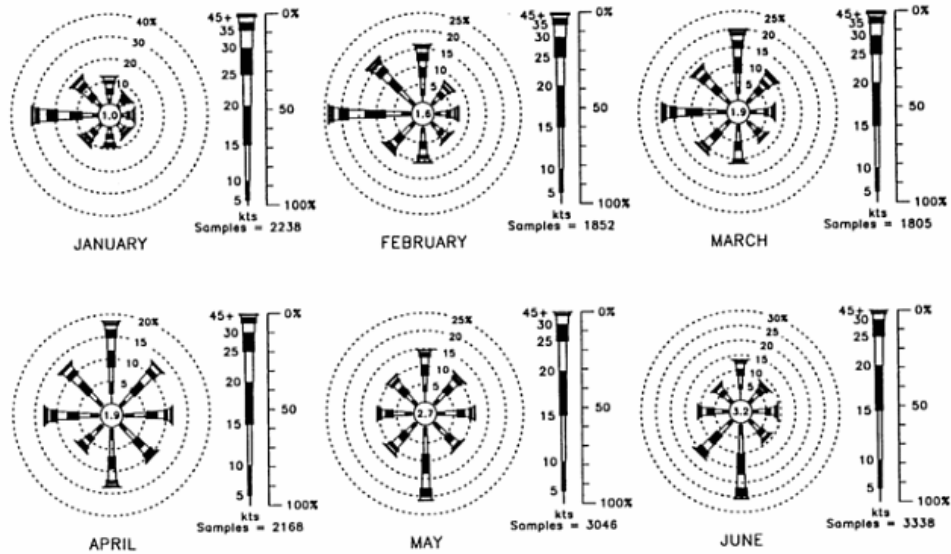


Figure 72 Monthly wind statistics: frequency of wind speed by direction for the Gulf of St. Lawrence, Magdalen taken from <http://www.meds-sdmm.dfo-mpo.gc.ca/alphapro/wave/TDCAtlas/TDCAtlasGS.htm>

4-4

MONTHLY WIND STATISTICS
GULF OF ST. LAWRENCE AREA 4 - MAGDALEN

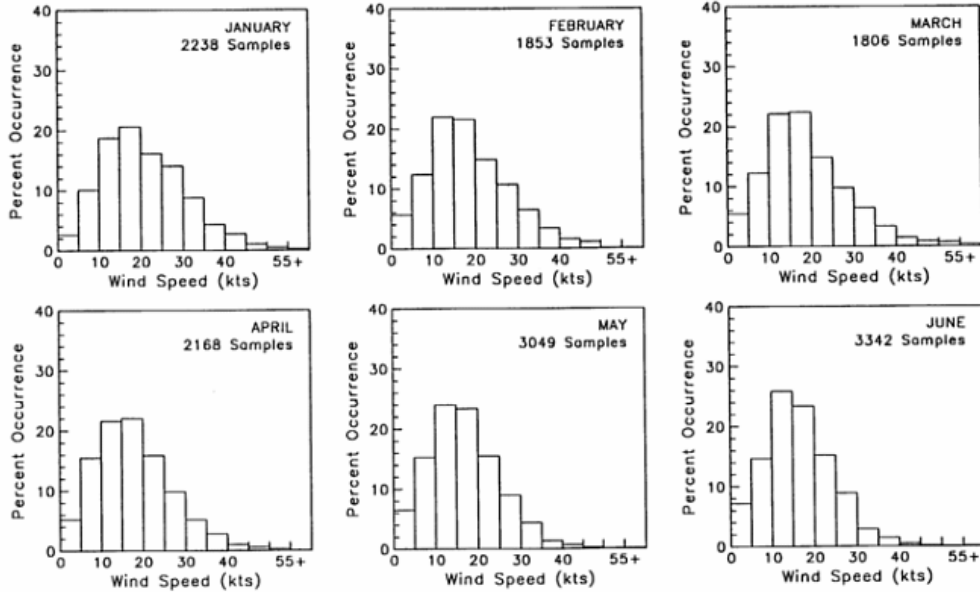


Figure 73 Monthly wind statistics: percent occurrence of wind speed for the Gulf of St. Lawrence, Magdalen taken from <http://www.meds-sdmm.dfo-mpo.gc.ca/alphapro/wave/TDCAtlas/TDCAtlasGS.htm>

4-6

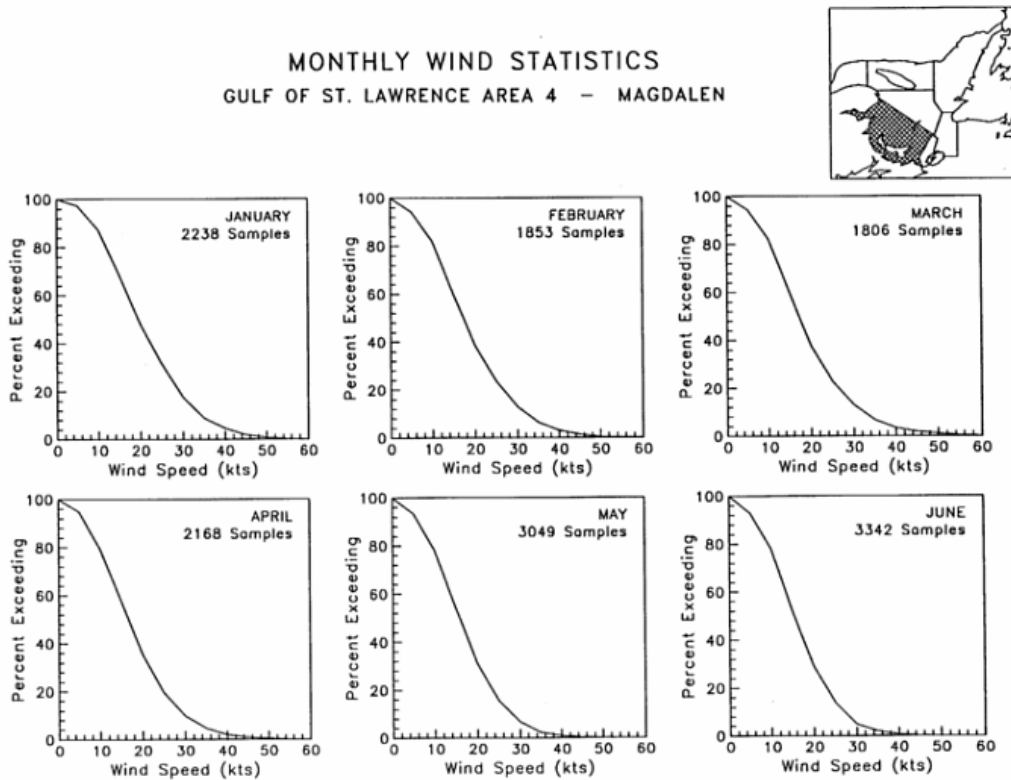


Figure 74 Monthly wind statistics: percent exceeding of wind speed for the Gulf of St. Lawrence, Magdalen taken from <http://www.meds-sdmm.dfo-mpo.gc.ca/alphapro/wave/TDCAtlas/TDCAtlasGS.htm>

4.2 Analysis

The model output was interpolated to match the time that of data and at the locations of each of the wave buoys and the weather stations. A simple correlation was performed to see how closely the scalar observations were related from each pairing of model output and observations. A complex least squares fit was performed to see how closely the vectors were related (model wind velocities to the observed wind velocities). Results for each pairing are given in graphic and tabular form.

From Table 6 we see that the scalar quantity correlations are high between each of the three land stations and the three different model output records (0.8 to 1.0) in winter. Table 7 lists the correlation coefficients for the summer data sets. It shows high correlations for all four parameters (>0.85) when model output are correlated with the buoy data but lower values when model output are correlated with land station data ($>0.67-0.97$). In both sets of observation data the mean sea level pressure gave the best correlation with model output.

Table 6 Coefficient of correlation: winter forecast and analysis output with observed winter data

R (coefficient of correlation)	Analysis	6-hrly low res.	3-hrly high res.
WINTER			
Charlottetown			
	U	0.79	0.81
	V	0.81	0.83
	MSLP	0.96	0.96
	T	0.86	0.86
Summerside			
	U	0.75	0.78
	V	0.80	0.82
	MSLP	0.97	0.97
	T	0.81	0.81
Iles de la Madeleine			
	U	0.83	0.84
	V	0.90	0.90
	MSLP	0.97	0.97
	T	0.90	0.90

Table 7 Coefficient of correlation: summer forecast and analysis output with observed summer data

R (coefficient of correlation)	Analysis	6-hrly low res.	3-hrly high res.	
SUMMER				
Buoy 44150				
	U	0.93	0.88	0.87
	V	0.93	0.88	0.92
	MSLP	1.00	1.00	0.99
	T	0.86	0.83	0.93
Buoy 44161				
	U	0.92	0.81	0.81
	V	0.93	0.88	0.91
	MSLP	1.00	1.00	0.99
	T	0.86	0.83	0.94
Charlottetown				
	U	0.70	0.67	0.79
	V	0.79	0.75	0.79
	MSLP	0.97	0.97	0.96
	T	0.82	0.73	0.70
Summerside				
	U	0.79	0.76	0.68
	V	0.80	0.77	0.76
	MSLP	0.97	0.97	0.96
	T	0.79	0.75	0.57
Iles de la Madeleine				
	U	0.78	0.77	0.79
	V	0.85	0.83	0.84
	MSLP	0.98	0.97	0.96
	T	0.87	0.88	0.81

Table 8 and Table 9 show that the wind speed is overestimated by the models for the winter and summer land stations and Table 9 shows that it is underestimated in the summer for the offshore buoys. The analysis wind produced the best R^2 results when regressed to summer wind observations (Table 9) explaining more than 86% of the variance in the offshore data and more than 60% of the variance in the land station data. Also, for the summer data, the models overestimated the wind speed more for the more sheltered wave buoy, 44161, than for the one in north-western Northumberland Strait (44150).

Table 8 Regression statistics: winter forecast and analysis wind velocity output to observed winter wind velocity data

Least Squares Fit Statistics				
WINTER				
Charlottetown		Analysis	6-hrly low res.	3-hrly high res.
	R^2	0.72	0.74	0.78
	$ \bar{\theta} $	0.04	0.00	0.03
	\bar{A} (%)	61.04	52.41	61.08
Summerside		Analysis	6-hrly low res.	3-hrly high res.
	R^2	0.75	0.77	0.80
	$ \bar{\theta} $	0.31	0.27	0.27
	\bar{A} (%)	71.16	72.03	72.26
Iles de la Madeleine		Analysis	6-hrly low res.	3-hrly high res.
	R^2	0.84	0.84	0.87
	$ \bar{\theta} $	0.15	0.13	0.14
	\bar{A} (%)	86.52	78.12	80.81

Table 9 Regression statistics: summer forecast and analysis wind velocity output to observed summer wind velocity data

Least Squares Fit Statistics				
SUMMER				
Buoy 44150		Analysis	6-hrly low res.	3-hrly high res.
	R^2	0.86	0.77	0.84
	$ \bar{\theta} $	-0.03	0.03	0.06
	\bar{A} (%)	106.29	98.43	89.47
Buoy 44161		Analysis	6-hrly low res.	3-hrly high res.
	R^2	0.86	0.73	0.82
	$ \bar{\theta} $	0.03	0.08	0.16
	\bar{A} (%)	118.10	110.11	107.74
Charlottetown		Analysis	6-hrly low res.	3-hrly high res.
	R^2	0.64	0.60	0.80
	$ \bar{\theta} $	-0.30	-0.28	-0.13
	\bar{A} (%)	62.91	53.32	62.24
Summerside		Analysis	6-hrly low res.	3-hrly high res.
	R^2	0.64	0.60	0.51
	$ \bar{\theta} $	0.06	0.11	-0.15
	\bar{A} (%)	75.75	75.36	54.36
Iles de la Madeleine		Analysis	6-hrly low res.	3-hrly high res.
	R^2	0.72	0.69	0.79
	$ \bar{\theta} $	-0.07	-0.07	0.00
	\bar{A} (%)	78.95	73.92	68.93

4.2.1 Compare Charlottetown; winter

4.2.1.1 Compare Charlottetown with analysis 6-hourly; winter

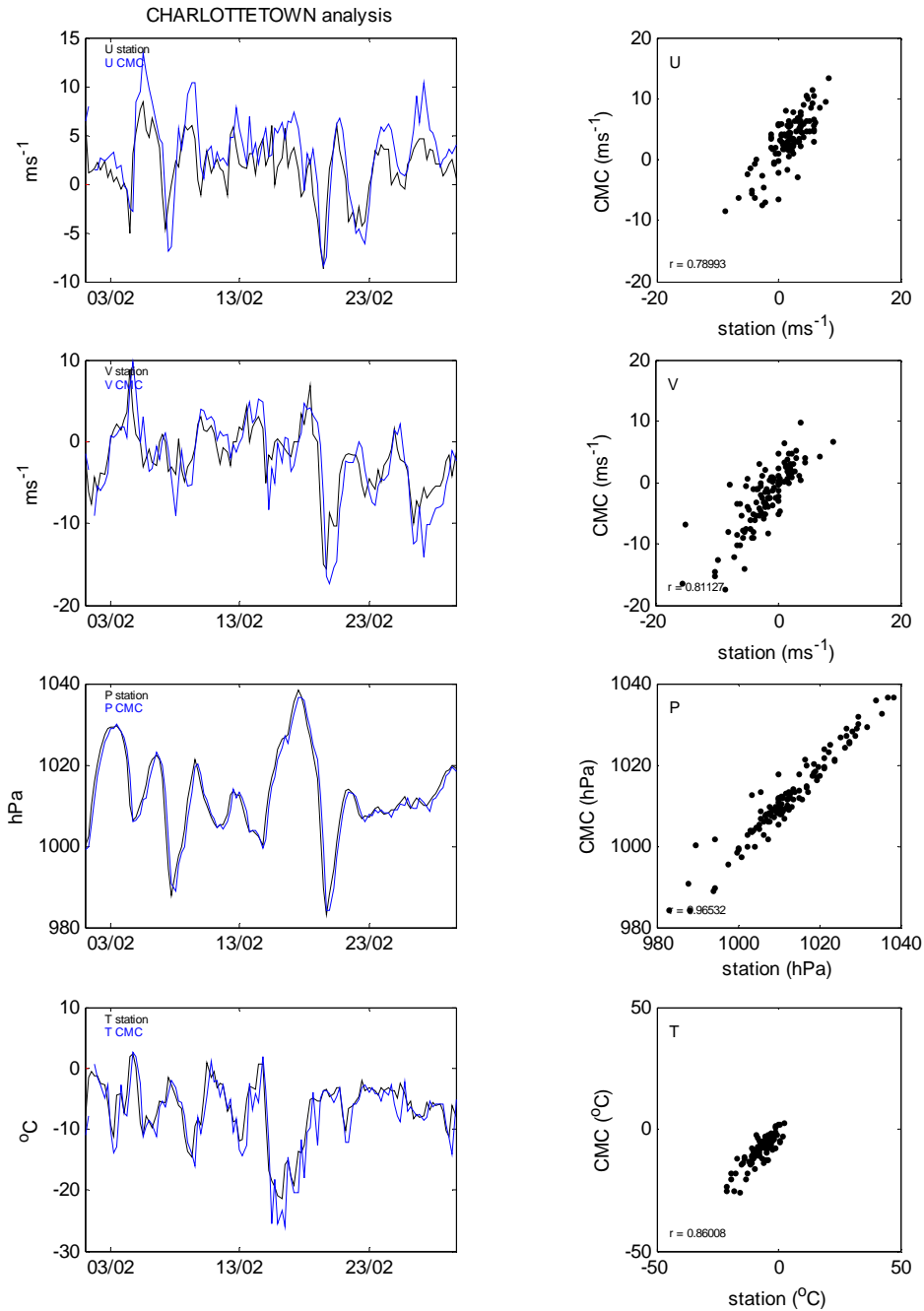


Figure 75 Time series of Charlottetown winter meteorological observations and 6-hourly analysis output; scatter plots of the same with correlation coefficients

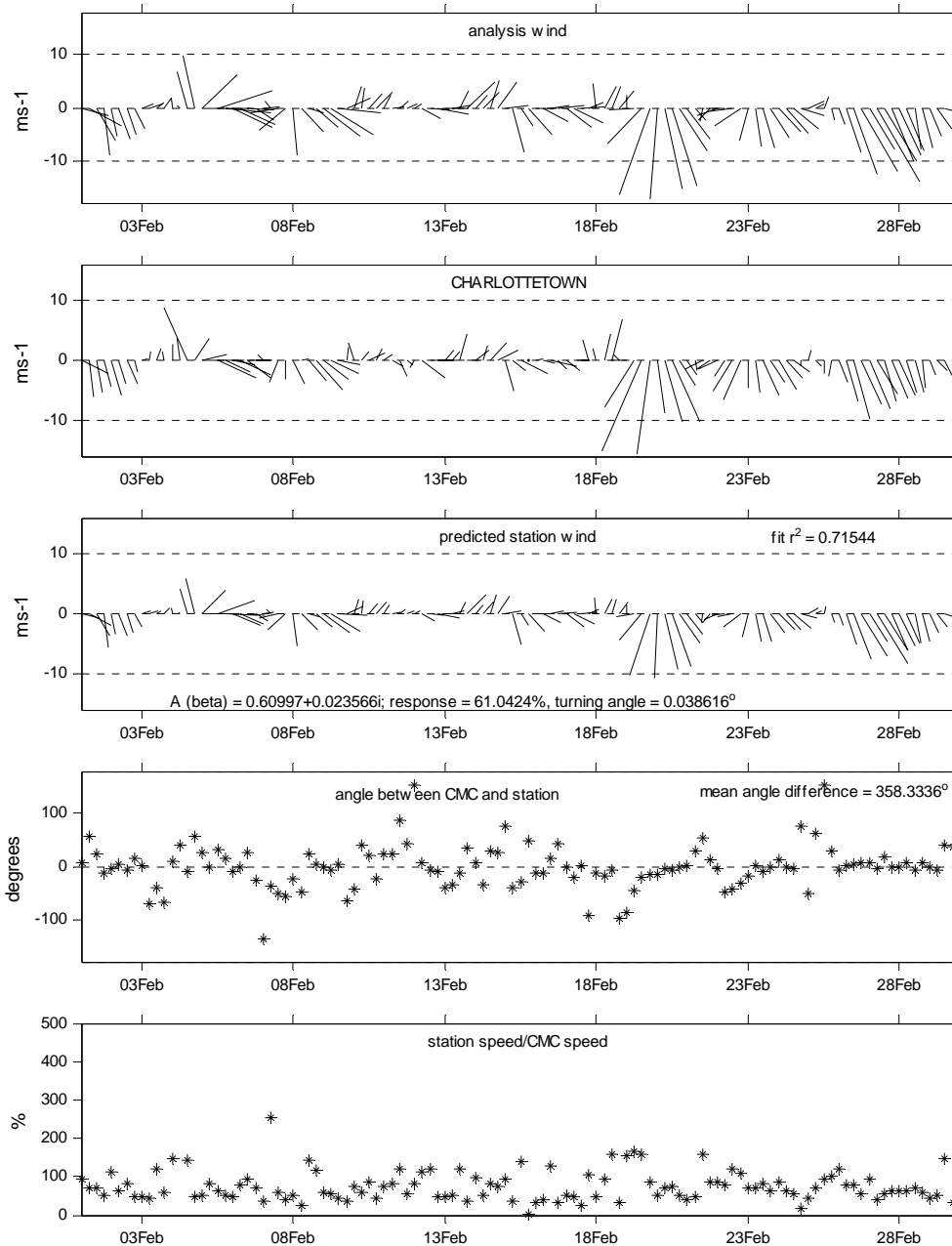


Figure 76 Time series of Charlottetown winter wind vector observations and 6-hourly analysis output with results of least squares fit

4.2.1.2 Compare Charlottetown with low resolution forecast 6-hourly; winter

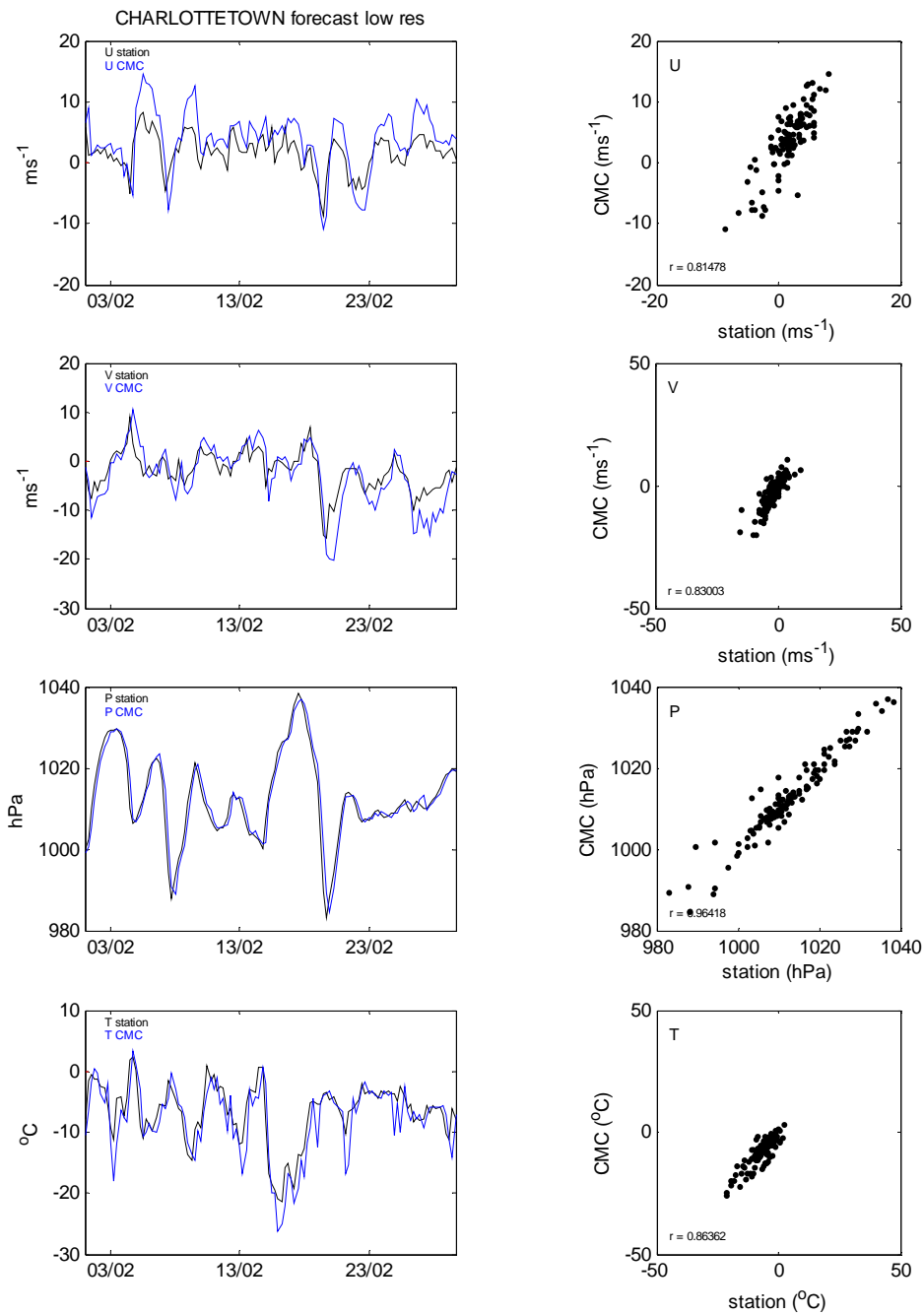


Figure 77 Time series of Charlottetown winter meteorological observations and 6-hourly low resolution forecast output; scatter plots of the same with correlation coefficients

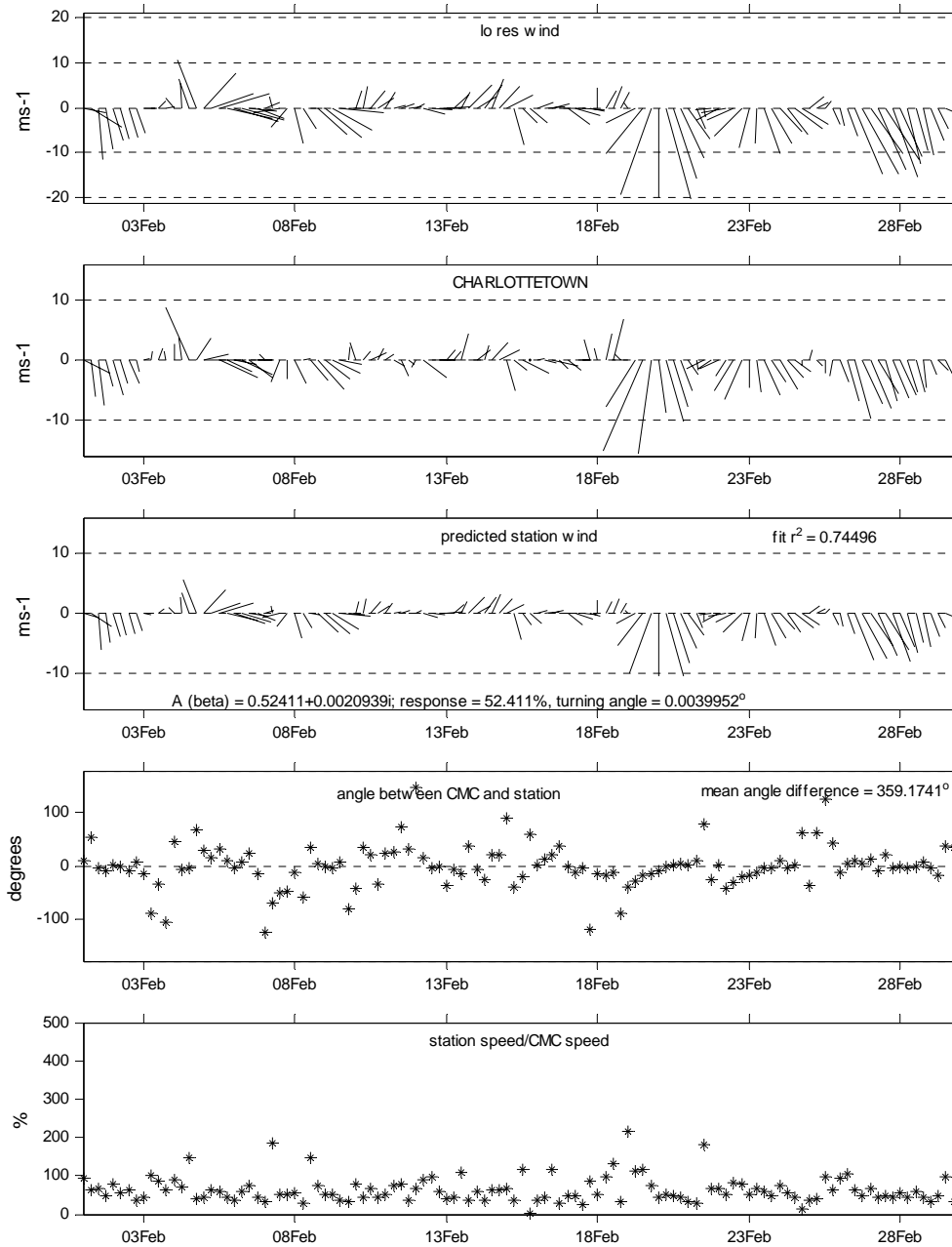


Figure 78 Time series of Charlottetown winter wind vector observations and 6-hourly low resolution forecast output with results of least squares fit

4.2.1.3 Compare Charlottetown with high resolution forecast 3-hourly

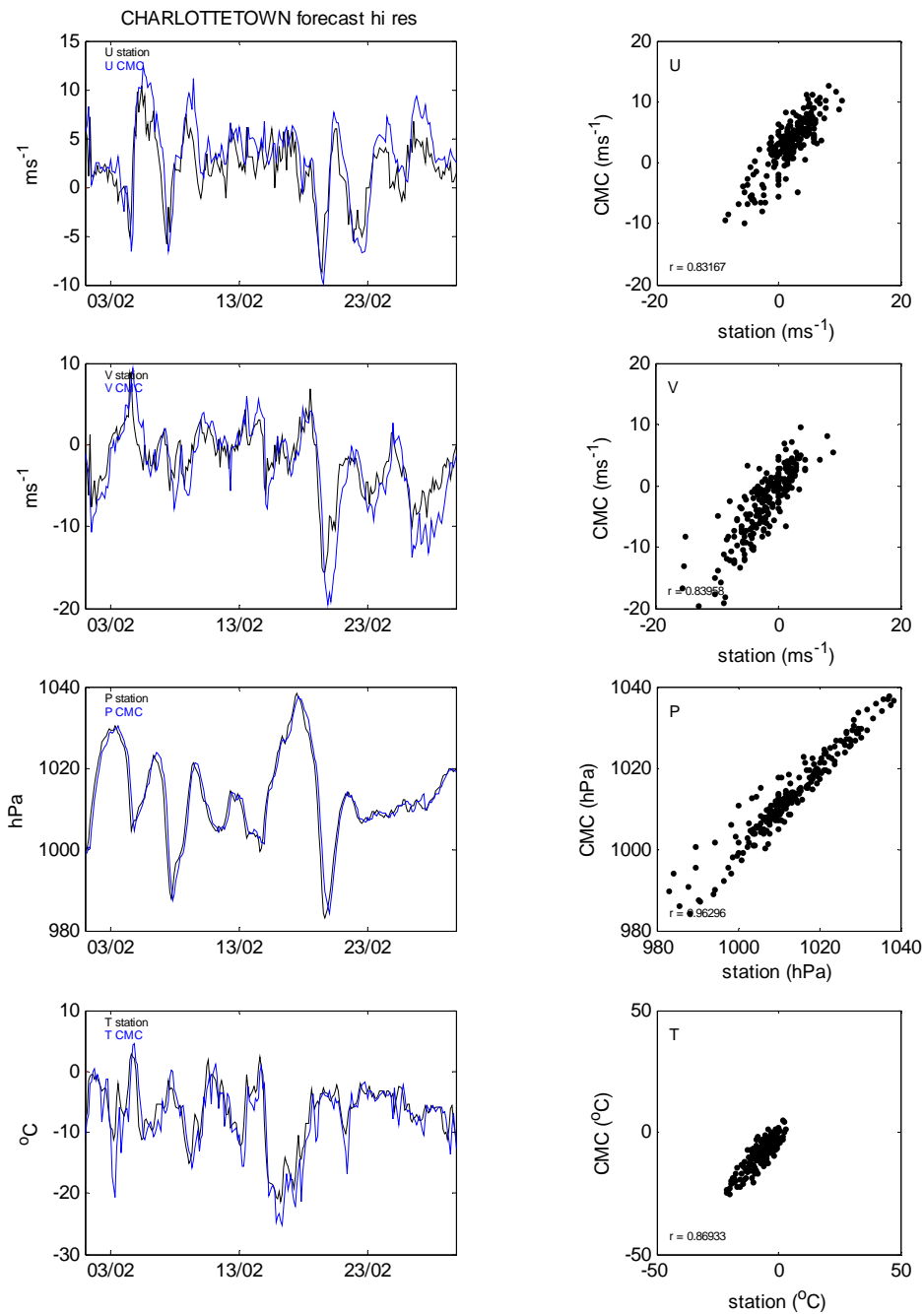


Figure 79 Time series of Charlottetown winter meteorological observations and 3-hourly high resolution forecast output; scatter plots of the same with correlation coefficients

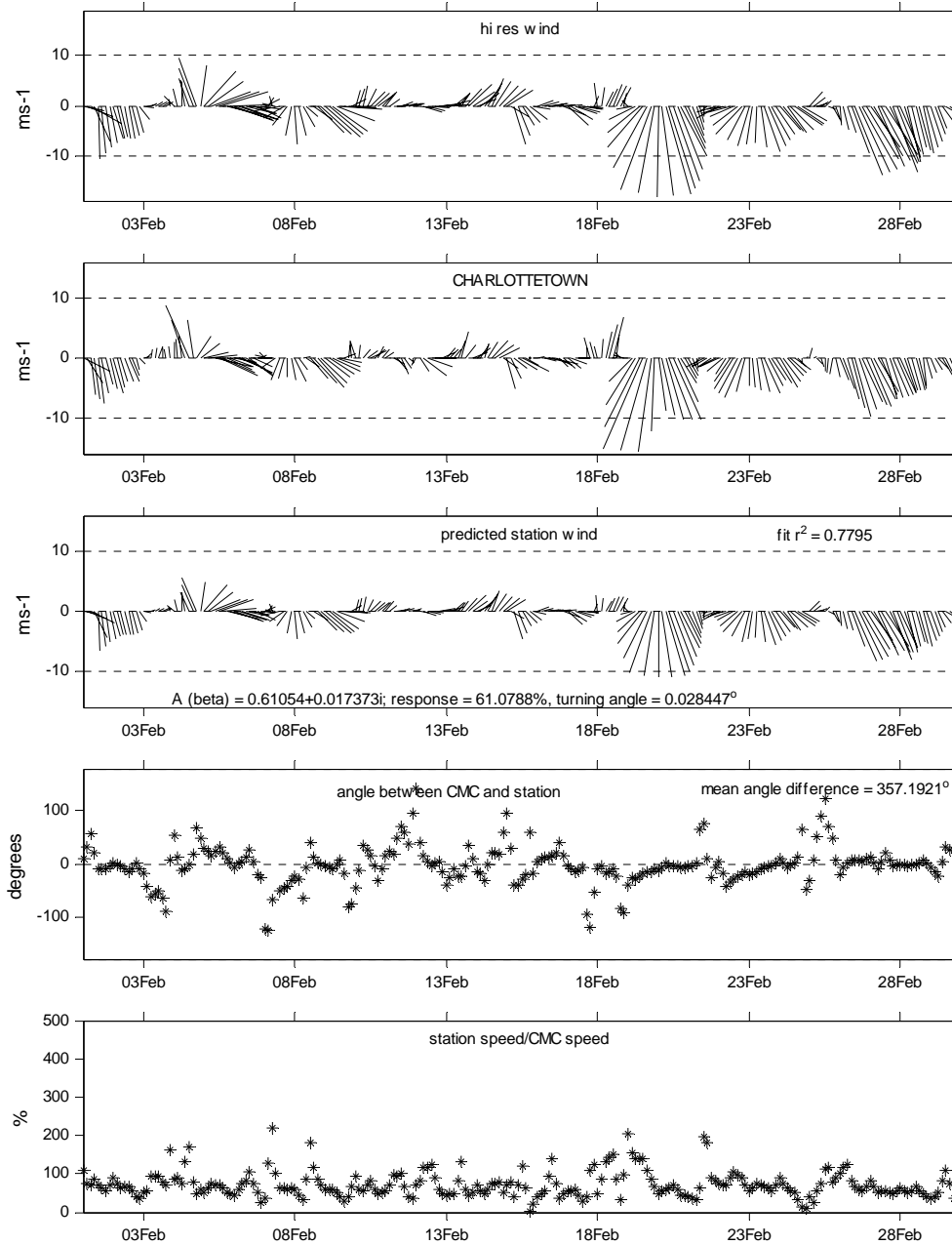


Figure 80 Time series of Charlottetown winter wind vector observations and 3-hourly high resolution forecast output with results of least squares fit

4.2.2 Compare Summerside; winter

4.2.2.1 Compare Summerside with analysis 6-hourly; winter

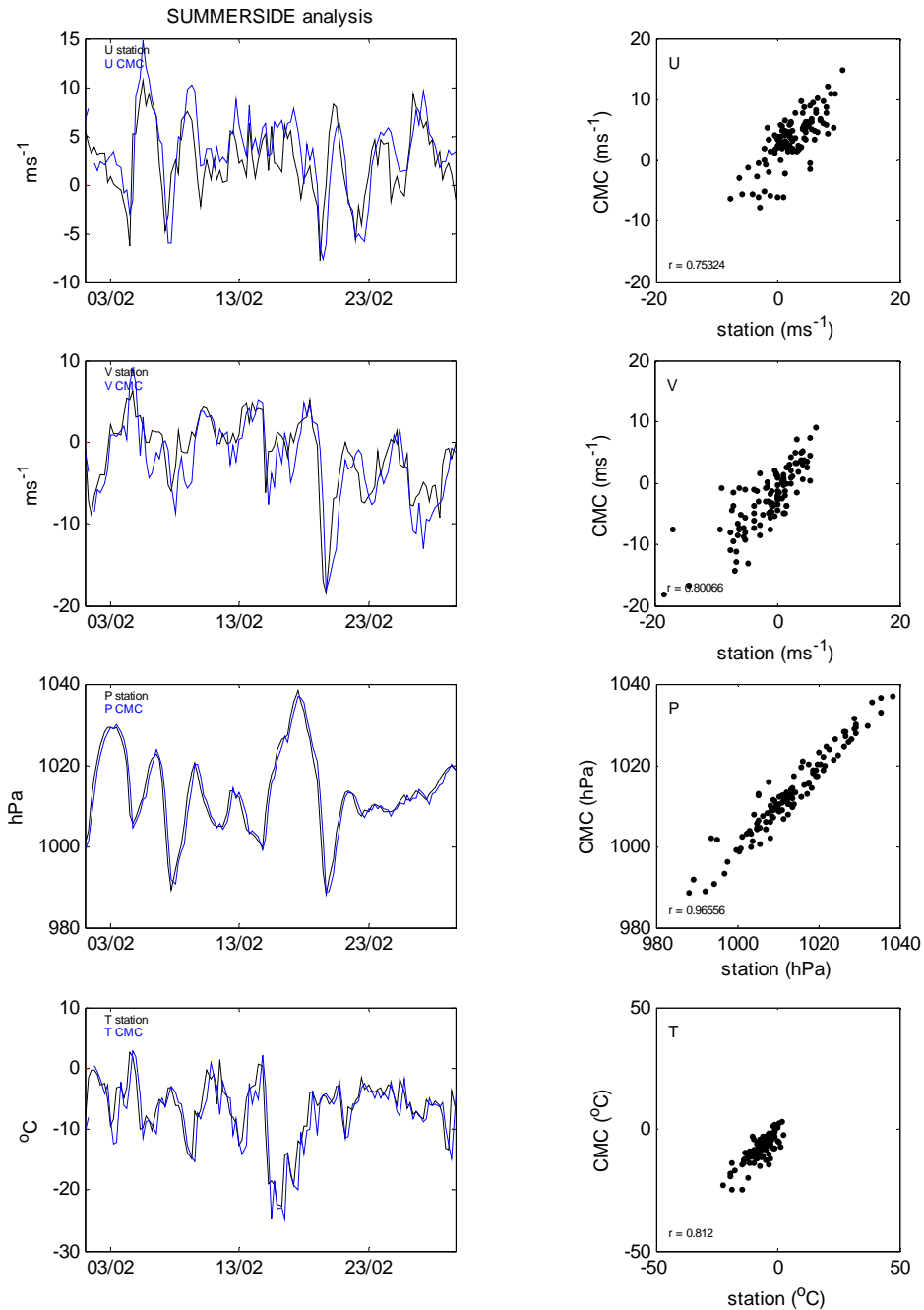


Figure 81 Time series of Summerside winter meteorological observations and 6-hourly analysis output; scatter plots of the same with correlation coefficients.

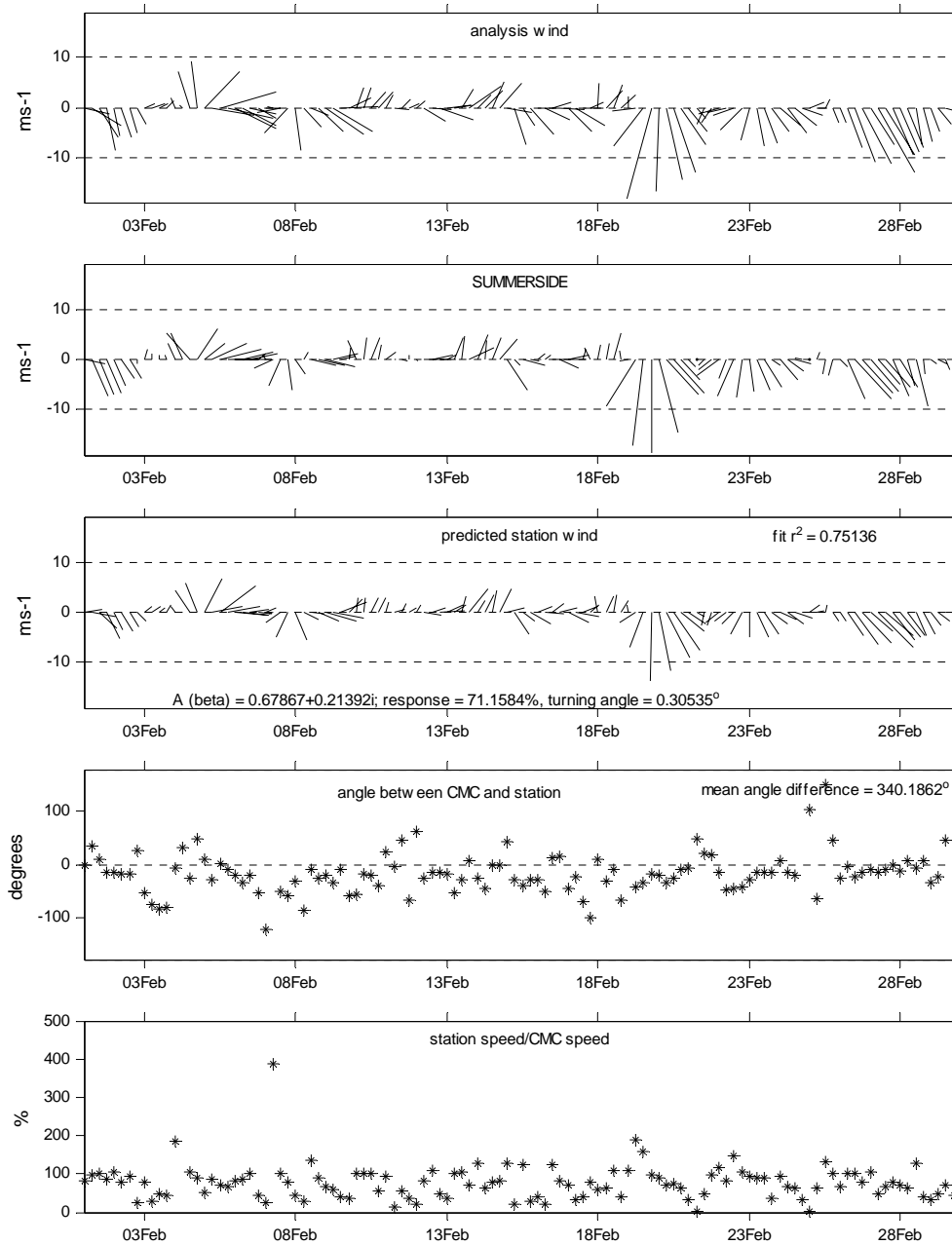


Figure 82 Time series of Summerside winter wind vector observations and 6-hourly analysis output with results of least squares fit

4.2.2.2 Compare Summerside with low resolution forecast 6-hourly; winter

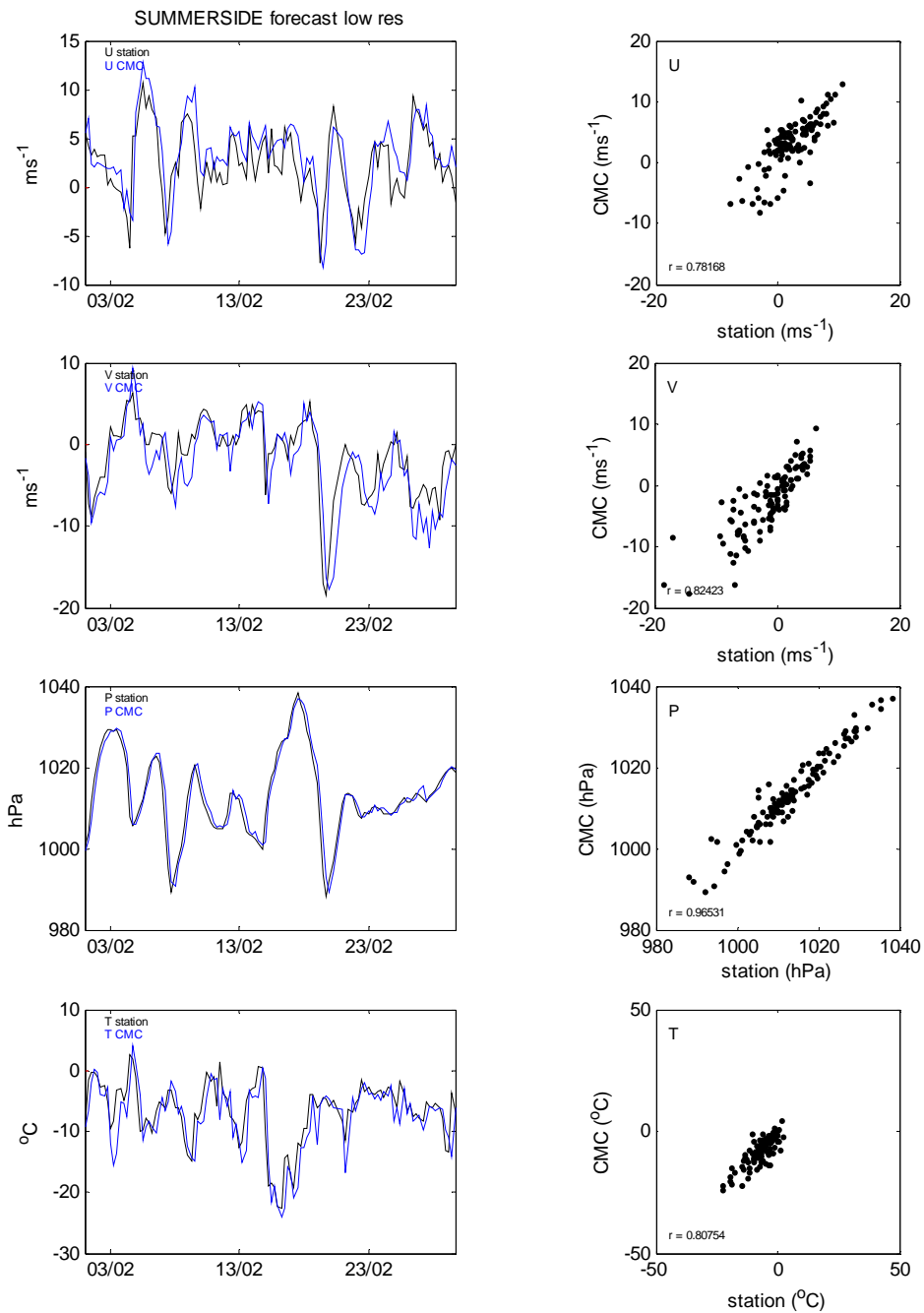


Figure 83 Time series of Summerside winter meteorological observations and 6-hourly low resolution forecast output; scatter plots of the same with correlation coefficients

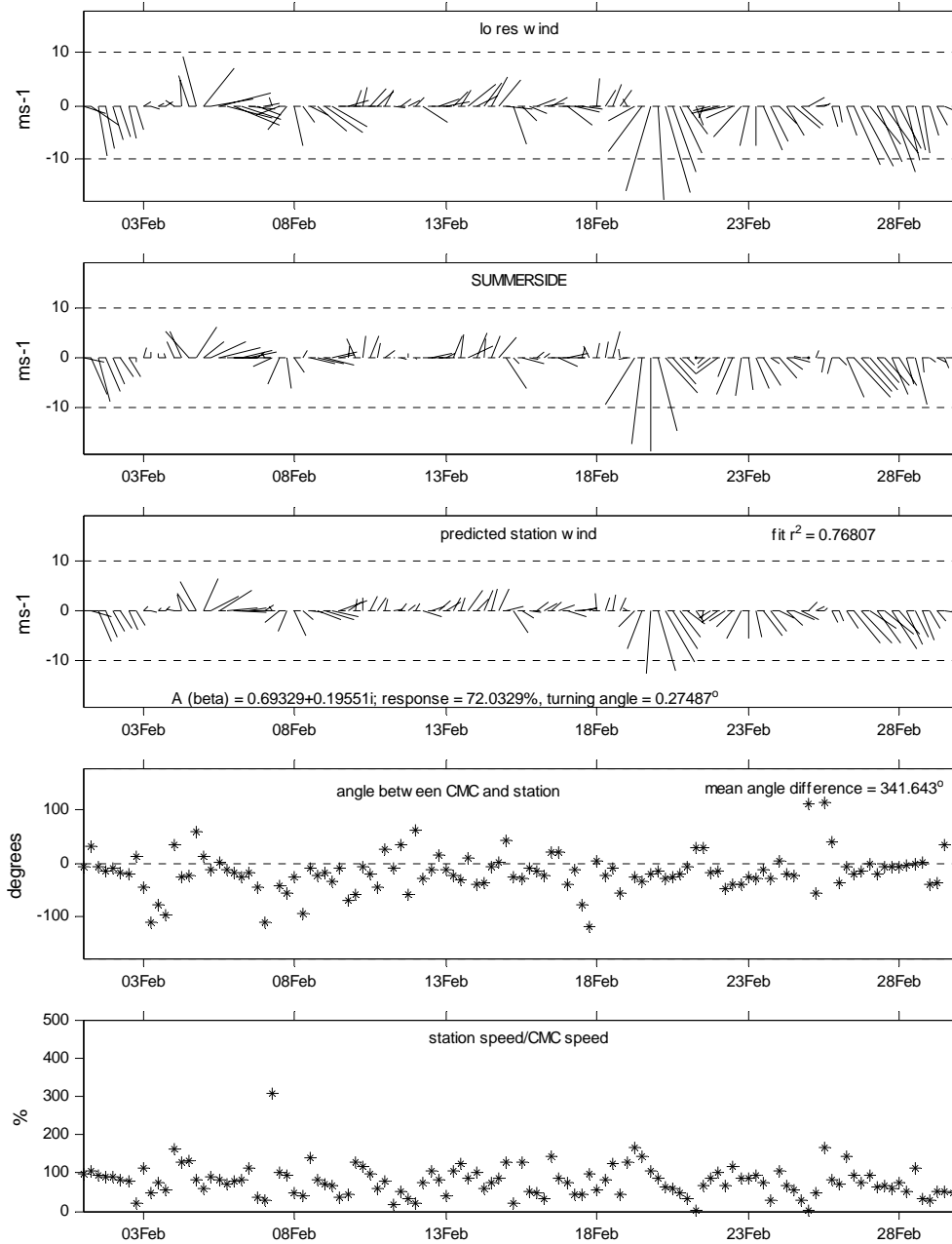


Figure 84 Time series of Summerside winter wind vector observations and 6-hourly low resolution forecast output with results of least squares fit

4.2.2.3 Compare Summerside with high resolution forecast 3-hourly; winter

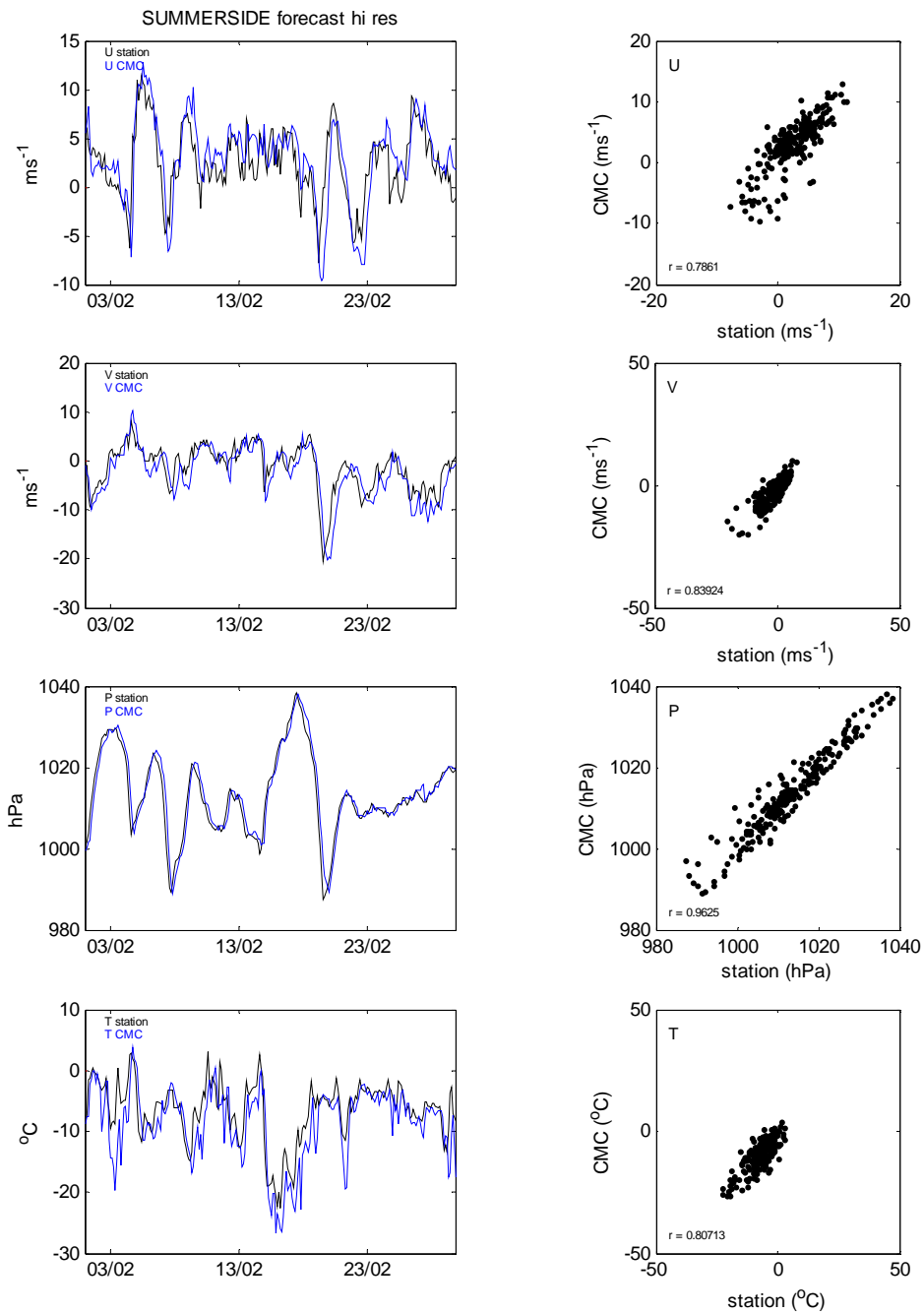


Figure 85 Time series of Summerside winter meteorological observations and 3-hourly high resolution forecast output; scatter plots of the same with correlation coefficients

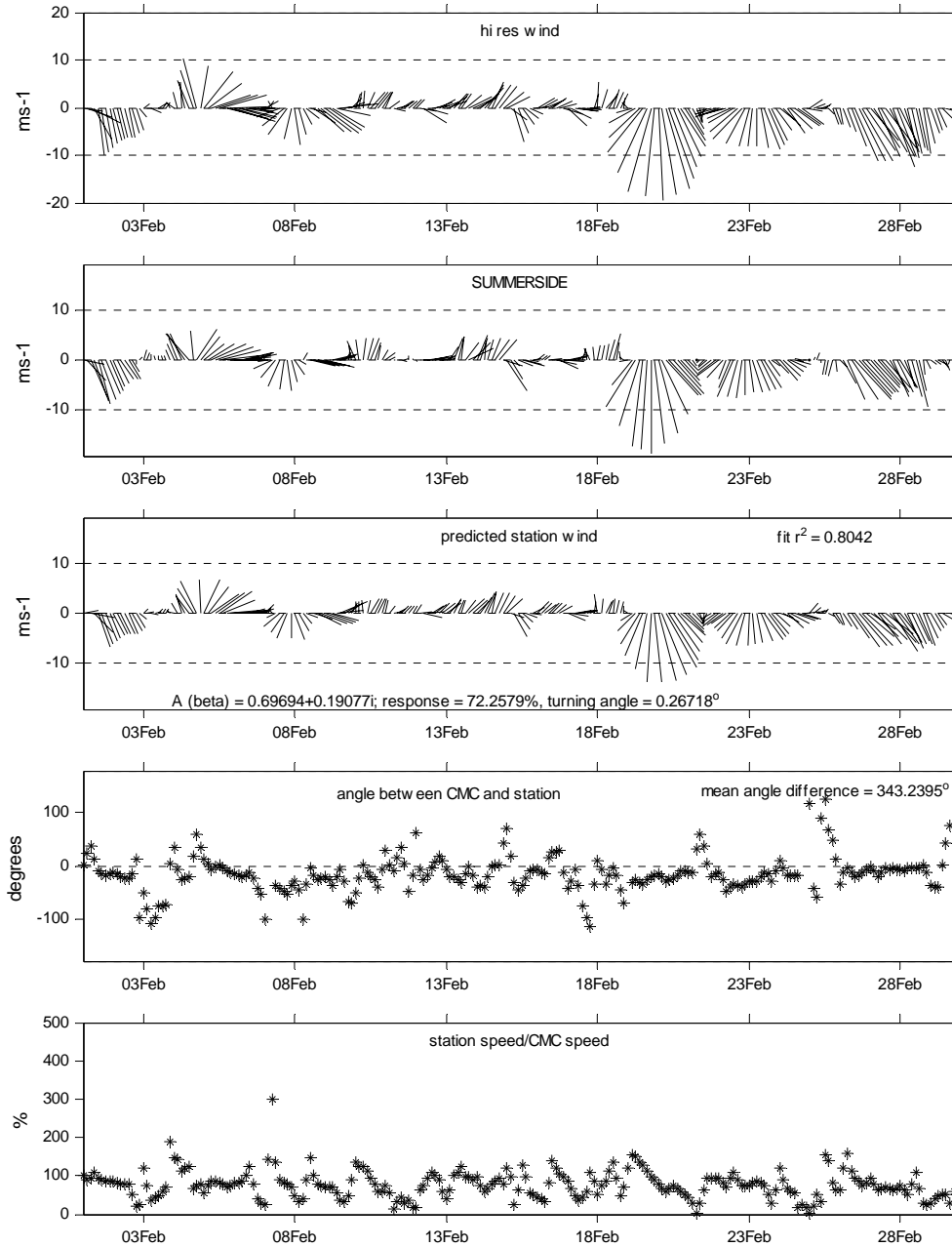


Figure 86 Time series of Summerside winter wind vector observations and 3-hourly high resolution forecast output with results of least squares fit

4.2.3 Compare Iles de la Madeleine; winter

4.2.3.1 Compare Iles de la Madeleine with analysis 6-hourly; winter

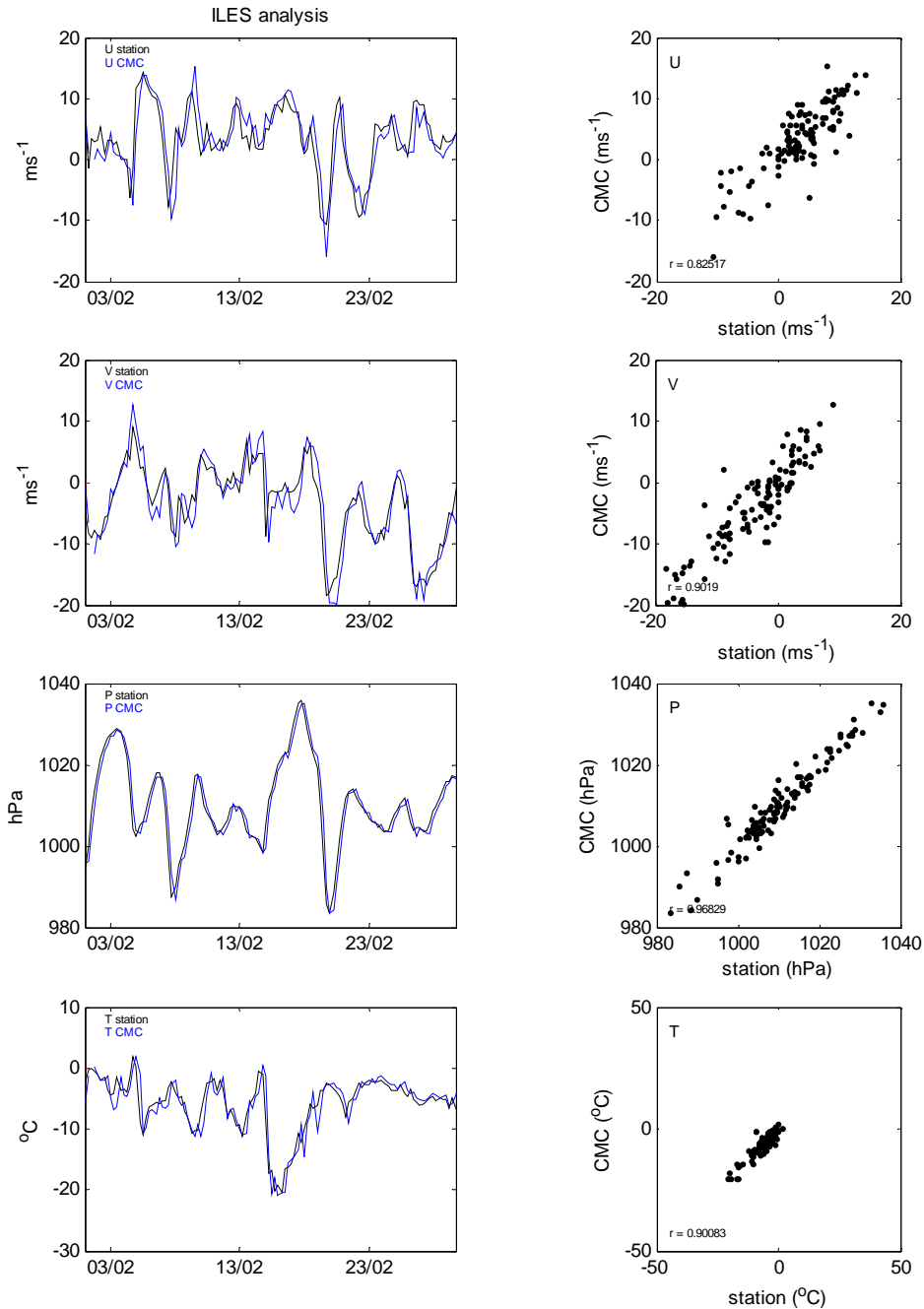


Figure 87 Time series of Iles de la Madeleine winter meteorological observations and 6-hourly analysis output; scatter plots of the same with correlation coefficients

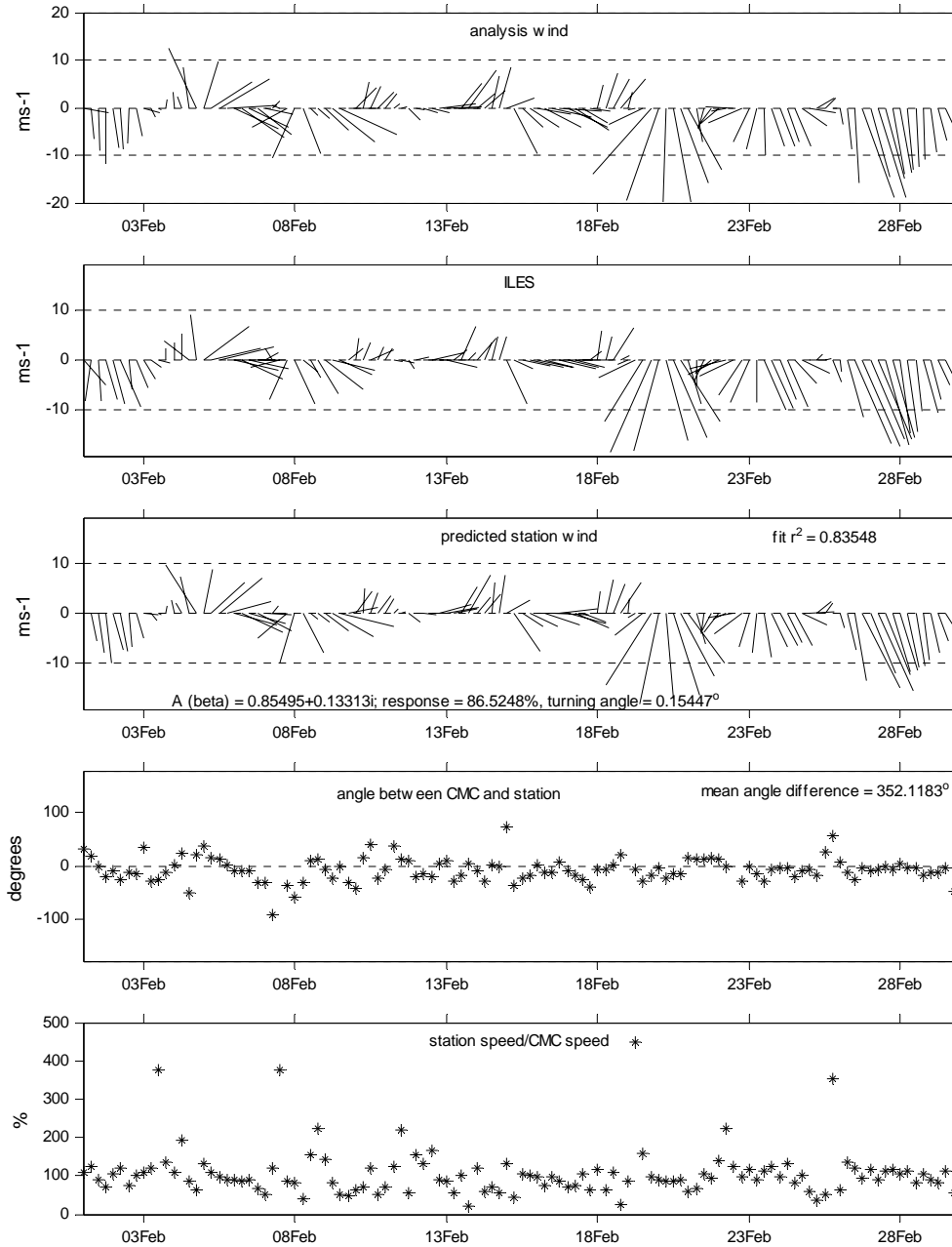


Figure 88 Time series of Iles de la Madeleine winter wind vector observations and 6-hourly analysis output with results of least squares fit

4.2.3.2 Compare Iles de la Madeleine with low resolution forecast 6-hourly; winter

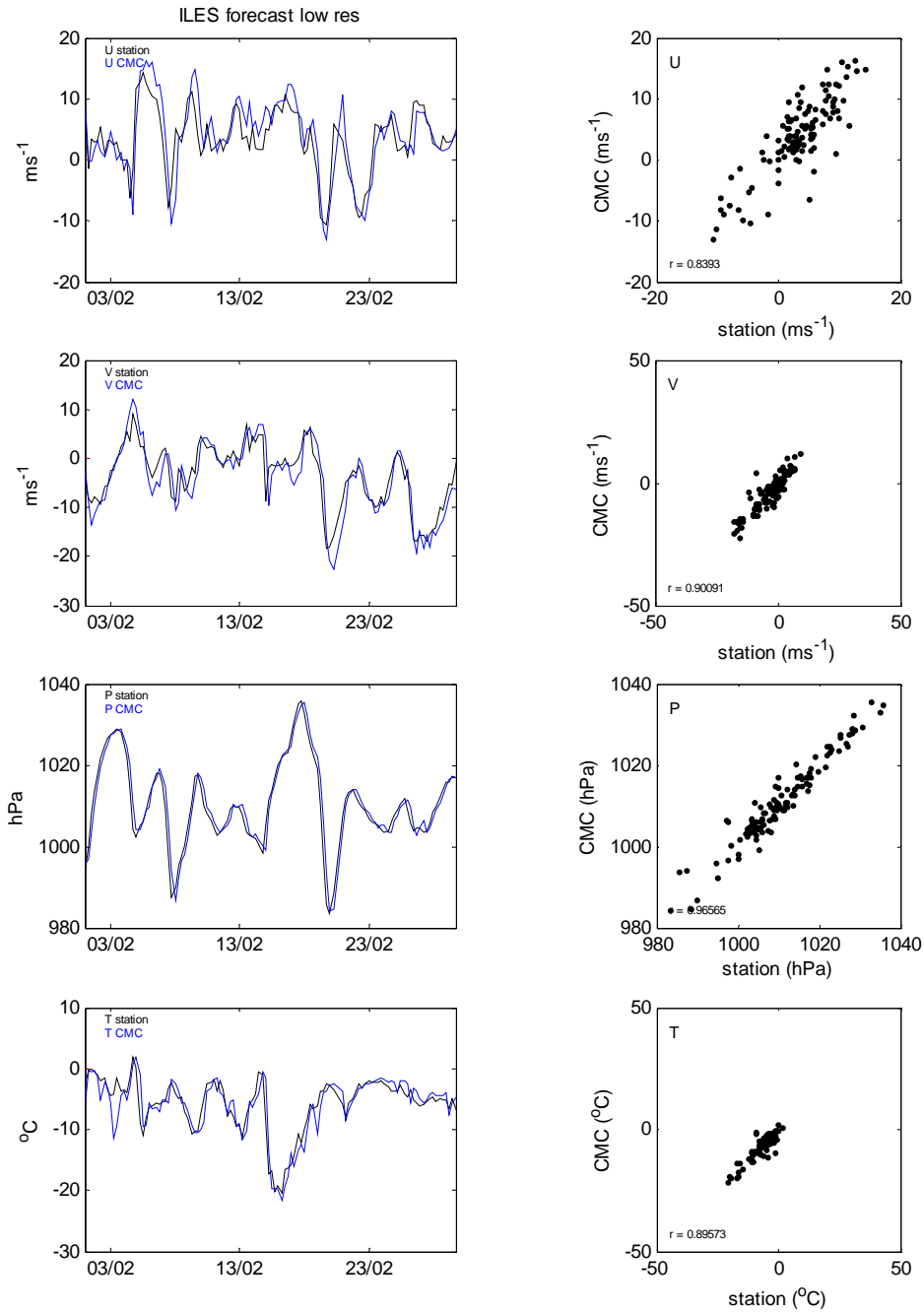


Figure 89 Time series of Iles de la Madeleine winter meteorological observations and 6-hourly low resolution forecast output; scatter plots of the same with correlation coefficients

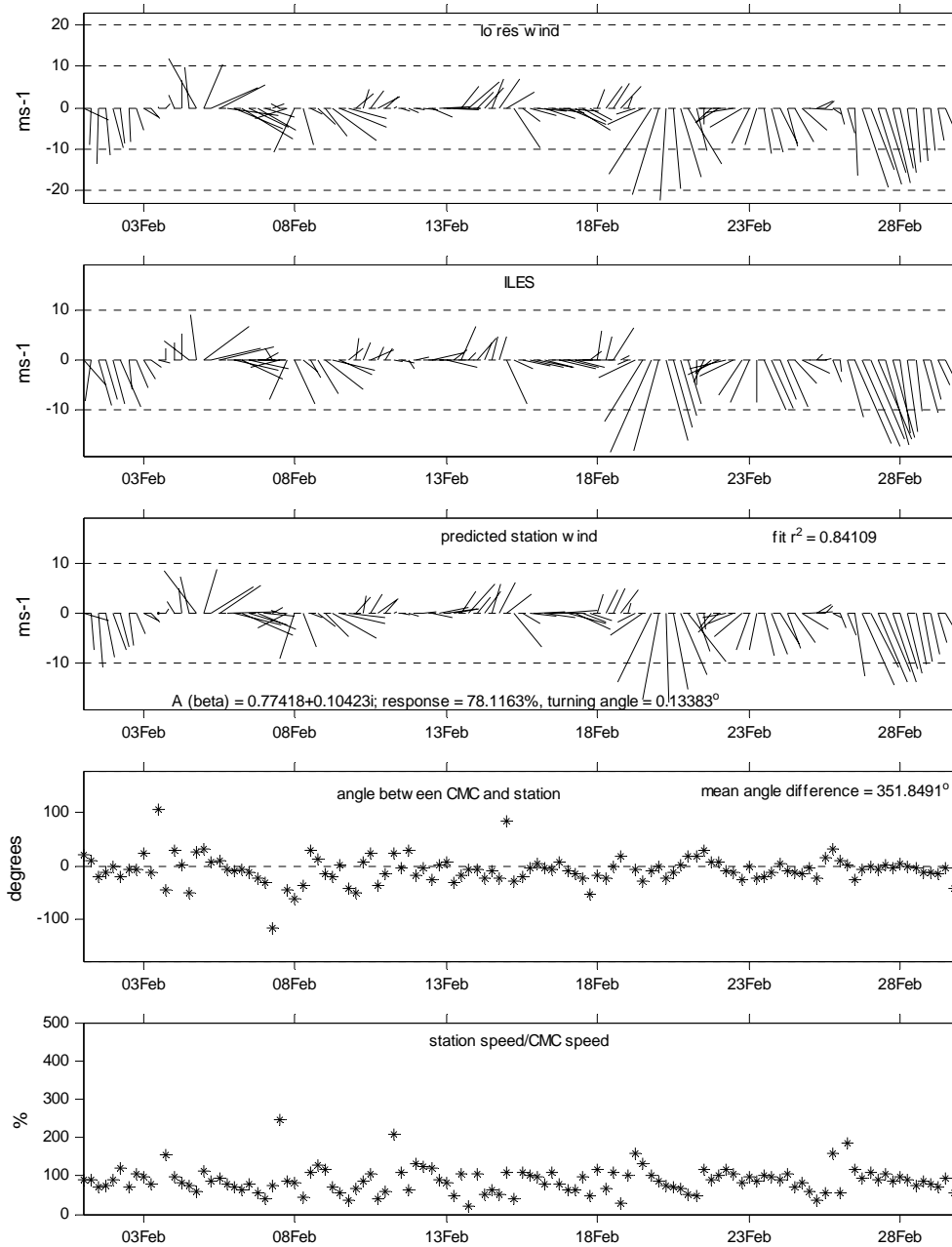


Figure 90 Time series of Iles de la Madeleine winter wind vector observations and 6-hourly low resolution forecast output with results of least squares fit

4.2.3.3 Compare Iles de la Madeleine with high resolution forecast 3-hourly; winter

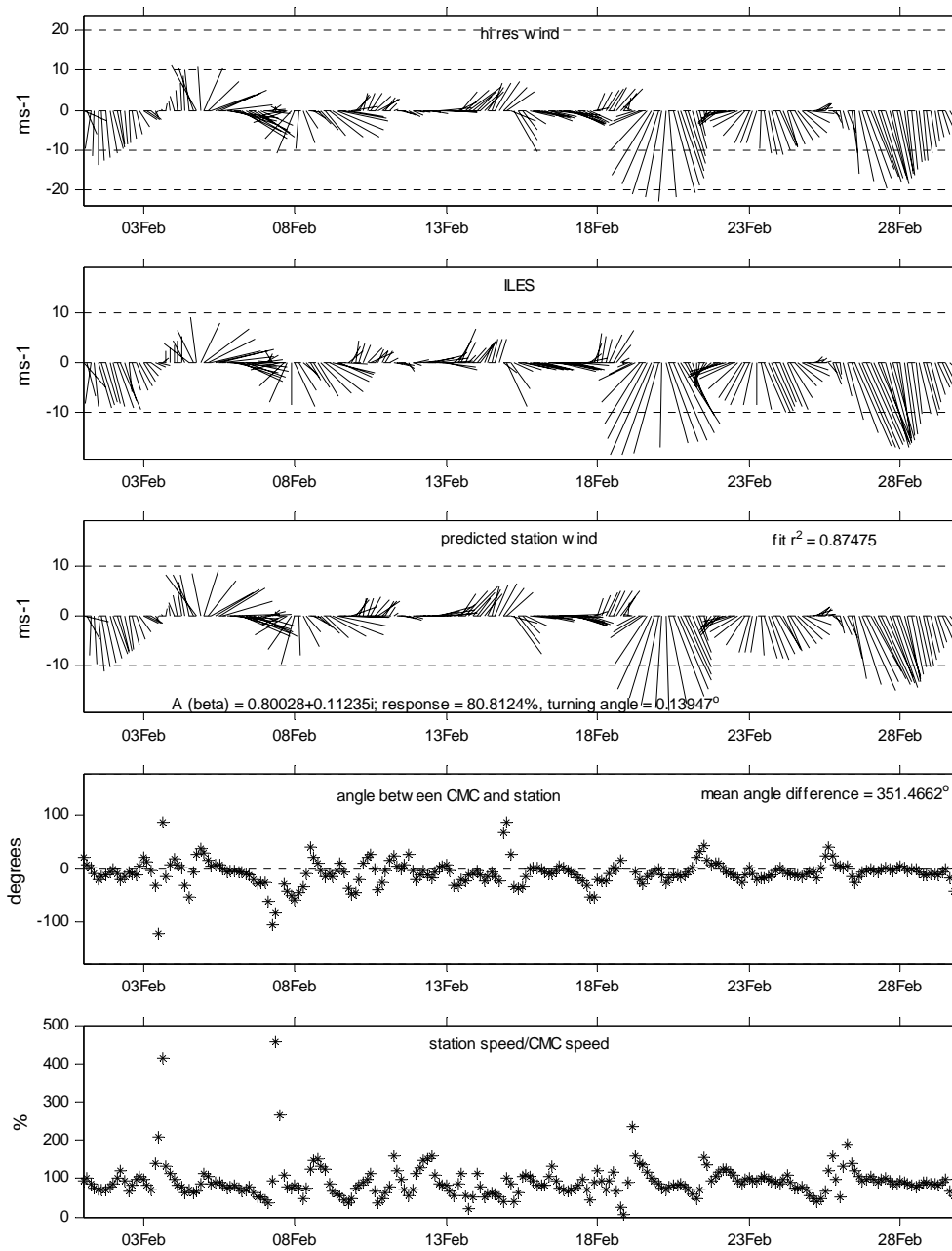


Figure 91 Time series of Iles de la Madeleine winter meteorological observations and 3-hourly high resolution forecast output; scatter plots of the same with correlation coefficients

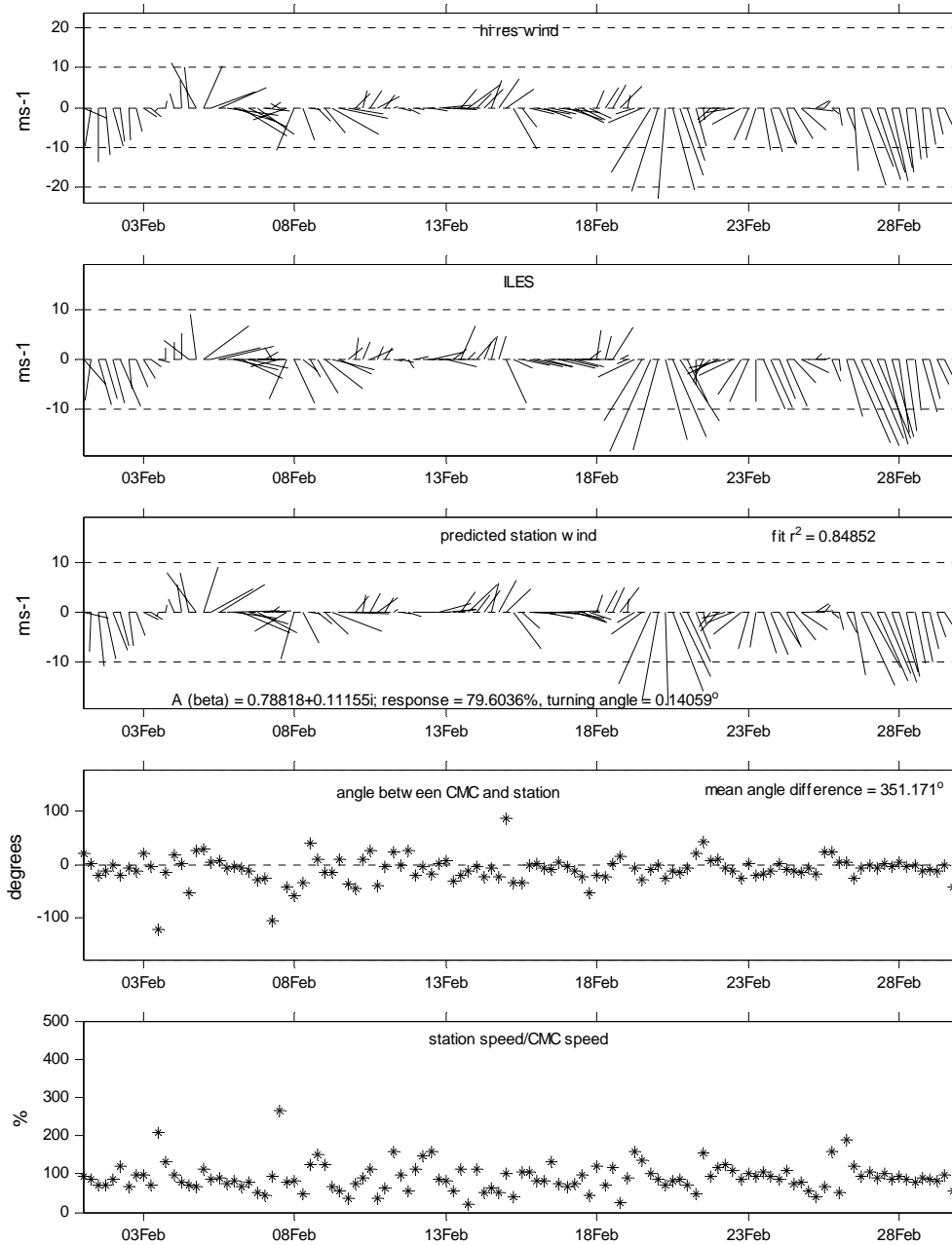


Figure 92 Time series of Iles de la Madeleine winter wind vector observations and 3-hourly high resolution forecast output with results of least squares fit

4.2.4 Compare wave buoy 44150; summer

4.2.4.1 Compare wave buoy 44150 with analysis 6-hourly; summer

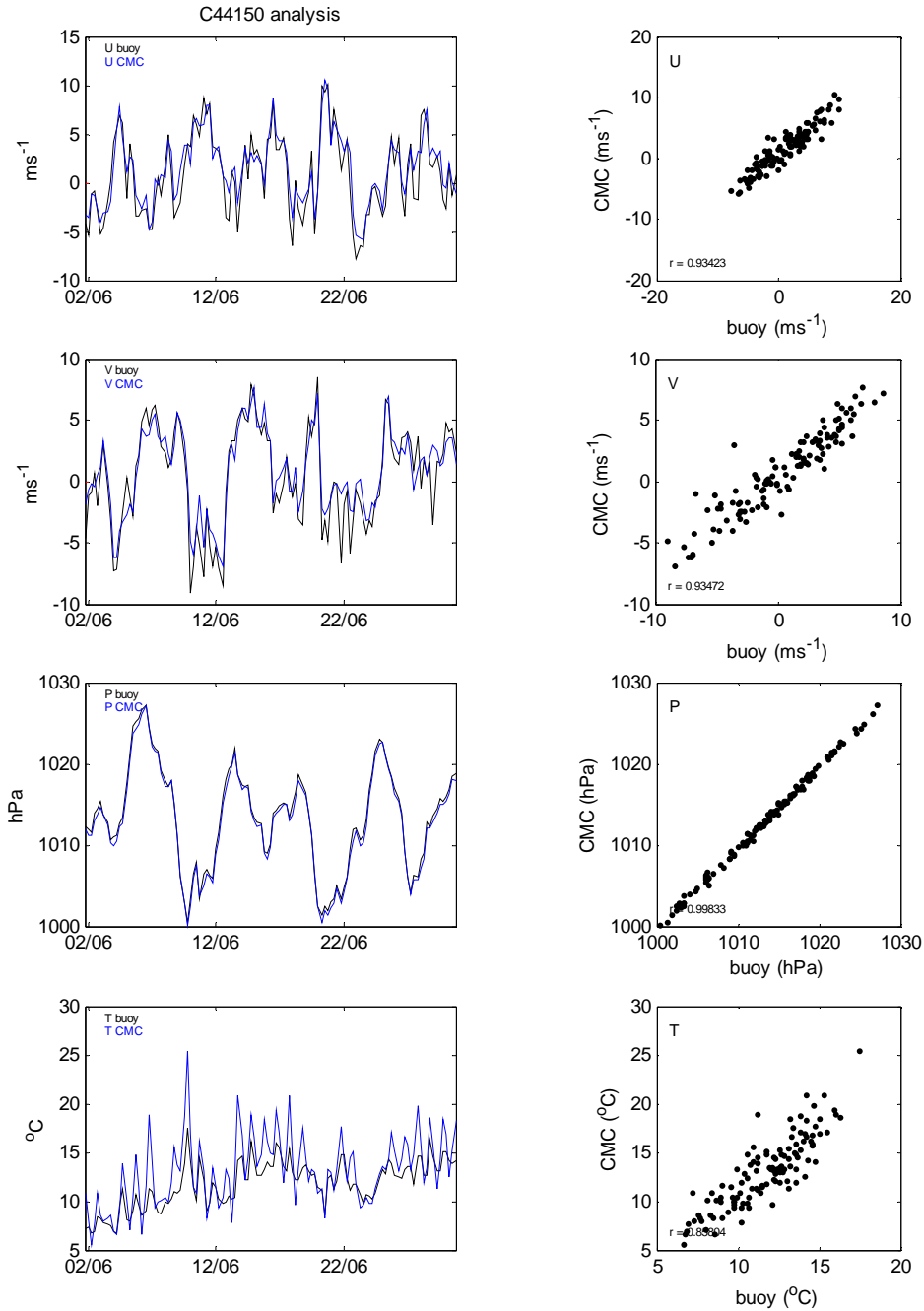


Figure 93 Time series of wave buoy 44150 summer meteorological observations and 6-hourly analysis output; scatter plots of the same with correlation coefficients

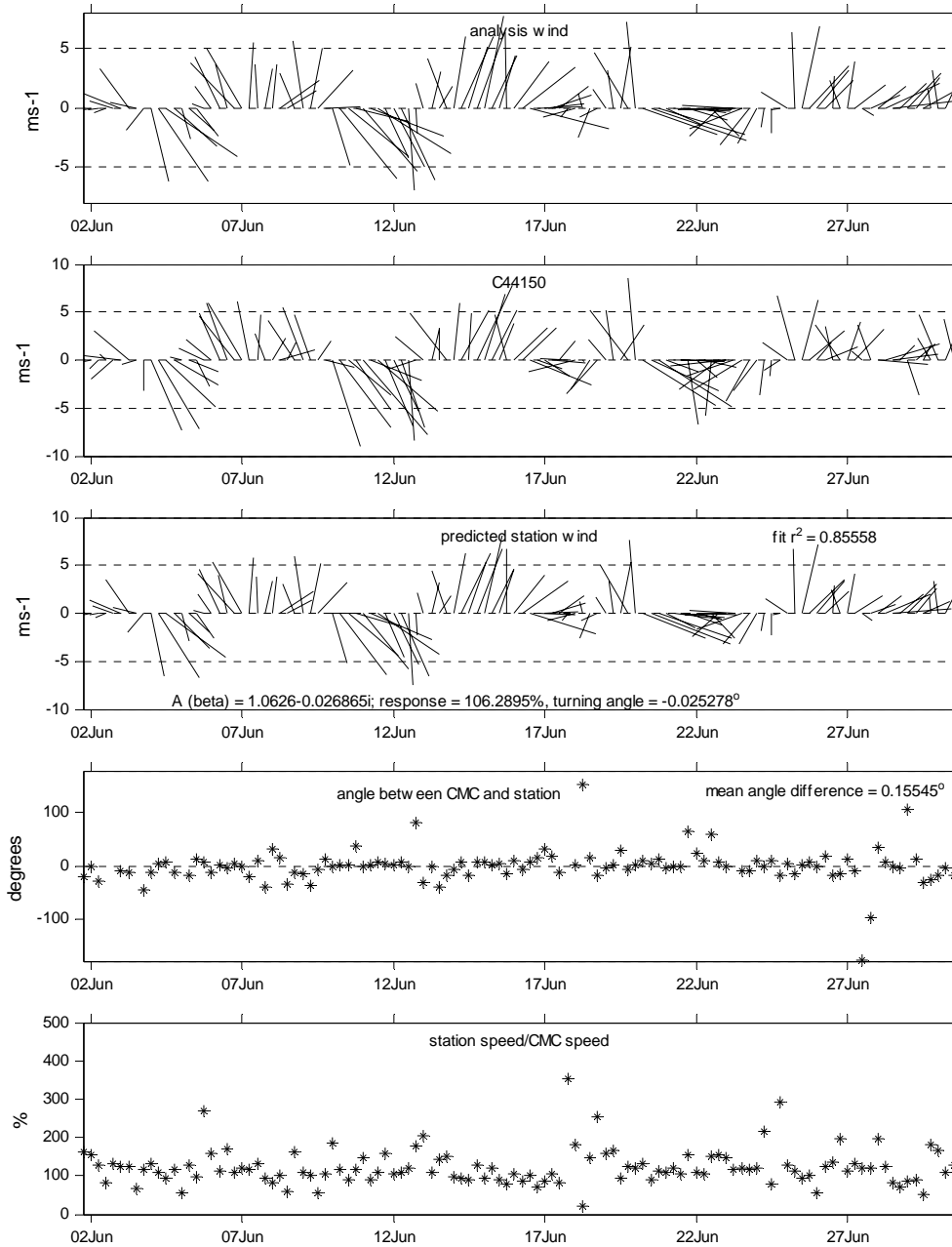


Figure 94 Time series of wave buoy 44150 summer wind vector observations and 6-hourly analysis output with results of least squares fit

4.2.4.2 Compare wave buoy 44150 with low resolution forecast 6-hourly; summer

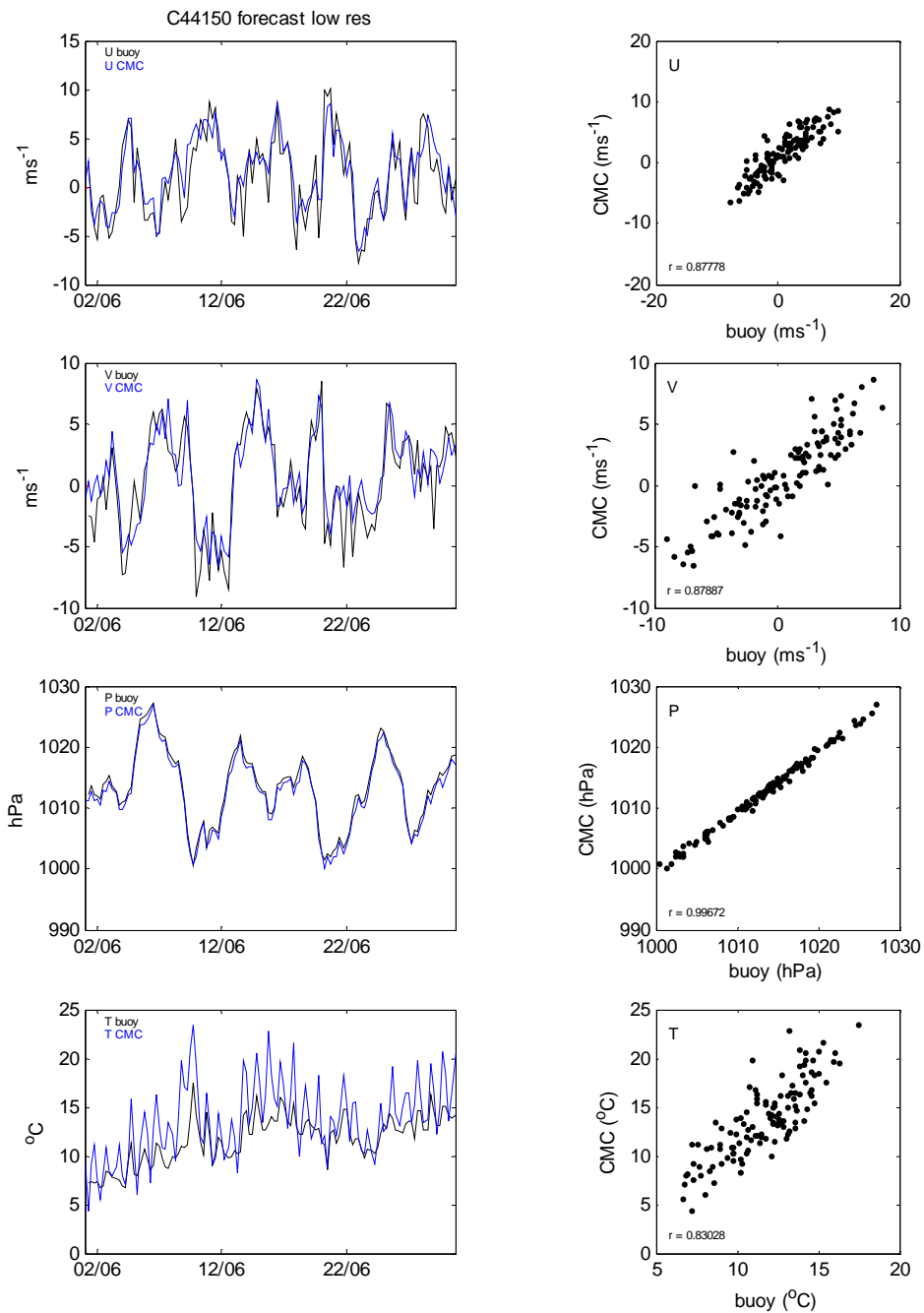


Figure 95 Time series of wave buoy 44150 summer meteorological observations and 6-hourly low resolution forecast output; scatter plots of the same with correlation coefficients.

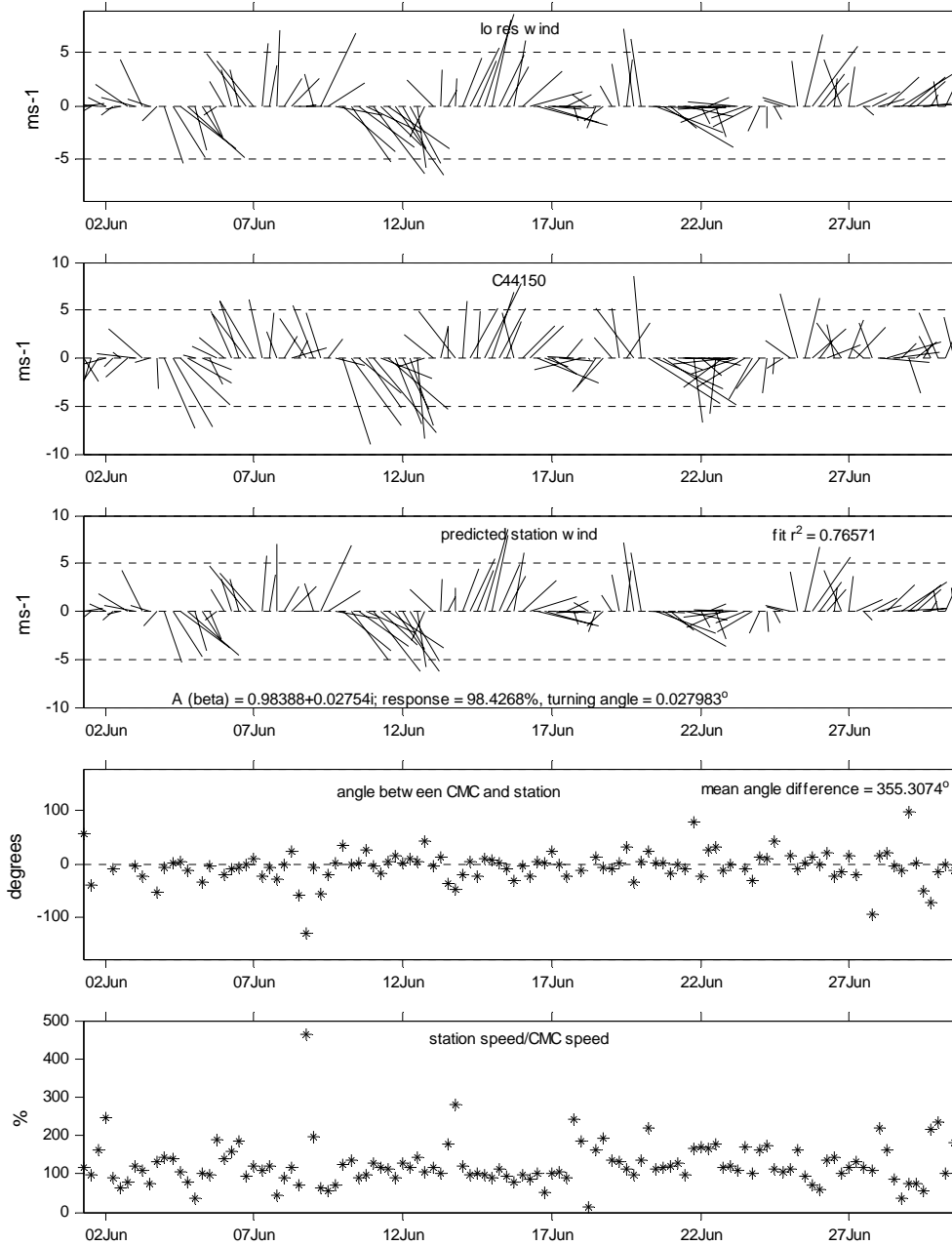


Figure 96 Time series of wave buoy 44150 summer wind vector observations and 6-hourly low resolution forecast output with results of least squares fit.

4.2.4.3 Compare wave buoy 44150 with high resolution forecast 3-hourly; summer

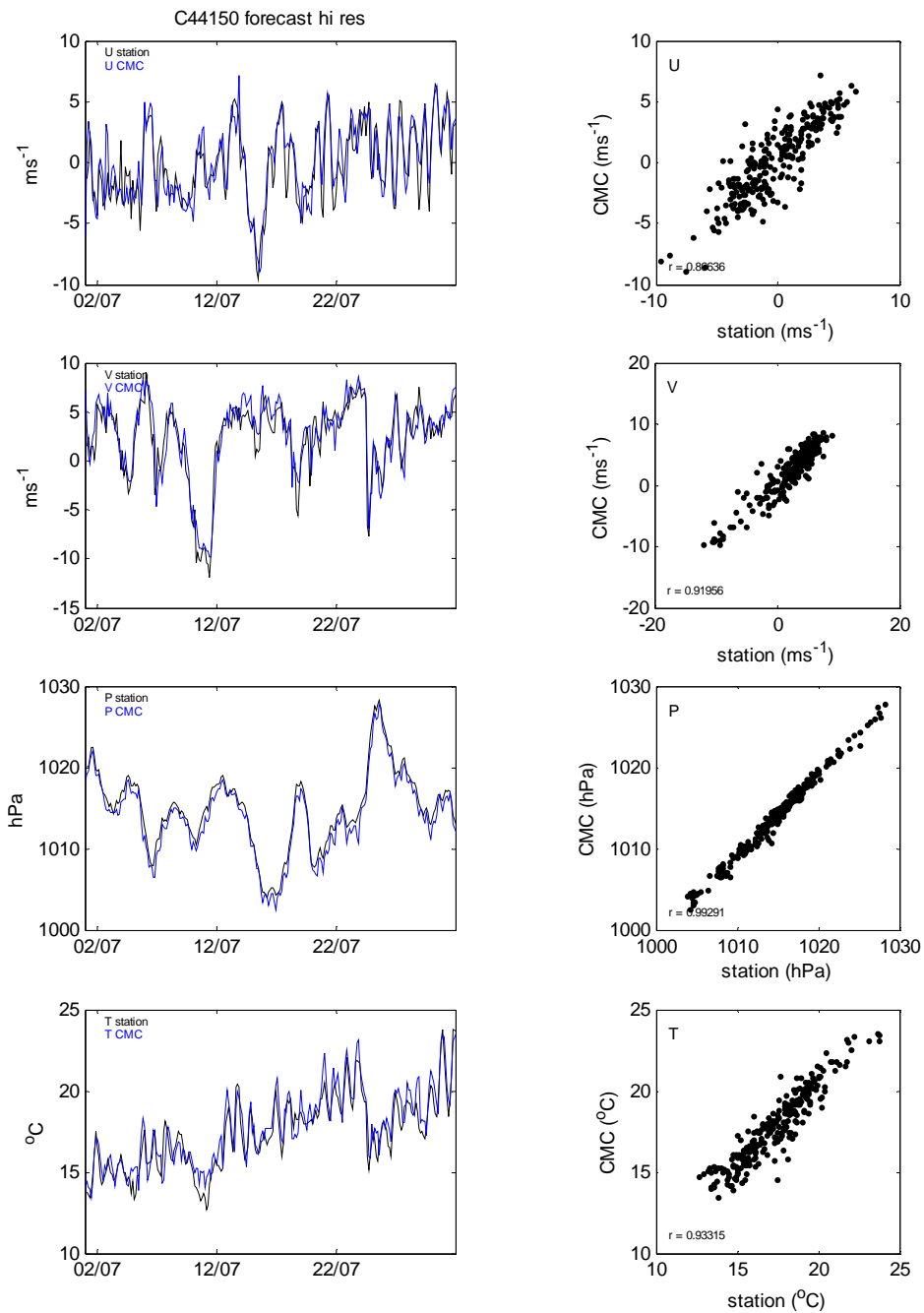


Figure 97 Time series of wave buoy 44150 summer meteorological observations and 3-hourly high resolution forecast output; scatter plots of the same with correlation coefficients.

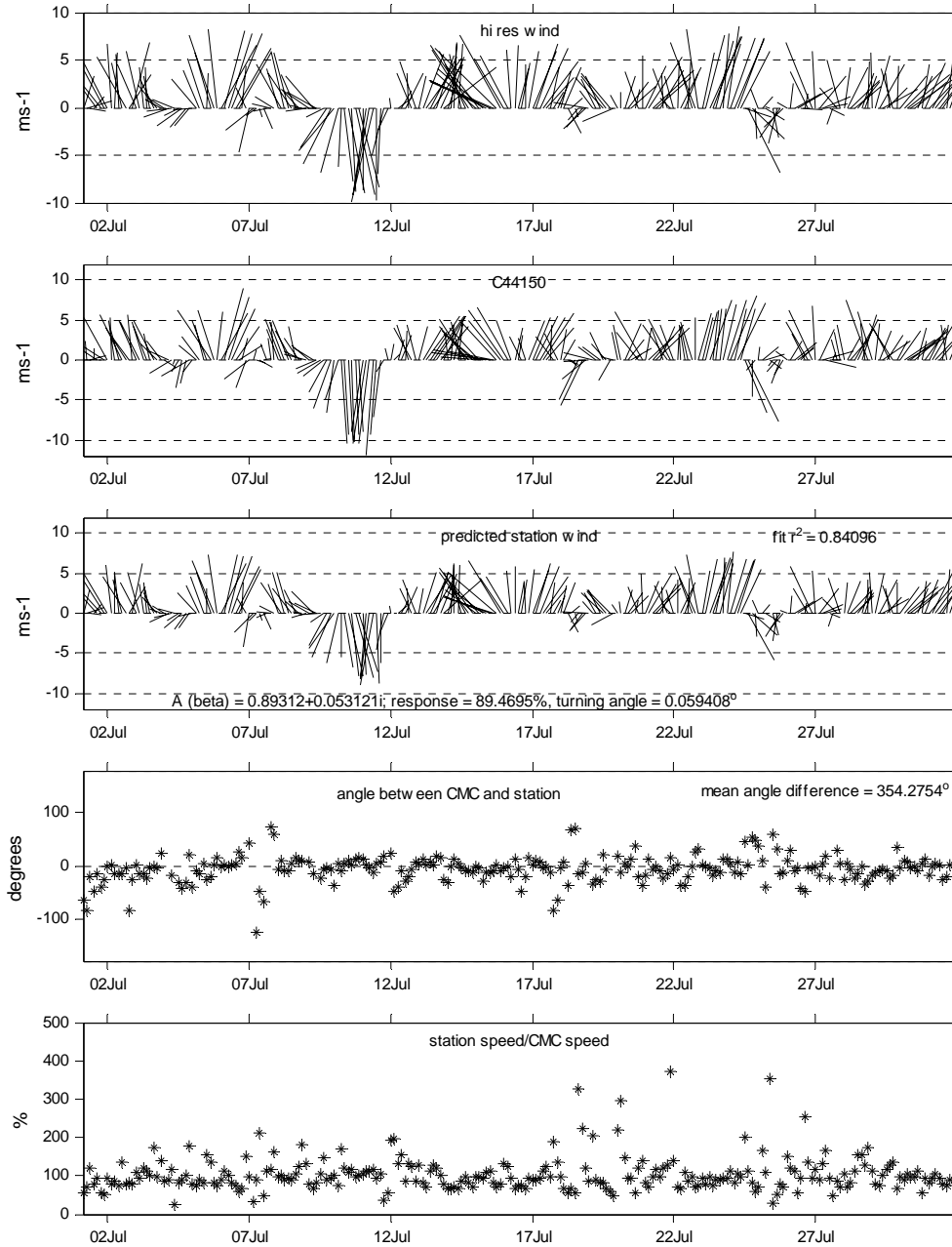


Figure 98 Time series of wave buoy 44150 summer wind vector observations and 3-hourly high resolution forecast output with results of least squares fit

4.2.5 Compare wave buoy 44161; summer

4.2.5.1 Compare wave buoy 44161 with analysis 6-hourly; summer

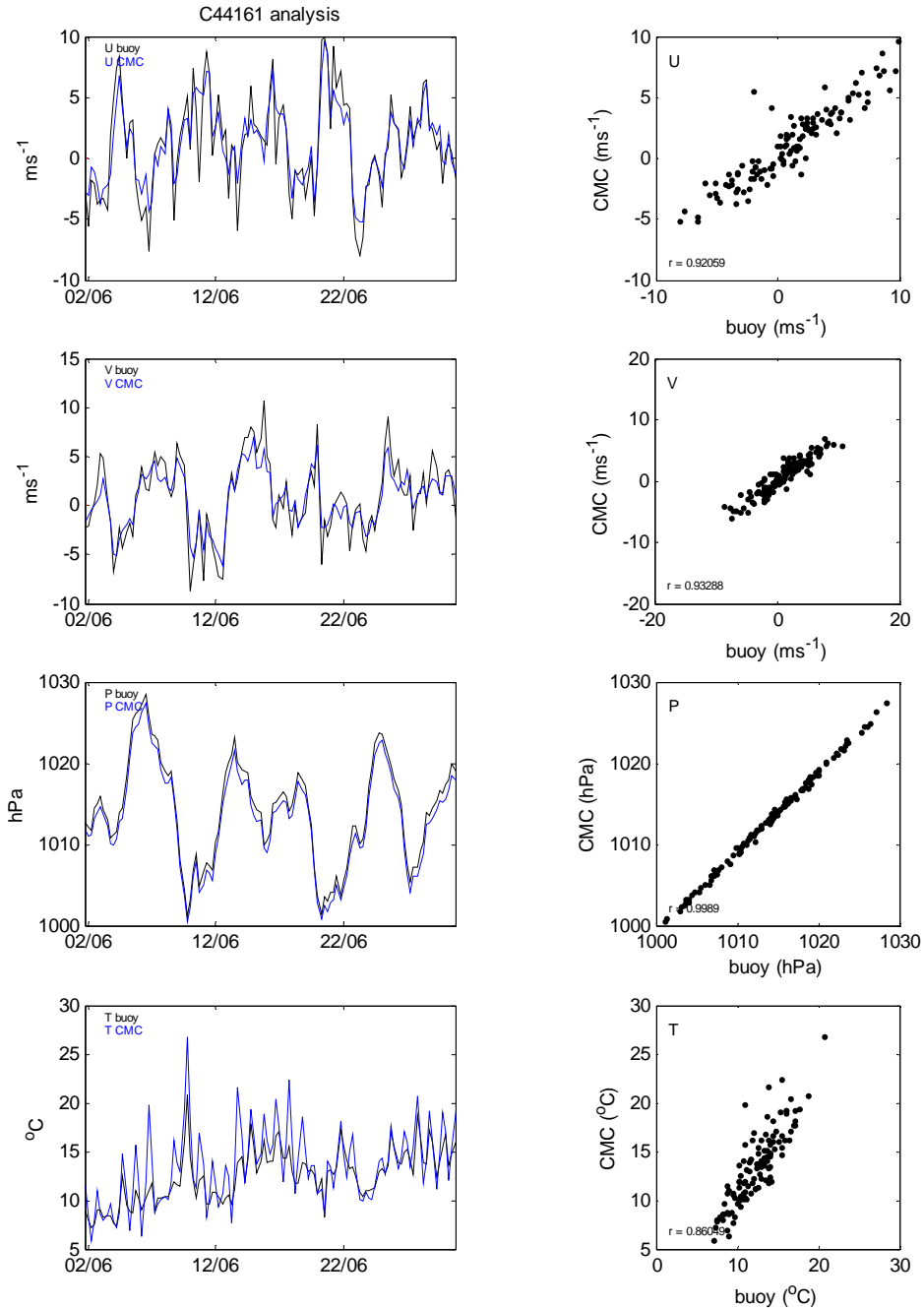


Figure 99 Time series of wave buoy 44161 summer meteorological observations and 6-hourly analysis output; scatter plots of the same with correlation coefficients.

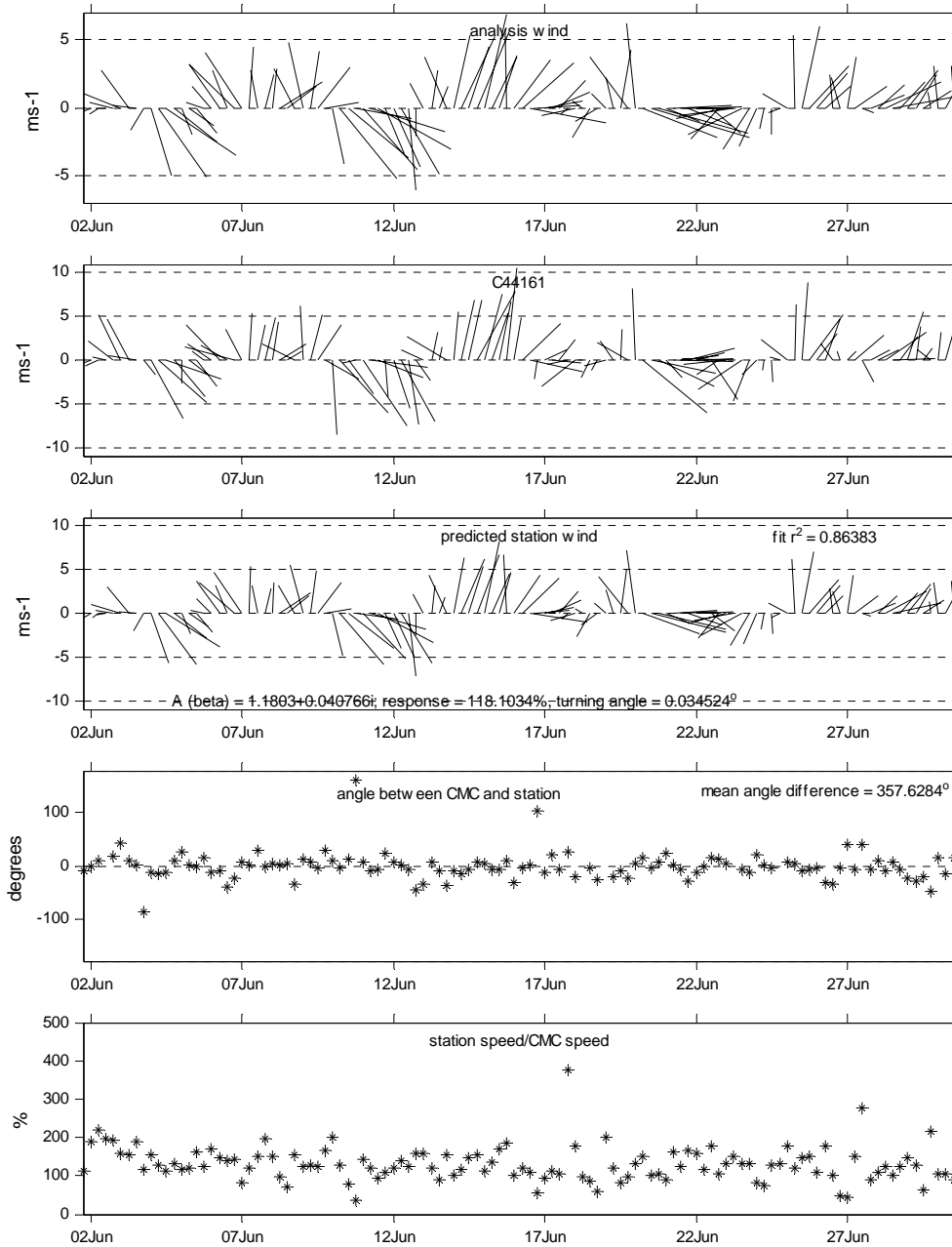


Figure 100 Time series of wave buoy 44161 summer wind vector observations and 6-hourly analysis output with results of least squares fit

4.2.5.2 Compare wave buoy 44161 with low resolution forecast 6-hourly; summer

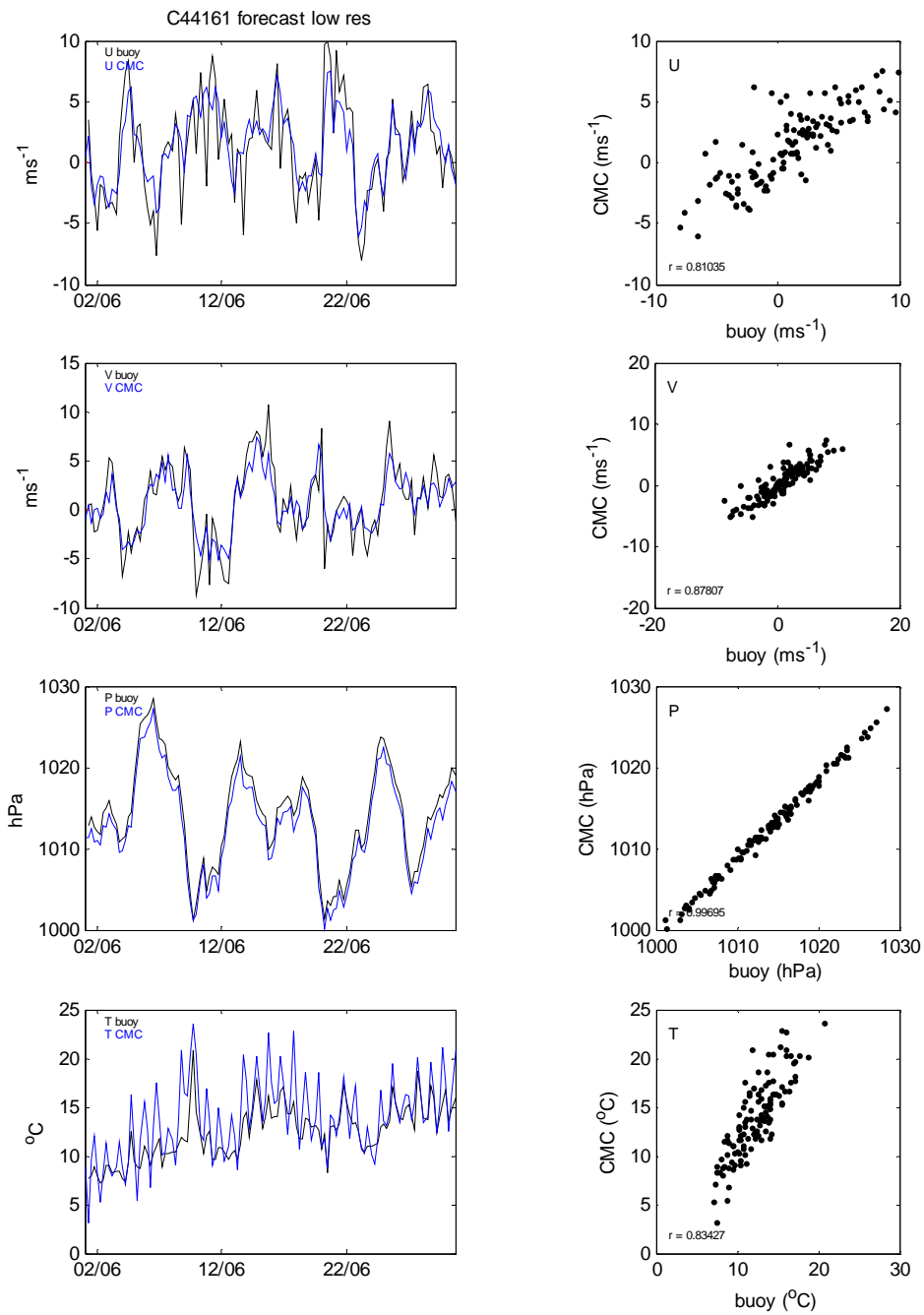


Figure 101 Time series of wave buoy 44161 summer meteorological observations and 6-hourly low resolution forecast output; scatter plots of the same with correlation coefficients

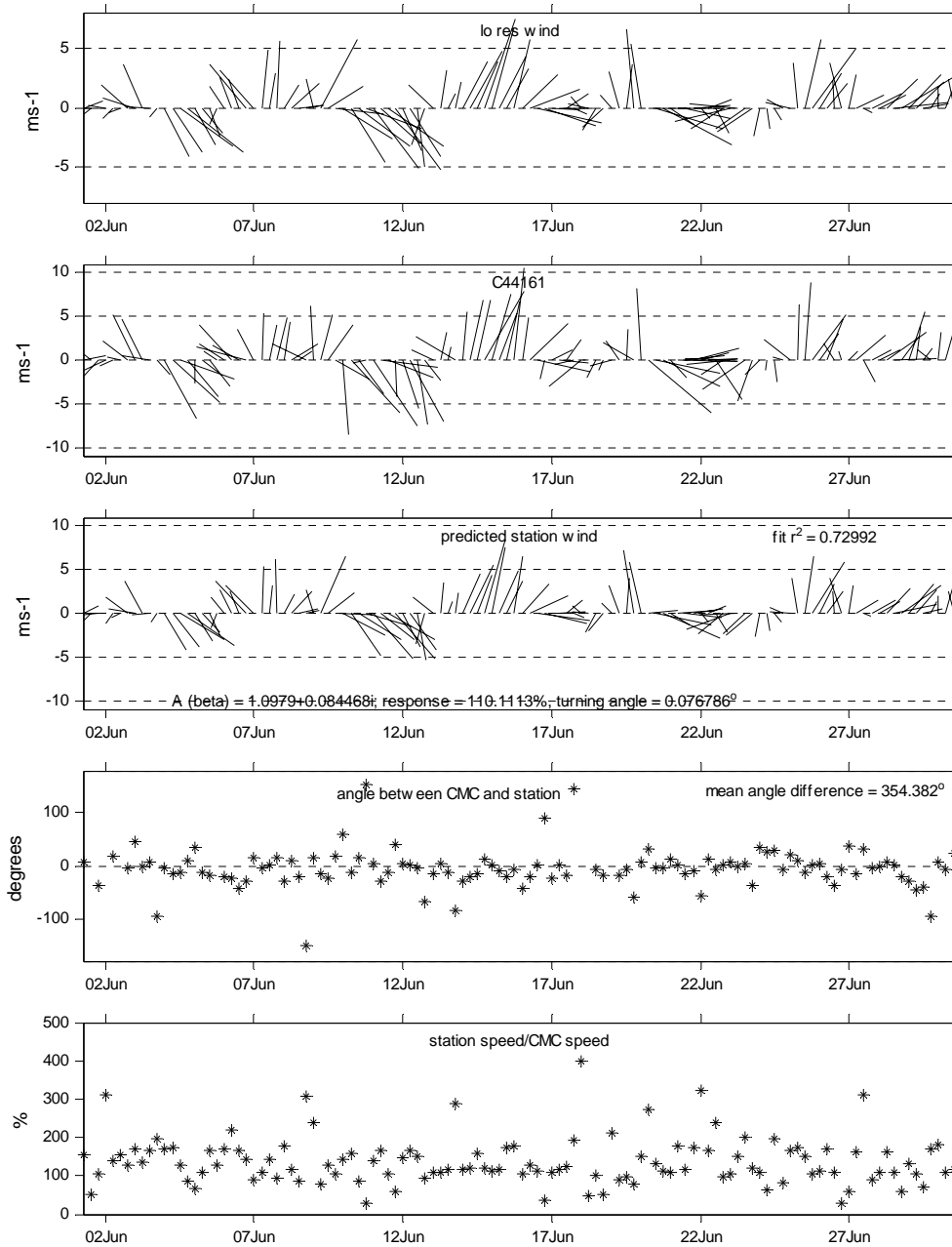


Figure 102 Time series of wave buoy 44161 summer wind vector observations and 6-hourly low resolution forecast output with results of least squares fit

4.2.5.3 Compare wave buoy 44161 with high resolution forecast 3-hourly; summer

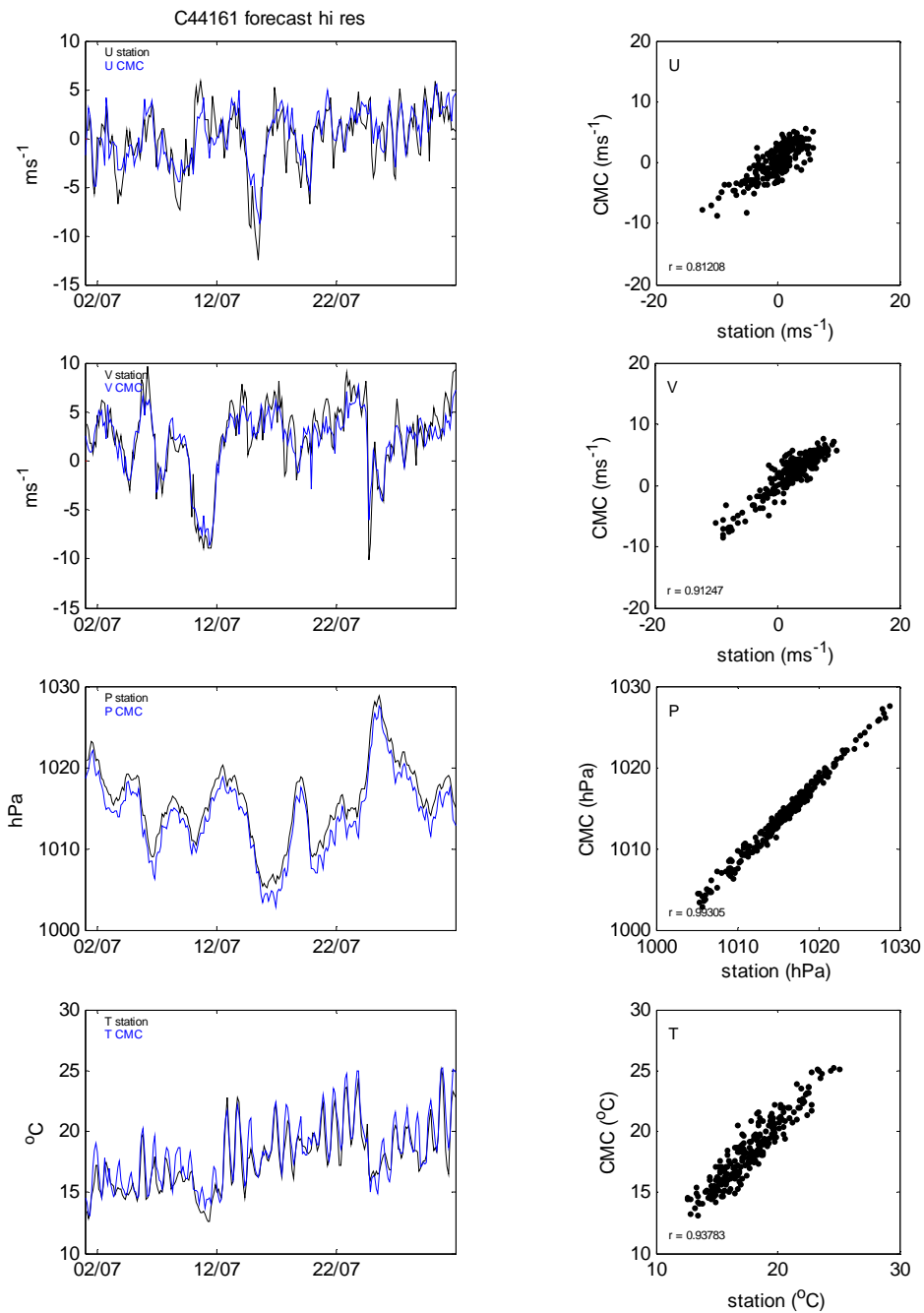


Figure 103 Time series of wave buoy 44161 summer meteorological observations and 3-hourly high resolution forecast output; scatter plots of the same with correlation coefficients

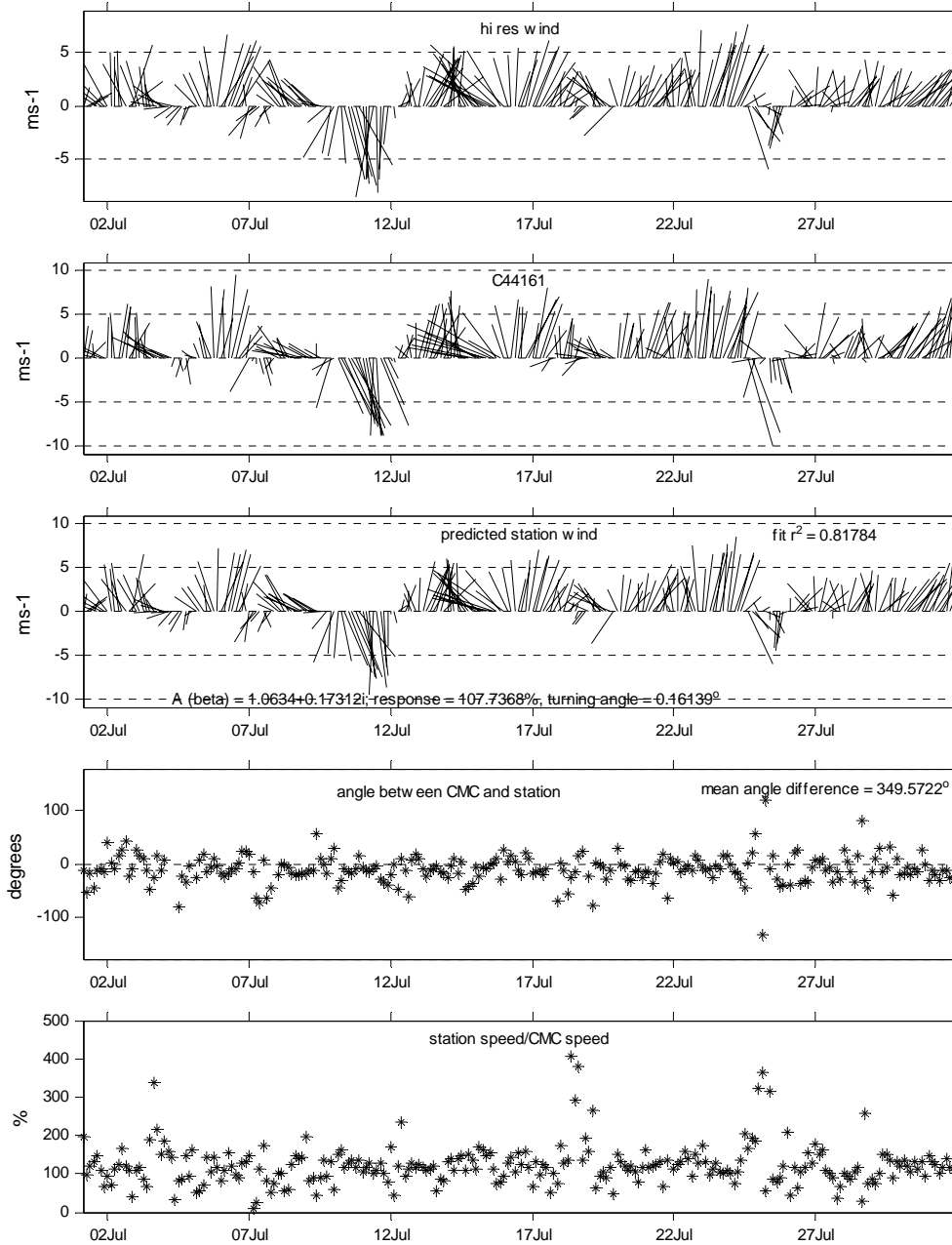


Figure 104 Time series of wave buoy 44161 summer wind vector observations and 3-hourly high resolution forecast output with results of least squares fit

4.2.6 Compare Charlottetown; summer

4.2.6.1 Compare Charlottetown with analysis 6-hourly; summer

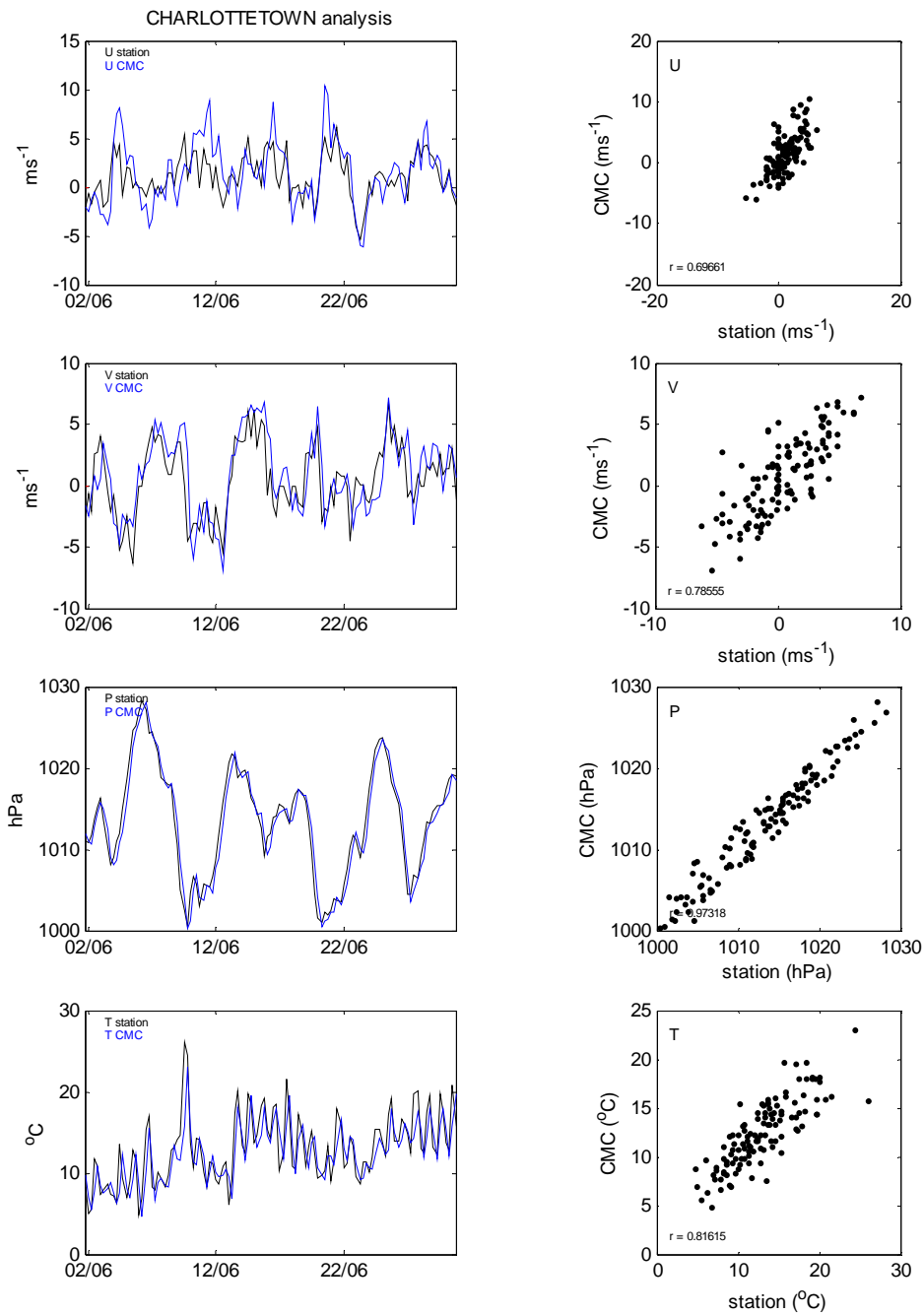


Figure 105 Time series of Charlottetown summer meteorological observations and 6-hourly analysis output; scatter plots of the same with correlation coefficients

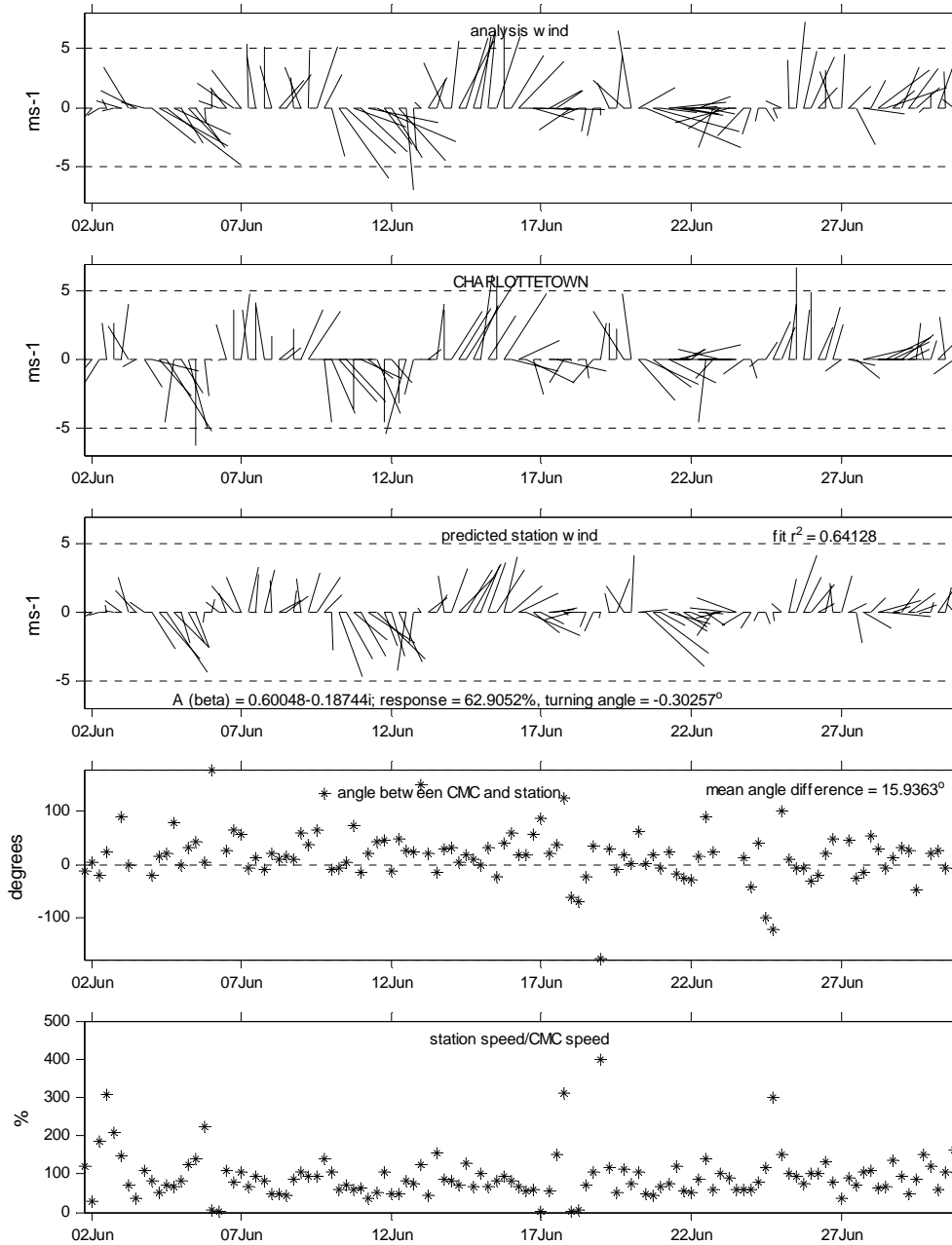


Figure 106 Time series of Charlottetown summer wind vector observations and 6-hourly analysis output with results of least squares fit

4.2.6.2 Compare Charlottetown with low resolution forecast 6-hourly; summer

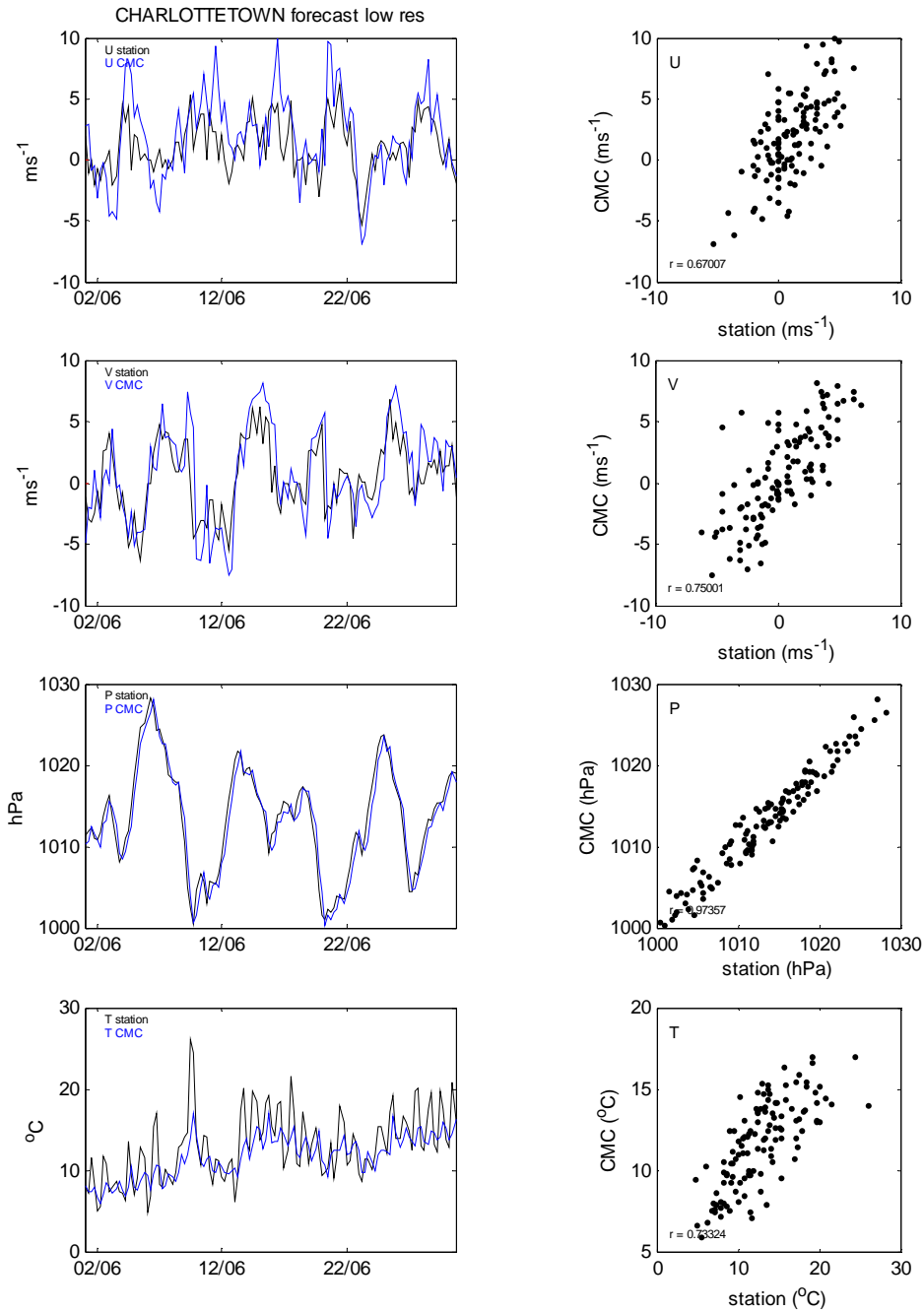


Figure 107 Time series of Charlottetown summer meteorological observations and 6-hourly low resolution forecast output; scatter plots of the same with correlation coefficients

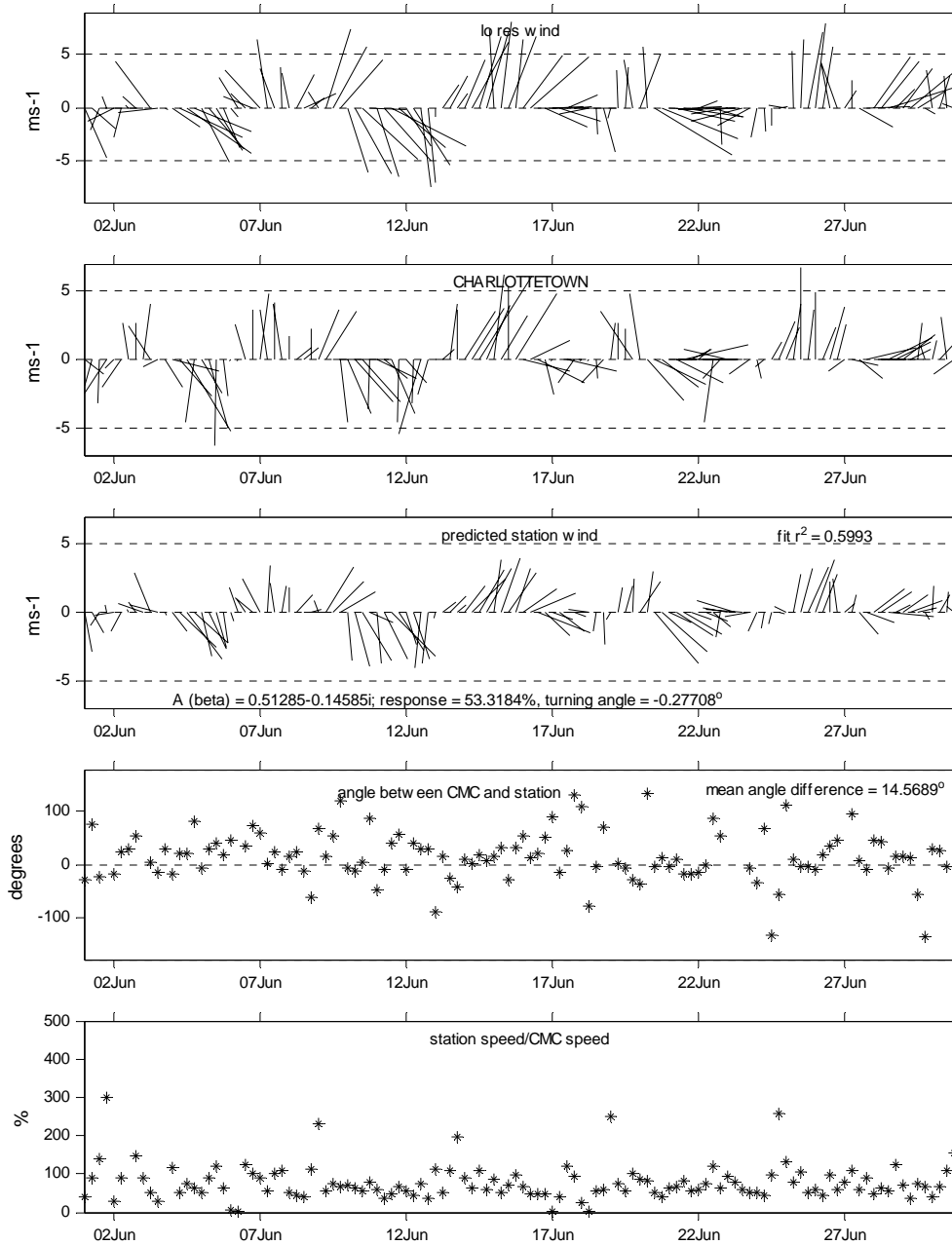


Figure 108 Time series of Charlottetown summer wind vector observations and 6-hourly low resolution forecast output with results of least squares fit

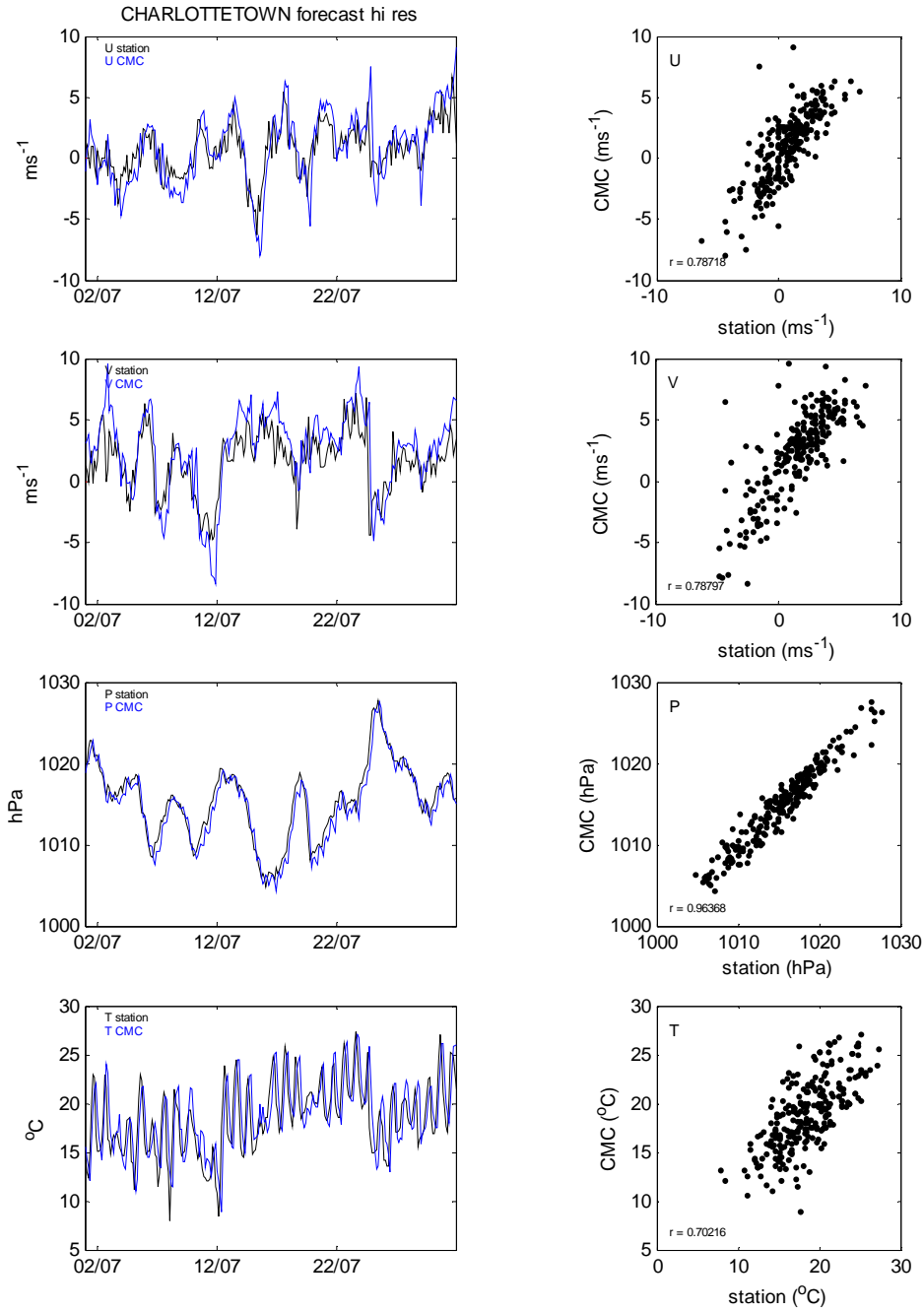


Figure 109 Time series of Charlottetown summer meteorological observations and 3-hourly high resolution forecast output; scatter plots of the same with correlation coefficients

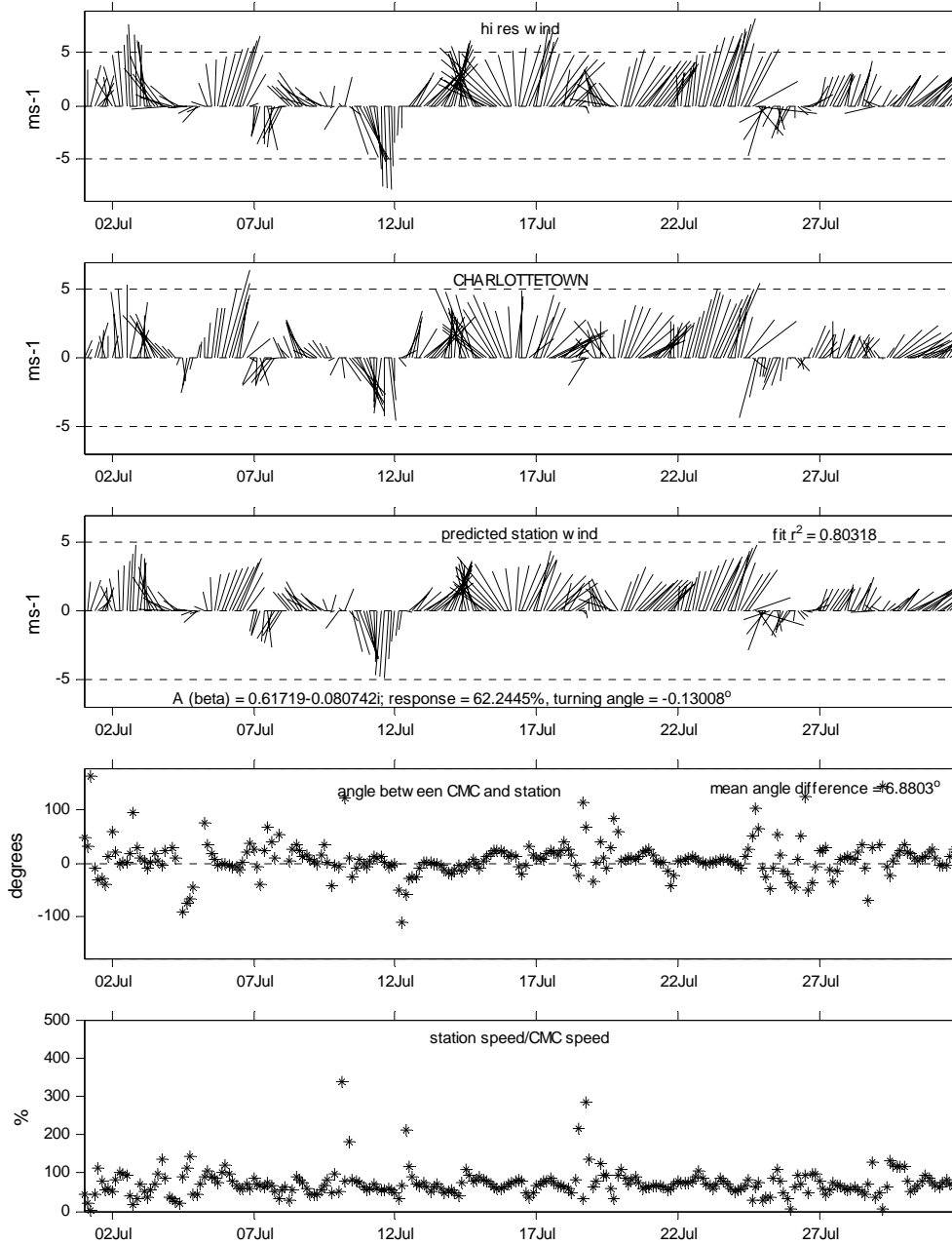


Figure 110 Time series of Charlottetown summer wind vector observations and 3-hourly high resolution forecast output with results of least squares fit

4.2.7 Compare Summerside; summer

4.2.7.1 Compare Summerside with analysis 6-hourly; summer

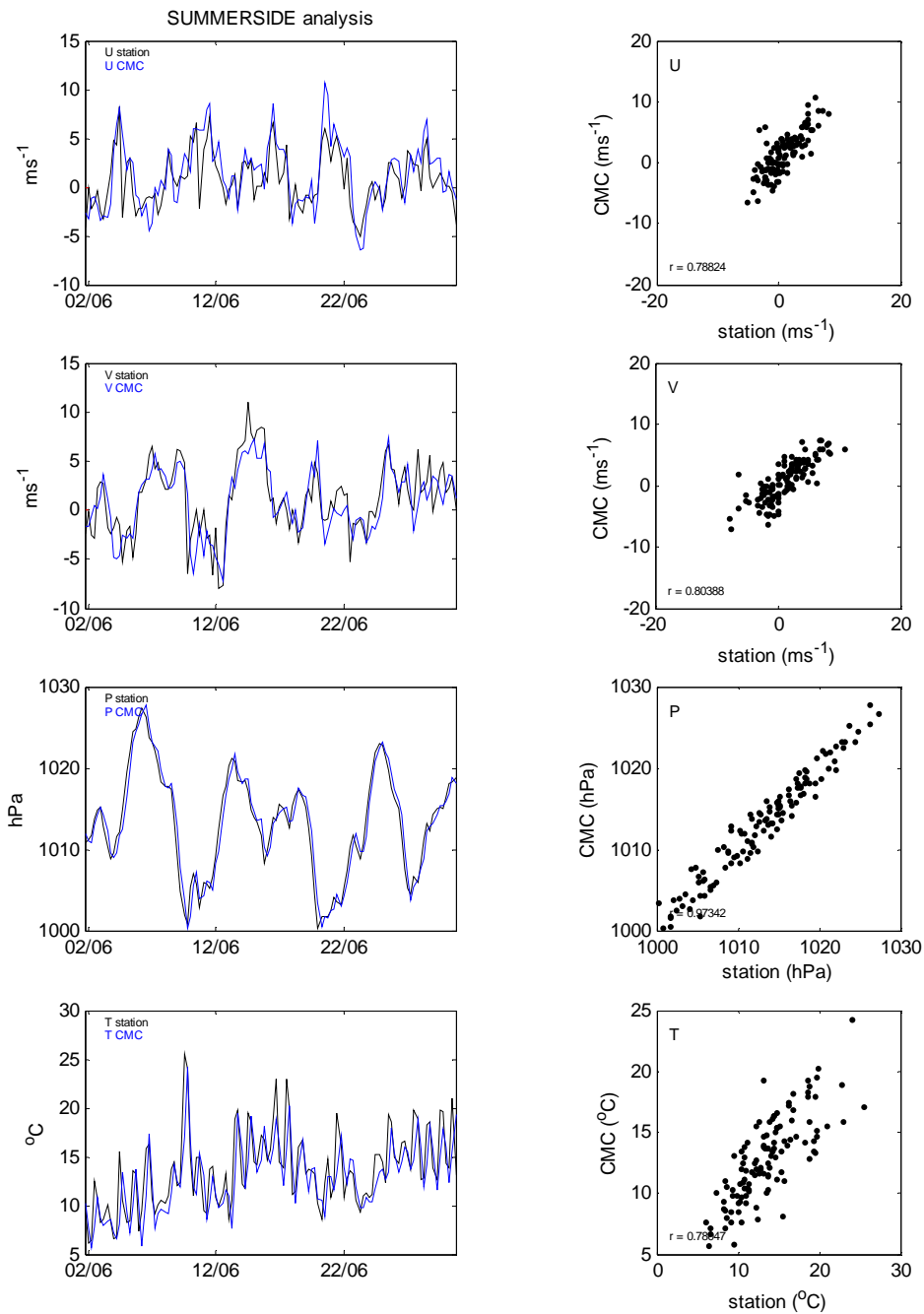


Figure 111 Time series of Summerside summer meteorological observations and 6-hourly analysis output; scatter plots of the same with correlation coefficients

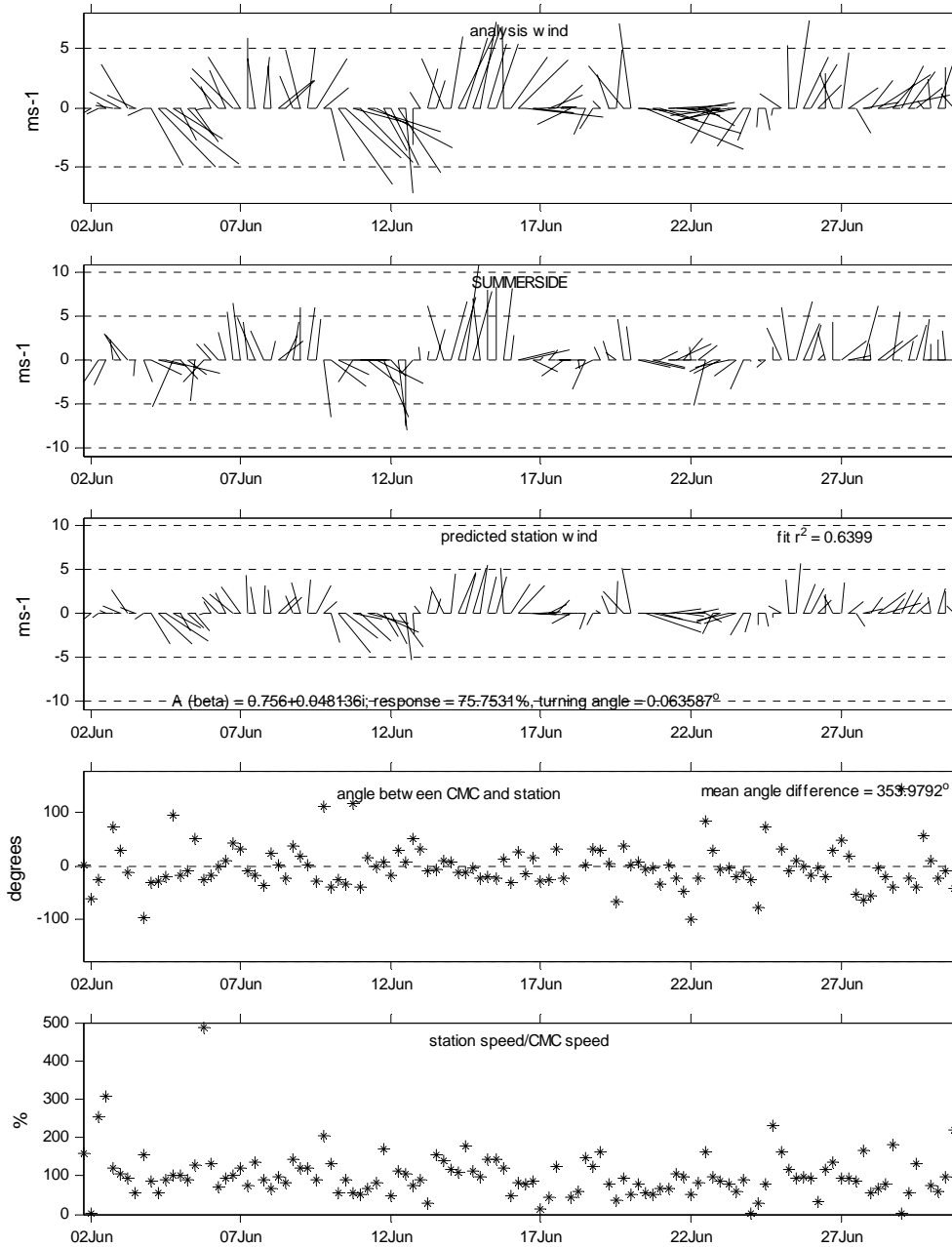


Figure 112 Time series of Summerside summer wind vector observations and 6-hourly analysis output with results of least squares fit

4.2.7.2 Compare Summerside with low resolution forecast 6-hourly; summer

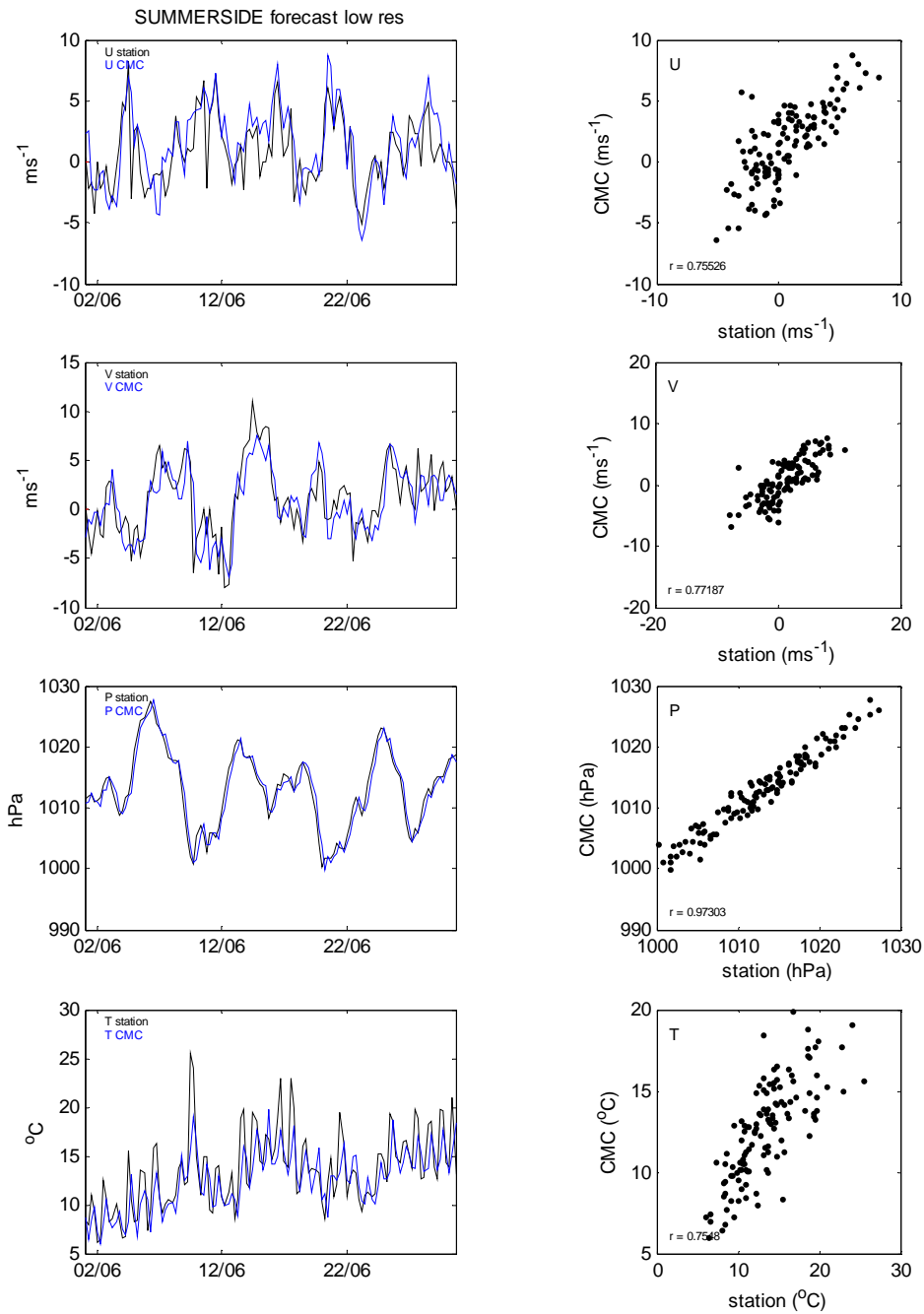


Figure 113 Time series of Summerside summer meteorological observations and 6-hourly low resolution forecast output; scatter plots of the same with correlation coefficients

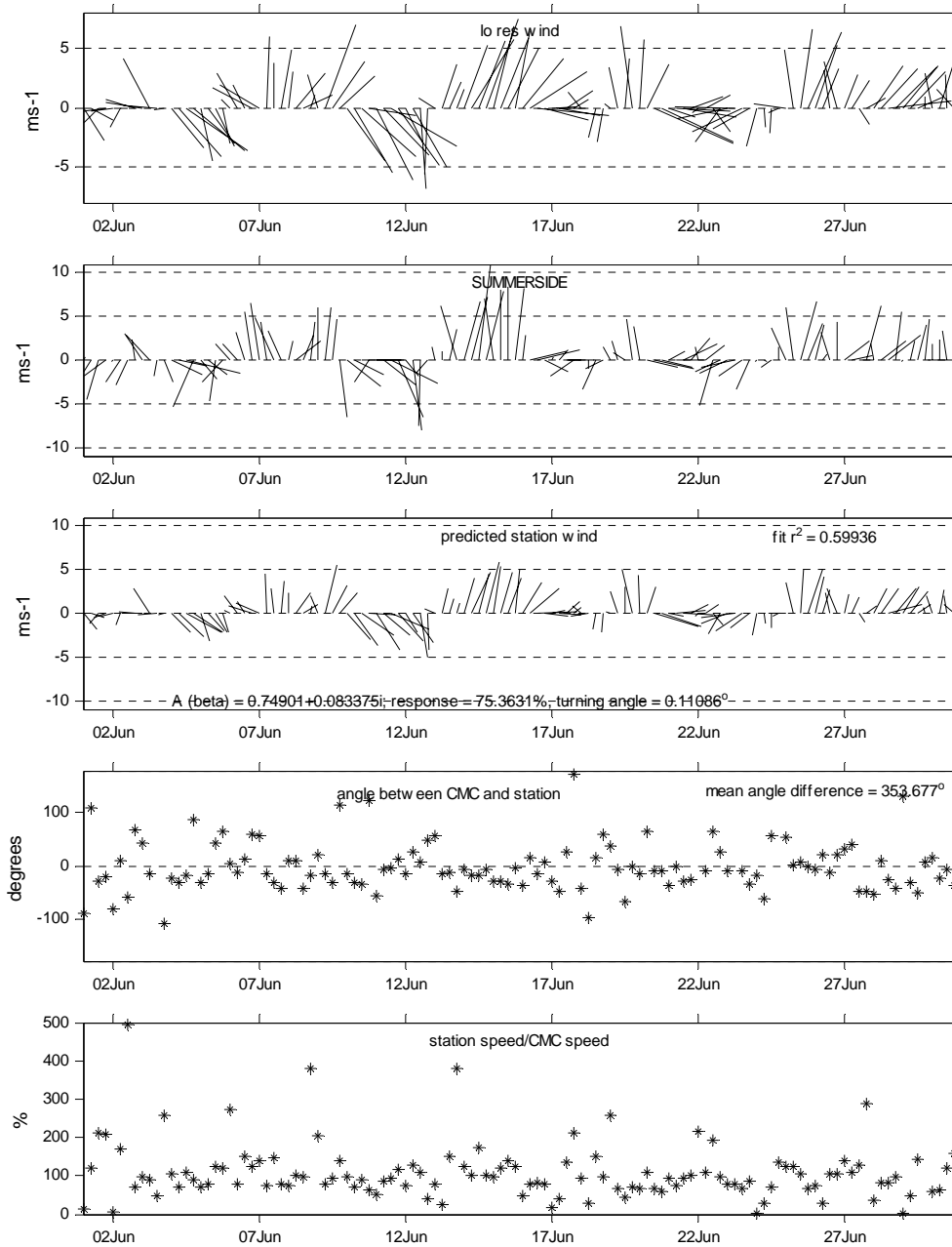


Figure 114 Time series of Summerside summer wind vector observations and 6-hourly low resolution forecast output with results of least squares fit

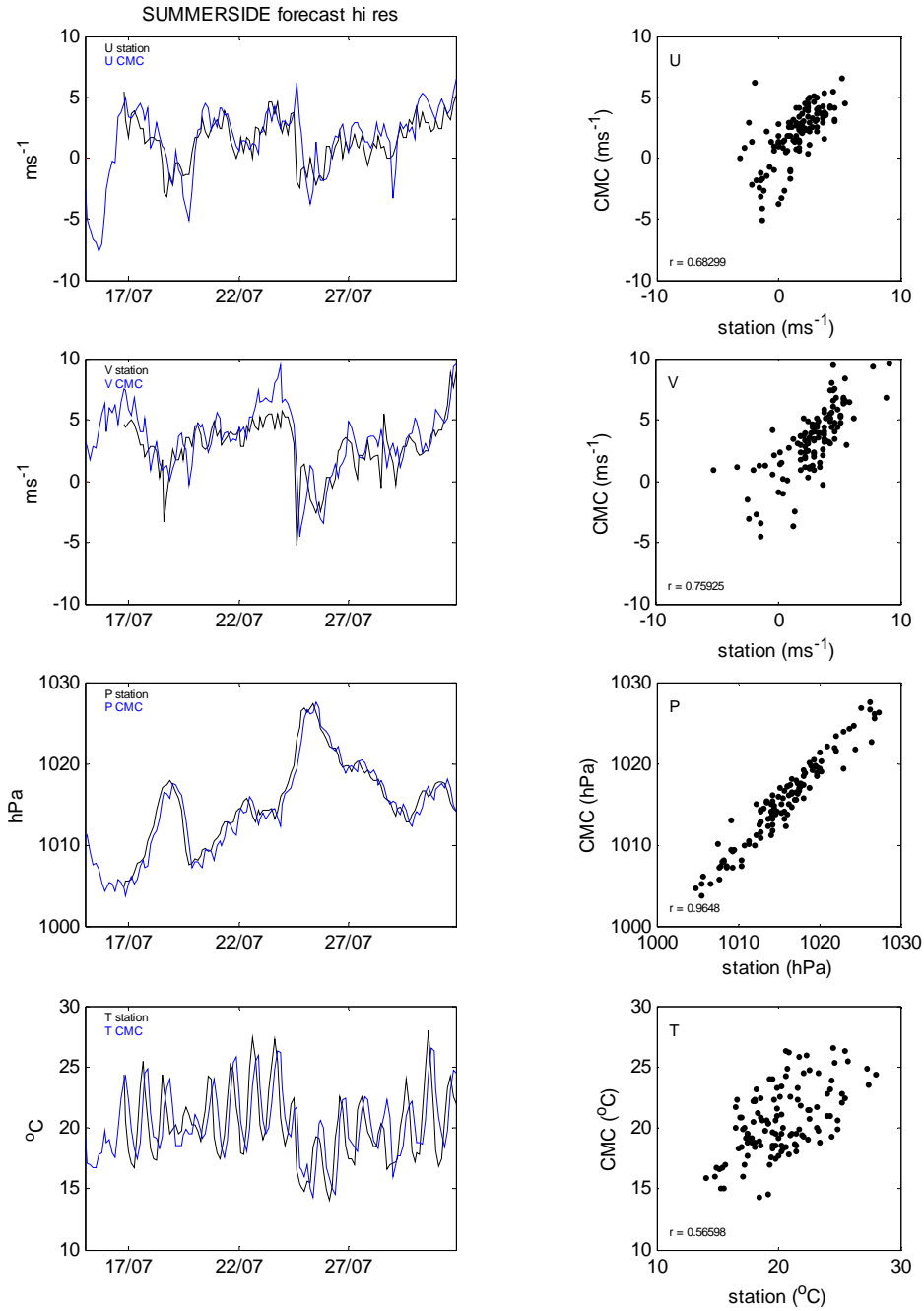


Figure 115 Time series of Summerside summer meteorological observations and 3-hourly high resolution forecast output; scatter plots of the same with correlation coefficients

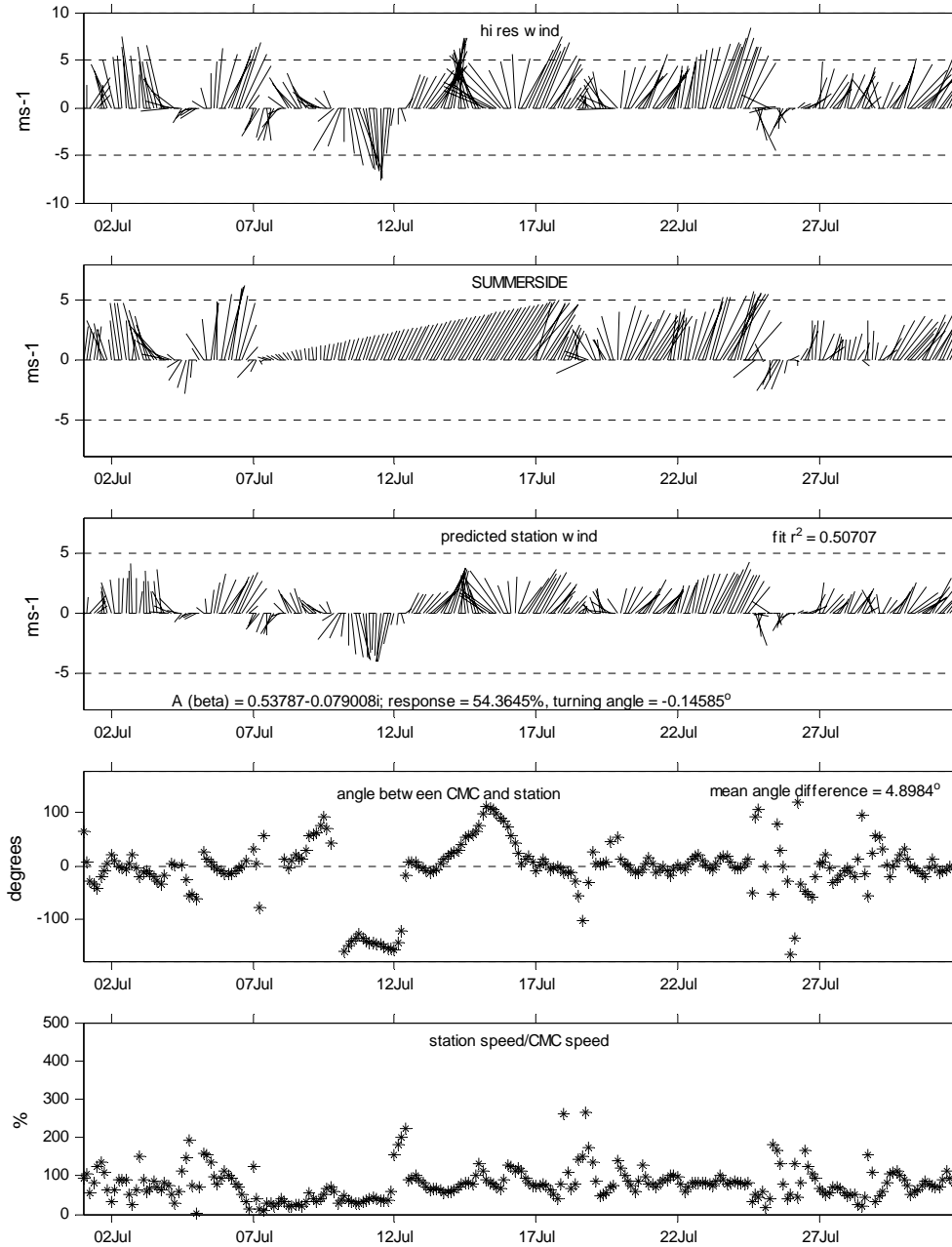


Figure 116 Time series of Summerside summer wind vector observations and 3-hourly high resolution forecast output with results of least squares fit

4.2.8 Compare Iles de la Madeleine; summer

4.2.8.1 Compare Iles de la Madeleine with analysis 6-hourly; summer

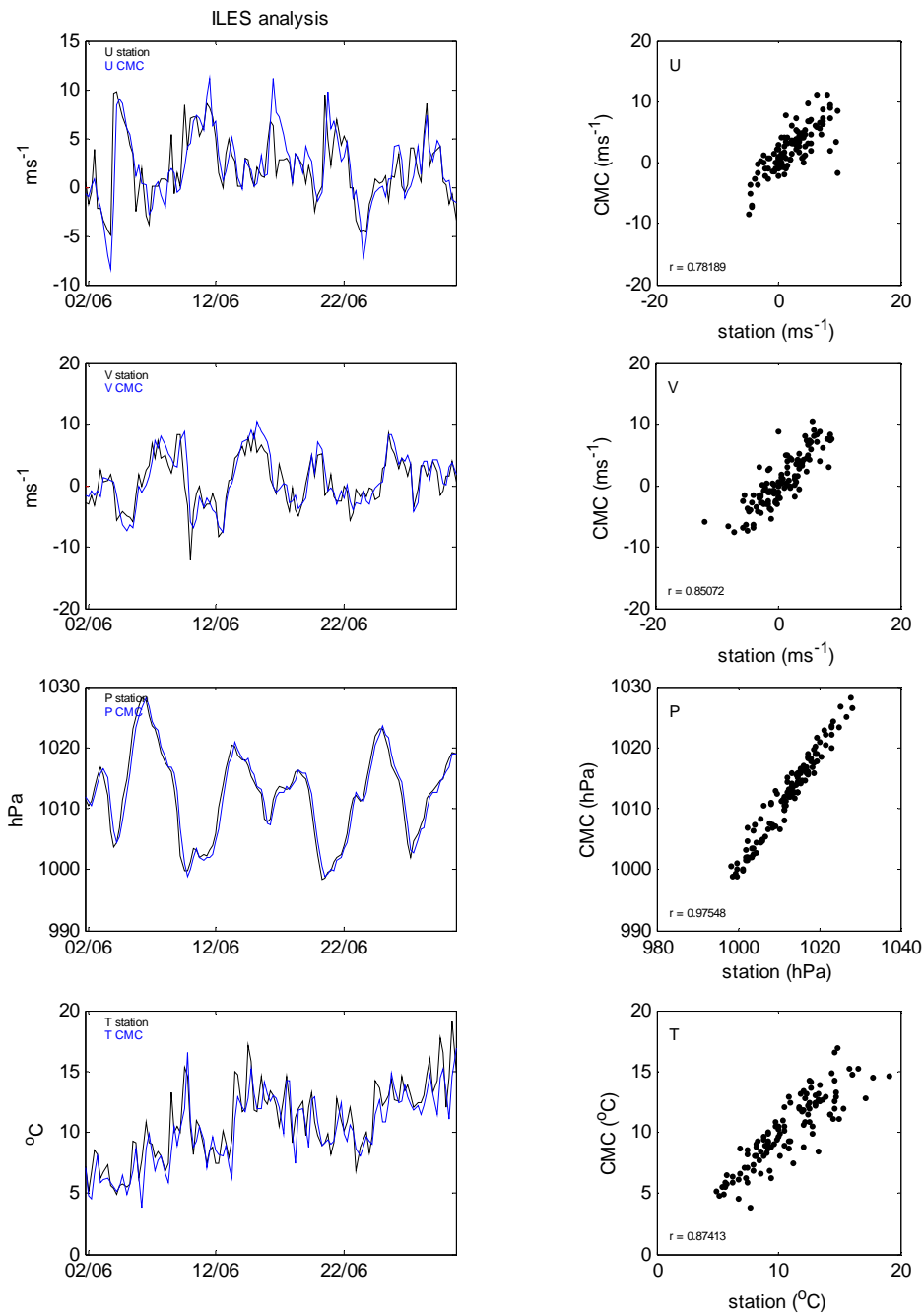


Figure 117 Time series of Iles de la Madeleine summer meteorological observations and 6-hourly analysis output; scatter plots of the same with correlation coefficients.

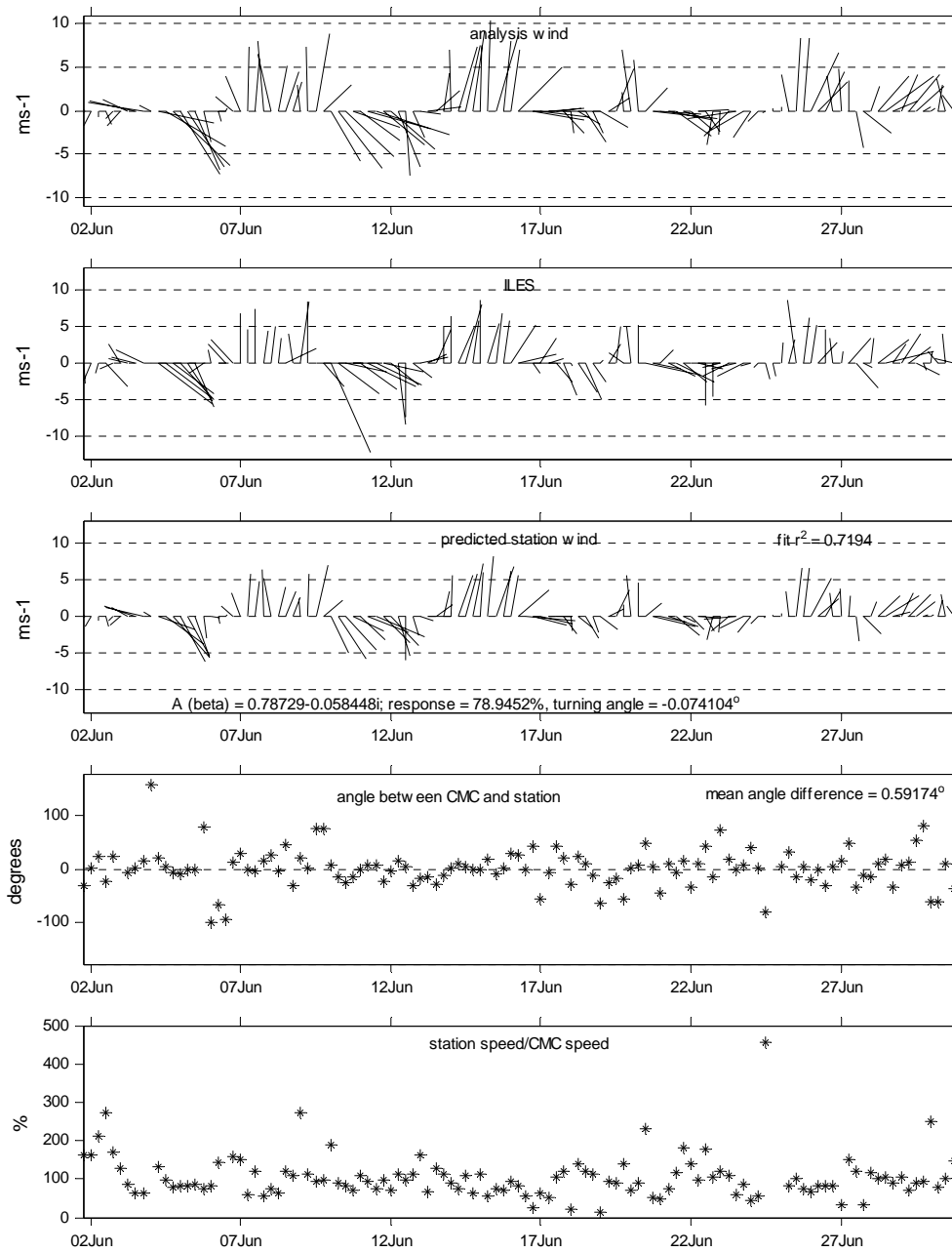


Figure 118 Time series of Iles de la Madeleine summer wind vector observations and 6-hourly analysis output with results of least squares fit.

4.2.8.2 Compare Iles de la Madeleine with low resolution forecast 6-hourly; summer

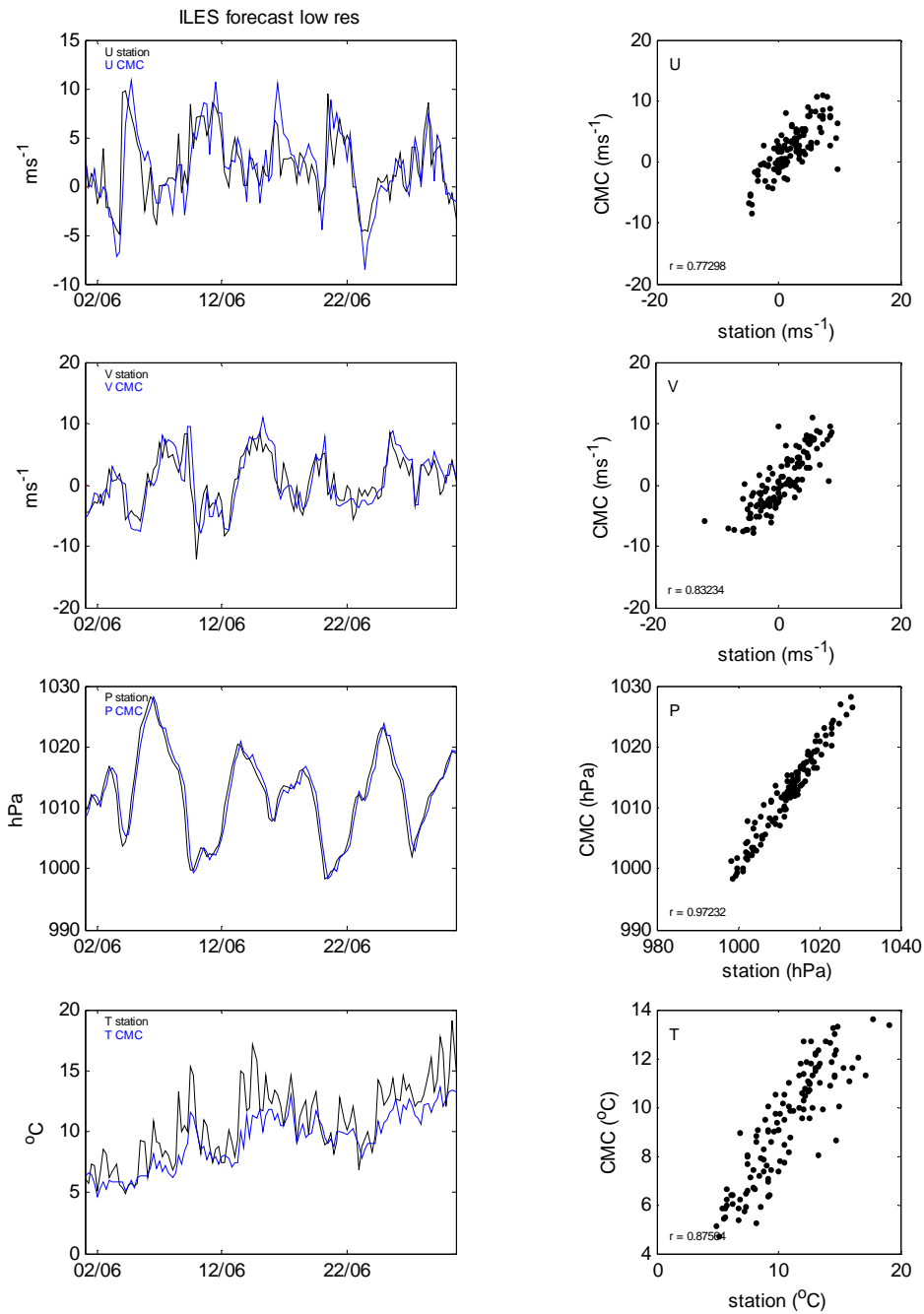


Figure 119 Time series of Iles de la Madeleine summer meteorological observations and 6-hourly low resolution forecast output; scatter plots of the same with correlation coefficients

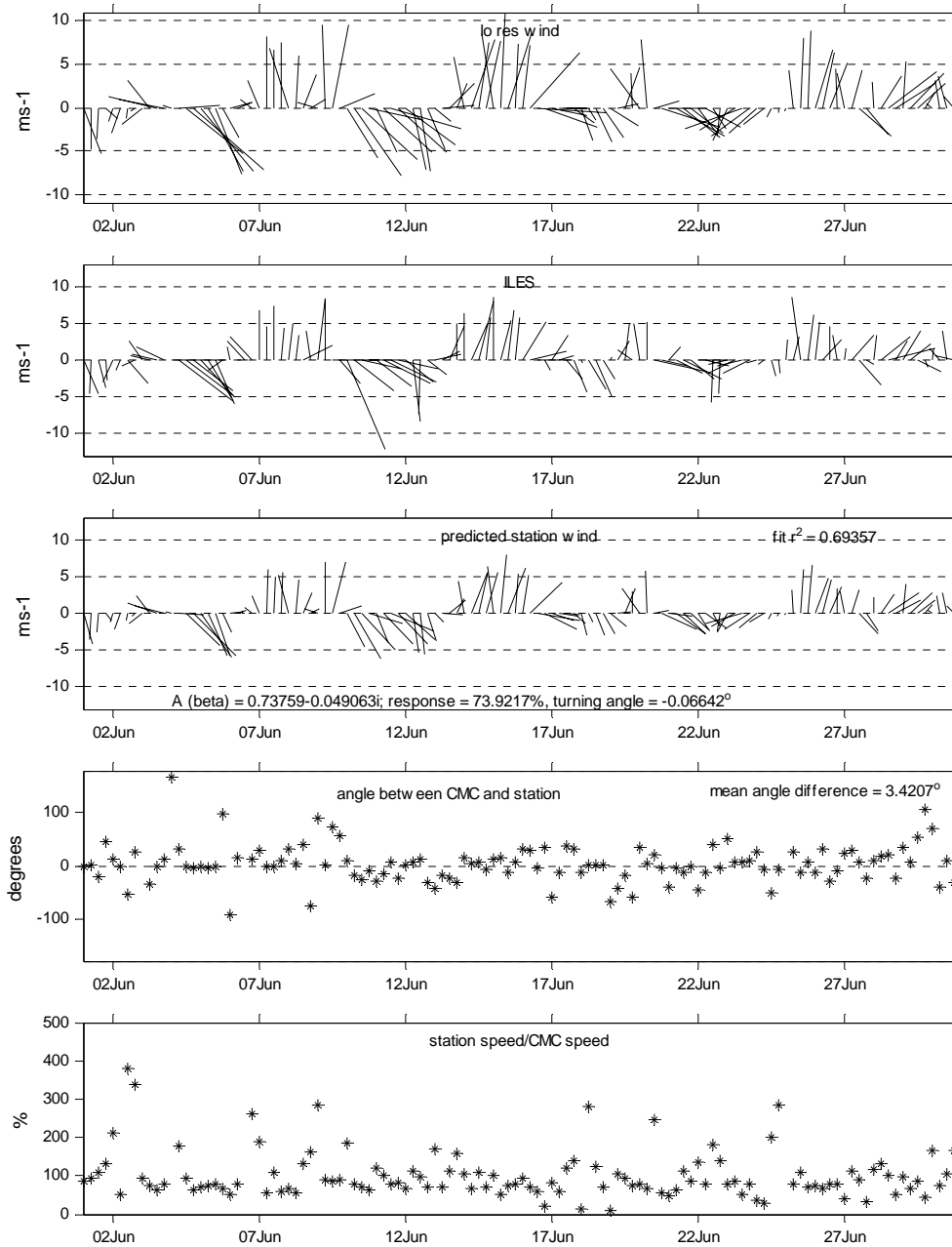


Figure 120 Time series of Iles de la Madeleine summer wind vector observations and 6-hourly low resolution forecast output with results of least squares fit

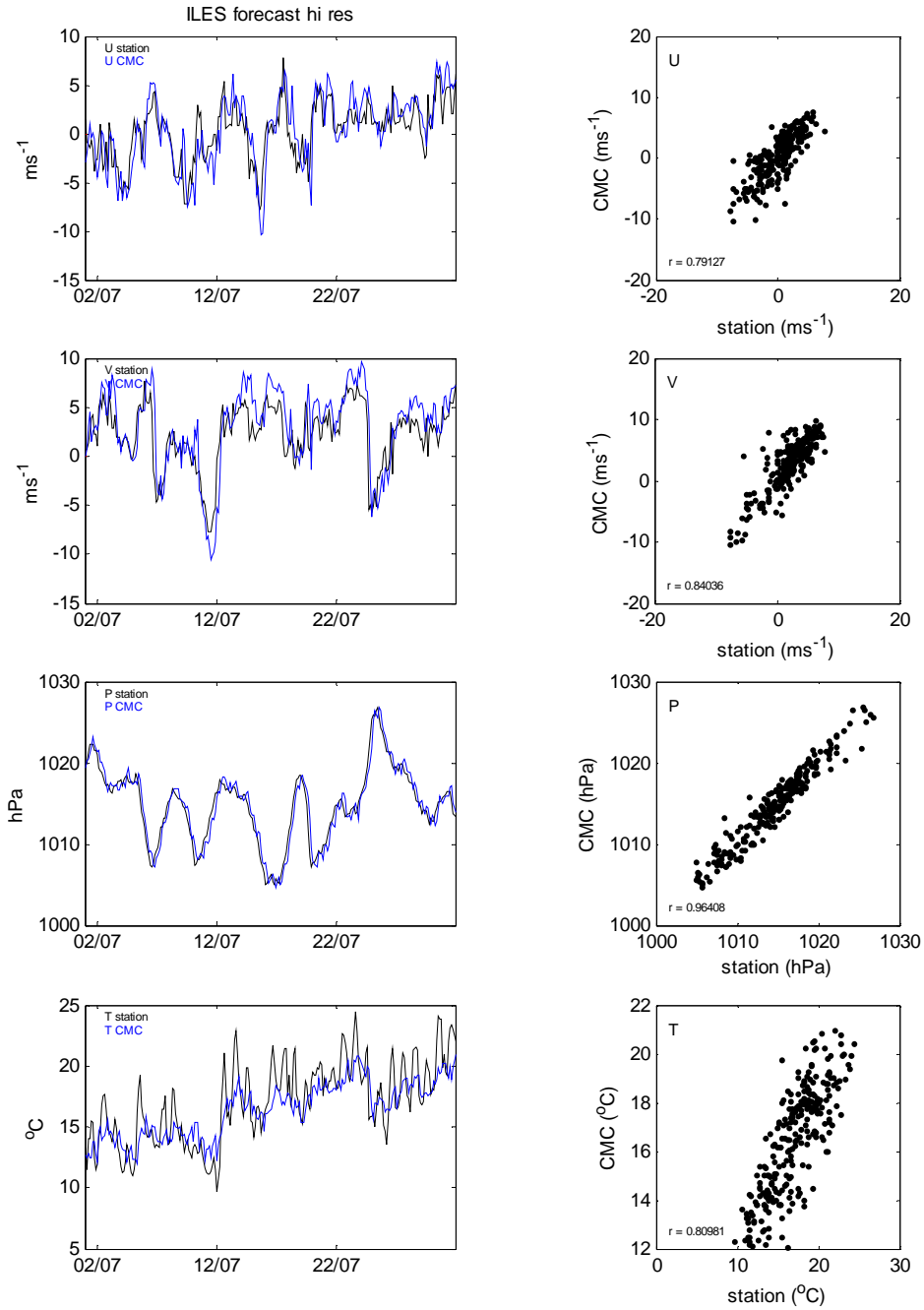


Figure 121 Time series of Iles de la Madeleine summer meteorological observations and 3-hourly high resolution forecast output; scatter plots of the same with correlation coefficients

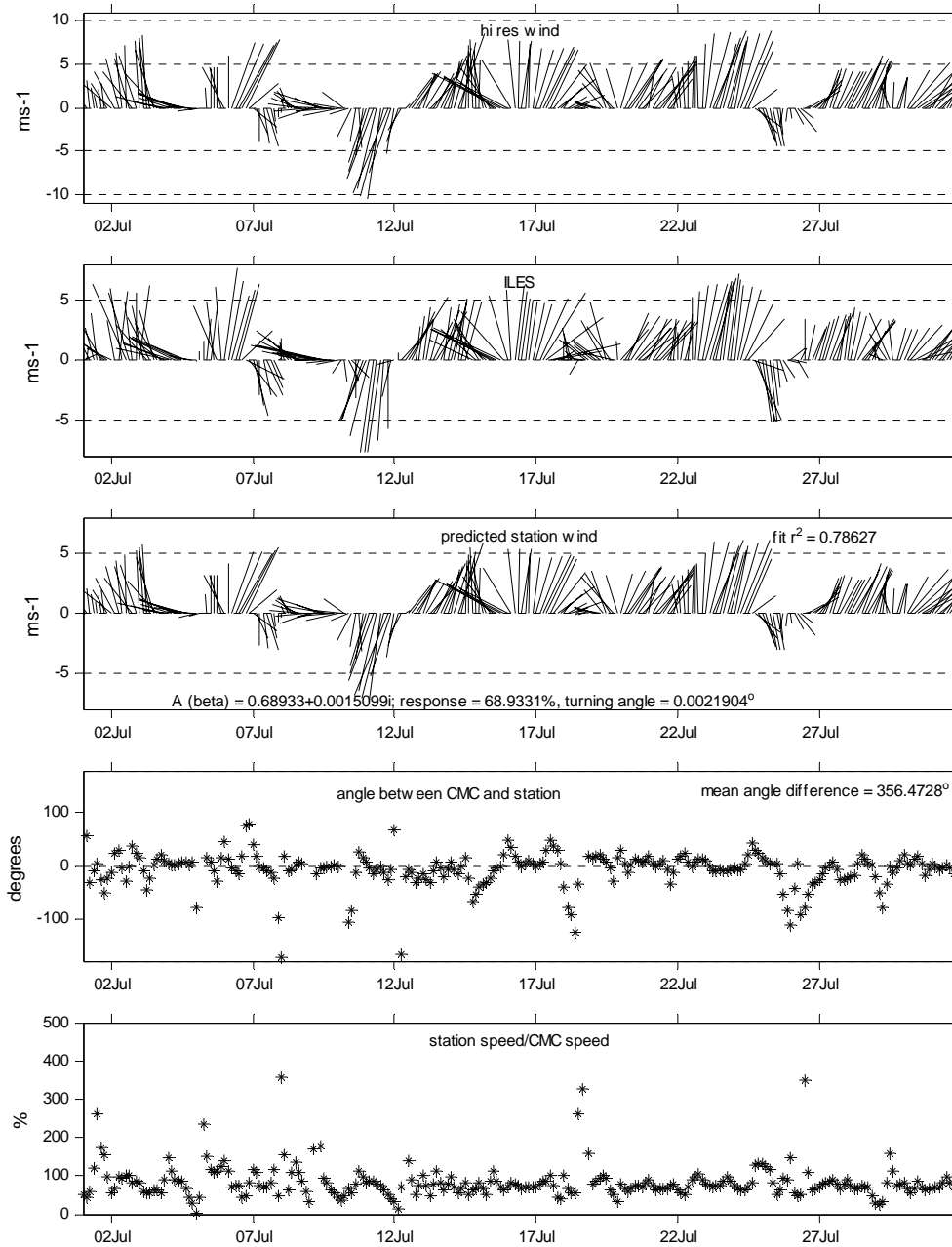


Figure 122 Time series of Iles de la Madeleine summer wind vector observations and 3-hourly high resolution forecast output with results of least squares fit

4.3 Beacon drift analysis with 6-hourly analysis winds

In this section the 6-hourly low resolution analysis wind data were used to complete a regression analysis with ice drift for beacons 26370 and 26386 for the entire drift record and for the time up to but not including Feb. 20. The method is the same as that reported in the main part of this report, except that for a second analysis the beacon positions were interpolated to be 6-hourly to create 6-hourly drift records. Results of the least squares regressions are given in tables and figures. Tides have not been filtered from drift records.

Beacon position data were used to compute drift (distance between beacon at time, t , and the beacon position at time, $t-1$; converted to m/s) and 6-hourly wind data were interpolated to match beacon positions in time (hourly or 6-hourly) and space to produce wind records for each beacon.

Table 10 Regression results for least squares fit of drift to 6-hourly analysis wind. $R^2 > 50\%$ and Gain $\geq 1.9\%$ are in bold.

Beacon	R^2	Turning angle θ (deg)	Gain (%)
<i>Entire data record hourly</i>			
26370	0.10	-4.40	0.53
26386	0.08	9.41	0.62
<i>Until 20 Feb hourly</i>			
26370	0.87	-12.60	3.48
26386	0.86	-17.82	3.10
<i>Entire data record 6-hourly</i>			
26370	0.13	-12.19	0.51
26386	0.09	0.12	0.53
<i>Until 20 Feb 6-hourly</i>			
26370	0.90	-18.48	3.07
26386	N/A	N/A	N/A

Results were similar to those using the low resolution forecast winds and for data before Feb. 20, gains were in the right ball-park (3%) and there are good R^2 values: 86% and 887% for hourly data up to Feb. 20 and 90% variance for 6-hourly data to Feb. 20.

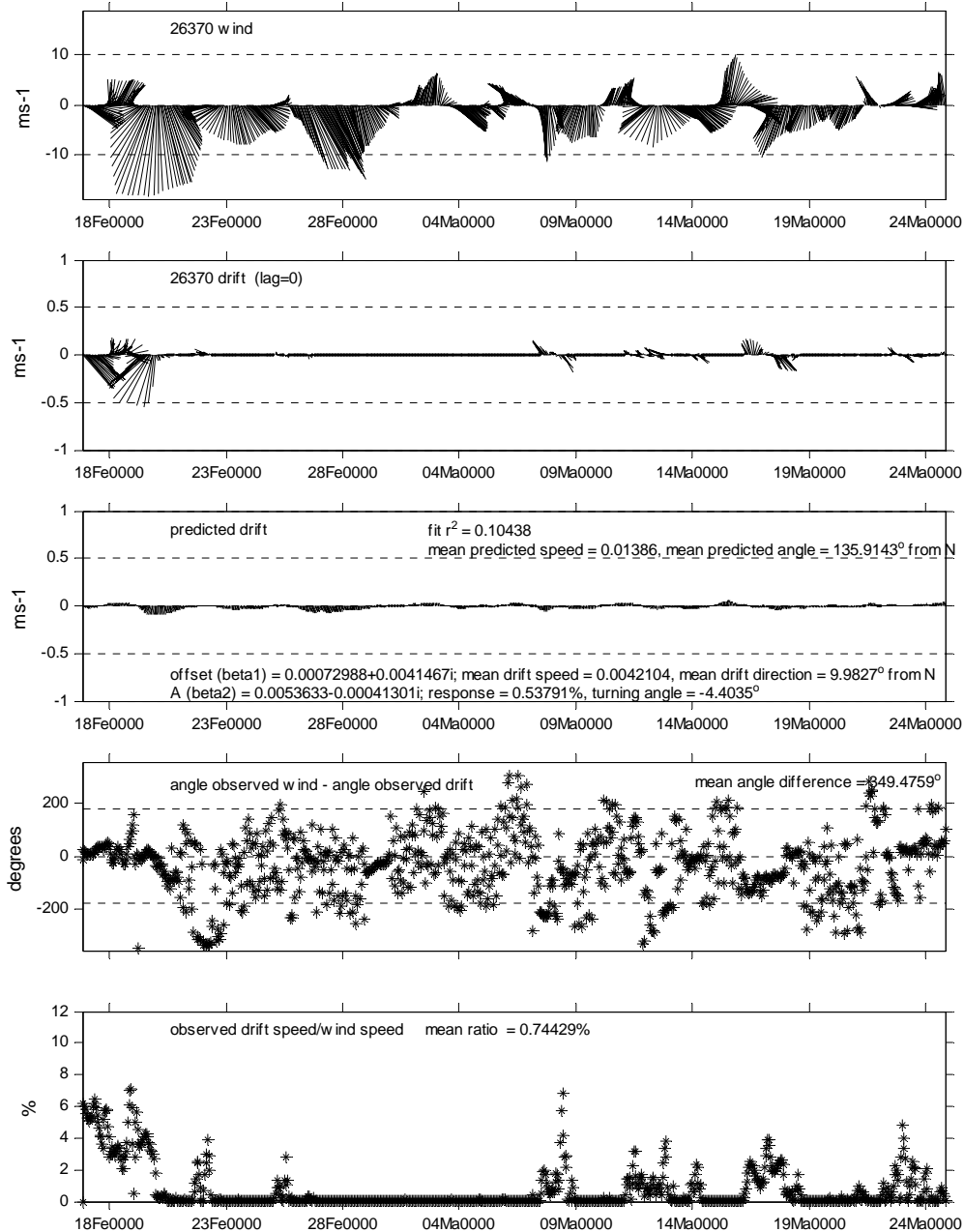


Figure 123 Results of complex least squares regression of 1-hourly analysis wind and drift data for beacon 26370. The figure shows hourly wind and beacon drift, the predicted drift values (ie. fitted series), the angle difference between wind vectors and drift vectors (with mean angle difference), and the ratio of drift speed to wind speed (with mean ratio).

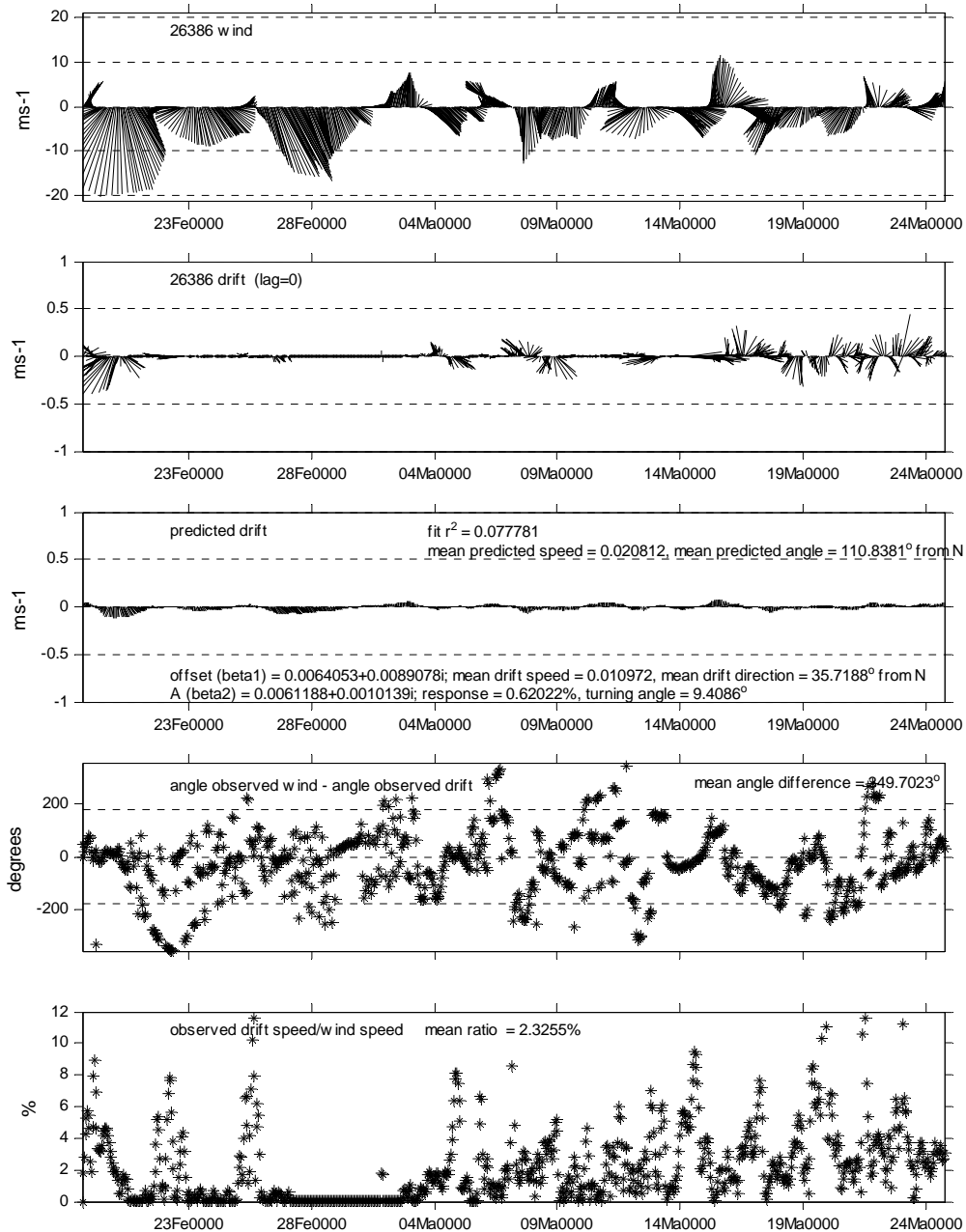


Figure 124 Results of complex least squares regression of 1-hourly analysis wind and drift data for beacon 26386. The figure shows hourly wind and beacon drift, the predicted drift values (ie. fitted series), the angle difference between wind vectors and drift vectors (with mean angle difference), and the ratio of drift speed to wind speed (with mean ratio).

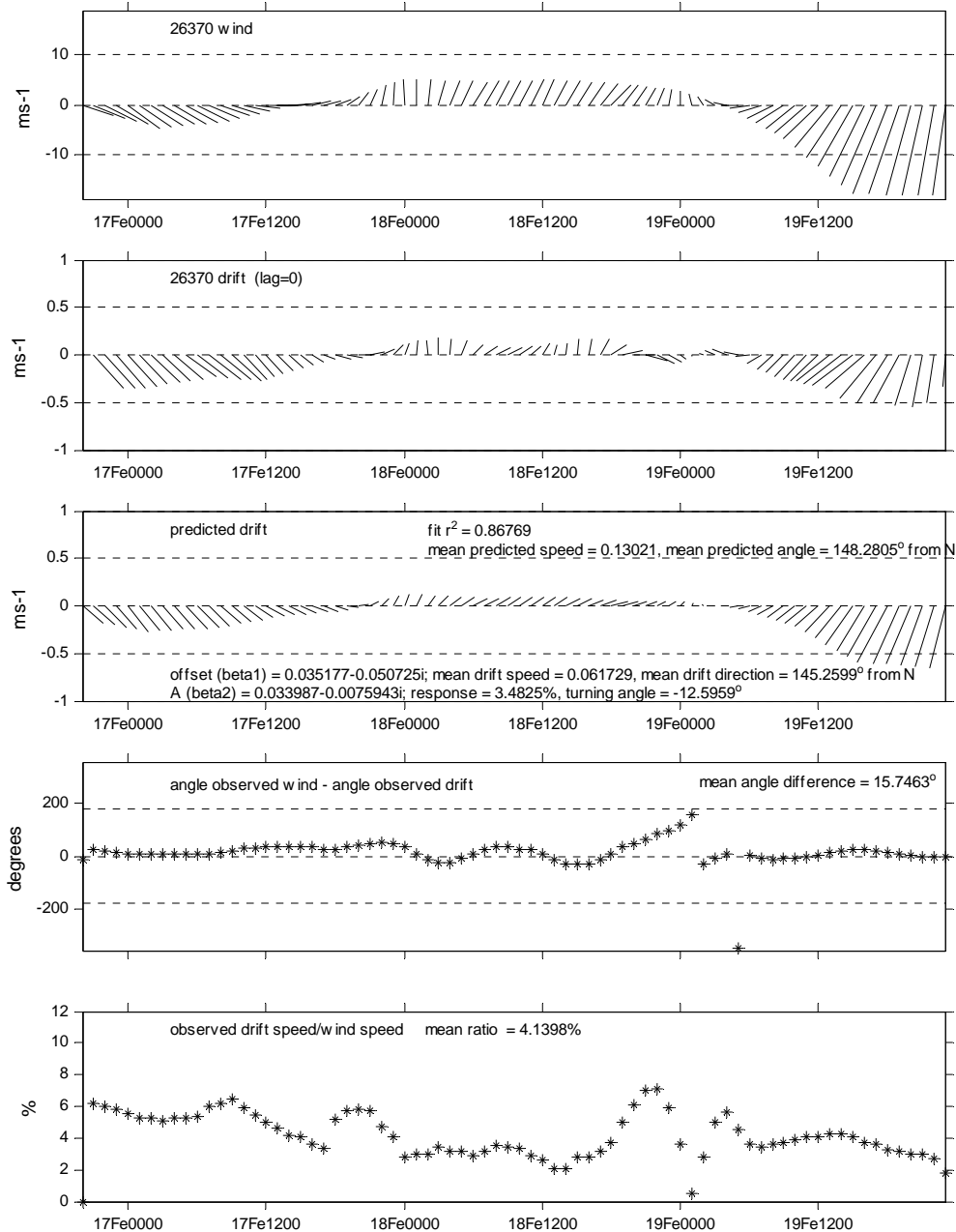


Figure 125 Results of complex least squares regression of 1-hourly analysis wind and drift data for beacon 26370 until 20 February only. The figure shows hourly wind and beacon drift, the predicted drift values (ie. fitted series), the angle difference between wind vectors and drift vectors (with mean angle difference), and the ratio of drift speed to wind speed (with mean ratio).

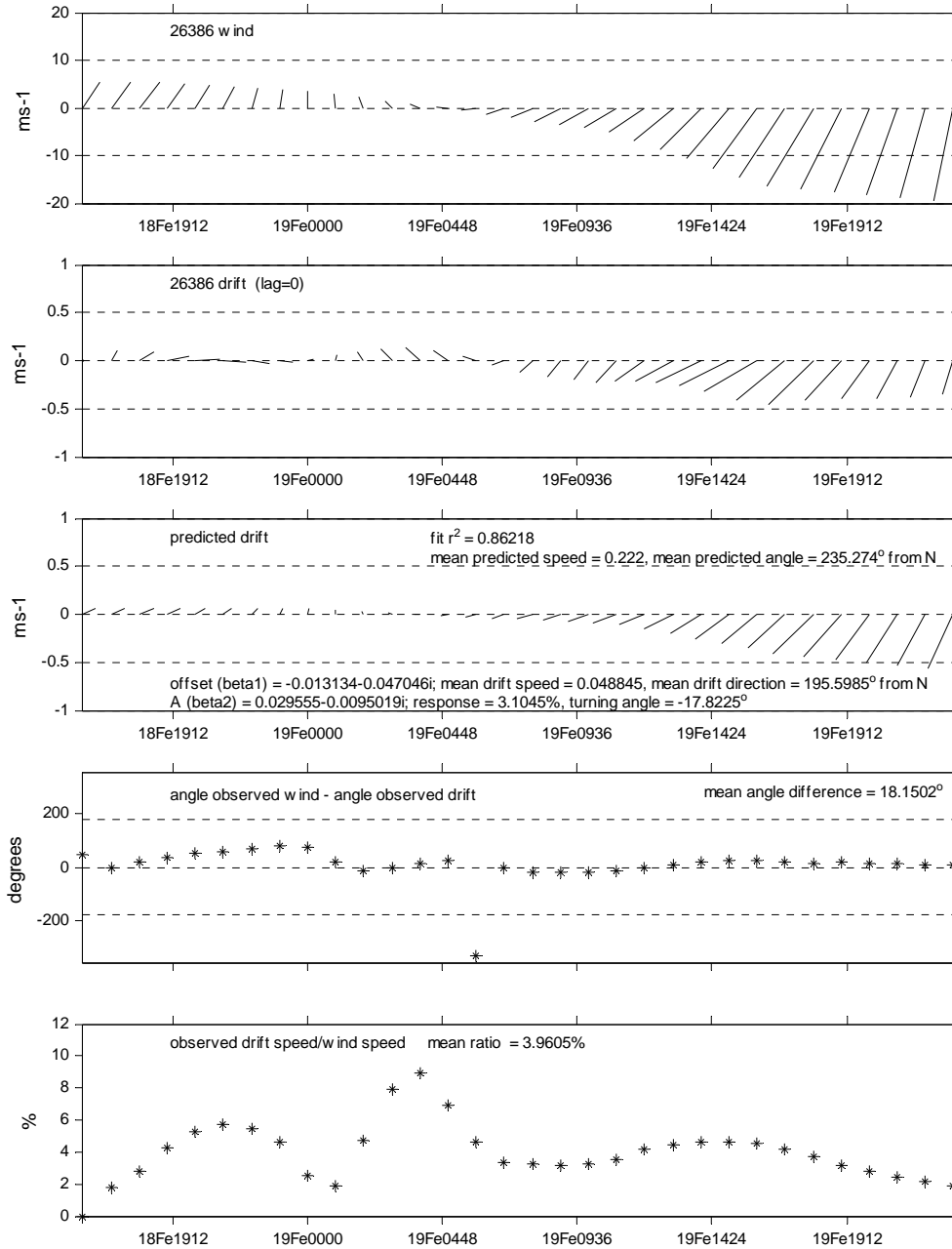


Figure 126 Results of complex least squares regression of 1-hourly analysis wind and drift data for beacon 26386 until 20 February only. The figure shows hourly wind and beacon drift, the predicted drift values (ie. fitted series), the angle difference between wind vectors and drift vectors (with mean angle difference), and the ratio of drift speed to wind speed (with mean ratio).

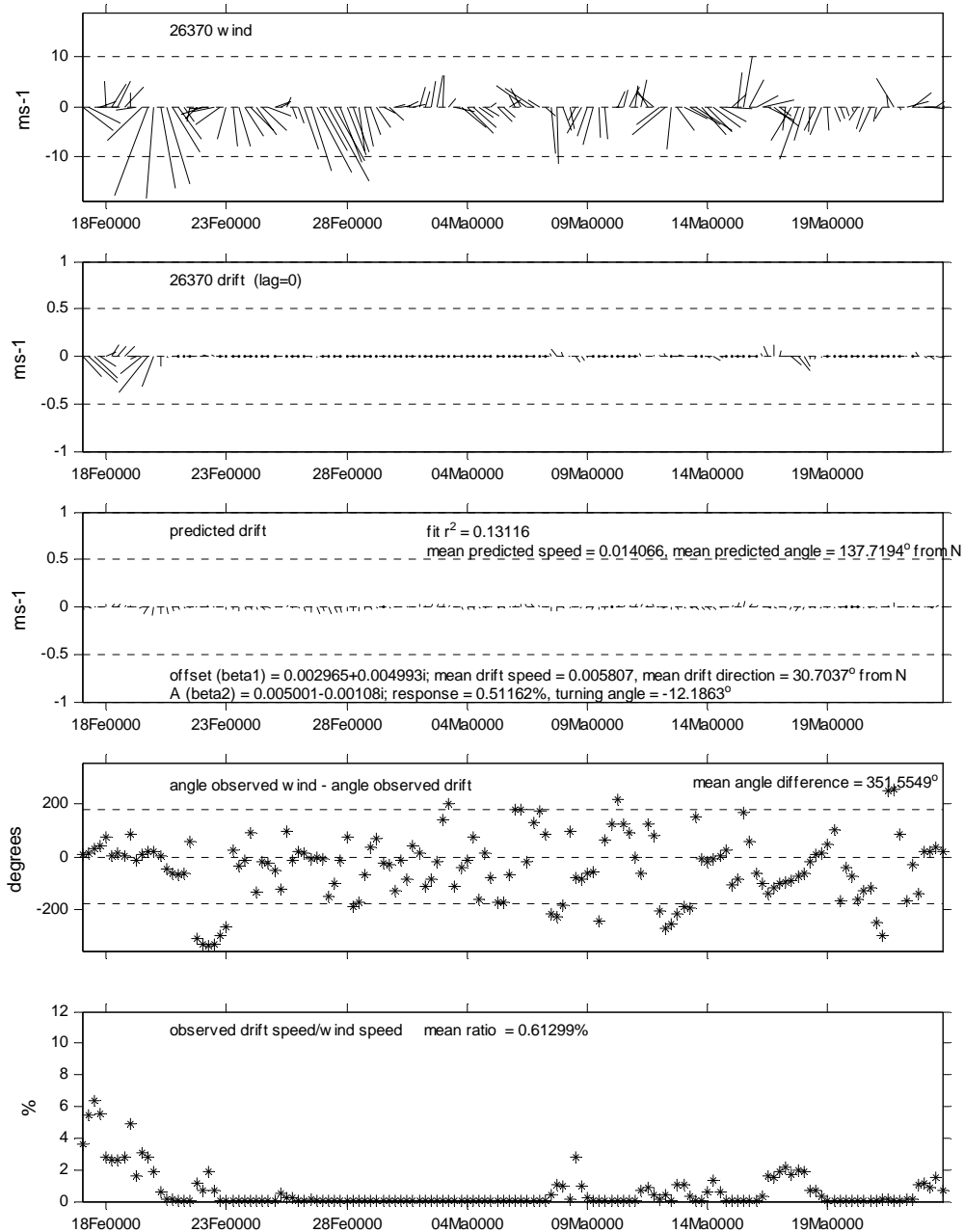


Figure 127 Results of complex least squares regression of 6-hourly analysis wind and drift data for beacon 26370. The figure shows hourly wind and beacon drift, the predicted drift values (ie. fitted series), the angle difference between wind vectors and drift vectors (with mean angle difference), and the ratio of drift speed to wind speed (with mean ratio).

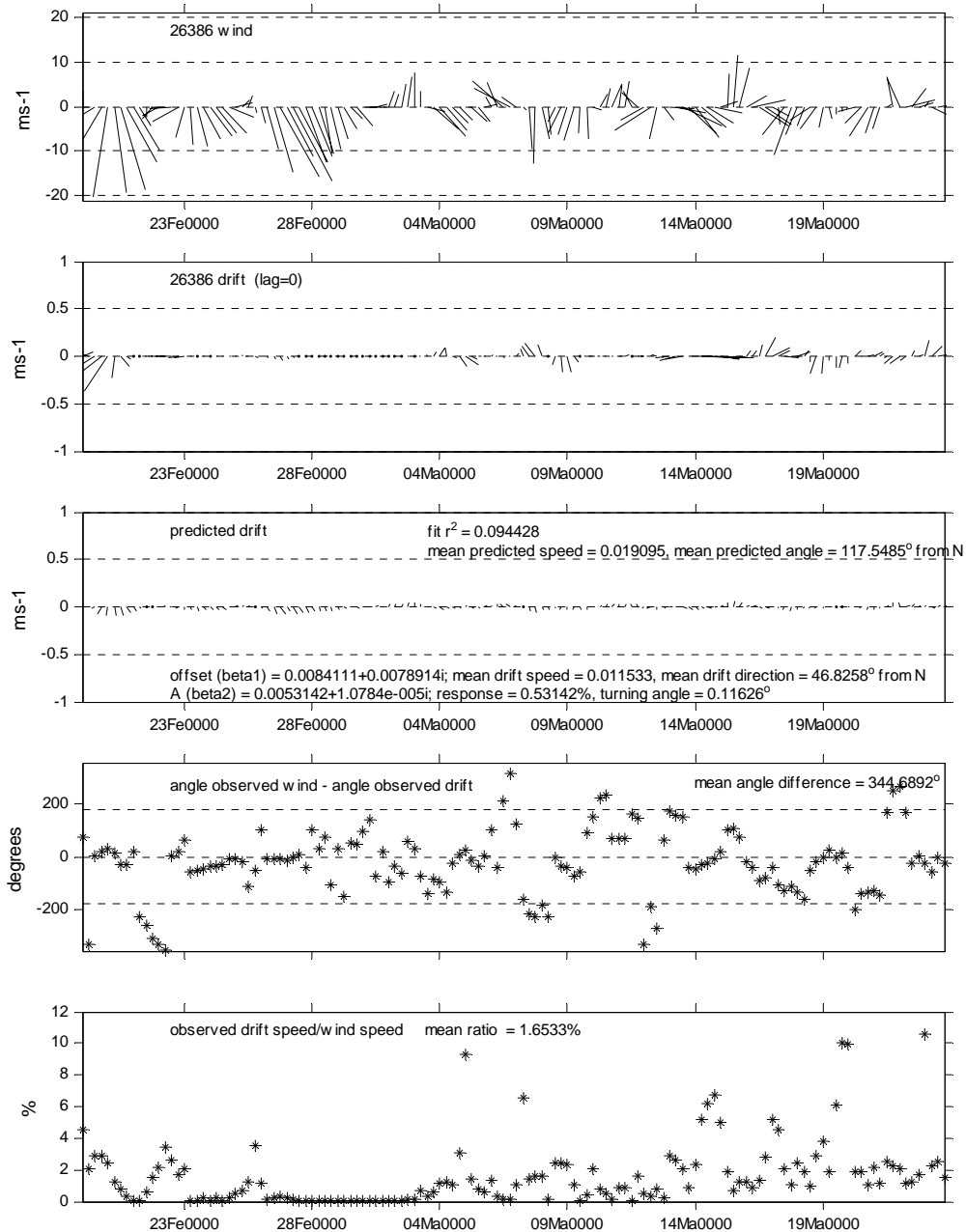


Figure 128 Results of complex least squares regression of 6-hourly analysis wind and drift data for beacon 26386. The figure shows hourly wind and beacon drift, the predicted drift values (ie. fitted series), the angle difference between wind vectors and drift vectors (with mean angle difference), and the ratio of drift speed to wind speed (with mean ratio).

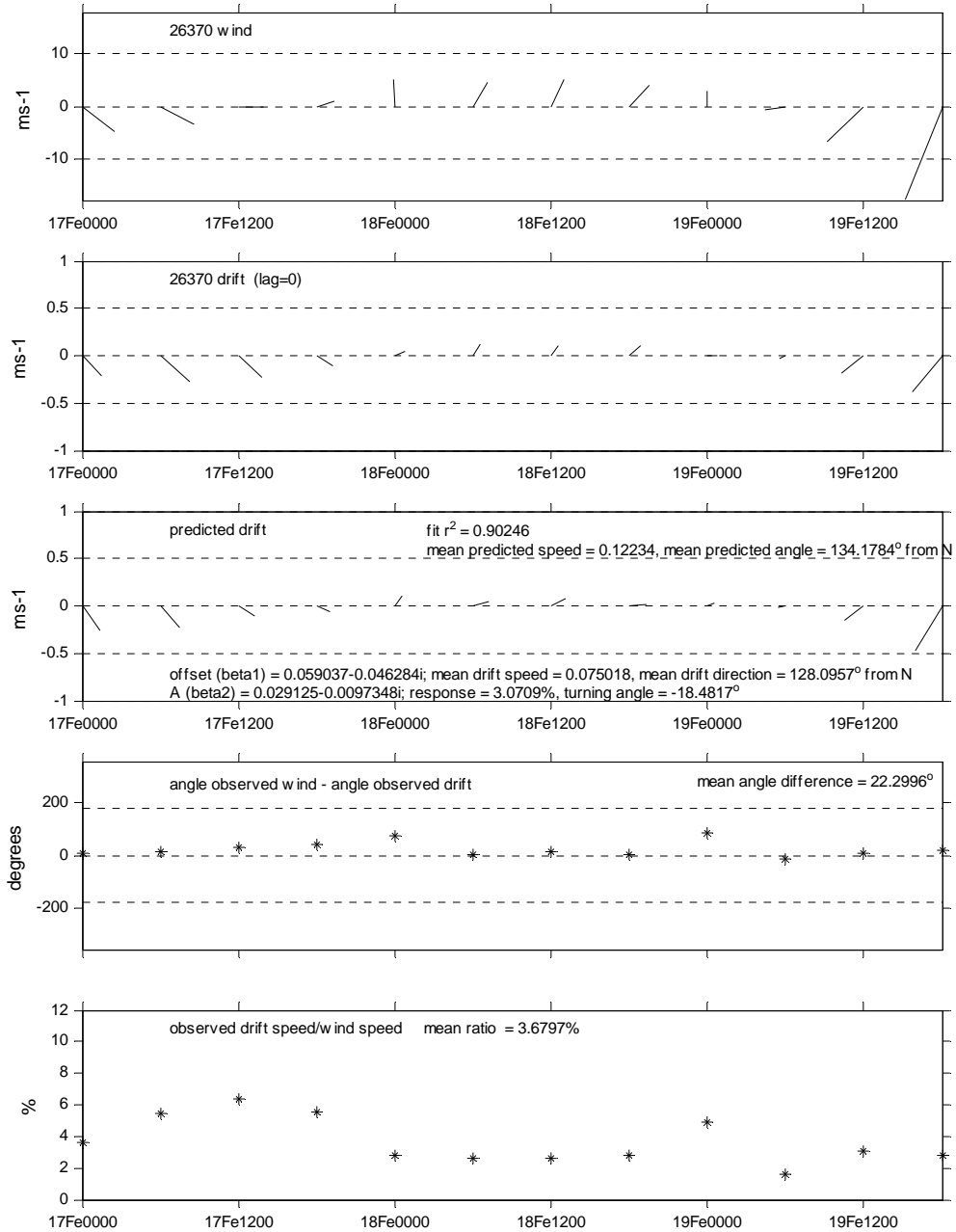


Figure 129 Results of complex least squares regression of 6-hourly analysis wind and drift data for beacon 26370 until 20 February. The figure shows hourly wind and beacon drift, the predicted drift values (ie. fitted series), the angle difference between wind vectors and drift vectors (with mean angle difference), and the ratio of drift speed to wind speed (with mean ratio).

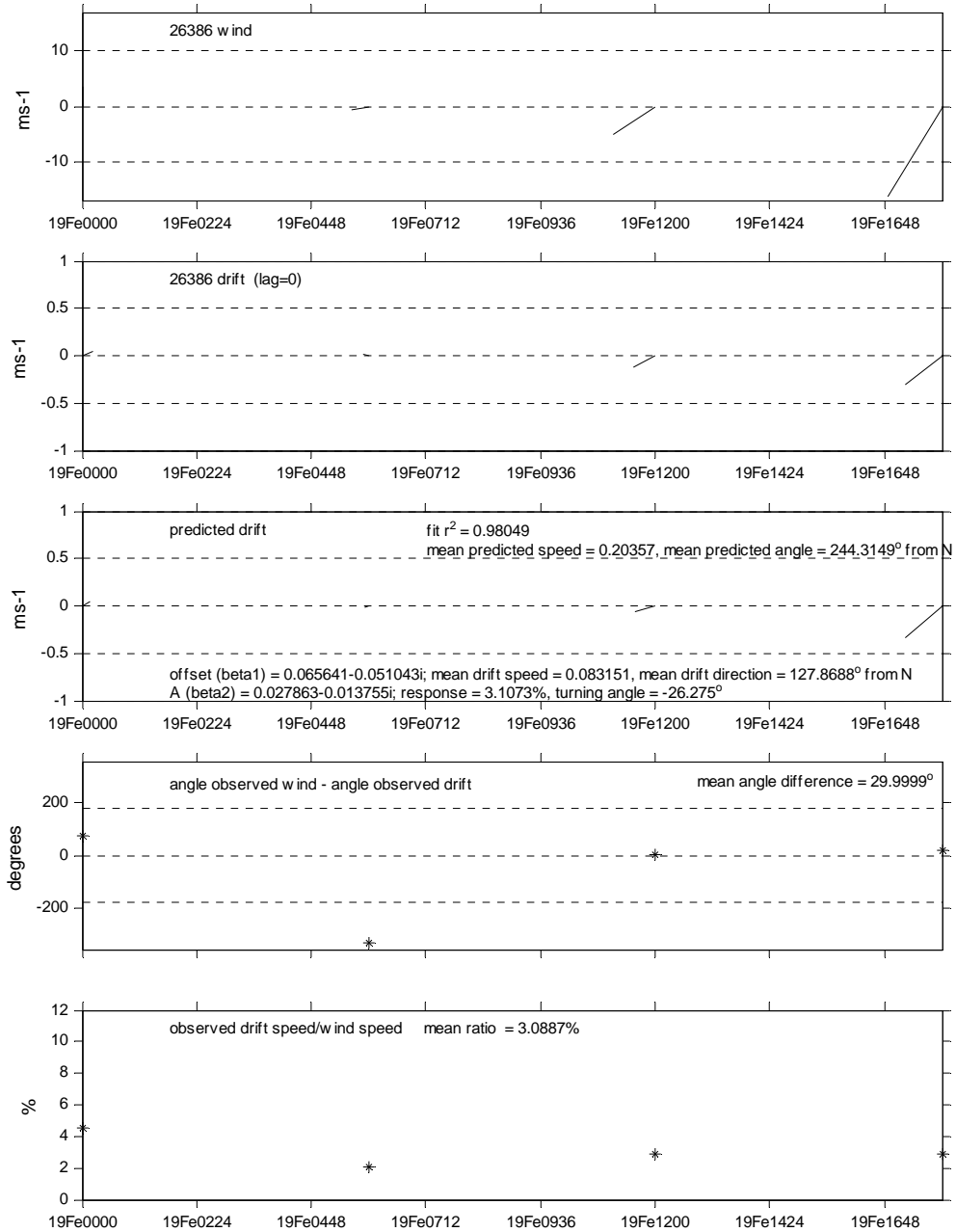


Figure 130 Results of complex least squares regression of 6-hourly analysis wind and drift data for beacon 26386 until 20 February. The figure shows hourly wind and beacon drift, the predicted drift values (ie. fitted series), the angle difference between wind vectors and drift vectors (with mean angle difference), and the ratio of drift speed to wind speed (with mean ratio).

4.4 Beacon drift analysis with 3-hourly high resolution forecast model wind output

In this section the 3-hourly high resolution model output wind data were used to complete an analysis of ice drift for beacons 26370 and 26386 up to but not including Feb. 20. It has been seen that using the data from after Feb. 20 produces poor results since the beacons were essentially not moving. The method is the same as that reported in the main part of this report; however, drift data were also lagged for 1 to 6 hours. Results of the least squares regressions are given in tables and figures.

Hourly beacon position data were used to compute drift (distance between beacon at time, t , and the beacon position at time, $t-1$; converted to m/s) and 3-hourly wind data were interpolated to match beacon positions in time (hourly) and space to produce hourly wind records. Drift data retained the tidal signal.

R^2 values were less for 26370 using these forecast winds than in the other two cases but still proved to be good (>80% variance in most cases). The gains were in the right ballpark but less than those obtained using the other two wind data sets.

Table 11 Results for least squares fit of drift to wind; data were *hourly*; drift lags were by the hour; data were up to but not including Feb. 20, 2004

Beacon	Lag (1-hour step)	R^2	Turning angle θ (deg)	Gain (%)
26370	0	0.86	-13.73	3.03
	1	0.87	-10.37	3.12
	2	0.87	-6.68	3.18
	3	0.86	-3.16	3.25
	4	0.85	0.25	3.30
	5	0.82	3.64	3.33
	6	0.78	7.07	3.35
26386	0	0.85	-19.91	2.69
	1	0.85	-15.24	2.76
	2	0.84	-11.17	2.80
	3	0.83	-6.80	2.82
	4	0.82	-1.93	2.79
	5	0.82	3.45	2.75
	6	0.83	9.14	2.71

Since original gridded winds were 3-hourly, a quick look at how a 3-hourly drift record would perform in a least squares fit was checked. The hourly beacon position data were interpolated to 3-hourly data and matched in time with the wind data. Beacon drift was computed from the 3-hourly records. Using the 3-hourly data, the results of lagging improved slightly for 3-hour and 6-hour lags R^2 increased slightly and gains were slightly less for 0-lag and 3-hour lag.

Table 12 Results for least squares fit of drift to wind; data were 3-hourly; drift lags were by the 3-hour; data were up to but not including Feb. 20, 2004

Beacon	Lag (3-hour step)	R^2	Turning angle θ (deg)	Gain (%)
26370	0	0.85	-17.36	2.94
	1	0.87	-7.40	3.20
	2	0.83	2.93	3.36
26386				
	0	0.85	-19.91	2.69
	1	0.85	-15.24	2.76
	2	0.84	-11.17	2.80

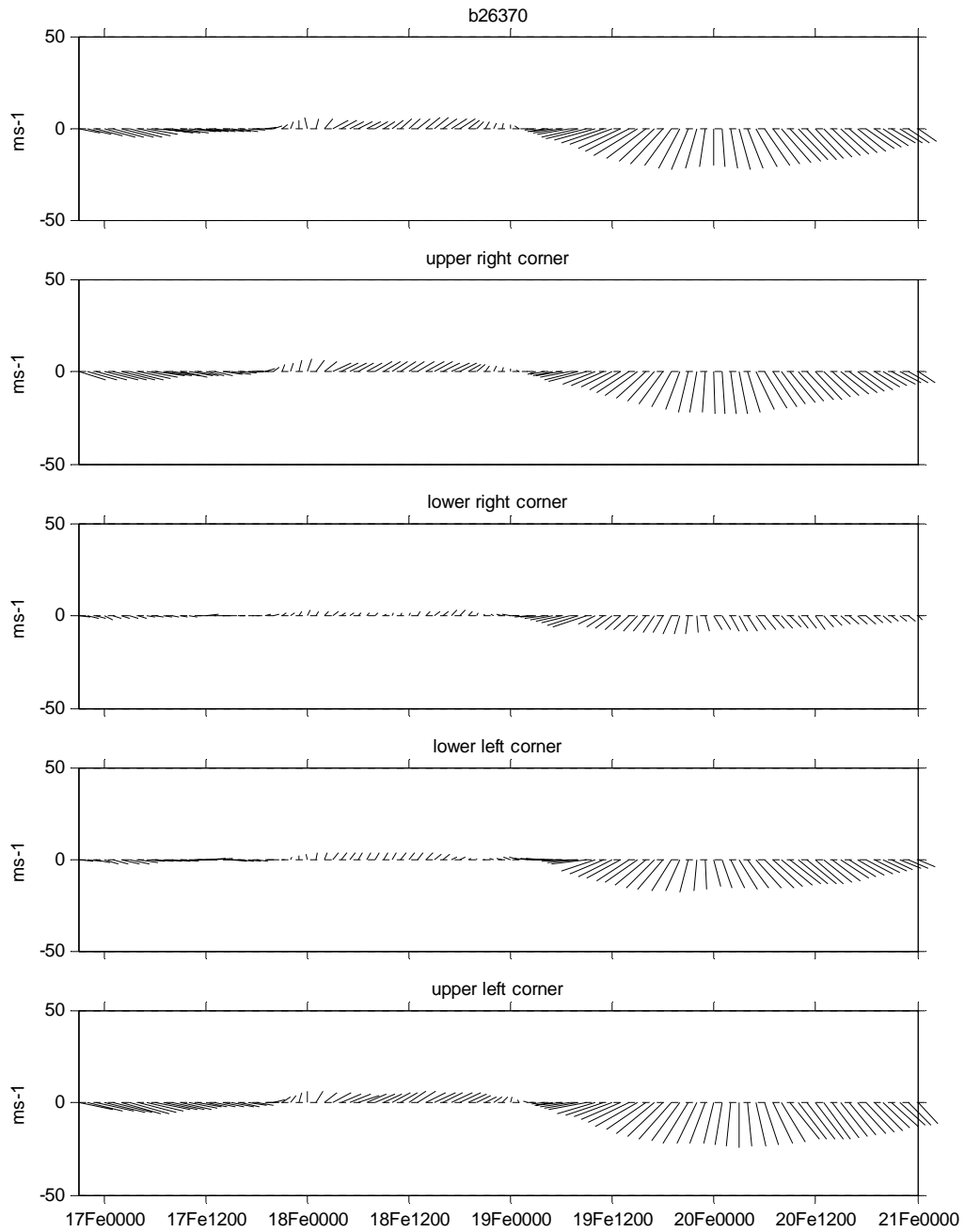


Figure 131 Time series of beacon 26370 wind obtained from CMC high resolution prognostic grid. Also shown are the 4 grid corners used to interpolate the wind at beacon positions.

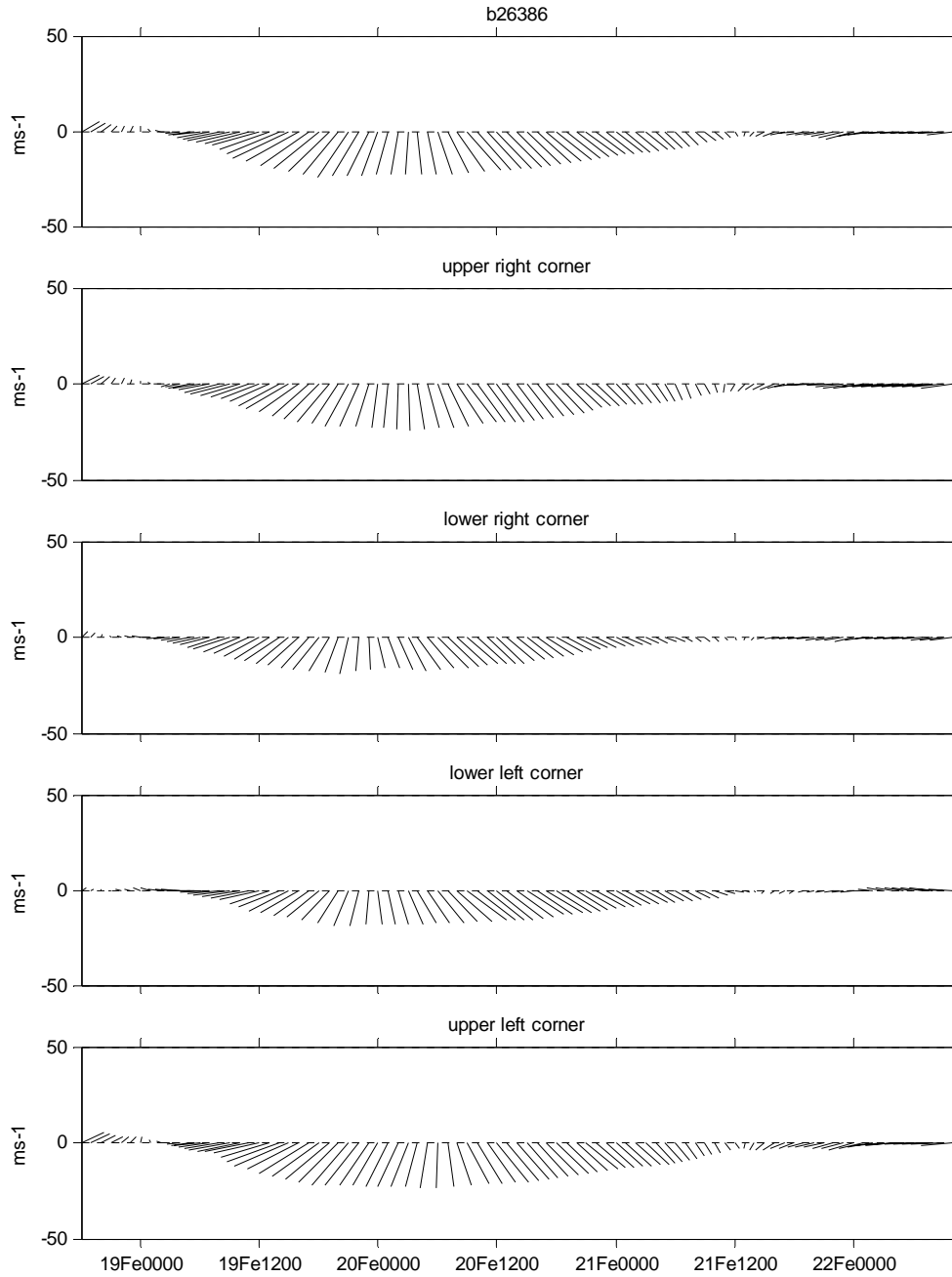


Figure 132 Time series of beacon 26386 wind obtained from CMC high resolution prognostic grid. Also shown are the 4 grid corners used to interpolate the wind at beacon positions.

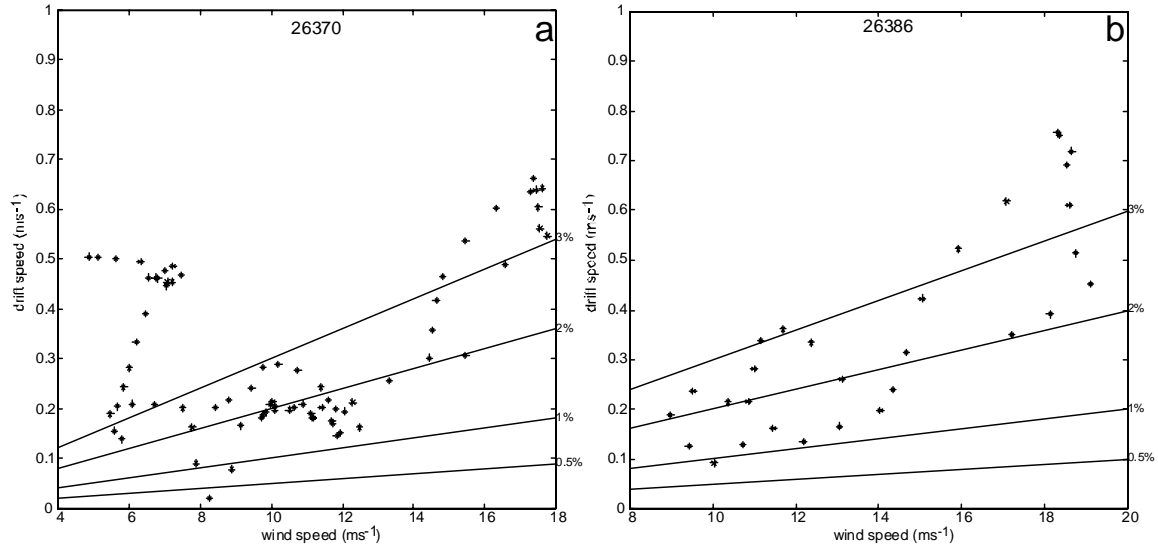


Figure 133 Scatter plot of hourly drift magnitude vs. hourly wind magnitude for both beacons: a) 26370 and b) 26386 with 0-hour lag. Tidal signal is retained in drift data.

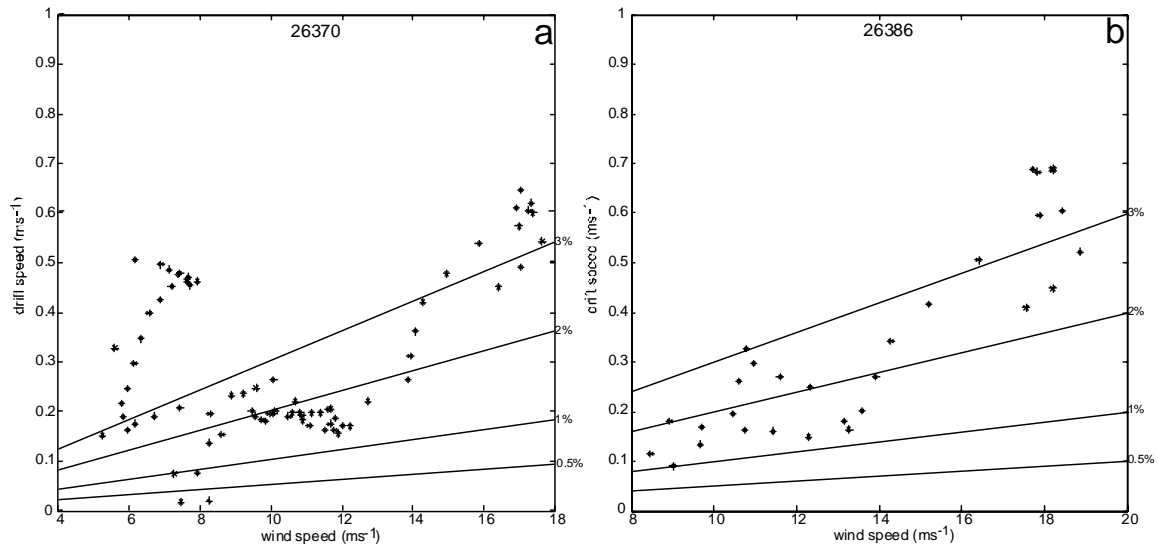


Figure 134 Scatter plot of 3-hourly drift magnitude vs. 3-hourly wind magnitude for both beacons: a) 26370 and b) 26386 with 0-hour lag. Tidal signal is retained in drift data.

The next figures are results for the least squares fits for the two beacons from lag=0 hours to lag=6 hours. The first 7 are for beacon 26370 and the next 7 are for beacon 26386. The data are hourly.

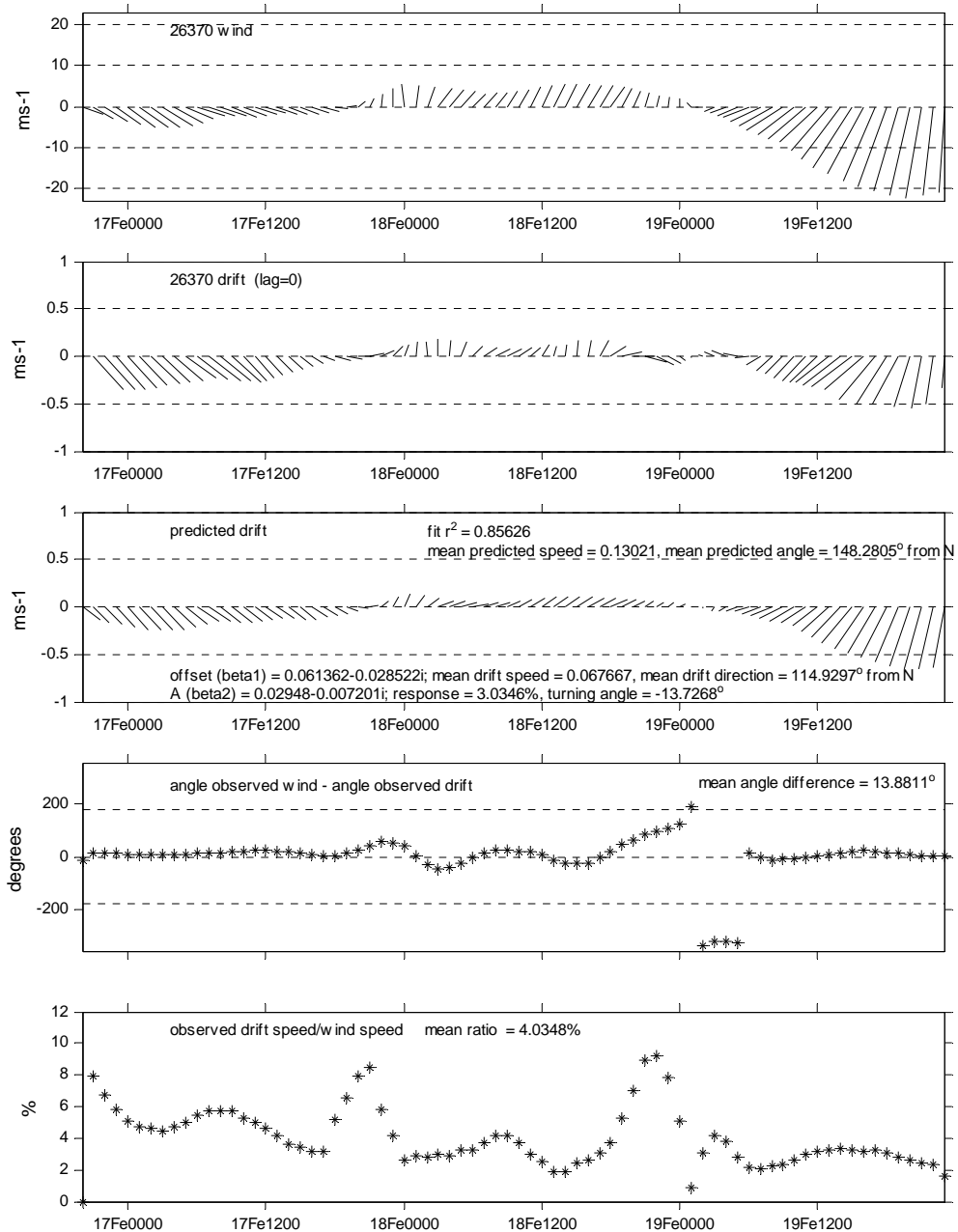


Figure 135 Hourly time series of least squares fit for beacon 26370 drift and 3-hourly high resolution forecast wind to 20 Feb. Wind has been interpolated to be hourly. Lag is 0 hours.

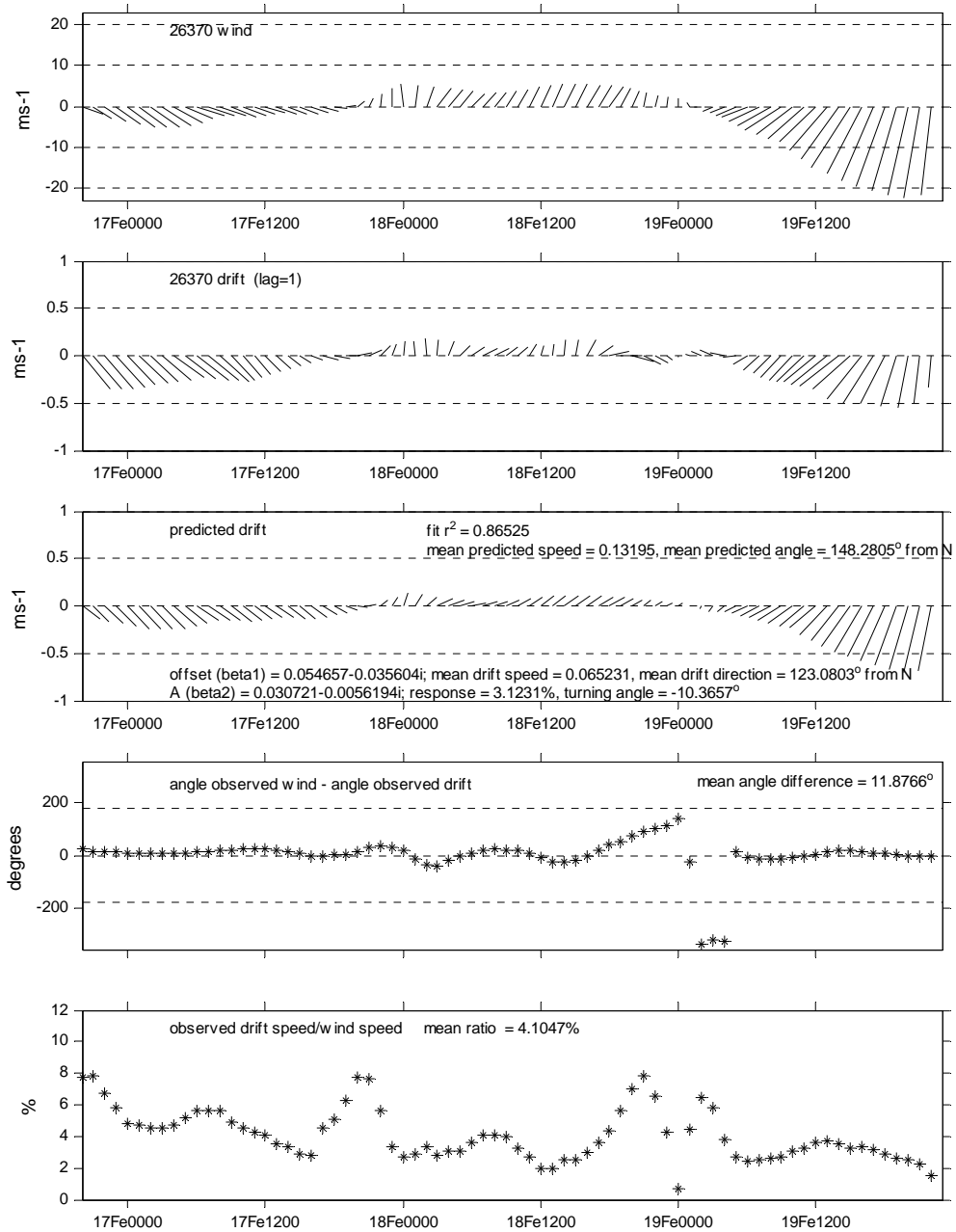


Figure 136 Hourly time series of least squares fit for beacon 26370 drift and 3-hourly high resolution forecast wind to 20 Feb. Wind has been interpolated to be hourly. Lag is 1 hour.

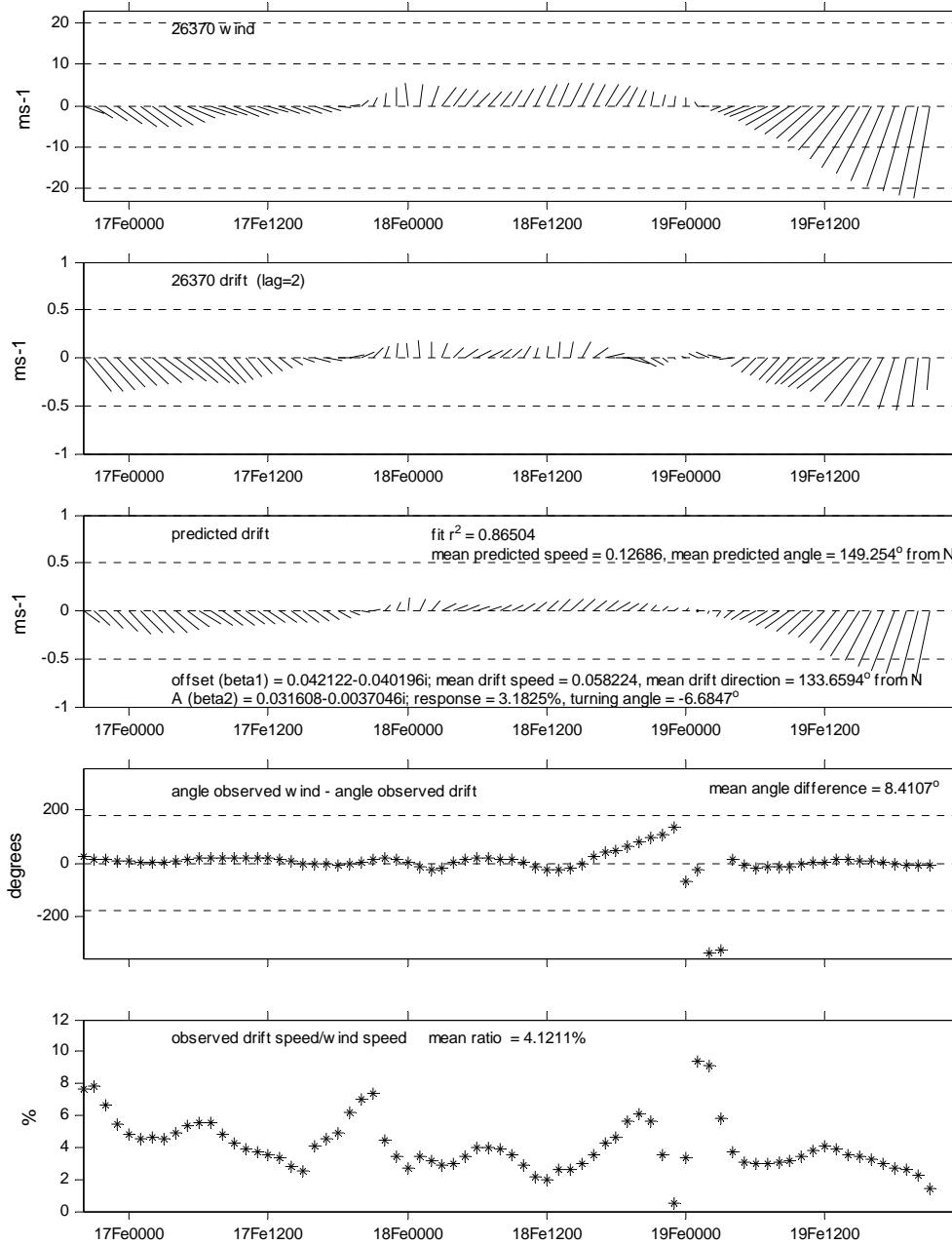


Figure 137 Hourly time series of least squares fit for beacon 26370 drift and 3-hourly high resolution forecast wind to 20 Feb. Wind has been interpolated to be hourly. Lag is 2 hours.

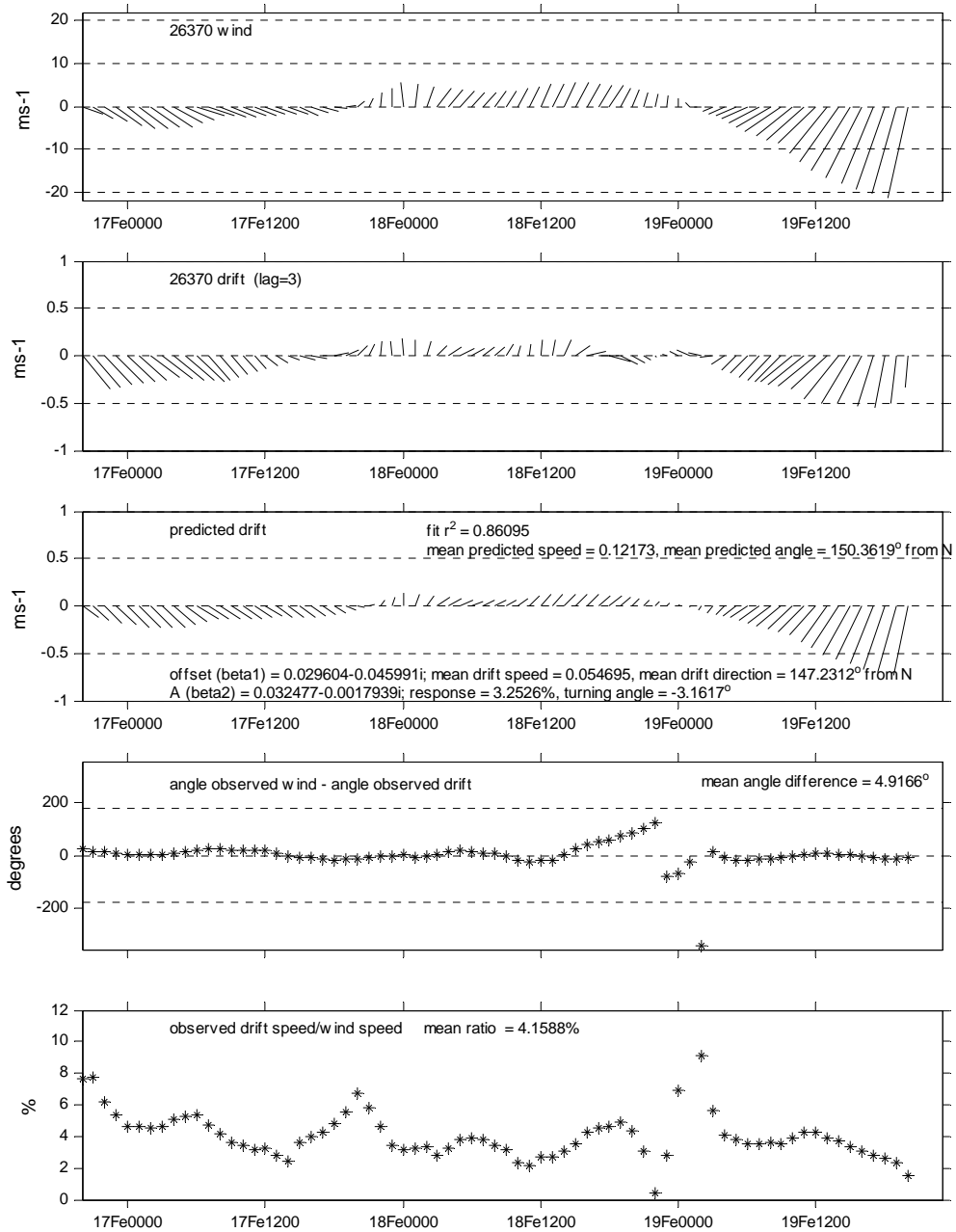


Figure 138 Hourly time series of least squares fit for beacon 26370 drift and 3-hourly high resolution forecast wind to 20 Feb. Wind has been interpolated to be hourly. Lag is 3 hours.

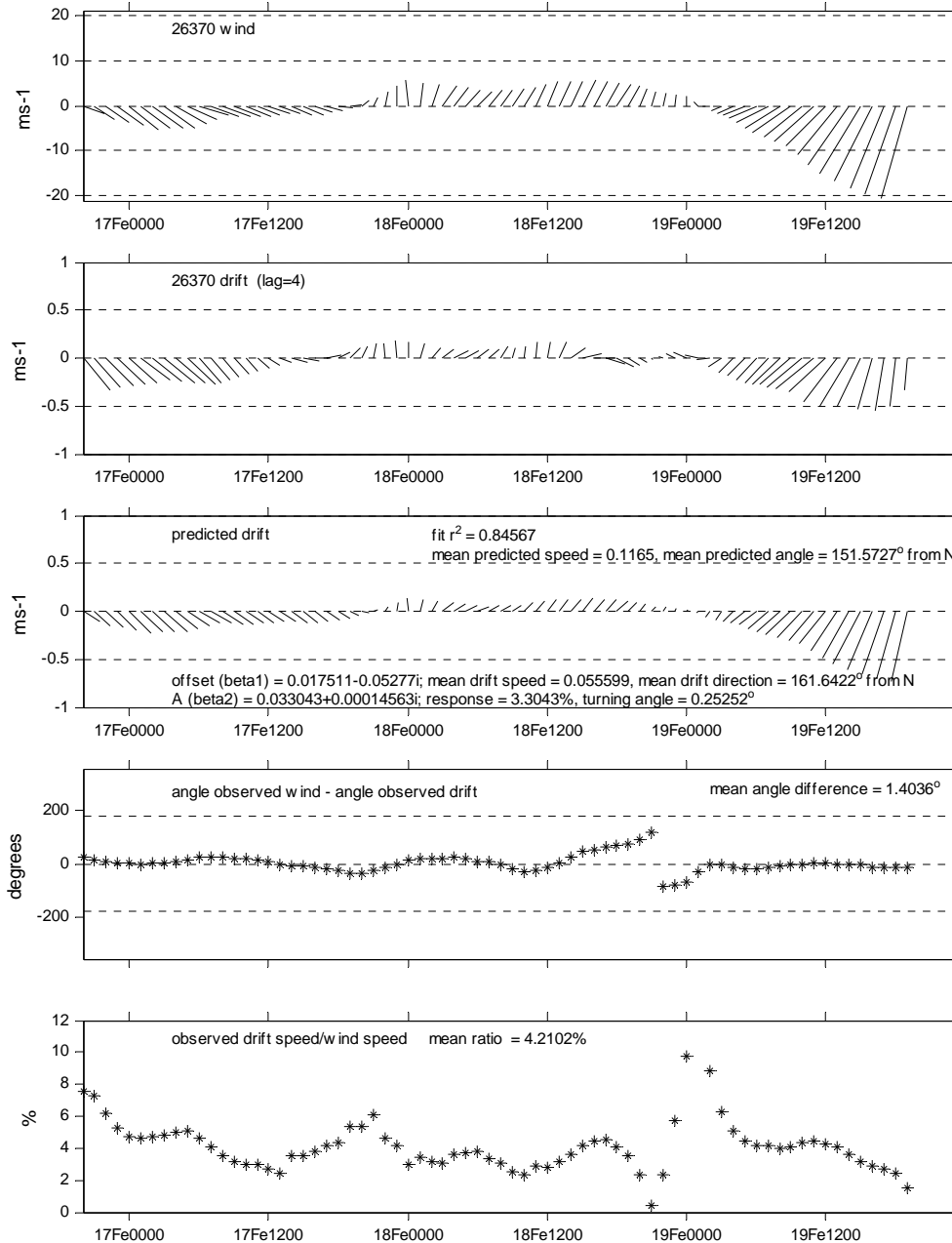


Figure 139 Hourly time series of least squares fit for beacon 26370 drift and 3-hourly high resolution forecast wind to 20 Feb. Wind has been interpolated to be hourly. Lag is 4 hours.

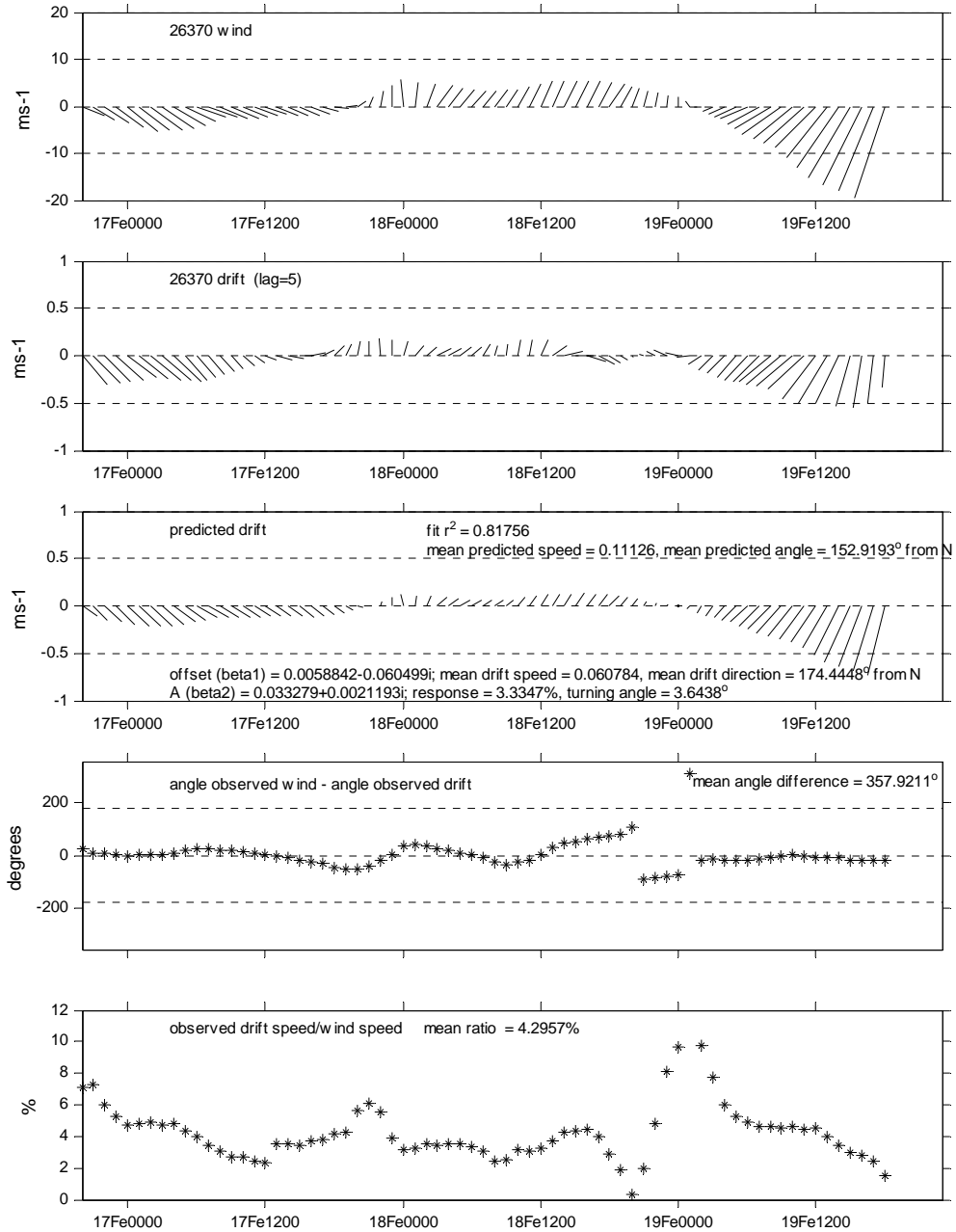


Figure 140 Hourly time series of least squares fit for beacon 26370 drift and 3-hourly high resolution forecast wind to 20 Feb. Wind has been interpolated to be hourly. Lag is 5 hours.

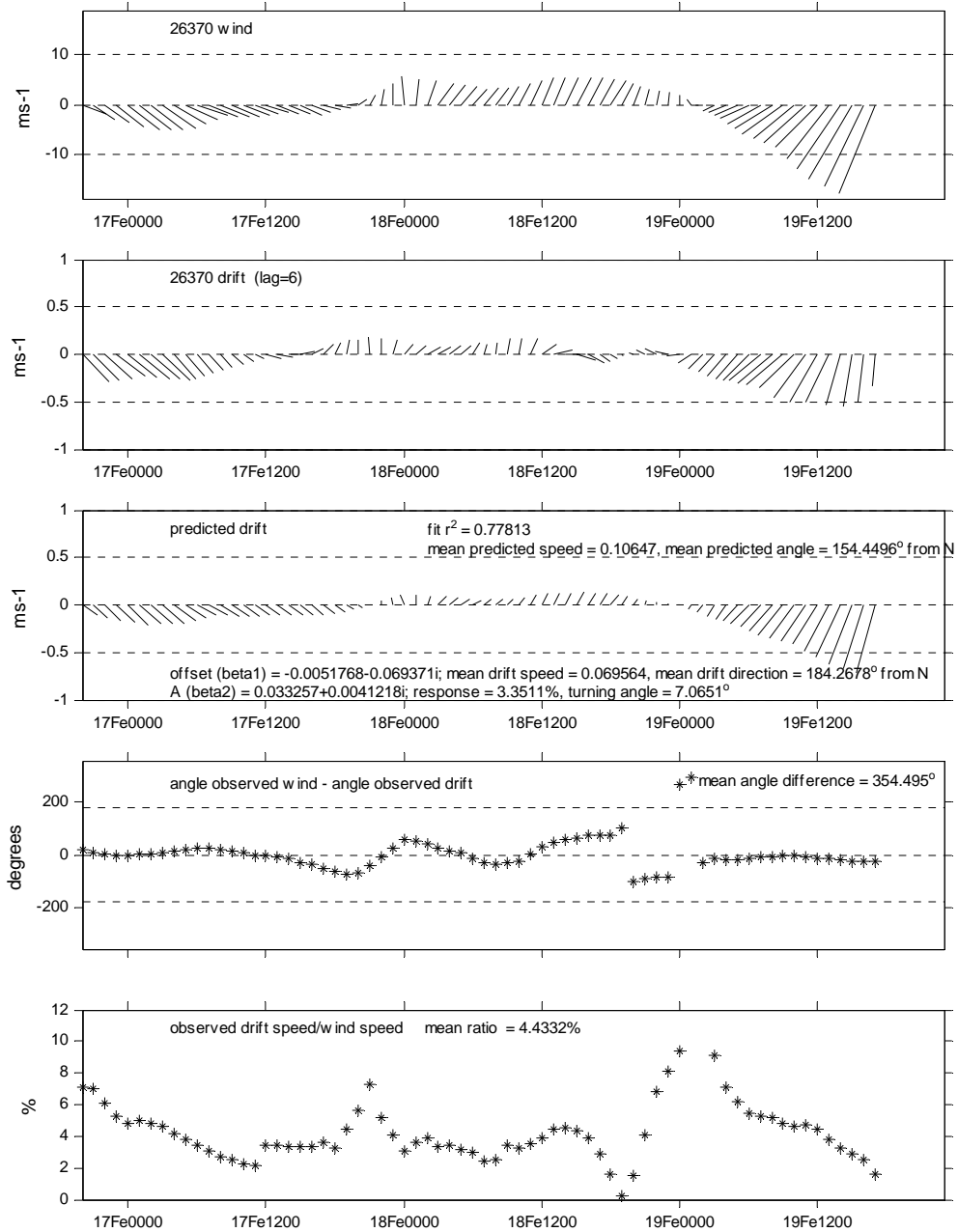


Figure 141 Hourly time series of least squares fit for beacon 26370 drift and 3-hourly high resolution forecast wind to 20 Feb. Wind has been interpolated to be hourly. Lag is 6 hours.

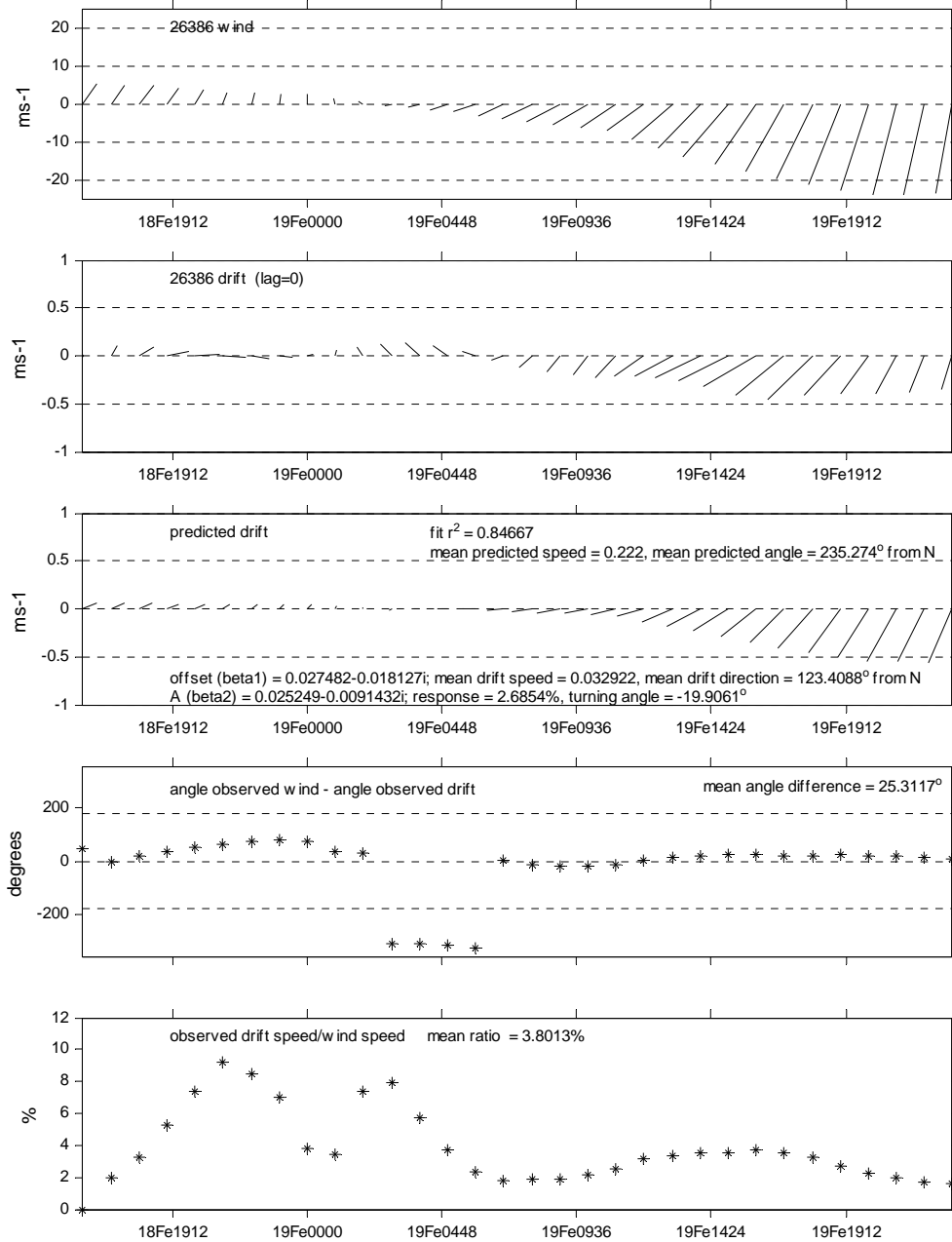


Figure 142 Hourly time series of least squares fit for beacon 26386 drift and 3-hourly high resolution forecast wind to 20 Feb. Wind has been interpolated to be hourly. Lag is 0 hours.

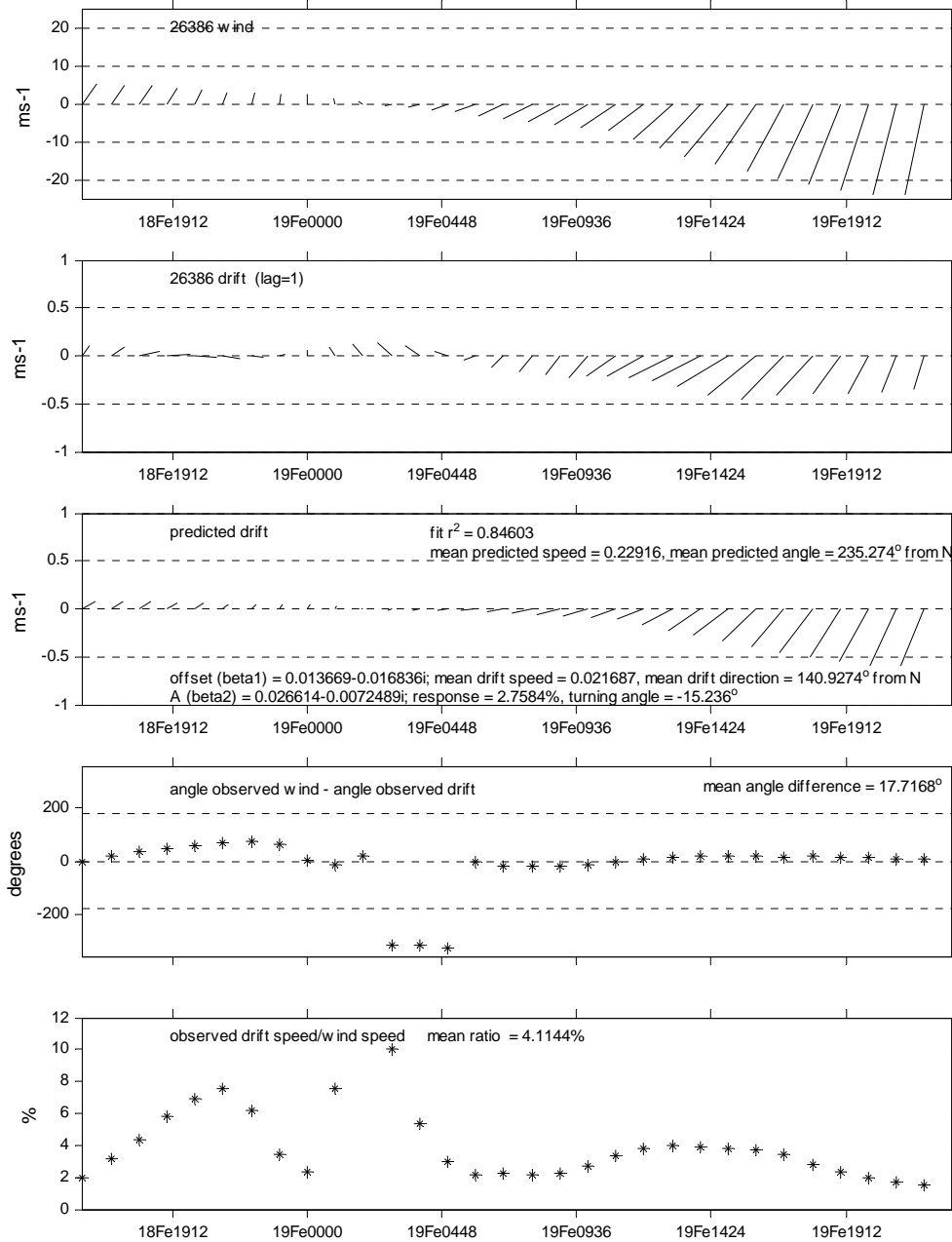


Figure 143 Hourly time series of least squares fit for beacon 26386 drift and 3-hourly high resolution forecast wind to 20 Feb. Wind has been interpolated to be hourly. Lag is 1 hour.

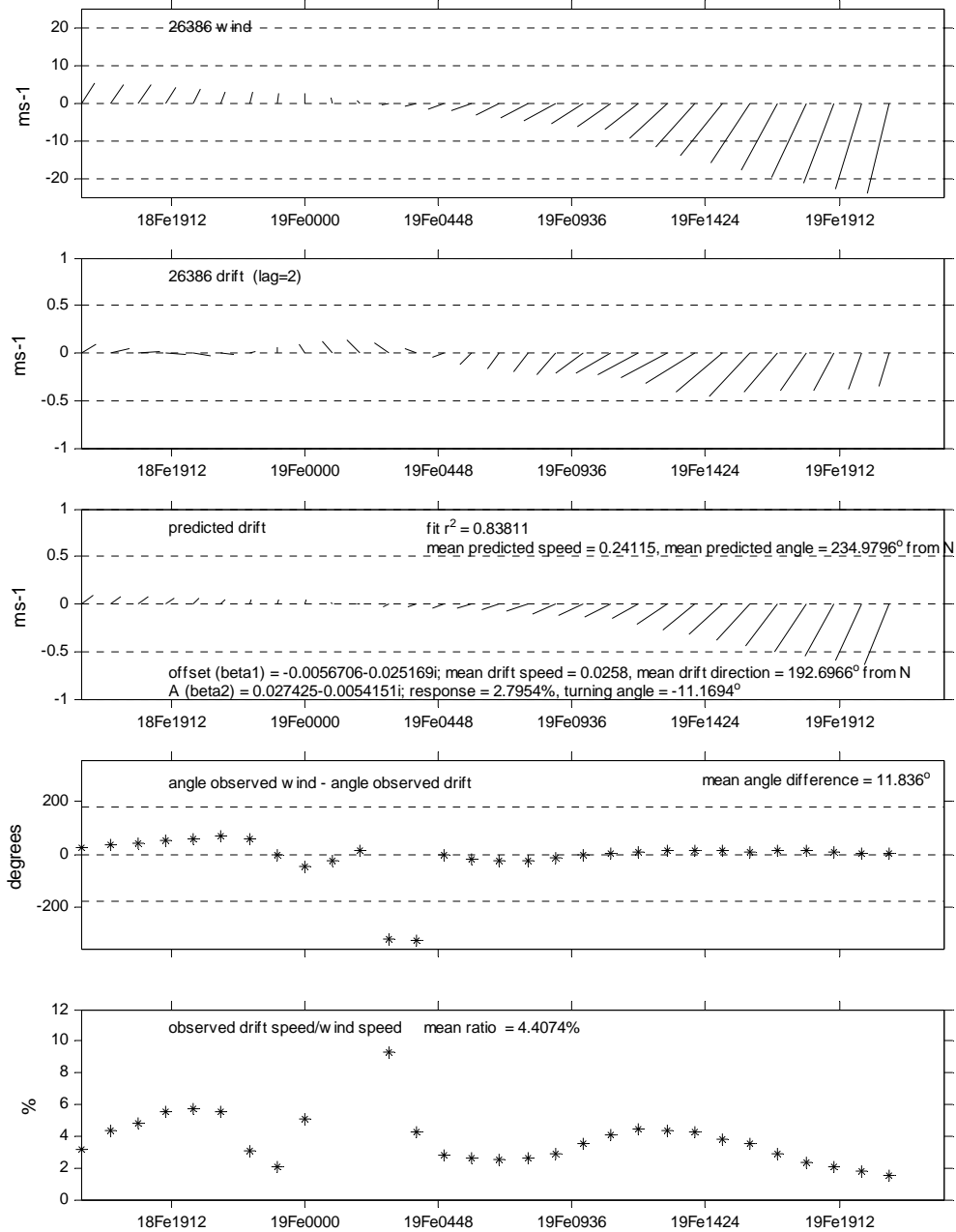


Figure 144 Hourly time series of least squares fit for beacon 26386 drift and 3-hourly high resolution forecast wind to 20 Feb. Wind has been interpolated to be hourly. Lag is 2 hours.

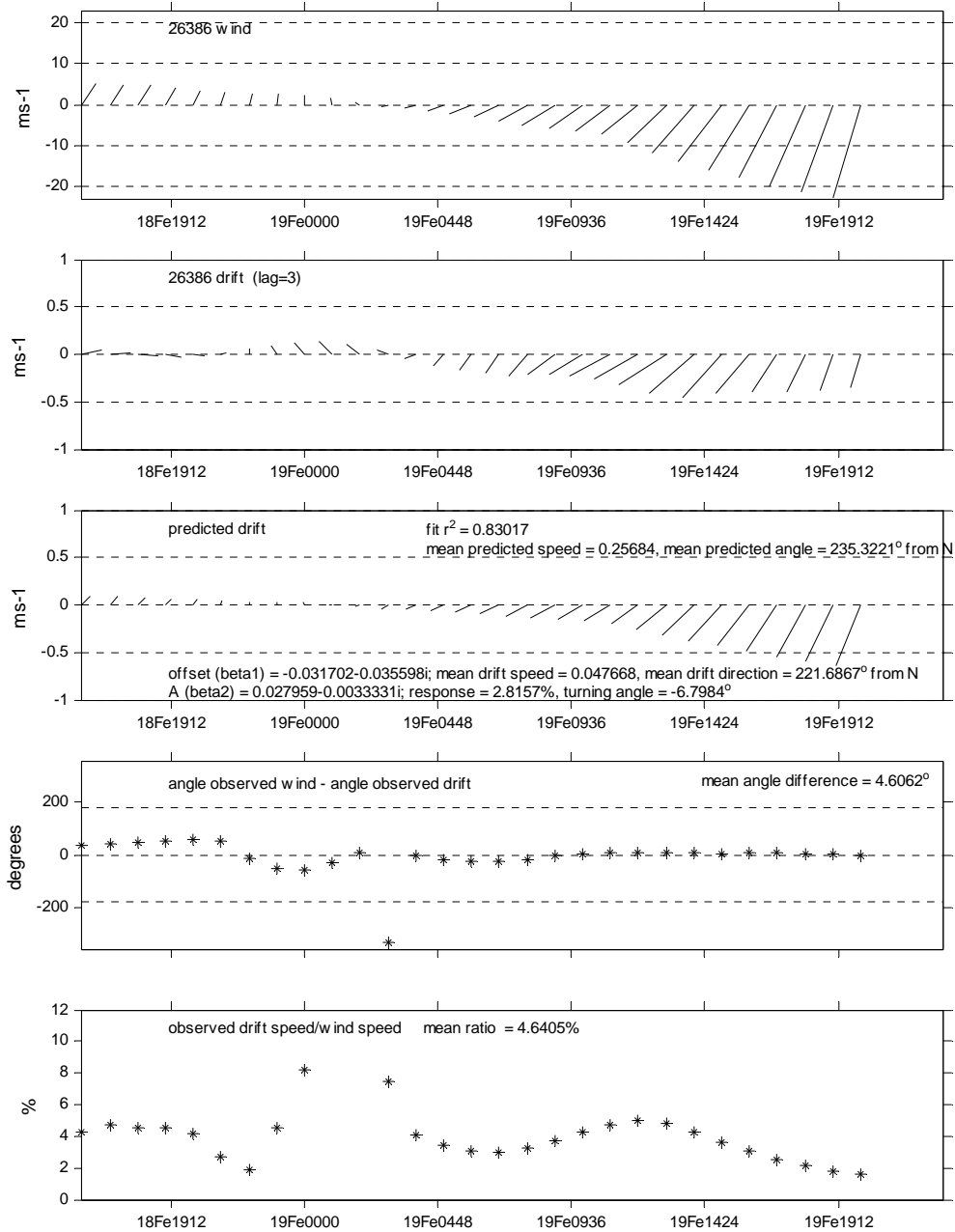


Figure 145 Hourly time series of least squares fit for beacon 26386 drift and 3-hourly high resolution forecast wind to 20 Feb. Wind has been interpolated to be hourly. Lag is 3 hours.

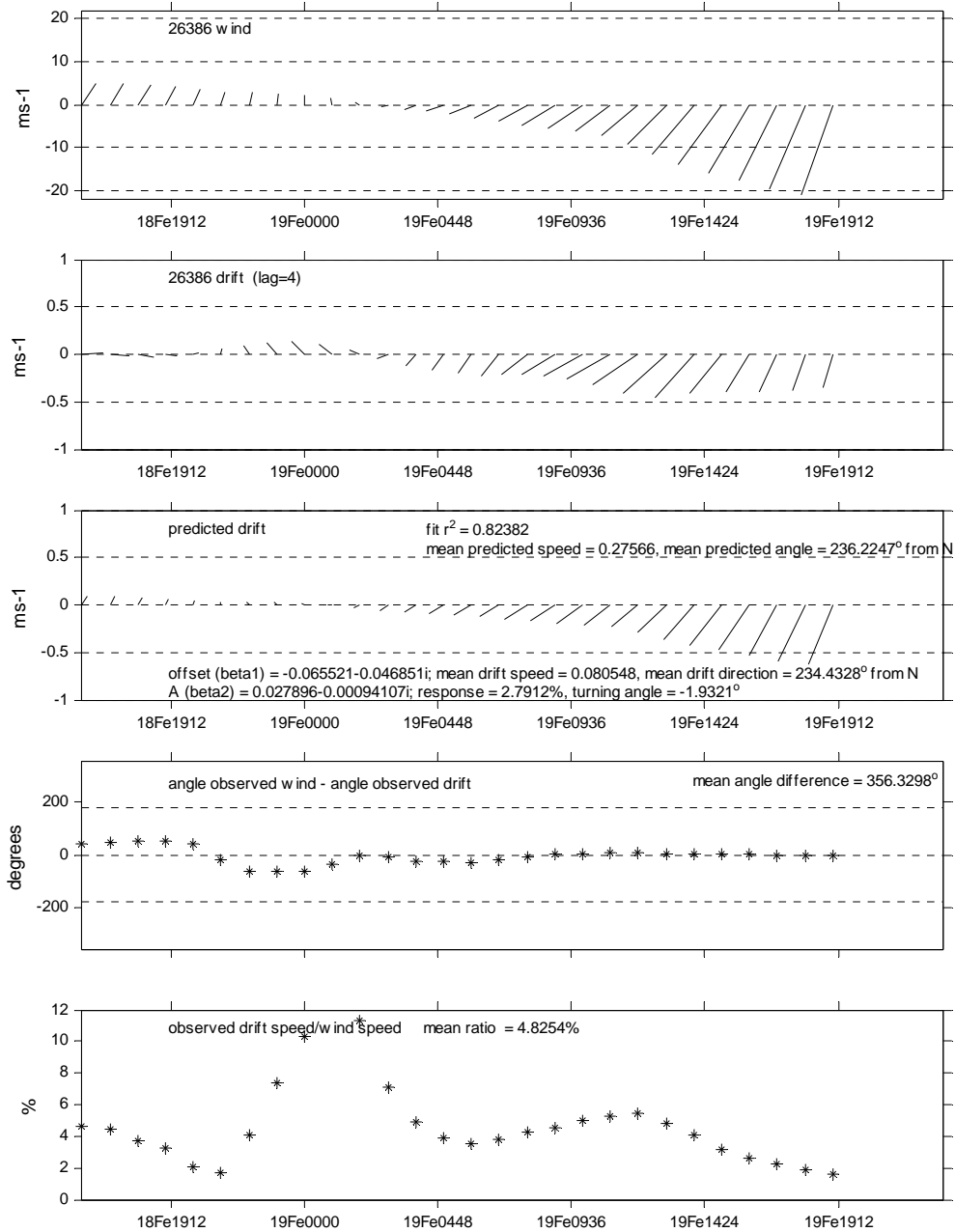


Figure 146 Hourly time series of least squares fit for beacon 26386 drift and 3-hourly high resolution forecast wind to 20 Feb. Wind has been interpolated to be hourly. Lag is 4 hours.

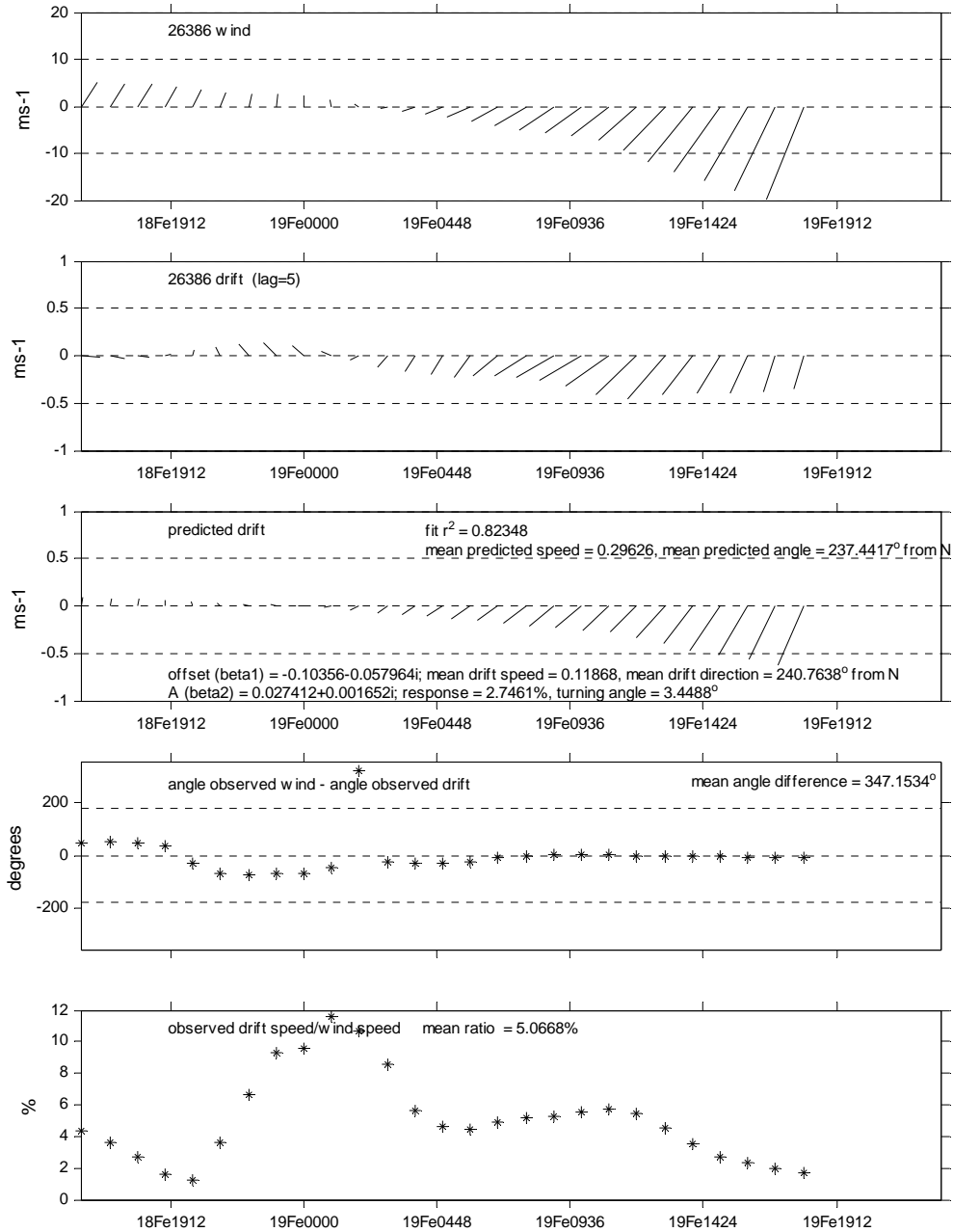


Figure 147 Hourly time series of least squares fit for beacon 26386 drift and 3-hourly high resolution forecast wind to 20 Feb. Wind has been interpolated to be hourly. Lag is 5 hours.

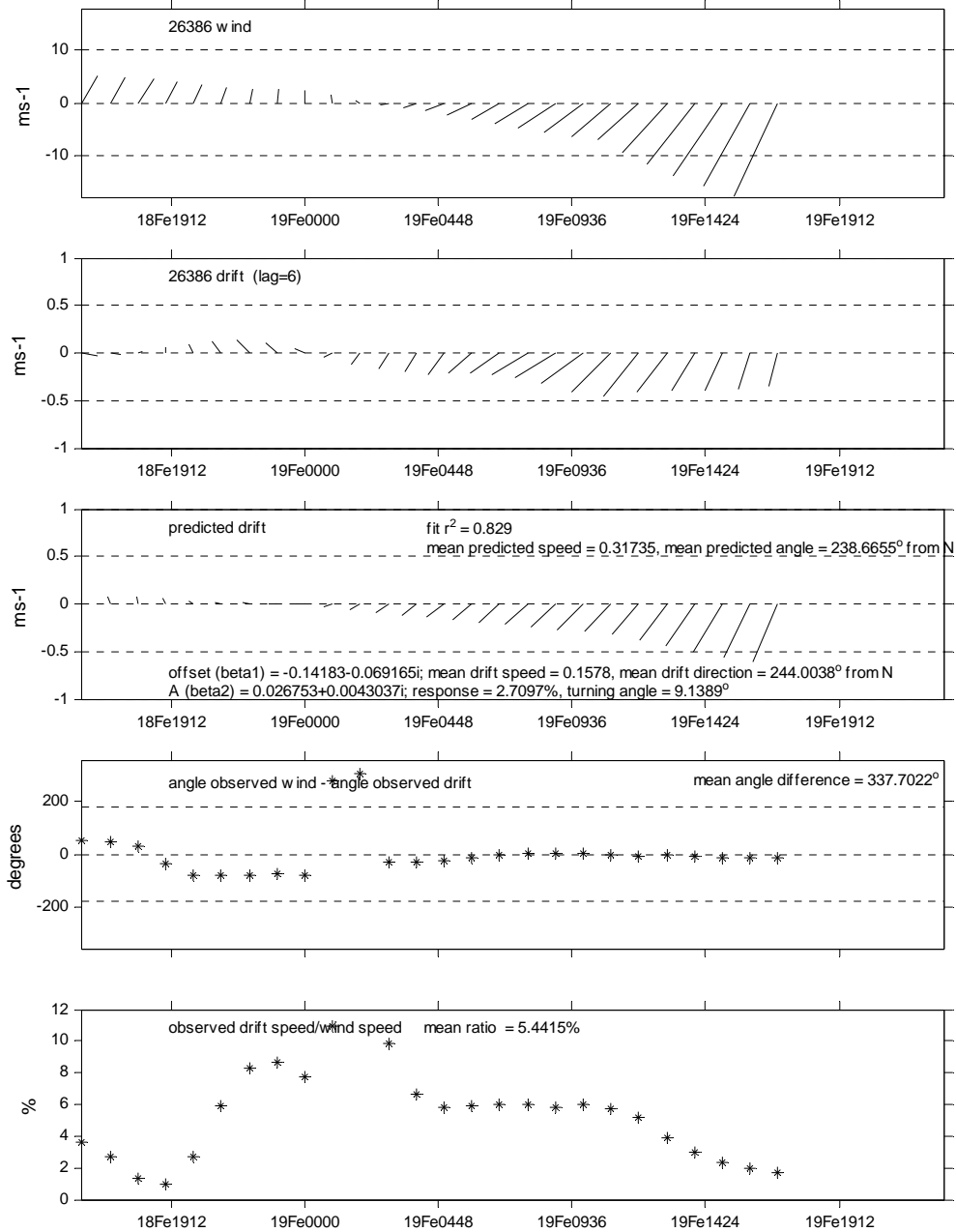


Figure 148 Hourly time series of least squares fit for beacon 26386 drift and 3-hourly high resolution forecast wind to 20 Feb. Wind has been interpolated to be hourly. Lag is 6 hours.

The next set of figures are the same least squares fit results but for 3-hourly data. Lag=1 means a lag of 3 hours and lag=2 means a lag of 6 hours.

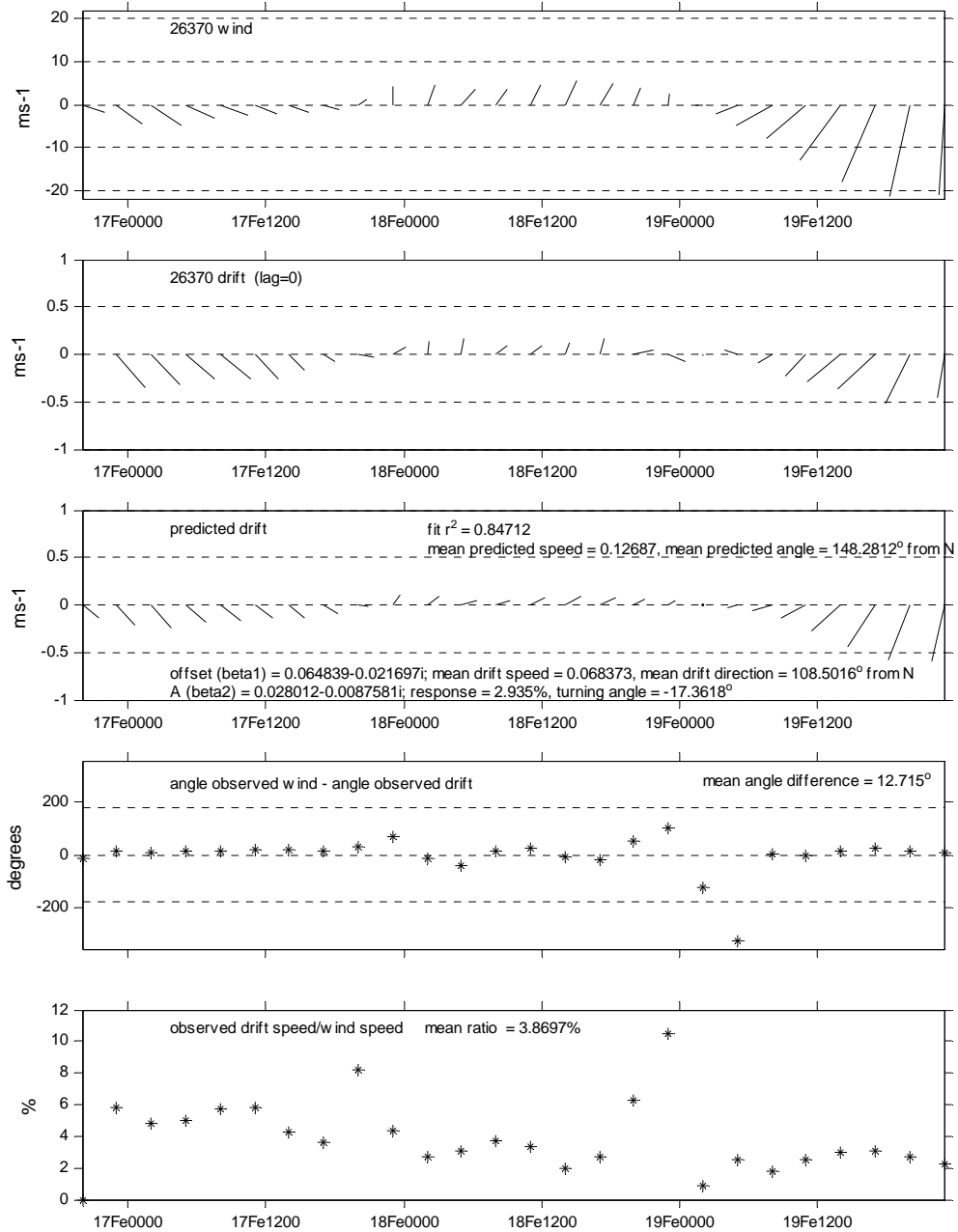


Figure 149 Time series of least squares fit for beacon 26370 drift and 3-hourly high resolution forecast wind to 20 Feb. Wind and drift are both 3-hourly. Lag is 0 hours.

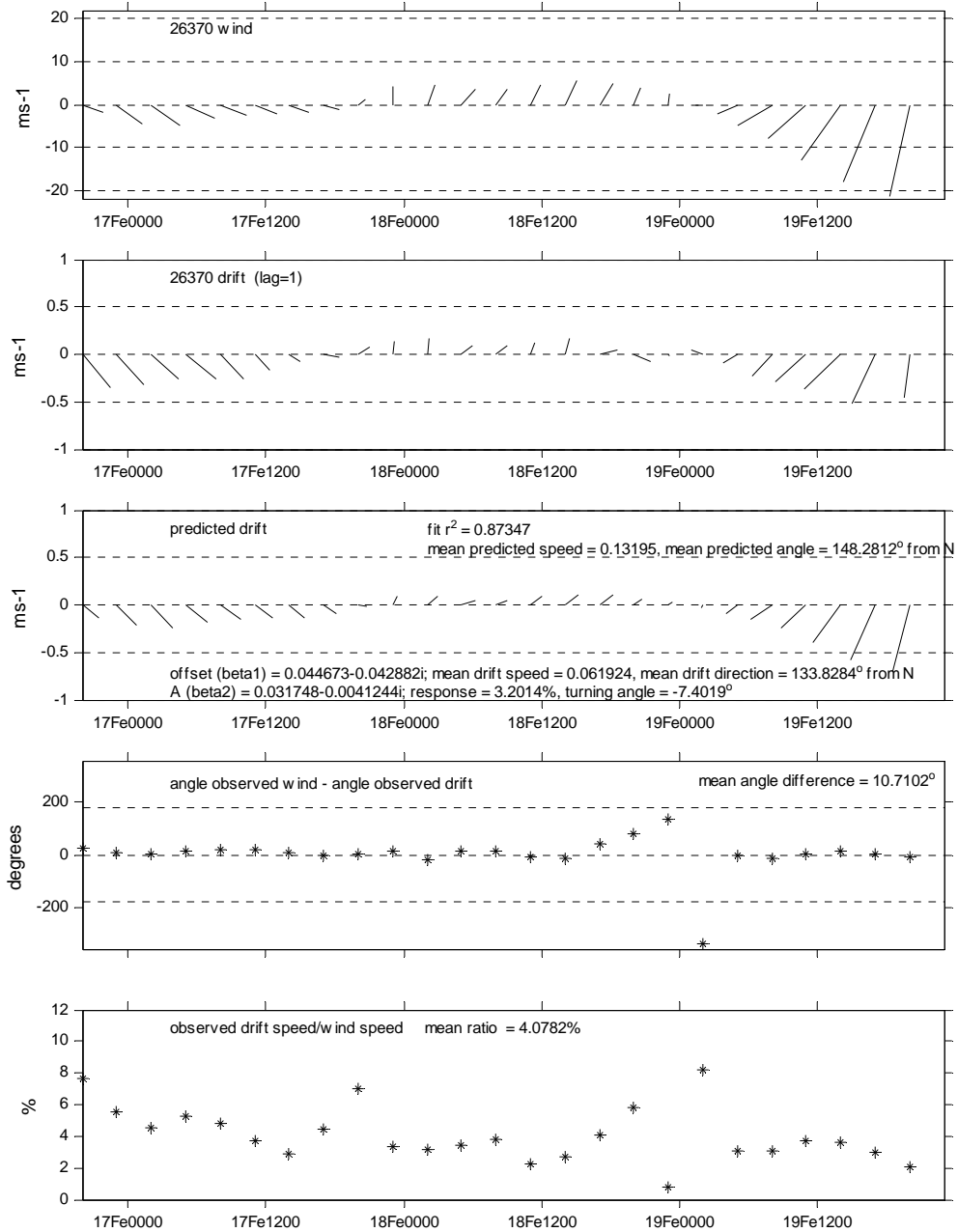


Figure 150 Time series of least squares fit for beacon 26370 drift and 3-hourly high resolution forecast wind to 20 Feb. Wind and drift are both 3-hourly. Lag is 3 hours.

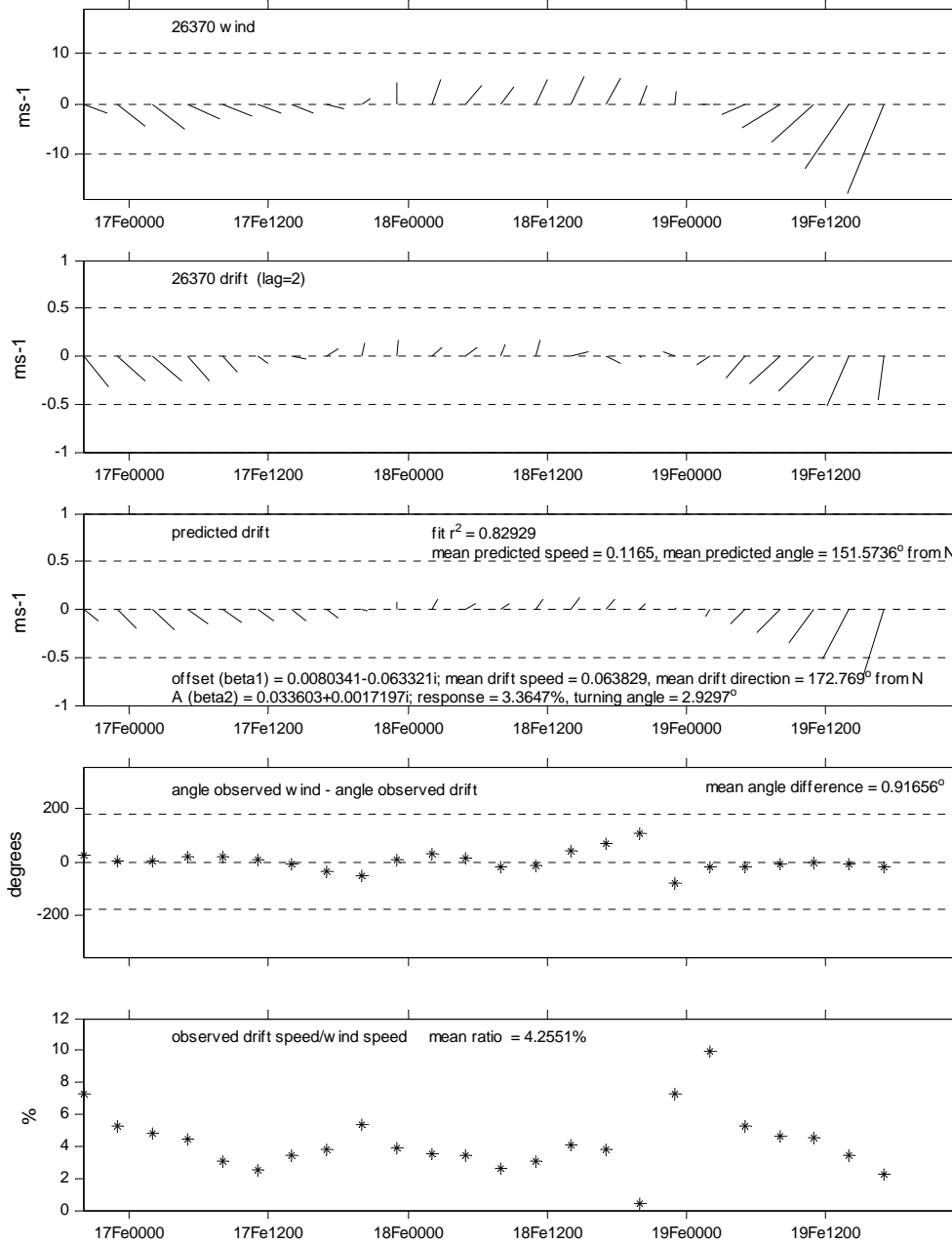


Figure 151 Time series of least squares fit for beacon 26370 drift and 3-hourly high resolution forecast wind to 20 Feb. Wind and drift are both 3-hourly. Lag is 6 hours.

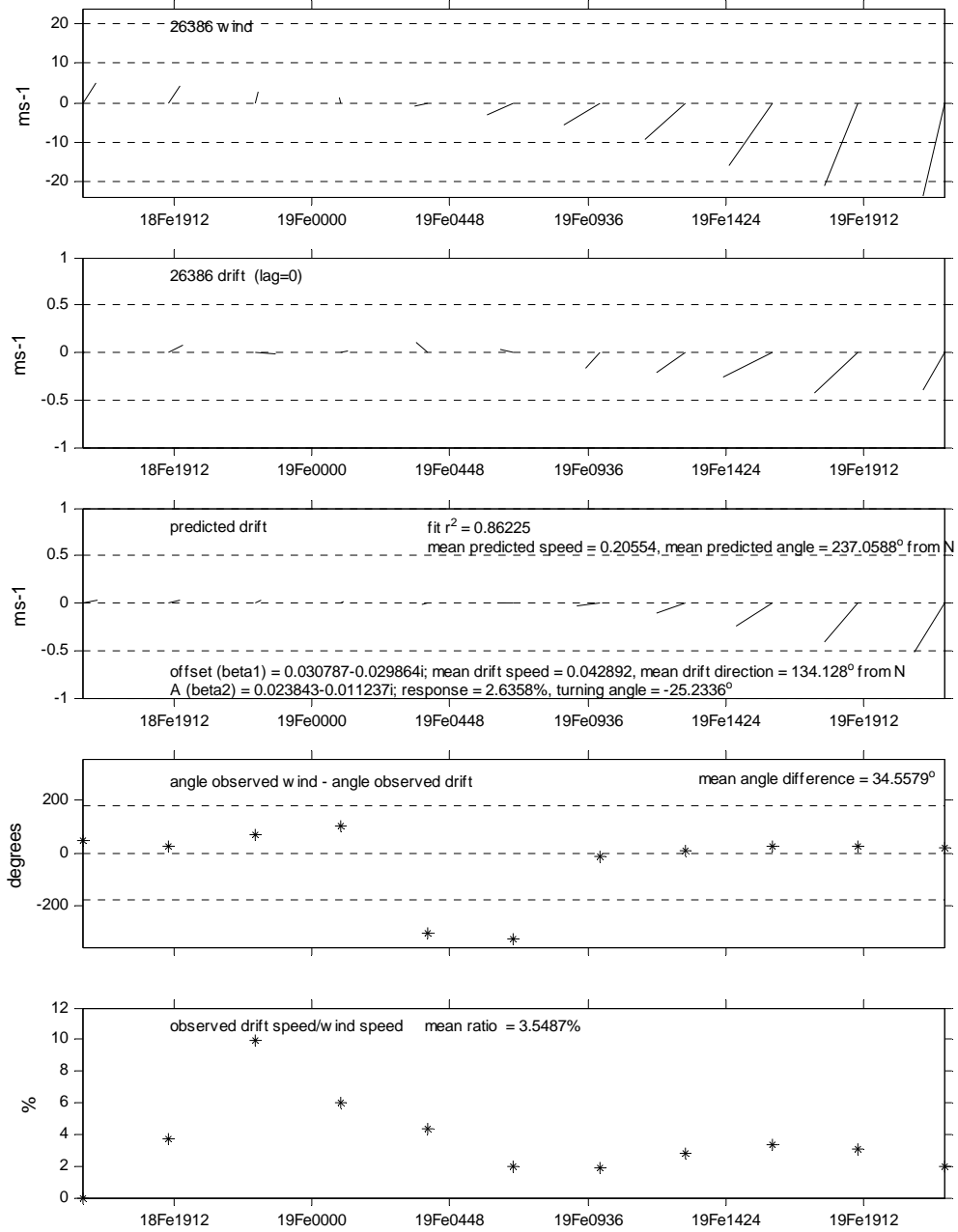


Figure 152 Hourly time series of least squares fit for beacon 26386 drift and 3-hourly high resolution forecast wind to 20 Feb. Wind and drift are both 3-hourly. Lag is 0 hours.

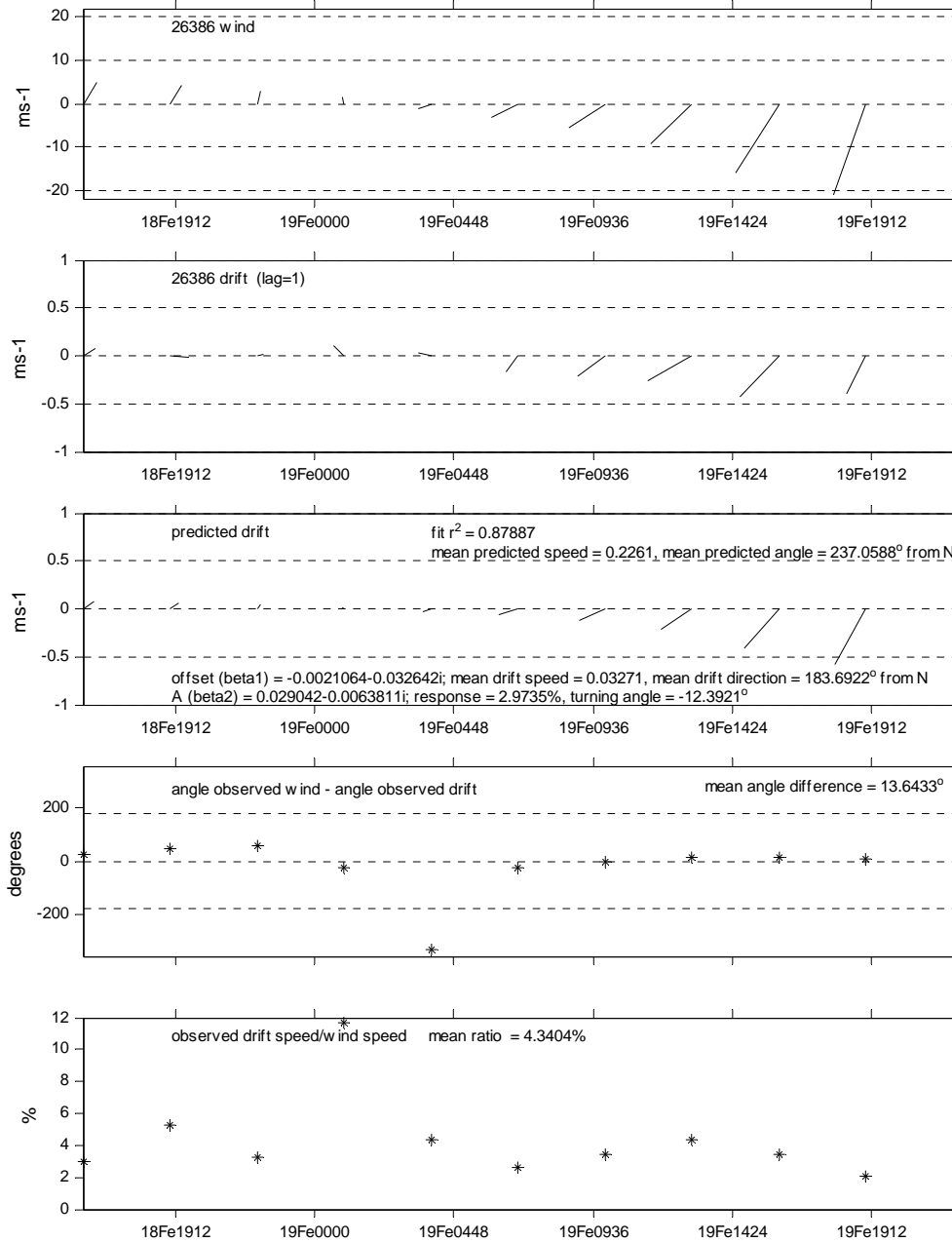


Figure 153 Hourly time series of least squares fit for beacon 26386 drift and 3-hourly high resolution forecast wind to 20 Feb. Wind and drift are both 3-hourly. Lag is 3 hours.

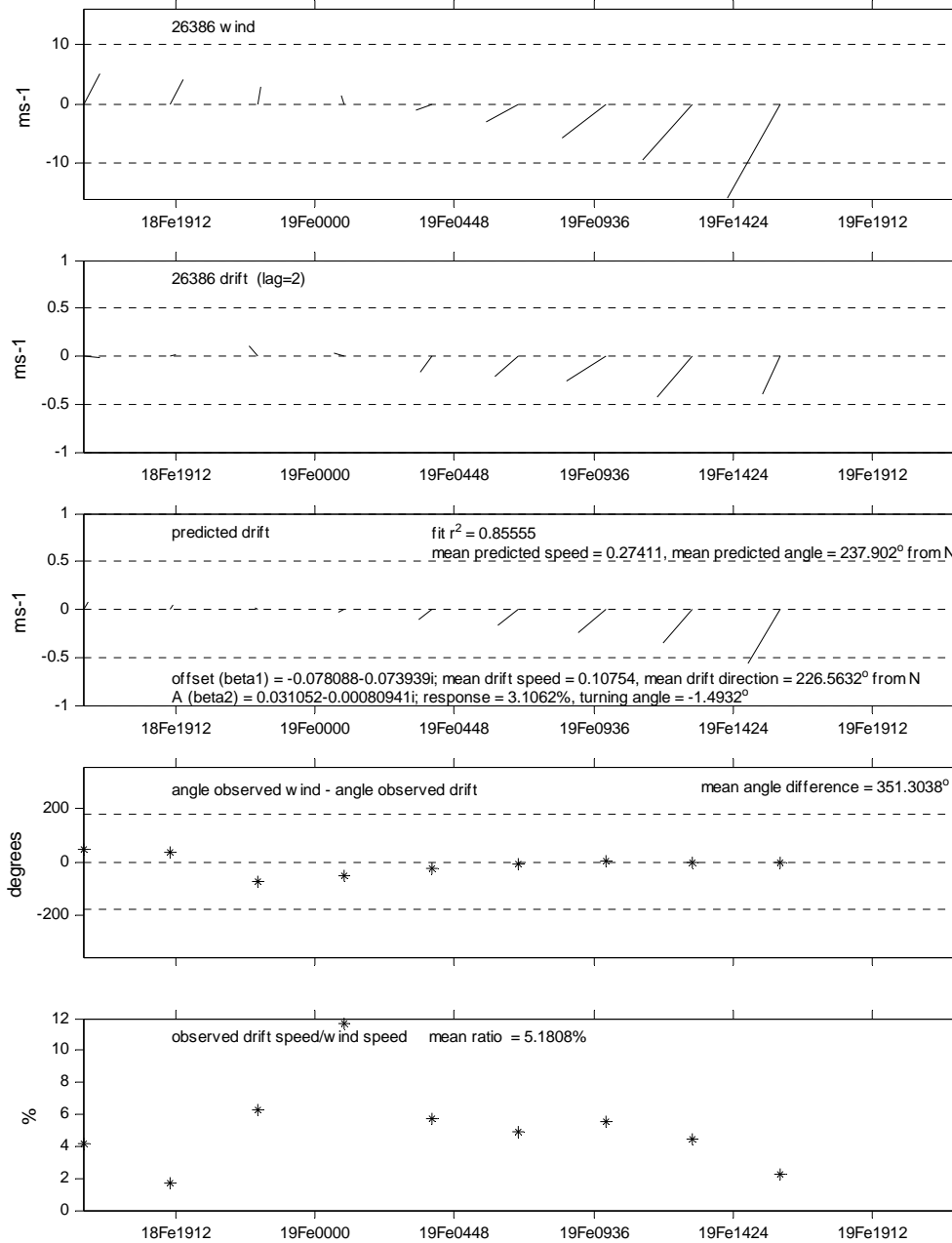


Figure 154 Hourly time series of least squares fit for beacon 26386 drift and 3-hourly high resolution forecast wind to 20 Feb. Wind and drift are both 3-hourly. Lag is 6 hours.

4.5 References Appendix I

- Cardone, V. J., J. G. Greenwood, and M. Cane, 1990. "On Trends in Historical Marine Wind Data", *Journal of Climate*, Vol. 3, No. 1, p. 113-127.
- Eid, B., E. Dunlap, M. Henschel, and J. Trask (MacLaren Plansearch Ltd.), 1991. Wind and Wave Climate Atlas, Vol. II, The Gulf of St. Lawrence, Transport Canada Publication #TP10820E (1991; *out of print*; also published @ <http://www.meds-sdmm.dfo-mpo.gc.ca/alphapro/wave/TDCAtlas/TDCAtlasGS.htm>)
- Greenan, B. J. W., S. J. Prinsenberg. 1998. "Wind Forcing of Ice Cover in the Labrador Shelf Marginal Ice Zone". *Atmosphere-Ocean* 36(2), 71-93.
- Smith, S. D., 1988. "Coefficients for Sea Surface Wind Stress, heat Flux, and Wind Profiles as a Function of Wind Speed and Temperature", *Journal of Geoph. Res.* Vol. 93, No. C12, p 15467-15472.

5 APPENDIX II: FIELD REPORT AND FIELD NOTES

NOTE: Field report and field notes are not edited.

5.1 Sea Ice 2004 Gulf Field Report

S. J. Prinsenberg
Bedford Institute of Oceanography
Dartmouth, N. S.
Canada, B2Y 4A2

and

S. Holladay
Geosensors Inc.
Toronto, Ont.
Canada, M4S 2Y3

This report documents the fieldwork undertaken during the 2004 ice season by Ocean Sciences personnel and co-investigators in support of several joint scientific projects in the southern Gulf of the St. Lawrence and Northumberland Strait. The report provides a list of daily work undertaken and data files collected. The work was supported by Can. Coast Guard helicopter personnel stationed in Charlottetown, PEI and funded through the Can. Space Agency GRIP program. The field report lists first the daily work done during the field survey, then lists the data files collected and finally reports the work done as recorded separately by Scott Holladay. Most pertinent data files can be provided by the co-investigators through CD distributions with this report; not all files will be provided as there are approximately 20CDs with video images alone.

Field notes from 2004 Gulf Sea Ice Survey

Friday, Feb.13, 2004

Overcast, -4°C
Light NW winds

11:00 left Bedford Institute for PEI in SUV cramped with equipment

13:00 at Confederation Bridge. Winds light from NW.

Small lead on NB side; very flat light and ice covered with snow.

15:45 Unpacked SUV and put gear into hanger.

Probe cradle need to be fixed; all boxes from Toronto are here.

Read new video laptop procedures.

Saturday, Feb. 14, 2004

Clear, -8°C

Light NW winds

08:00 Weight and measured boxes to be sent up to CASES.

Put together video sensor and mounted system in helicopter

Mounted PIC with Ian and picked up Scott from airport.

Tested probe in Hanger and ARGOS beacons

15:30 SH/SP off with PIC and video over harbour.

16:40 Flew icebreaker track into Charlottetown.

Two icebreakers in the harbour, Terry Fox and the Earl Grey.

Bought supplies on way back to hotel.

Sunday, Feb 15, 2004Clear, -17°C
Light NW Winds

08:00 Clouds over open water area north of PEI
 Put out two beacons 26384 and 2754 left here in PEI
 Scott is fixing second operator's control box.
 Checked cotter pin of probe, E-mailed Feb. 14 plots.
 13:10 PIC flight to harbour and set out line in Hillsborough Bay.
 Scott testing new sled sensor.

Hillsborough Bay line east to west

	Distance	Ice (cm)	snow (cm)	sample bag
Bag 1	0m	50	4/9/8	#19 water
			Up to 19cm	
Bag2	50m	46	4/8/8	
Bag3	100m	42	4/8/10	small ridge
	140m	48	8/8/9	
Ridge	150m	85	up to 75	
	160m	25	6/4/4	#18 snow top #10 snow bottom
Bag5	200m	25	5/5/5	
Bag6	250	26	4/3/4	
Bag7	300	26	4/3/4	

Water depth at both ends 12.9m

Salinities:

Water #19 = 25ppt Top of snow #18 = 11ppt Bottom of snow #10 = 25ppt

15:15 Video run E-W #139 over ridge

Video run W-E

No laser PIC data-----too cold after being on the ice 2hrs

Video: F001-F002

16:40 Back to Hillsborough Bay with Probe

Several restarts as not all switches were on.

No Probe but did several video flights over line.

Video: F003 – F013

Monday, Feb. 16, 2004

Clear, -18°C
Light NW Winds

Made up flags and poles.
Loosen PIC cables; PIC laser is working again.

10:40 Flight with Dan (CIS) to North Cape to do E-W line and put beacon out.

Small area of heavy ice now North of Summerside.
East end of line 47 04N and 63 50.3W
Track of line is 318 magnetic just hitting top of Island
Beacon near west end of line; beacon **26375** at 47 06N and 64 08W.
Beacon out at 11:40, telonics not working but range finder did.
Ridge area at beacon 60-71cm of ice but flat area only 35cm
At beacon E-W with PIC; W-E PIC east of line.
E-W video 4130; W-E PIC west of line and to North Cape
Video on the way to Summerside at 160m
Video: F014 – F018.

14:35 Probe flight but there is still a cable problem

15:15 Flight with Dan (CIS) to put beacon out north of PEI

Flight to small area of heavy pack ice north of Summerside
Ice thickness 37cm PIC and auger 36cm plus 4cm of snow
Beacon **26370** out at 16:10 at 46 45N and 63 28W.

E-W PIC line; W-E line Video missed to North
E-W Video line to find lat/long better variable height
W-E PIC line north of line, E-W video line at 70m (200ft)
Beacon at Video#8990; W-E line south of flag.
Video: F019 - F023

16:45 Three pictures approaching beach high up.

17:00 Over Hillsborough Bay

Laser acted up again but started after Video line
W-E line at 200ft (9570); W-E PIC line.
Video: F024-F026

Tuesday, Feb. 17, 2004

Clear, -17°C
Light NW Winds

08:25 Trip with Dan (CIS) to sample ENVISAT and fixed wing track west of Bridge.

PIC line out of harbour, turned to bridge; Video at 65m up to frame #9891.

Two pictures to PEI coast along video line

09:01 Background; then PIC line #2, three pictures low while profiling.

09:06 Background, Video at 150m frame #9920

Three pictures taken

PIC #3 line to bridge

No ice east of bridge, the floes are stalled against the bridge; winds are pushing them against it but weak tidal current slowed them down enough.

09:15 PIC #4 line west and // to bridge from PEI to NB

Thick floe at PEI side several bridge spans stuck against piers

Midway thinner ice to grey ice

Pancake in composite floe, no leads and sharp shear zone at NB side.

Video lines to bridge: F027 – F029.

09:20 Video along bridge NB to PEI at 400ft; Video F030.

Background over PEI and PIC line #5 starting towards west Point.

09:28 to 09:33; Video line all grey ice; whiter ice near PEI coast.

09:27 PIC #6 thin grey ice but rafting at places.

Short Video line end at 10529

Flight path // to thicker ice along the PEI coast

PIC #7 line S to N direction to sample from thin the thick ice.

09:43 Video line at 95m (300ft) N to S feature changed at 10956.

PIC #8 sampled to West Point; Video frame 10962 at 300-400m?

Past West Point flying high to North

West of West Point bright band along the old shear zone

New shear zone in middle of band.

Landed helicopter on mobile W side in granular ice band.

Beacon **4725** out at 10:20. Sample bag 13 of granular ice (salinity = 9.0ppt)

Video lines bridge to Beacon: F031 – F035; after beacon deployment F036-37

12:25 To Pictou Islands with Dan (CIS) taken beacon out.

Video and PIC line to beacon.

Beacon 0973 at 45 51.755N and 62 29.014W at 13:00

1.20m of ice with PIC, thinner but rafted area 60cm with Auger.

Flat floe near by away from rafts 35cm with 2cm of snow.

Video: F038

- 13:10 Beacon **0973** out; snow drifts up to 20cm, but mostly 2 – 3cm.
 PIC line due east from beacon for 8miles; Video back to beacon
 Flag/Beacon at frame 12508, three pictures taken.
 PIC line west of beacon; video was left on.
 Video at 13.38 frame 12800.
- Moved over to CCG track at 13:41 thinner ice closer to PEI.
 Video 13:50 over track to west Point.
 Video, beacon to Point Prim: F039 – F042
- 15:10 CIS flight to western ENVISAT area around North Cape area.
 From land point to NE triangle corner.
 Video lines: F043 – F053.
 Video 13320 F043 at 90m.
 Small waves in open water areas ~10- 20cm long and ~ 2 – 3 cm height.
 Video line #2 frame 13525 – 13557 some land fast ice
 PIC #2 15:50 some finger rafting.
 Video into heavier ice and Background at end 13869 (15:54)
 Video 13880 grey ice now (15:57)
 Grey ice with PIC 5miles to corner (15cm)
 Background in clockwise loop; pictures taken.
- 16:08 Video 142xx large leads and large floes of grey ice.
 Floes recent broken very sharp straight edges.
 Directly north of Cape 16:10 frame 14414.
 PIC line after background.
 Older grey ice with rafted areas 3 pictures low latitude.
 Video line section grey ice area with 3 pictures high latitude (16:15).
 Background at 16:20; more wind from south now.
 All grey ice fast video section again.
 Brighter area on Image – smaller pancake ice; newer ice.
 Looped around to take pictures.
 Short video of it (Low latitude)
 Video at 16:25 frame at 15293 - 15566.
 2.0 miles to end with some fast video.
- 16:30 End of East to West line.
 A clock-wise loop; picture at loop.
 Very thin ice still has open water round holes in it.
 PIC at 16:31 into the pancake ice
 Video at 16:35 going to SE frame area 15580 file 52.
 Lots of pancake ice in between grey flat ice + holes.
 Video at 15740; solid grey ice less pancake ice.
 Floes cracked; sharp edges floes of pancake and grey mixed.
 Video frame area 15833.

- 16:40 PIC background; area has large leads.
 Mostly thin grey ice but here and there still pancake ice.
 Heavier ridging in grey ice starting to appear.
 16:44 white band ~ ½ mile wide to SW of flight path; probably pancake ice.
- 16:49 Background of PIC; into pancake ice later rough ice and rubble.
 Loop to take picture of rough ice 16:52.
 Rough ice in shore with bright rubble field; end with PIC run.

Wednesday, Feb. 18, 2004

Overcast, -9°C
 Light SE Winds

- 09:40 Test flight with Probe to Hillsborough Bay (Scott and John)
 Probe worked well, refueled and left for Northern PEI pack ice.
 Probe did not start up and returned to Hanger.
 Video lines: F055 – F060.
- 10:24 Flight north of PEI with Dan (CIS) with PIC and Video.
 Video lines: F061 – F073.
 Video shore waves F061; Background 10:30 to beacon/floe.
 Waves // to shore; different wind than over land.
 Pic #1 shore fast ice to open water.
 Shore fast very rough up to 4.5m thick, thin ice 3 –5cm.
 Band of ice of grey thicker ice before another lead with grey – grease ice.
 Older grey ice before thick floe with beacon on it.
 Background at 10:36 some fast video.
- 10:37 Grey, young ice, Video end logging over floe 26370.
 Pic line over floe and edges.
- Continue due east from floe/beacon.
 Alternating video PIC every 3 – 4 minutes
 10:53 saw some 20-15 thick ice, floes within pack ice small 2m.
 10:56 Video over dull grey ice very flat; bright is rafted older ice.
- 11:06 Landed on the grey ice PIC said 25cm; two 25cm auger holes confirmed it.
 Salinity of grey ice bag #11 = 10ppt.
 Beacon **26386** out at 11:37 at 46 43N and 62 07.7W
 File going south then west F067.
 Background at 11:41. PIC 11:42 – 11:45 rafted/ridge bright area band.
 Video all grey ice.

12:00 Video over bright area F069.

Landed besides a grey ice lead on rubble bright floe with a very straight edge.
Other broken are in a band towards the east; PIC W to E.
Floes within rubble look like old pancake ice 2m and bigger.
Thickness 100 and 120cm; rubble blocks thin 15 – 20 cm.
Helicopter parked at edge on small pan.

12:15 PIC flight over the area from N to S then going to PEI.

Video at 12:23 thin ice still some round pod holes not frozen.
Background 12:29 large flat floes grey ice no ridging but rafting.
Video. More open water present and finger rafting end at 12:40.
PIC 12:39 ice along the coast. Winds 10-15 knts SW
Glassy ice 3-5cm cuts short water out but not long waves.
Open water – stopped PIC.
Video open water to land-fast ice 12:43.

14:15 CIS Flight to targets NE and E of PEI.

Video lines: F074 – F080.
Video shore lead towards the east. Target #1.
Dull grey floe 35cm thick but at places up to 1m thick;
6-8 cm of snow of wet-salty snow on it.
Auger holes 33 and 34cm plus 4cm of snow.
PIC measured 36cm snow + Ice.
Bag of wet snow taken Salinity of bottom snow layer = 33.0ppt.

15:03 Off from dull flow Target #1; run PIC over it.

Line S – N; rough ice, dull floe; rough ice and just into grey ice.
Pic second run over bright but rubble ice; up to 5m thick.
Video run to east at 400m, then at 21525 turn to south now at 270m.
PIC profile rough ice to just into grey ice east of East Point.
Did a loop to take pictures of it.
Back over it with video end at rough ice at 21800.

15:43 Bright target #3 east of PEI was pancake ice wind drift band.

PIC over it dull area on both side was 25 – 30 cm thick.
Pancake region up to 65 cm thick.
Target #4 E-W line between dull inshore and old offshore pack ice.
PIC W – E flat to rough ice passing over icebreaker track.
Video E – W same path. Track at 22229 at 15:50.

16:40 Scott and John to Hillsborough Bay line.

Some video/PIC lines and sled runs.

Thursday, Feb. 19, 2004

Storm, -5°C
Strong NE winds

Snow storm, just writing CDs and typing notes.

Friday, Feb. 20, 2004

Clear, -5°C
Light NW Winds

Digging car out of snowdrift, packing gear and writing CDs.

Tuesday, Feb. 24, 2004

Overcast, -6°C
15mph NW Winds

07:25 Left Bedford for PEI.

10:25 At Bridge Winds perpendicular to bridge from the NW
Ice moving to the East; Southern half of Strait covered with pack ice.
Large floes $\frac{1}{4}$ to PEI; Grease ice $\frac{1}{2}$ to $\frac{3}{4}$ across the Strait.
 $\frac{3}{4}$ open water started; not much land-fast ice along PEI

12:00 At hanger; mounted video camera; downloaded Ingrid's beacon map.

13:00 Off the NW beacon 26370 found it by eyeball; range finder too slow.

E-W PIC may not be good.

E-W video at 100m flag at 22536; 13:13

W-E PIC at 13:16

E-W video at 100 flag to left 22657 at 13:18

13:15 Background; W-E PIC at 13:22.

80cm at flag by PIC

Thin snow 10/12/15cm; snow drifts 30-50cm.

13:40 PIC to North slower speed due to bad contrast.

13:44 Video and then turn to east 13:52 Background at 13:48

Grey ice now covered with snow but around 29cm on average.

Several video and PIC lines; turned south at 14:04 and did a wide loop.

No beacon on range finder.

14:10 Went to beacon last coordinates placed a flag there for reference.

PIC line W-E and video E-W 23995 flag.

PIC line south of flag W-E; video E-W left (south) of flag 24140.

PIC W-E North of flag.; Video flag line at 14:45 E-W 24234.

Wednesday, Feb. 25, 2004

Overcast, -2°C
Light NNW winds

08:30 Waiting for low mist to burn off.

10:25 At beacon 26370 46 28.398 and 63 14.965 at 10:52

Beacon had drifted 2.13kmiles SE.

Ice thickness just NE of beacon in flat ice 45/47cm with 9/8/8cm of snow

11:10 PIC W_E (actually NW-SE) more open water areas; 2miles on each side.

Video (91) flag at 24380 E-W.

Video flag at 24466 11:16

PIC at 11:24 grey ice with snow at start W-E

11:20 Video flag to south end at 11:24

11:23 Video E-W north of line; flag at 24660 to south.

South PIC line 11:27 more open water and rougher ice inshore.

11:30 Video south of flag at distance 290m (PIC or Video?)

End in land-fast ice rubble.

Video to East to ridge at 24774; start land-fast ice rubble
south of flag at 11:34 24868.

11:36 Passing over ridge W-E.

Landed; water depth 8.80m; ridge over 10m.

46 26.953 and 63 14.427.

Negative 8cm freeboard; snow 45/40cm at places.

12:05 PIC to beacon 26386 then video 12:09 at 100m.

12:13 after video PIC measured grey ice plus snow as 30-40cm.

Video into beacon area; found beacon by eye ball and other flag to NW 2miles.
(i.e. lines flown day before do represent area)

1.4miles west of last beacon location 46 35.442 and 62 32.587 at 12:35.

Range finder finally woke up at 2m from flag.

Hand held video of PIC sampling. First W-E line and then E-W line right over flag. 13:00
to hanger for fuel.

13:50 Back to beacon 26383 for more lines and video lines.

Video to beacon and right over beacon on W-E line; flag at 25903.

Large N-S lead to East of beacon.

14:10 PIC line E-W to north of beacon

Video at 500ft W-E over beacon; 26022 at about 200ft north of flag.

Back Ground; a distinguishable square floe in lead to east of flag.

PIC E-W over flag; small leads forming

Video W-E at 500ft flag at 26095.

PIC line E-W; video was on!

14:25 Video from west end of lines to NW direction.

PIC at 14:32- 14:35.

The video and PIC lines; turn to Maggies and run into seals.

15:03 Towards Hanger video and PIC lines

16:00 Files 33 and 34 did not download.

Thursday, Feb. 26, 2004

Storm, -5°C
Strong NE Winds

Snow storm, just writing CDs and typing notes.

Down laded files 33 and 34 but GPS is missing

Friday, Feb. 27, 2004

Storm, -5°C
Strong NE Winds

Took sensors off helicopter; typing notes and packing.

Monday, Mar. 22, 2004

Clear, -10°C
Light NW Winds

13:00 Installed video and PIC on helicopter.

Installed updated Video logging software, and Pant-shop
on both helicopter laptops.

Fixed crate for Probe, Scott working on Probe.

Tuesday, Mar. 23, 2004

Clear, -14°C
Light NW Winds

09:15 To ICYCLER location

Video Ferry to location 4 miles; F105

Low at spot and up again for BG

09:23 On ice to put temp. flag out, found visually. Range finder??

Some ice ridged up to 5m.

Try to beacon out but no response on range finder even close 10m from
Beacon 26370 nor the beacon at the airport.

E - W PIC lines (3): centre; north and south

W - E video lines (F107 and F108)

9:35 at 86m flag at 28857

9:40 at 150m flag at 29101.

Some fast video at end.

- 12:15 Off with Probe; its data is intermittent.
 Video hard to start.
 Probe-video data at 12:37 but laser intermittent.
 Flying along the bridge; Scott not happy with Probe.
- 12:40 N to S on east side of bridge F110
 12:50 S to N west of bridge; halfway at 12:50 F111
 N to S F112 31445 midway east of bridge.
 Large lead on NB side
- 13:03 Video back out 310m F113
 Back sampling to Hanger.
- 14:11 Range finder now works on tarmac (temp dependent??)
- 15:16 Going to the east beacon 26386
 Found beacon by range finder on a small flow; flag there but faded.
 I kept the box warm away from the floor??
 PIC lines E to W and Video W to E
 Flag at 33302 85m on F115 at 15:20
 Flag at 33410 150m on F116
- 16:46 W to E PIC plus low video flag at 34121 on F117
 Video E to W at 88m F118 at 16:51 flag at 34177
 PIC south of flag centre at 16:55.15
 Video E-W at 415m 35259 flag
 17:00 west end of line maybe landfast ice (17:00)
- 17:01 Flag at beacon 0.87 snow+ice
 17:05 Beacon recovered.
 PIC line over beacon and into shore.

Wednesday, Mar. 24, 2004

Snow, -2°C
 Light SE Winds

- 13:20 Off the bridge but returned due to snow showers.

Thursday, Mar. 25, 2004

Clear, -5°C
 SW Winds

- Probe still not working; PIC to do seal test.
- 12:49 to 12:52 seals with PIC
 Video 15:52 on F121
 S – N PIC 2.2 miles; centre at 13:18.05
 Video N to S centre at 35990 at 86m F122
- 13:23 BG some video (low) at end of F122
 S to N PIC lots of seals at N end
 Video at 600ft; centre at 37433 at 13:308

13:39 No seal area north of other area and just south of large lead.

N to S PIC line ends at start of seals.

S to N video at 86 m (300ft)

PIC second line; then video at 175m or 600ft.

37700 at 13:46

16:00 Probe flight along land-fast ice north of PEI.

First no power cable disconnected.

No laser probably snow plug.

Three landings Probe static problem does not occur.

Video could not be started as the breaker was off on the Probe PC

Video finally on F128 at 16:28 –16:35

Packed all boxes for CASES (also on Friday morning)

Video files:

Day	Time	CD #	video file #s	Fem file #s	Areas
Feb. 14	15:30 - 16:45	-----	-----	04001- 02	Hillsborough Bay
Feb. 15	15:19 - 17:25	2004 -1	F001 - F013	04003 - 05	Hillsborough Bay
Feb. 16	11:03 - 11:13	2004 -2	F014 - F016	04006 - 08	Cape North
Feb. 16	11:52	2004 -3	F017 start	04006 - 10	Cape North
Feb. 16	12:52 - 12:02	2004 -4	F017 - F018	04010	Cape North (#26370)
Feb. 16	16:19	2004 -4	F019	04011 - 12	North of PEI
Feb. 16	16:23 - 17:00	2004 -5	F020 - F026	04013 - 14	N of PEI/ Hillsb. Bay
Feb. 17	08:57 - 09:43	2004 -5	F027 - F033	04015	Hillsb. Bay – Bridge
Feb. 17	09:49 - 10:31	2004 -6	F034 - F037	04015	Bridge – West Point
Feb. 17	12:48 - 13:52	2004 - 6, -7	F038 - F042	04016 - 17	Pictou Isl. to Point Prim
Feb. 17	15:44 - 16:25	2004 - 7	F043 - F049	04018	Cape North
Feb. 17	16:26 - 16:44	2004 - 8	F050 - F053	04018	Cape North
Feb. 18	08:44 - 09:03	2004 - 8	F054 - F060	04019	Probe test
Feb. 18	10:27 - 11:36	2004 - 8, -9	F061 - F067	04025 - 27	N and NE of PEI (#26368)
Feb. 18	11:44 - 15:30	2004 - 10	F068 - F078	04028	N and NE of PEI
Feb. 18	15:32 - 15:52	2004 - 11	F079 - F080	04029	N and NE of PEI
Feb. 18	16:30 - 17:30	-----	-----	04030 - 31	Hillsborough Bay
Feb. 24	13:07 - 15:10	2004 - 13	F081 - F090	04032	N of PEI - beacons
Feb. 25	10:00 - 12:45	2004 - 14	F091 - F098	04033 - 34	N of PEI beacon 26370
Feb. 25	13:55 - 15:52	2004 - 15	F099 - F104	04035 - 36	N of PEI beacon 26386
Mar. 23	09:17 - 09:45	2004 - 16	F105 - F108	04038	ICYCLER
Mar. 23	12:34 - 13:13	2004 - 16,17	F109 - F114	Probe	Bridge area
Mar. 23	12:20 - 15:28	2004 - 17	F115	04039	Beacon 26368
Mar. 23	16:49 - 16:59	2004 - 17,18	F116 - F118	04040	Beacon 26370
Mar. 25	12:42 - 13:36	2004 - 19	F120 - F125	04043	Seals
Mar. 25	15:57 - 16:38	2004 - 19	F126 - F130	Probe	N of PEI

5.2 2004 DFO Ice Pic and Probe Field Program Field Notes 14-20 February

J. S. Holladay

14 February

Weather: Clear, -5°C(?) Winds low to moderate

Activities:

Travel Toronto-Charlottetown.

Pic mostly mounted by time of arrival.

Turned on Pic and Probe in hangar—both OK.

Short test flight with Pic in Hillsborough Bay (HBB)—ran lines ~NS between Governor's Island and Point Prim. Landed to drill some test holes and validate Pic on two different ice types. First one—semi-landfast ice, good agreement with Pic (Pic ~3 cm low compared to single auger hole).

Second floe had been through bridge (~square) had slushy snow (wet with brine) and was thin and soft—Pic read slightly (5 cm) low, as expected due to conductive ice and brine in snow.

Files: FEM04001 Hillsborough Bay (no test line yet)

15 February

Weather: Clear, very cold -15 to -19 over day, winds NW 15 dropping in late aft

Activities:

Checked out small sensor off landing pad, then took it out with Pic to establish test line on semi-landfast ice.

JSH tested small sled sensor, SP and HM set up test line.

Test line: 300m line with ridge in middle, older ice to E, small hummock of ice in center of thinner floe (to W).

On ice ~1.5 hr.

After takeoff—no laser altimeter. Pilot's display only showed altitudes above 100m—when below this, cut out (above 100m, used radar).

Diagnosis of Pic laser problem—no laser in RAW files after line setup, so appears laser was either too cold to operate properly, or cables to Pic might have contracted enough to affect contact (seems unlikely but possible). These had been set up rather tight in warm hangar, so would have contracted a fair bit over ~1m span.

Flew Probe test.

Turned on at pad. EM froze during takeoff (remember, only turn on after takeoff!)

Verified that nav, pitch and roll all OK, laser OK before takeoff.

Worked fine initially EIS04004, but did not seem to get good base levels for drift correction.

Restarted EIS04005, again worked fine at start and didn't baseline properly

[Note: these data can be post-processed to obtain nominal accuracy—problem was with baselining and radio transmissions—see below.]

Files: EIS04003-5: Hillsborough Bay test line

16 February

Weather: Clear, cold (-21C in morning), winds NW ~15 kts.

Activities:

Pic checkout: turned on in hangar, showed no problems. Rerouted cables to reduce stress at sensor connectors. Positioned helicopter outside to cool off while SP prepared for field. Laser operated properly when turned on after ~1 hr at -20C.

During a flight later today, laser shut down briefly after getting cold—leaving Pic on warmed it up again and it resumed operation after a few minutes.

Later, Pic sat on pad for > 1 hr in -20, again laser failed to start. Heated aluminum shell with heat gun, avoiding telescope lenses—laser resumed operation after a few minutes. This seems to confirm that the new Optech laser (brass-anodized finis) does not start up well at very cold temperatures. See notes below on short and long-term solutions for Pic laser issue.

Probe data analysis. Determined that baseline errors are caused by starting baseline measurement too soon after radio transmissions. After end of transmission, there is a long period (over 20 sec) during which some EM channels are strongly affected (during transmission, effect is even stronger). Away from radio bursts, data look normal.

Conclusion: we were not following proper procedure during test flight—pilot should avoid unnecessary radio transmissions, operator should wait for 30 seconds after last radio transmission before zeroing. Avoid radio transmission after zeroing and before profiling. This problem seems much stronger than any I have seen with this system. Has radio been changed or serviced recently? Power wiring changed?

Will need to post-process data to correct baseline errors etc.

Test flight of Probe to verify efficacy of procedural changes—bird failed to initialize, returned to base.

Troubleshoot Probe. Ethernet card (Probe console) front end chip blown.

Restarted Pic, laser not operating. Heated shell of laser with heat gun for a few minutes—resumed operation.

Files: Pic

FEM04006 Test line vicinity (no laser?)

FEM04007 3 lines, just west of Cape North

FEM04008 2 landings, just west of Cape North

FEM04009 x

FEM04010 3 profiles, 2 west of Cape North, 1 thick to open water to E

FEM04011 1 profile, thin ice, 63.4W, 46.73N

FEM04012 1 profile plus landing, same spot as 04011

FEM04013 4 profiles, same spot as 04011

FEM04014 2 profiles, 1 short, 1 including test line (?)

FEM04015 X

FEM04016 X

Short-term Pic laser workaround

—rerouted cables, leaving small slack and tying off to base of mounting bar before running to mirror supports and on back. Plan to keep Pic running as much as possible when outside, and when shut down, wrap laser part of Pic with blanket or coat (to be removed before takeoff!) to keep it from cooling down too much.

--(late evening) added foam pad with cutouts for telescope sightlines to provide insulation and reduce airflow around base of laser unit.

--No further problems were reported after this change (though temperatures moderated a few degrees at the same time).

--Long term Pic Laser changes—may need to install heater(s) for laser altimeter, should perform some tests on unit when time permits to identify extent of temperature sensitivity.

Note that the geophysical industry routinely operates equipment overnight when in cold conditions to prevent such effects. Also, original Pic laser seems to have better thermal tolerance than new one, although new one has superior performance over open water.

17 February

Weather: clear, cold -17 in morning, winds W 15 kts.

Activities:

Completed troubleshooting of Probe system by noon.

Pic flew several flights with Dan Fequette and Simon.

Files:

FEM04017 5 profiles, E to W, from N of Pictou to Hillsborough

FEM04018 11 profiles triangular track N, W, then SE

18 February

Weather: high overcast, moderating temperatures, winds S 15 kts.

Activities:

Install and test Probe in morning. First flight over Hillsborough Bay, with John Iacozza operating VGPS in back, no problems. Returned to base to refuel before long flight to north of island with Simon. After refuel—Probe failed to initialize. 3 retries, then returned to base and swapped back to Pic, Dan and Simon took off to perform the flight with the Pic.

Test Probe—spare Ethernet in Probe console failed—same chip, slightly different expression (won't receive or transmit). Tried to locate a more robust replacement—could not obtain unit before next week. One interesting possibility obtain a robust AUI transceiver (interfaces between AUI port on Ethernet board and thin-wire 10Base2 Ethernet cable (this would work with the existing boards, since their AUI ports are apparently not damaged)

ground shield of Ethernet cable to main helicopter power supply ground to prevent common-mode surges due to electrostatic events.

After Simon's main data acquisition complete—take John Iacozza out with Pic and sled sensor to train him on Pic use and let him test the sled sensor. Acquired 3 passes with Pic, and 2-1/2 lines with sled.

John operated Pic during return to base—ran a few lines enroute.

Files Probe:

EIS4008, simultaneous VGPS data. No data after this.

Pic:

FEM04019 1 short profile over northern arm of Hillsborough River

FEM04020 6 profiles NW from Tracadie, then E

FEM04021 2 WE profiles plus ?? N of East Point.

FEM04022 3 profiles to SW, end at north shore

FEM04023x

FEM04024x

FEM04025 1 profile plus landing N of East Cape

FEM04026 1 profile EW N of East Cape

FEM04027 1 profile WE N of East Cape

FEM04028 1 profile NS E of East Cape

FEM04029 3 profiles in Strait S of eastern PEI

FEM04030?: test lines in Hillsborough Bay. Shutdown at end

FEM04031?: training flight for John Iacozza (not over line). Shutdown prior to landing at base.

19 February

Weather: Nor-Easter, 100 km/hour winds, 50 cm snow, heavy drifting, moderate temp, big storm surge forecast.

Activities:

No flying—could not even reach hangar by road. Worked on data at hotel.

6 APPENDIX III: COMPUTATIONAL CODE

The following code was used to compute U_{10} using Matlab[®] v6.05, Release 13. It was found @ <http://woodshole.er.usgs.gov/operations/sea-mat/>; Air-Sea Toolbox.

function [cd,u10]=cdntc(sp,z,Ta)

```
% CTDTC: computes the neutral drag coefficient following Smith (1988).
% cd = CDNTC(sp,z,Ta) computes the neutral drag coefficient given the
% wind speed and air temperature at height z following Smith (1988),
% J. Geophys. Res., 93, 311-326. Assumes sp and Ta are both column
% or row vectors and z a fixed scalar.
%
% INPUT: sp - wind speed (m/s)
%        z - measurement height (m)
%        Ta - air temperature (deg C) (optional)
%
% OUTPUT: cd_10 - neutral drag coefficient at 10m
%         u_10 - wind speed at 10m (m/s)
%%%%%%%%%%%%%%%%%%%%%%%%%%%%%%%%%%%%%%%%%%%%%%%%%%%%%%%%%%%%%%%%%%%%%%%%
% 3/8/97: version 1.0
%%%%%%%%%%%%%%%%%%%%%%%%%%%%%%%%%%%%%%%%%%%%%%%%%%%%%%%%%%%%%%%%%%%%%%%%
% Vectorized RP 26/8/98

as_consts: % Define constants

if nargin==2,
    Ta=Ta_default;
end;

% Iteration endpoint
tol=.00001;

visc=viscair(Ta);

% remove any sp==0 to prevent division by zero
i=find(sp==0);
sp(i)=.1.*ones(length(i),1);

% initial guess
ustaro=zeros(size(sp));
ustarn=.036.*sp;

% iterate to find z0 and ustar
```

```
ii=abs(ustarn-ustaro)>tol;  
while any(ii(:)),
```

```
ustaro=ustarn;  
z0=Charnock_alpha.*ustaro.^2./g + R_roughness*visc./ustaro;
```

```
ustarn=sp.*(kappa./log(z./z0));
```

```
ii=abs(ustarn-ustaro)>tol;  
end
```

```
sqrzd=kappa./log((10)./z0);  
cd=sqrzd.^2;
```

```
u10=ustarn./sqrzd;
```